

**Regulation of inflammation in canine species:
a role for macrophages and Hsp70**

Qingkang Lyu

吕庆康

© 2021 Qingkang Lyu

All rights reserved. Published papers were reprinted in this publication under CC license. No parts of this thesis may be reproduced or transmitted in any form or by any means without prior permission of the author.

ISBN: 978-94-6416-849-5

The research described in this thesis was performed at the Division of Immunology, Department of Biomolecular Health Sciences, Utrecht University, The Netherlands.

Cover design: Qingkang Lyu conceives the idea and makes the final layout, Liyao Jiao draws the elements. Joint hands mean collaboration and cast the shadow of a dog on the macrophage. The curl bands in the background are Hsp70 molecules. All the elements are relevant to the content of this thesis.

Layout and design: Qingkang Lyu

Printing: Ridderprint | www.ridderprint.nl

Printing of this thesis was financially supported by Infection & Immunity Center Utrecht and by the Division of Immunology, Department of Biomolecular Health Science, Utrecht University

Regulation of inflammation in canine species: a role for macrophages and Hsp70

Regulatie van ontsteking bij honden: een rol voor macrofagen en
Hsp70

(met een samenvatting in het Nederlands)

Proefschrift

ter verkrijging van de graad van doctor aan de Universiteit Utrecht op
gezag van de rector magnificus, prof. Dr. H.R.B.M. Kummeling,
ingevolge het besluit van het college voor promoties in het openbaar
te verdedigen op dinsdag 2 november 2021 des middags te 12.15
uur

door

Qingkang Lyu

Geboren op 18 oktober 1988 te Handan City, China

Promotoren:

Prof. dr. W. van Eden

Prof. dr. F. Broere

Copromotor:

Dr. E.J.A.M. Sijts

Qingkang Lyu was financially supported by China Scholarship Council (CSC).

Table of contents

Chapter 1	General introduction	7
Chapter 2	The anti-inflammatory properties of heat shock proteins and therapeutic tolerance induction in chronic inflammatory diseases	36
Chapter 3	Leucinostatin acts as a co-inducer for Heat Shock Protein 70 in cultured canine retinal pigment epithelial cells	62
Chapter 4	Hsp70 and NF- κ B mediated control of innate inflammatory responses in a canine macrophage cell line	80
Chapter 5	Comprehensive characterization of dog monocyte-derived macrophages at different polarization statuses: M1 and M2	110
Chapter 6	A canine macrophage cell line that can be polarized into classically activated M1 and alternatively activated M2 macrophages provides a model for the study of canine macrophage differentiation	144
Chapter 7	General discussion	180
Chapter 8	Summary in English Nederlandse samenvatting	200
Appendix	Acknowledgements Curriculum Vitae List of publications	212

1



General introduction

Preface

Inducible Hsp70 is a representative of the family of HSPs, and has been well-examined for its functions in cell stress, such as in stressed eyes and macrophages of many species (1-3). In the eye, the retinal pigment epithelium (RPE) constitutes a single layer of polarized pigmented cells between the retina and the choroid. Maintaining the physiological function of RPE contributes to remission of a number of ocular disorders, such as age-related macular degeneration (AMD) and uveitis (4, 5). Boosting of Hsp70 expression in RPE cells has been shown to improve the physiological function of RPE cells (6).

In addition, macrophages are key components involved in the regulation of chronic inflammatory diseases, and autoimmune diseases. An increasing number of studies have shown that overexpression of Hsp70 has an anti-inflammatory role in macrophages (7). Dogs are susceptible species for chronic and immune diseases, but little is known about the role of Hsp70 in dogs. Therefore, understanding the effects of Hsp70 in dogs RPE cells and macrophages, and exploring novel ways to upregulate Hsp70 expression by use of Hsp70 inducer/co-inducers might lead to new therapeutic strategies for eye diseases.

Macrophages are a heterogeneous population, mainly consisting of two extreme phenotypes, M1 and M2 macrophages. The balance between M1 and M2 macrophages is tightly associated with the process of inflammation and the immune response (8, 9). Well-defined macrophage subsets *in vitro* are useful tools for studies of macrophage-related diseases. Unfortunately, the lack of a canine macrophage model *in vitro* has hampered the progress of studies on the canine immune system. Therefore, it is urgent to develop a well-characterized canine macrophage model *in vitro*.

Taken together, the overall aim of this thesis is to have a better understanding of Hsp70 in canine RPE cells and macrophages, and to establish well-characterized canine macrophages. In this introduction, a background on canine Hsp70, RPE cells and macrophages, and the relationship between them are provided.

Function of Hsp70

The heat shock response was first reported by Ritossa et al. in 1962 due to induction of new puffing patterns in the salivary gland chromosomes of *Drosophila busckii* by heat shock (10). Over 10 years later, heat shock genes and proteins coded by these genes were identified and termed as “heat shock proteins” (11). Since then, great progress has been made in elucidating the function of heat shock proteins (HSPs)

at the molecular level. So far, HSPs have been found to be ubiquitously present in almost all studied organisms from microbe to human, even in plants. They are highly conserved among diverse species during evolution. HSPs play a critical role in maintaining cellular homeostasis and defending against extreme environment. In animals, cells express HSPs in different ways, by constitutive expression and inducible expression. Constitutively expressed HSPs in resting cells participate in nascent protein synthesis, facilitate assembly, folding and transportation of proteins, and prevent aggregation and mis-folding. Thus, they are also referred to as molecular chaperons. Upon stress, a large amount of inducible HSPs is produced, which assist in the refolding of damaged proteins or facilitate the degradation of proteins damaged beyond repair. Recent research showed that HSPs can also be released into extracellular compartments. Some extracellular HSPs were found to modulate innate immunity by activating antigen presentation, inducing the secretion of inflammatory cytokines, or affecting cellular signaling (12).

With increasing knowledge of HSPs, the members of HSP families have been largely extended, containing proteins of molecular weight ranged from 8 to 200 kDa (13). According to the new guideline proposed by Kampinga et al. in 2009, human HSPs are named and classified as HSPH (Hsp110), HSPC (Hsp90), HSPA (Hsp70), DNAJ (Hsp40), and HSPB (small Hsp), HSPD/E (Hsp60/Hsp10) and CCT (TRiC) (14). Among these, the HSP70 family encoded by the gene HSPA1A is one of the most studied members, which is characterized by ubiquitous spread and conservation. The Hsp70 family consists of at least eight structurally homologous chaperone proteins, residing in different cellular compartments (mitochondria, cytosol, endoplasmic reticulum etc.) and with different functions. Three of them are strongly up-regulated under stresses: HSPA1A, HSPA1B and HSPA6 (15). The structure of Hsp70 is different from that of other HSPs; instead of having a cylindrical structure (16), iHsp70 contains a 45 kDa N-terminal ATPase domain and a 25 kDa C-terminal peptide-binding domain (17). It has been shown that Hsp70 recognizes short hydrophobic stretches within a protein sequence (18, 19). The vast majority of proteins carry (multiple) Hsp70 binding sites (18, 20), as such hydrophobic peptides are required for holding the 3D fold of a globular protein, by constituting a hydrophobic core. Meanwhile, Hsp70 requires an extended conformation of its substrate in order to bind (21).

As a molecular chaperon, Hsp70 has been implicated in diverse cellular functions, such as in maintaining cellular homeostasis, preventing cell death, in cell differentiation, protein synthesis, and proliferation. Early studies show that around 15% of newly synthesized proteins in bacteria is associated with the assistance of Hsp70 (22, 23). Furthermore, Hsp70 also has anti-apoptotic effects by regulating apoptosis related signaling at different levels (24).

In addition, Hsp70 has been reported to play a crucial role in multiple inflammatory and immune diseases, such as cancer, rheumatoid arthritis, neurodegenerative disorders, and asthma (24, 25). Hsp70 is found to accumulate in breast, lung, and gastric cancer, suggesting it might be a potential diagnostic biomarker for various cancers (26). Moreover, increasing studies have shown that overexpression of Hsp70 has a remedying effect in many diseases. Sun et al. demonstrated that overexpressing Hsp70 by using an inducer can ameliorate neurodegeneration of Alzheimer's disease by decreasing the production of inflammatory cytokines and inhibiting ERK/p38 MAPK signaling (27). Increased Hsp70 was observed to inhibit inflammation by inhibiting the activation of NLRP3 inflammasomes (28). Similarly, Samborski et al. showed that pharmacologically elevating Hsp70 expression can dampen the inflammatory process in inflammatory bowel diseases (IBD) (29). Besides, overexpression of endogenous Hsp70 also could enhance its presentation by MHC molecules and modulate adaptive immune response by inducing Tregs (12).

Taken together, overexpression of Hsp70 might be a promising approach to treat Hsp70 associated diseases. Although Hsp70 is strongly inducible, its expression is very low and difficult to induce under physiological conditions. Therefore, pharmacological induction of Hsp70 has been focused. Since activation of HSF1 highly induces Hsp70, HSP inducers or co-inducers are a matter of great concern for the induction of Hsp70. So far, several Hsp70 inducers, such as celastrol, GGA, geldanamycin and ansamycins, and co-inducers, such as carvacrol and bimoclolmol have been studied. However, few of them can be used in the clinic because of their toxicity or side effects, thus there still is a need for new inducers.

Regulation and induction of HSPs

The expression of inducible HSP family members is triggered mainly by physiological stress such as chemical stressors and heat shock, and environmental stress such as inflammation and aging. In response to stress, transcription of inducible HSPs is initiated by the nuclear translocation of heat shock factor (HSF). Translocated HSF can bind to heat shock element (HSE) containing a 5'-nGAAn-3' sequence in the HSP gene promoter region, initiating the transcription of HSPs (30, 31). So far, at least four HSF genes (HSF1-4) have been found in mammalian cells (32). Among these HSFs, HSF1 has been demonstrated to be the main regulator of synthesis of inducible HSPs in HSF1 gene knock-out studies (33-35). The exact activation mechanism of HSF1 is still controversial. The one that is widely accepted in mammals is that under normal conditions, HSF1 is in an inactive state in the cytoplasm where it is bound to Hsp70, Hsp90 and Hsp40; upon stress, HSF1 is separated from other HSPs and phosphorylated, subsequently undergoes nuclear translocation, binds to heat shock promoter elements, and induces transcription of

heat shock genes (Figure 1). This theory is supported by the discovery of Hsp70/HSF1 (36) and Hsp90/HSF1 complexes (37) in the cytosol of resting cells. Thus, the activation of HSF1 is indispensable to the expression of inducible HSPs (Figure 1). HSFs are potent therapeutic targets for HSP-related diseases.

Recently, a great number of studies have shown that many compounds derived from food, herb or approved drugs can elevate iHSP expression by activating HSF1, such as carvacrol and celastrol (38, 39). According to whether compounds directly activate HSF or not, these compounds can be divided into HSP inducers and co-inducers (40). In other words, HSP inducers can elevate HSP expression by activating HSF, in contrast, HSP co-inducers do not interact with HSF and do not induce HSPs directly, but lower the threshold of heat shock response and assist other stressors do that. Thus, HSP inducers or co-inducers can activate HSF and induce HSPs in different ways. Some compounds can disrupt HSF/HSPs complexes, releasing HSF, which prompts translocation of HSF and the combination of HSF and HSE. For example, Otaka et al showed that geranylgeranylacetone (GGA) could release HSF1 by binding to the C-terminus of Hsp70, resulting in induction of Hsp70 (41); geldanamycin binds to Hsp90 to dissociate HSF1, leading to HSP induction (37); and boosting of Hsp70 by celastrol (39) and paeoniflorin (42) is mediated by HSF1 activation (Figure 1).

The location and function of RPE cells

During embryonic development, the retinal pigment epithelium (RPE) and the neural retina originate from the outer layer and the inner layer of optic cup in the optic vesicle neuroectoderm respectively (43). Due to the structural relationship between RPE and retina, the RPE is adjacent to and tightly linked with the neural retina throughout life. In adult eyes, the RPE consists of a single layer of cells closely connected by tight junctions lying at the interface of neural retina and choroid. Due to this special structure, the RPE can perform numerous important functions to protect and support the neural retina, and maintain normal visual function during embryonic development and throughout adult life course. These functions include transportation of trophic substances and the end-product of metabolism, enhancement of visual acuity by absorbing stray light, protection of the retina from oxidative damage by transferring free radicals, and phagocytosis of photoreceptor outer segments (44). The intercellular tight junctions between RPE cells constitute the outer blood-retinal barrier which maintains the immune privilege environment of the eye, together with the inner blood-retinal barrier composed of endothelial cells, which selectively transports specific biomolecules and prevents toxic molecules and plasma components from entering the retina (45). Therefore, maintaining the health and integrity of RPE is essential for retinal health and vision. Defects in the RPE,

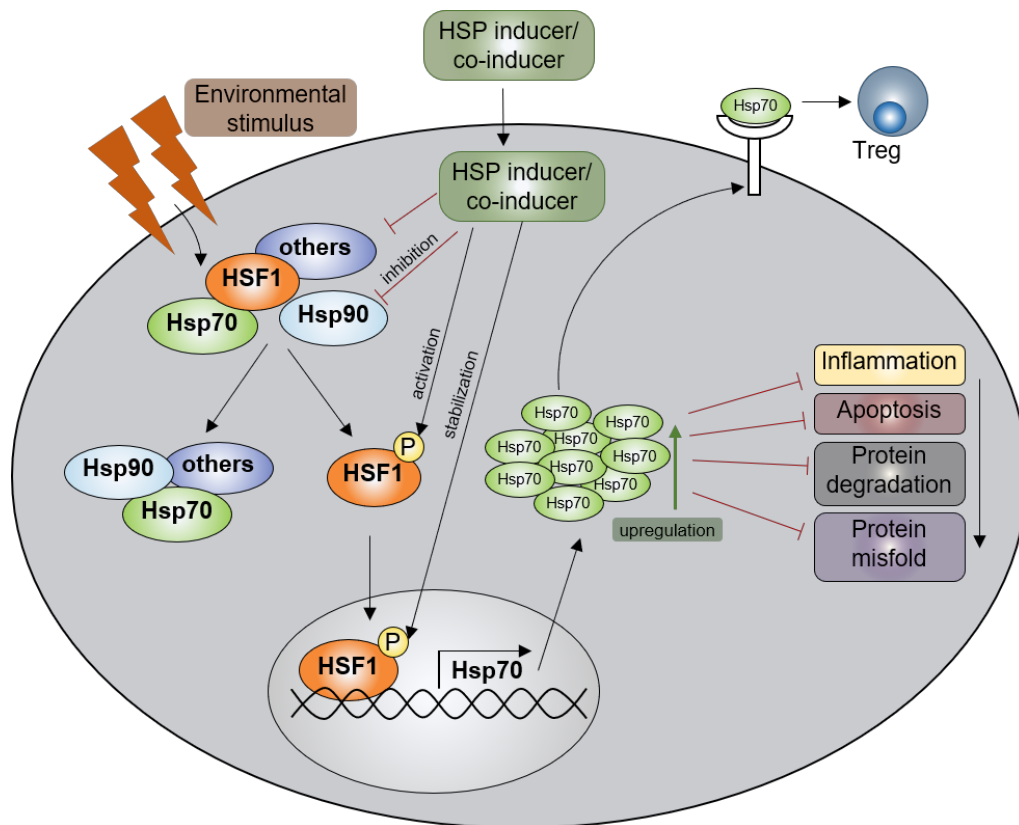


Figure 1 The induction of Hsp70 by its inducers or co-inducers. Under normal conditions, HSF1 resides in the cytoplasm in an inactive state bound to Hsp70, Hsp90 and Hsp40; in response to environmental stress, HSF1 is separated from other HSPs, phosphorylated, translocated into the nucleus, binds to heat shock promoter elements, and so induces the transcription of Hsp70. HSP inducers or co-inducers are able to upregulate Hsp70 by inhibiting Hsp90, 40 or other components of HSF complexes, activating HSF1 or stabilizing the binding of HSF1 and heat shock elements. Upregulated Hsp70 has suppressive effects on inflammation, apoptosis, protein degradation and protein misfolding. HSP: heat shock protein, HSF: heat shock factor, Treg: regulatory T cell.

especially morphologic abnormalities and changes in functionality, have been implicated in the etiology of various human eye diseases which result in vision loss, such as retinitis pigmentosa and age-related macular degeneration (46, 47). Diagnosis and therapies targeting the RPE layer have been documented for numerous eye diseases in humans (48). Also, many canine eye diseases are

associated with RPE degeneration, such as Retinal Pigment Epithelial Dystrophy (49) and Stationary retinal disorders (50), making dogs an important intermediate model to study the role of RPE in eye diseases. So far, many therapeutic strategies have been proposed to prevent disease progression, including transplantation of the RPE layer and improvement of RPE functionality, probably, the latter is one of the most promising treatments for early phases of RPE-related diseases.

Anti-apoptosis and anti-inflammatory role of Hsp70 in RPE

Due to its special location and functions, RPE cells fight off environmental insults every day, they consume high levels of oxygen, accumulate lipid peroxidation by ingesting photoreceptor outer segments, and are exposed to light stimuli for a long time. Thus, RPE cells are exposed continuously to oxidative stress (51, 52). Excessive reactive oxygen species resulting from oxidative stresses are a major risk factor for RPE apoptosis. Previous studies have shown that oxidant-induced RPE cell loss is associated with both caspase-dependent and independent pathways. Activation of caspase-8 and caspase-3 was observed in RPE cells, under oxidative stress and TNF- α stimulation respectively (53, 54). The activation of Bcl-2 family proteins followed by Bax subfamily activation activated the intrinsic (or mitochondrial) apoptotic pathway, which results in activation of the caspase cascade. A study performed by Y. Liang et al. shows that Bcl-2, Bax, and c-Fos expression contribute to RPE cell apoptosis following UV-light exposure (55). Also, a release of apoptosis-inducing factor (AIF) and Bax translocation into mitochondria were detected when RPE cells were exposed to appropriate doses of H₂O₂ (56). Hsp70 functions as a crucial regulator of the apoptotic pathway, by inhibiting the release of pro-apoptosis factors, such as Bcl-2 family proteins and Apaf-1 (24). There is considerable evidence suggesting that Hsp70-mediated regulation involves both pre- and post-mitochondrial steps. At pre-mitochondrial level, Hsp70 interferes with upstream signaling in the apoptotic pathway. Hsp70 can directly bind and inhibit Akt and c-Jun N-terminal Kinase (JNK1), which have a critical role in the regulation of apoptosis (57). At the mitochondrial level, Hsp70 suppresses the translocation of Bax into mitochondrial membrane and the release of cytochrome c (58). At the post-mitochondrial level, Hsp70 suppresses the activation of pro-apoptotic factors, such as Apaf-1, Bid and Bax, blocking the formation of the apoptosome, which prevents apoptosis. In RPE cells, this anti-apoptotic role of Hsp70 is also observed. Accumulated Hsp70 attenuates RPE cell apoptosis, induced by the activation of caspase-3, which suggests an association between Hsp70 and caspase-3 (59). Kayama, Maki, et al. demonstrated that increased Hsp70 significantly prevents photoreceptor apoptosis by inhibiting the activation of PI3K-Akt pathway (60). However, Hsp70 can also prevent apoptosis without caspase activation, suggesting caspase-independent pathways (61). The formation of apoptosome, cytochrome

c/Apaf-1/caspase, is the key feature of apoptosis. Studies show that over-expression of Hsp70 can prevent apoptosis in Apaf-1^{-/-} mouse embryo fibroblasts induced by serum-deprivation (62). In RPE cells, oxidant-induced cell death led to the release of cytochrome c, but no caspase 9 and 3 cleavage was observed, indicating the existence of caspase-independent signals (63). Due to the anti-apoptotic and cyto-protective characteristics of Hsp70, induction of Hsp70 production might be an alternative approach to block RPE death.

Hsp70 has also been shown to have a neuroprotective and anti-inflammatory role by preventing detrimental pro-inflammatory responses in eye diseases, such as AMD, glaucoma, and RP. Those diseases are strongly linked to death and dysfunction of RPE cells resulting from exposure to oxidative stress. A crucial regulator in acute and chronic inflammation is nuclear factor kappa B (NF- κ B). A variety of factors can lead to the activation of NF- κ B, including oxidative stress and ischemia. Activated NF- κ B dissociates from its inhibitor I κ B and translocates into the nucleus of cells, to induce the transcription of pro-inflammatory cytokines such as TNF- α , IL-6 and IL-1 β . Increased levels of Hsp70 suppress IL-6 secretion by human RPE cells. A potential mechanism by which Hsp70 may inhibit cytokine production is by interfering with phosphorylation of NF- κ B at Ser536 and thereby with DNA binding (64). Similarly, another study demonstrated that the overexpression of Hsp70 not only reduces the secretion of pro-inflammatory cytokines like TNF- α , IL-6 and IL-1 β , but also promotes the expression of the anti-inflammatory cytokines IL-10 and TGF- β 1 (65). It is speculated that Hsp70 interacts with IKK, thereby preventing the phosphorylation of I κ B and NF- κ B translocation (66). In addition to inducing Hsp70 endogenously, exogenous delivery of recombinant human Hsp70 (rh Hsp70) to RPE cells was also reported to protect RPE against oxidative stress. Exogenous rhHsp70 could be taken up by ARPE-19 cells and ARPE-19 cells, pre-treated with rhHsp70, showed a reduced inflammation, higher cell viability and lower cytotoxicity (67).

Due to characteristics of Hsp70 upregulation in inflamed or injured tissues of the eye and its role in RPE cells, upregulation of Hsp70 expression has been postulated as a therapeutic strategy for eye diseases. In recent years, enhanced Hsp70 expression by non-damaging laser treatment has been introduced into the clinic, with the purpose to avoid detrimental effects for vision (68, 69). Studies in human and mouse showed that Hsp70 expression was highly induced by sublethal photothermal stimulation, which protected RPE cells from oxidative stress and avoided cellular damage of the neural retina (70-74). Selective photocoagulation by multiple short argon laser pulses was performed by Roeder et al. to investigate the healing response of the RPE in rabbits (75). Their study showed that 4 weeks after healing, the RPE was replaced by a single layer of hypertrophic RPE cells; the blood-retinal barrier was re-established and the inflammatory response in RPE was decreased.

Further studies showed that upregulated Hsp70 expression in the RPE may have contributed to the therapeutic effects of non-damaging laser treatment (76). Besides, low power laser irradiation also facilitated RPE proliferation and increased the production of growth factors such as TGF- β 1, EGF and insulin-like growth factor (77). However, the exact threshold of laser energy is hard to control. Over-dose of laser energy may cause damage of RPE cell and retina.

In recent years, the use of pharmacological inducers of HSP70 has, due to only minor side effects, been posited as a promising way to increase Hsp70 expression in RPE cells. Several compounds like celastrol, arimoclolomol, and geranylgeranylacetone have been shown to induce Hsp70 production by activating HSF-1 (64, 78, 79). But the efficiency of such compounds varies and the exact mechanism in treating eye diseases still needs to be validated. In this thesis a novel HSP (co-)inducing compound is proposed and tested in canine primary RPE cells. Induction mechanism of Hsp70 by this co-inducer was investigated.

Polarization and characterization of macrophages

Macrophages are present nearly in all organs and tissues, and are considered as a group of heterogeneous cells due to their high plasticity and functional diversity. Biological functions of macrophages can be significantly changed by different micro-environmental stimuli, which provide macrophages with diverse polarization signals and induce them to differentiate into different functional subsets, known as the classically activated macrophage (M1) and the alternatively activated macrophage (M2) (80). The physiological functions of each subset seem to be contrary, but these subsets work together to form a well-balanced network to regulate the immune response (81). M1 cells, regarded as a pro-inflammatory subtype, are polarized by TLR agonists (such as lipopolysaccharide) and cytokines such as IFN- γ or TNF- α in the presence of granulocyte macrophage stimulating colony factor (GM-CSF), serving as an effector in immune responses mediated by Th1 and Th17 cells (Figure 2). M1 phenotype macrophages secrete abundant amounts of pro-inflammatory cytokines like IL-6, IL-12, IL-23, IL-1 β and TNF- α , thereby displaying pro-inflammatory properties (82). The activation of M1 cells leads to the activation and production of iNOS and the release of reactive oxygen species (ROS), facilitates the metabolism of arginine, and eventually increases reactive oxide (NO) release, which exerts a cytotoxic function (83, 84). Moreover, M1 macrophages express higher levels of major histocompatibility complex class II (MHC II) and co-stimulatory molecules like CD80 and CD86, leading to the enhancement of their antigen presenting capacity. Furthermore, the expression of Fc receptors (CD32 and CD64), TLR2 or 4 and chemokines (CXCL5) in M1 macrophages contributes to an increased phagocytic activity and recruitment of lymphocytes (85). As a result, functionally, M1

macrophages facilitate the inflammatory response and foster a highly microbicidal and tumoricidal environment, having a strong ability to combat pathogens and cancer cells.

In contrast, M2 macrophages have anti-inflammatory properties and are functionally involved in parasite clearance, wound repair, tissue remodeling, allergy associated responses and tumor progression. The polarization state of M2 cells is associated with Th2 responses, so M2 differentiation can be induced by the Th2 cytokines IL-4, IL-10, IL-13, as well as by other stimuli, such as glucocorticoids, immunoglobulin complexes and Toll-like receptor (TLR) ligands (86). M2 cells in the presence of macrophage colony stimulating factor (M-CSF) can be shaped into different subpopulations defined as M2a, M2b and M2c macrophages in response to diverse micro-environmental factors (Figure 2). In vitro, the M2a subtype is induced by exposure to IL-4 and/or IL-13, which both decrease the expression of pro-inflammatory cytokines such as IFN- γ , TNF- α , IL-6, and IL-1 β (86). Activated M2a cells produce a series of chemokines like CCL22 (in mice) and CCL17 (in human), which promote the recruitment of Th2 cells, basophils, and eosinophils (87). They also express a higher level of IL-10, TGF- β and IL-1ra, which enhances the Th2 response and regulates Th2-type allergic immune activation. M2a macrophages can be characterized by an increase of surface markers, such as CD163, CD86 and CD206 in human and arg-1 in mouse (88). Besides, M2a also participate in fibrogenesis, tissue repair by producing extracellular matrix (ECM) protein. M2b macrophages, also known as regulatory macrophages or type II macrophages, can be polarized by treatment with the combination of immune complex and TLR agonists or IL-1R agonists. By chemokine production (CCL1 in mice) M2b cells recruit eosinophils and regulatory T cells (Tregs), promoting Th2 response (87). Although M2b cells exert an anti-inflammatory role by secreting IL-10, the pro-inflammatory cytokines IL-6, TNF- α , and IL-1 β as well as iNOS also can be found in M2b cells (89). M2b cells are characterized by relatively high levels of CD14 and CD80 in human (90). Through the secretion of those cytokines, chemokines, and other regulatory factors, M2b cells modulate the inflammatory reaction and the immune response. When exposed to glucocorticoids, IL-10, or TGF- β , macrophages polarize to the M2c phenotype. M2c cells, also named deactivated macrophages, are characterized by increased expression of CD163, CD206 and Mer receptor tyrosine kinase (MerTK) (91). M2c also produce a high level of IL-10 and TGF- β , both of which are anti-inflammatory cytokines that contribute to the development of Tregs and Th2 cells. This function is further enhanced by the expression of CCL18 and CCL16 by M2c cells (8). Metalloproteinases (MMPs) like MMP-9 are also activated in M2c cells, which are engaged in extracellular matrix (ECM) remodeling (89). Furthermore, increased arginase-1 expression is found in M2c cells. In addition, some studies showed that M2c cells secrete a higher level of placental growth factor

(PGF), which is involved in M2c induced angiogenesis. As can be deduced from this profile, M2c cells exert their functions to promote tissue repair, angiogenesis, and resolution of inflammation; they suppress T cell proliferation, and restore homeostasis (92-94). The three subtypes of M2 (M2a, M2b and M2c) cells can shift among each other (95). They share certain features like IL-10 production, suppression of the immune response, and down-regulation of costimulatory molecules (CD40, CD80/86).

Recently, a further M2 subtype, named M2d macrophage, was found (Figure 2). This type is induced by the treatment of IL-6 and adenosine (89, 96). Because they are very common in tumoral tissues, they are also known as tumor associated macrophages (TAMs). M2d cells display similar functions as other types of M2 cells, they show an increased expression of IL-10 and TGF- β , and decrease in expression of IL-12 and TNF- α (96). Besides, the expression of vascular endothelial growth factor (VEGF) is also increased, but no increased CD206 and dectin-1 expression has been observed (88). M2d cells are believed to be associated with angiogenesis and tumor metastasis (97). In addition, several other phenotypes of macrophage have been described, such as Mhem, M4 and Mox. They are believed to be involved in certain diseases, for example, M4 cells induced by the C-X-C motif chemokine ligand (CXCL4) stimulation, serve as athero-protective cells in atherosclerosis (8).

Based on the above, characterization of macrophages *in vitro* roughly includes four aspects, namely, morphological changes, surface marker expression, cytokine expression, and functional activity. Morphologically, monocyte or bone marrow-derived M1 macrophages of human and mice acquire a typical round-shaped morphology and display a fried egg-like shape under light microscope, while M2 macrophages display an elongated, spindle-like morphology (98). Phenotypically, the surface marker profiles of M1 macrophages in murine and human includes the MHC II, co-stimulatory molecules CD80 and CD86, Fc γ receptors CD64 (Fc γ R I), CD32 (Fc γ R II) and CD16 (Fc γ RIII). Moreover, signaling molecules, intracellular protein suppressor of cytokine signaling 3 (SOCS3), STAT1 and IRF5 have been shown to be upregulated in M1 cells, as well as iNOS, to promote NO production from L-arginase (99, 100). Besides, M1 macrophages have also been shown to upregulate TLR2 and 4, and IL-1R expression (99). On the other hand, M2 macrophages are characterized by an increased expression of arginase 1 (Arg1), CD209, the mannose receptor CD206, the scavenger receptors CD163 and CD204, Fc ϵ receptor II CD23, Fizz1 and Ym1 (85, 101). More specifically, M2a macrophages express high arg-1, CD206, Fizz1 and Ym1 (102). The M2b subtype shows an increased expression of CD86 and MHC II (103). The M2c polarization state is accompanied by increased expression of CD206, CD163 and arg-1 (104). M2d cells can be distinguished by high production of VEGF. In addition, transcription factors,

like PPAR γ , PPAR δ STAT6, IRF4, HIF-2 α , and JMJD3 have been shown to be associated with M2 polarity (99, 102). According to secretion profiles of M1 and M2 cells, pro-inflammatory cytokines and chemokines, such as IL-6, IL-12, TNF- α , IL-1 β , CXCL9 and CXCL10, are used to characterize M1 cells *in vitro*, while M2 cells are identified by expression of anti-inflammatory cytokines IL-10 and TGF- β (102, 105). Furthermore, functionally nitric oxide (NO) production and phagocytosis also reflect macrophage polarization states. However, the regulation of NO production and phagocytosis is complex, which may be associated with corresponding surface molecules expression, activation of signaling pathway and different macrophage activities.

In vitro culture of macrophages

Macrophages from different sources display various functionalities in immune responses. Thus, it is important to investigate the phenotype and functionality of macrophages from different organs or tissues individually. However, primary tissue macrophages are difficult to isolate and proliferate *in vitro*, therefore they can not be used for functional analysis. Analysis of macrophage cultures *in vitro* for phenotypic and function is an attractive alternative. To date, *in vitro* cultures of macrophages from different sources such as bone marrow, peripheral blood mononuclear cells, peritoneum and spleen have been studied (106). Bone marrow is a common source of macrophages, which can polarize to M1 and M2 phenotype in the presence of GM-CSF and M-CSF respectively. Bone marrow-derived macrophages have notable advantages such as homogeneity and proliferation capacity. Mouse peritoneal macrophages are one of the best-studied tissue resident macrophages (107). Peritoneal macrophages play crucial roles in controlling inflammatory and immune response. Splenic macrophages are mainly situated in the red pulp, and have a strong antigen-presentation capability. Monocyte-derived macrophages are a useful and widely used tool to study macrophages, due to their ability to give rise to different subsets of tissue macrophages in specific micro-environments. *In vitro*, monocytes can be differentiated into multiple phenotypes such as M1, M2a, M2b and M2c by different stimuli. Monocytes also can be passaged *in vitro* and have a good experimental reproducibility. In addition, considering the animal welfare issues, collecting blood monocytes is less invasive to animals. Above all, monocyte-derived macrophages are an ideal model for macrophage studies in animals including dog.

In contrast to primary macrophages, a monocyte-like cell line is another alternative for *in vitro* study. Monocyte-like cell lines from mouse, human and canine are generally originated from cancerous cells, which have similar genotypes and phenotypes as primary macrophages (108-110). Moreover, special characteristics of cell line, like unlimited proliferation, high homogeneity, and cost effective, make

them a powerful in vitro tool to study mechanisms, cellular functions, signaling pathways and drug transport. Importantly, most of monocyte-like cell lines have the potential to be differentiated into different macrophage-like states, such as M1 and M2 cells (111, 112). Thus, they are widely used in studies to immune response. In addition, polarization states of macrophages are determined by a complex regulatory network, including signaling molecules, regulators of inflammation, transcription factors, epigenetic mechanisms, and microRNAs. By modifying relative genes on monocyte-like cell line during polarization, polarization pathways can be investigated and understood better (113). However, the information on both canine monocyte- and monocyte-like cell line-derived macrophages is considerably lacking. Hence, in this thesis canine monocyte- and O30D-derived (canine monocyte-like cell line) macrophages will be investigated.

The role of Hsp70 in macrophages

In addition to the functions of chaperoning, anti-apoptosis and maintenance of protein homeostasis, a large number of studies have demonstrated that Hsp70 has a critical anti-inflammatory role, regulating immune responses and regulating signaling pathways (114-116). Studies show that macrophages express Hsp70 when exposed to stress stimuli like hyperthermia, oxygen free radicals and cytokines (117-119). Moreover, increased intracellular Hsp70 in macrophages has been found to inhibit cytokine production, suggesting the anti-inflammatory role of Hsp70. Previous studies have shown that heat-induction or overexpression of Hsp70 decreases LPS-induced pro-inflammatory cytokine TNF- α and IL-1 β production in both human and murine macrophages (120, 121). It is well known that the NF- κ B signaling pathway has a crucial role in the regulation both acute and chronic inflammation. Its activation and translocation promote cytokine production. Studies on the anti-inflammatory mechanism of Hsp70 show that intracellular Hsp70 may bind with TRAF6, an upstream molecule of NF- κ B, to inhibit the activation of NF- κ B, and suppressing inflammatory cytokines production (122). Furthermore, high mobility group box1 (HMGB1) secreted by activated monocytes and macrophages can activate NF- κ B through the HMGB1-TLR2/4-NF- κ B pathway. It has been reported that increased Hsp70 in macrophages suppresses the release of TNF- α and LPS induced HMGB1, thereby inhibiting NF- κ B activation and pro-inflammatory cytokine production such as that of TNF- α , IL-6 and IL-1 β (117, 123). Another study showed that febrile-range temperatures decreased LPS-induced recruitment of NF- κ B p65 to the TNF-promoter but increased its recruitment to the IL-1 β promoter (124). When human primary monocytes and murine macrophages were exposed to alcohol, the cellular stress protein HSF1 was induced and activated, which further promoted the induction of Hsp70. Upregulated Hsp70 inhibits the TLR4/MyD88/NF- κ B pathway, to

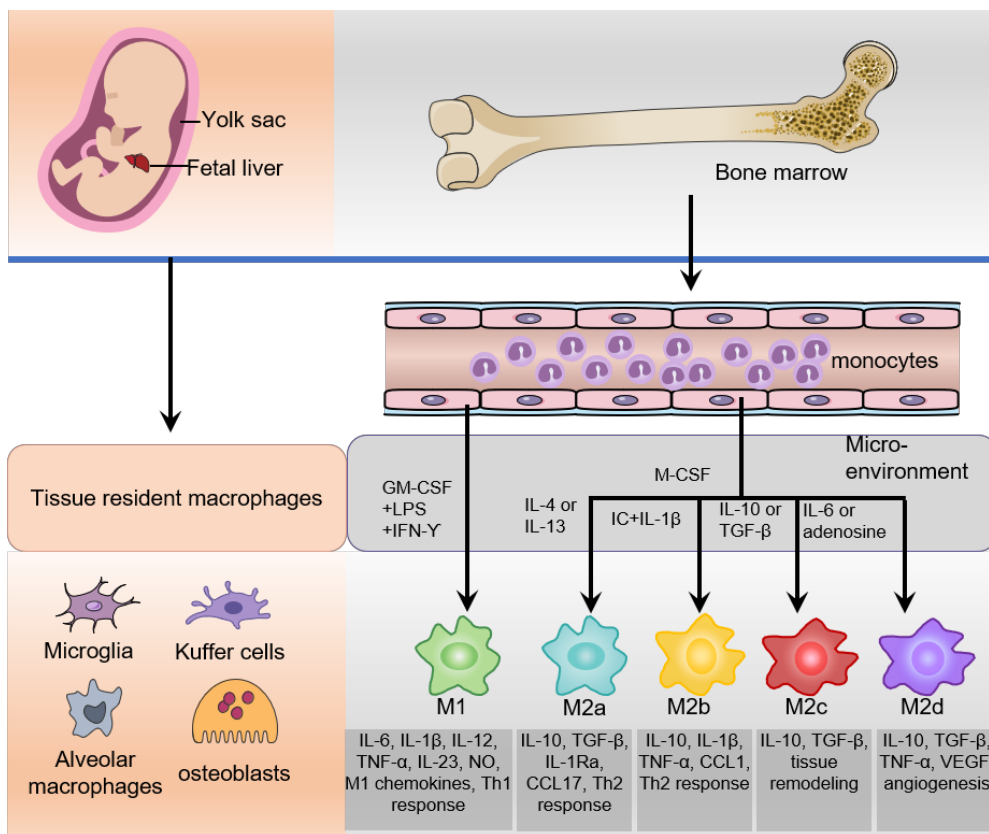


Figure 2 The origin and polarization of macrophages. Tissue macrophages such as microglia, Kupffer cells, alveolar macrophages, and osteoblasts, have two main origins, which are the yolk sac and fetal liver. In adults, the main source of macrophages are the bone marrow and blood monocyte intermediates. M1 macrophages are activated by LPS and IFN- γ in the presence of GM-CSF, associated with the pro-inflammatory response and Th1 response. In the presence of M-CSF, M2 cells can be differentiated into four subsets, M2a, M2b, M2c and M2d, which are related to Th2 response. M2a are induced by IL-4 or IL-13, which produce IL-10, TGF- β and IL-1Ra. M2b are induced by IC and IL-1 β and secrete IL-10, IL-1 β and TNF- α . M2c are activated by IL-10 or TGF- β and contribute to tissue remodeling. M2d are activated by IL-6 or adenosine, which is associated with angiogenesis. TGF- β : Transforming growth factor beta, GM-CSF: Granulocyte-Macrophage Colony-Stimulating Factor, M-CSF: Macrophage Colony-Stimulating Factor, TNF: Tumor Necrosis Factor, IL: Interleukin, VEGF: Vascular Endothelial Growth Factor, IC: immune complexes, CCL: C-C Motif Chemokine Ligand.

reduce TNF- α , IL-6 and IL-1 β production (125). In addition, the overexpression of Hsp70 in murine Bone Marrow-Derived Macrophages (BMDMs) reduces caspase-1 activation and IL-1 β production under NOD-leucine rich repeat and pyrin containing protein 3 (NLRP3) activator treatment, while Hsp70 deficiency increases caspase-1 activation and IL-1 β production under the same conditions, suggesting an inhibitory effect of Hsp70 on the NLRP3 inflammasome (28). Above evidence indicates that Hsp70 upregulation in macrophages has a significant anti-inflammatory effect and might be an alternative approach to treat inflammatory diseases.

At the individual level, induction of endogenous Hsp70 by raising the body temperature enhances the resistance of rats to the lethal activity of LPS (126). Further studies showed that upregulated Hsp70 also reduced LPS-induced cytokine TNF in serum of heat-conditioned rats, while the blockade of HSP accumulation led to an increase in serum levels of LPS induced cytokines (127, 128). Hsp70 overexpression decreased the level of TNF- α and IL-6 in the serum of LPS treated rats (129). Meanwhile, overexpressed Hsp70 also inhibited I κ B degradation and NF- κ B translocation. Besides, Hsp70 also reduced the mortality rate in a sepsis induced acute lung injury model (130). Taken together, these data suggest that the anti-inflammatory effect of Hsp70 in animals may be associated with its role at a cellular level (macrophage) to some extent.

Furthermore, Hsp70 release by stressed macrophages or dying cells serves as a danger signal to alert the immune system (131). In some chronic inflammatory diseases like rheumatoid arthritis, extracellular Hsp70 can prevent tissue from inflammatory damage by producing the anti-inflammatory cytokine IL-10 (132). Datanico et al. demonstrated that PBMCs from both RA patients and healthy controls produce IL-10 48h after treatment with Hsp70 (133). In addition, Hsp70 and 90 are able to combine with LPS and take part in innate recognition (134, 135). Further studies show that Hsp70 and 90 function as transfer molecule that delivers LPS to TLR4/MD2 complex, and then helps targeting this complex to the Golgi apparatus (136). These results indicate that regulation of the inflammatory responses by extracellular Hsp70 is a complex process, so more research is needed.

Besides the anti- and pro-inflammatory effects discussed above, also other functions of macrophages have been proposed to be regulated by Hsp70, including macrophages activation and maturation, phagocytosis, and antigen presentation. Hsp70 is reported as a potent activator of macrophages (137). After stress, Hsp70 is synthesized and anchored in the plasma membrane of cells. Afterwards, Hsp70 is released in exosomes, which serve as an effective danger signal to activate macrophages (138). Hsp70 also changes the morphological state of macrophages. Macrophages treated with Hsp70 display more surface ruffles and lamellipodia

enhancing the ability of adhesion to endothelial cells and antigen uptake (139). Furthermore, Hsp70 shifts tumor associated macrophages from the M2 phenotype to the M1 phenotype, helping tumor elimination (139). Extracellular Hsp70 is shown to interact with receptor molecules on the surfaces of cells such as monocytes, macrophages, and DC, and activate the related signaling pathways, finally to modulate the activation and maturation of macrophages and DC. It has been shown that Hsp70 is able to modulate cytokine secretion like that of IL-10 and IL-6, by activating MAPK, STAT3 and ERK signaling (12). These actions will further affect the maturation of immune cells. Studies in murine models show that LPS-free Hsp70 inhibits BMDCs maturation by decreasing MHC II and CD86 expression (140), while Hsp70 combined with high doses of endotoxin promotes the maturation of monocyte-derived DCs (141).

Phagocytosis is a protective cellular function of macrophages in response to microbial invasion. With regard to the phagocytic capacity of macrophages, exogenous Hsp70 without endotoxin increases the rate and capacity of phagocytosis of invaders such as bacteria and fungi, and further enhances the processing and presentation of antigens by MHC II (142). A study of the underlying cellular mechanisms shows that Hsp70 binds lipid rafts on the surface of macrophages and interacts with lipid raft-associated TLR7, to subsequently activate the p38 MAPK and PI3K pathways (143). The activation of these pathways can induce the expression of scavenger receptors by macrophages leading to enhanced phagocytic capacity.

Taken together, Hsp70 has broad biological functions. It is expressed in almost all eukaryotic cells including RPE cells and macrophages. Hsp70 is involved in many cellular processes which constitute a fine-tuned and complex regulatory network. Hsp70 plays a crucial role in inflammatory and immune responses, therefore it is proposed as a promising therapeutic target to cure many diseases. However, most of researches focus on mice and human, studies on other animals like dog is relatively behind. Thus, in our study, we investigated the role of Hsp70 on RPE cells and macrophages. Such studies will allow us to understand more the use of Hsp70 as a therapeutic target in inflammatory diseases and immune diseases in other species.

Scope of this thesis

In this thesis, we explored a new Hsp70 co-inducer on canine RPE cells and the role of Hsp70 on canine macrophages. Furthermore, we characterized both canine monocyte- and 030D-derived macrophages.

In the **first chapter**, we introduced the background for the studies in this thesis and summarized the latest research progress on Hsp70, RPE cells and macrophages in canine, humans, and mice. Subsequently, we pointed out the significance of our study.

In **chapter 2**, we reviewed potential mechanisms of T-cell driven autoimmune diseases including rheumatoid arthritis (RA), type 1 diabetes (T1D), and several eye diseases. We pointed out that the establishment of therapeutic tolerance in the inflamed tissues may inhibit or skew pro-inflammatory self-antigen-specific T cells, thereby curing autoimmune diseases with less side effects. Then we systematically elaborated on whether HSPs or HSP-based peptides could induce therapeutic tolerance in T Cell-mediated autoimmune diseases through the induction of regulatory T cells, which also provided clues for our follow-up research on eye diseases.

In **chapter 3**, we reported a modified protocol to isolate and characterize canine RPE cells. We identified leucinostatin as a novel HSP co-inducer and explored its Hsp70 enhancing effects in arsenite-stressed RPE cells. Our results indicated that leucinostatin, as a co-inducer, could enhance Hsp70 expression in canine RPE cells, most likely by activating heat shock factor-1.

In **chapter 4**, the anti-inflammatory role of Hsp70 and its underlying mechanisms was determined on both wild-type and Hsp70 knockout macrophages. Our data indicated that Hsp70 upregulation by cell stress can suppress the LPS-induced inflammatory response in canine macrophages by downregulating NF- κ B nuclear translocation and subsequent pro-inflammatory cytokine expression.

In **chapter 5**, we first polarized blood-derived canine monocytes into macrophages with M1 and M2 phenotype *in vitro*. Then, we described a comprehensive morphological, phenotypical, transcriptional, functional characterization of canine monocyte-derived M1 and M2 macrophages. Our results showed that polarized M1 and M2 macrophages from canine monocytes displayed distinct characteristics and functions.

Next, in **chapter 6**, we evaluated the differentiation potentials of a canine monocyte-

Chapter 1

like cell line, 030D cell, to generate macrophages with M0, M1 and M2 phenotype. We showed that 030D-derived M1 and M2 macrophages showed many similarities to M1 and M2 macrophages derived from other species.

Finally, in **chapter 7**, all findings in this thesis as well as future perspective and applications are discussed.

Reference

1. Wang C-H, Chou P-C, Chung F-T, Lin H-C, Huang K-H, Kuo H-P. Heat shock protein70 is implicated in modulating NF-κB activation in alveolar macrophages of patients with active pulmonary tuberculosis. *Scientific reports* (2017) 7(1):1-9.
2. Chen H, Tian A, Wu Y, Li R, Han R, Xu X, et al. HSP70 expression before and after treatment and its clinical value in patients with acute angle-closure glaucoma. *Exp Ther Med* (2021) 21(3):253. Epub 2021/02/20. doi: 10.3892/etm.2021.9683.
3. Salvermoser L, Dressel S, Schleißheimer S, Stangl S, Diederichs C, Wergin M, et al. 7Hsp70 serum levels in pet dogs-a potential diagnostic biomarker for spontaneous round cell tumors. *Cell Stress Chaperones* (2019) 24(5):969-78. Epub 2019/08/04. doi: 10.1007/s12192-019-01024-9.
4. Heller JP, Martin KR. Enhancing RPE Cell-Based Therapy Outcomes for AMD: The Role of Bruch's Membrane. *Transl Vis Sci Technol* (2014) 3(3):11. Epub 2014/07/30. doi: 10.1167/tvst.3.3.11.
5. Konda BR, Pararajasegaram G, Wu GS, Stanforth D, Rao NA. Role of retinal pigment epithelium in the development of experimental autoimmune uveitis. *Invest Ophthalmol Vis Sci* (1994) 35(1):40-7. Epub 1994/01/01.
6. Kern K, Mertineit CL, Brinkmann R, Miura Y. Expression of heat shock protein 70 and cell death kinetics after different thermal impacts on cultured retinal pigment epithelial cells. *Exp Eye Res* (2018) 170:117-26. Epub 2018/02/20. doi: 10.1016/j.exer.2018.02.013.
7. Zheng Z, Kim JY, Ma H, Lee JE, Yenari MA. Anti-inflammatory effects of the 70 kDa heat shock protein in experimental stroke. *Journal of Cerebral Blood Flow & Metabolism* (2008) 28(1):53-63.
8. Atri C, Guerfali FZ, Laouini D. Role of Human Macrophage Polarization in Inflammation during Infectious Diseases. *Int J Mol Sci* (2018) 19(6). Epub 2018/06/21. doi: 10.3390/ijms19061801.
9. Oshi M, Tokumaru Y, Asaoka M, Yan L, Satyananda V, Matsuyama R, et al. M1 Macrophage and M1/M2 ratio defined by transcriptomic signatures resemble only part of their conventional clinical characteristics in breast cancer. *Sci Rep* (2020) 10(1):16554. Epub 2020/10/08. doi: 10.1038/s41598-020-73624-w.
10. Ritossa F. A new puffing pattern induced by temperature shock and DNP in *Drosophila*. *Experientia* (1962) 18(12):571-3.
11. Tissieres A, Mitchell HK, Tracy UM. Protein synthesis in salivary glands of *Drosophila melanogaster*: relation to chromosome puffs. *J Mol Biol* (1974) 84(3):389-98. Epub 1974/04/15. doi: 10.1016/0022-2836(74)90447-1.
12. Borges TJ, Wieten L, van Herwijnen MJ, Broere F, van der Zee R, Bonorino C, et al. The anti-inflammatory mechanisms of Hsp70. *Front Immunol* (2012) 3:95. Epub 2012/05/09. doi: 10.3389/fimmu.2012.00095.
13. Shinozaki K, Yamaguchi-Shinozaki K. *Molecular responses to cold, drought, heat and salt stress in higher plants*: RG Landes Company Austin, TX (1999).
14. Kampinga HH, Hageman J, Vos MJ, Kubota H, Tanguay RM, Bruford EA, et al. Guidelines for the nomenclature of the human heat shock proteins. *Cell*

- Stress Chaperones* (2009) 14(1):105-11. Epub 2008/07/30. doi: 10.1007/s12192-008-0068-7.
15. Daugaard M, Rohde M, Jaattela M. The heat shock protein 70 family: Highly homologous proteins with overlapping and distinct functions. *FEBS Lett* (2007) 581(19):3702-10. Epub 2007/06/05. doi: 10.1016/j.febslet.2007.05.039.
 16. Frydman J. Folding of newly translated proteins in vivo: the role of molecular chaperones. *Annu Rev Biochem* (2001) 70(1):603-47. Epub 2001/06/08. doi: 10.1146/annurev.biochem.70.1.603.
 17. Zhuravleva A, Gierasch LM. Allosteric signal transmission in the nucleotide-binding domain of 70-kDa heat shock protein (Hsp70) molecular chaperones. *Proc Natl Acad Sci U S A* (2011) 108(17):6987-92. Epub 2011/04/13. doi: 10.1073/pnas.1014448108.
 18. Mayer MP, Bukau B. Hsp70 chaperones: cellular functions and molecular mechanism. *Cell Mol Life Sci* (2005) 62(6):670-84. Epub 2005/03/17. doi: 10.1007/s00018-004-4464-6.
 19. Rüdiger S, Germeroth L, Schneider Mergener J, Bukau B. Substrate specificity of the DnaK chaperone determined by screening cellulose-bound peptide libraries. *The EMBO journal* (1997) 16(7):1501-7.
 20. Srinivasan SR, Gillies AT, Chang L, Thompson AD, Gestwicki JE. Molecular chaperones DnaK and DnaJ share predicted binding sites on most proteins in the E. coli proteome. *Molecular BioSystems* (2012) 8(9):2323-33.
 21. Stein KC, Kriel A, Frydman J. Nascent polypeptide domain topology and elongation rate direct the cotranslational hierarchy of Hsp70 and TRiC/CCT. *Molecular cell* (2019) 75(6):1117-30. e5.
 22. Bukau B, Deuerling E, Pfund C, Craig EA. Getting newly synthesized proteins into shape. *Cell* (2000) 101(2):119-22. doi: Doi 10.1016/S0092-8674(00)80806-5.
 23. Hartl FU, Bracher A, Hayer-Hartl M. Molecular chaperones in protein folding and proteostasis. *Nature* (2011) 475(7356):324-32. Epub 2011/07/22. doi: 10.1038/nature10317.
 24. Ikwegbue PC, Masamba P, Oyinloye BE, Kappo AP. Roles of Heat Shock Proteins in Apoptosis, Oxidative Stress, Human Inflammatory Diseases, and Cancer. *Pharmaceuticals* (2018) 11(1):2. doi: 10.3390/ph11010002.
 25. Fontaine SN, Martin MD, Dickey CA. Neurodegeneration and the Heat Shock Protein 70 Machinery: Implications for Therapeutic Development. *Curr Top Med Chem* (2016) 16(25):2741-52. Epub 2016/04/14. doi: 10.2174/1568026616666160413140741.
 26. Murphy ME. The HSP70 family and cancer. *Carcinogenesis* (2013) 34(6):1181-8. Epub 2013/04/09. doi: 10.1093/carcin/bgt111.
 27. Sun Y, Zhang JR, Chen S. Suppression of Alzheimer's disease-related phenotypes by the heat shock protein 70 inducer, geranylgeranylacetone, in APP/PS1 transgenic mice via the ERK/p38 MAPK signaling pathway. *Experimental and therapeutic medicine* (2017) 14(6):5267-74.
 28. Martine P, Chevriaux A, Derangere V, Apetoh L, Garrido C, Ghiringhelli F, et al. HSP70 is a negative regulator of NLRP3 inflammasome activation. *Cell Death & Disease* (2019) 10(4):1-11. doi: 10.1038/s41419-019-1491-7.
 29. Samborski P, Grzymislawski M. The Role of HSP70 Heat Shock Proteins in the Pathogenesis and Treatment of Inflammatory Bowel Diseases. *Adv Clin Exp Med* (2015) 24(3):525-30. Epub 2015/10/16. doi: 10.17219/acem/44144.

30. Wu C. Heat shock transcription factors: structure and regulation. *Annu Rev Cell Dev Biol* (1995) 11(1):441-69. Epub 1995/01/01. doi: 10.1146/annurev.cb.11.110195.002301.
31. Fernandes M. Structure and regulation of heat shock gene promoters. *The biology of heat shock proteins and molecular chaperones* (1994):375-93.
32. Akerfelt M, Trouillet D, Mezger V, Sistonen L. Heat shock factors at a crossroad between stress and development. *Ann N Y Acad Sci* (2007) 1113:15-27. Epub 2007/05/08. doi: 10.1196/annals.1391.005.
33. Xiao X, Zuo X, Davis AA, McMillan DR, Curry BB, Richardson JA, et al. HSF1 is required for extra - embryonic development, postnatal growth and protection during inflammatory responses in mice. *The EMBO journal* (1999) 18(21):5943-52.
34. Akerfelt M, Morimoto RI, Sistonen L. Heat shock factors: integrators of cell stress, development and lifespan. *Nat Rev Mol Cell Biol* (2010) 11(8):545-55. Epub 2010/07/16. doi: 10.1038/nrm2938.
35. Jin X, Eroglu B, Moskophidis D, Mivechi NF. Targeted Deletion of Hsf1, 2, and 4 Genes in Mice. *Methods Mol Biol* (2018) 1709:1-22. Epub 2017/11/28. doi: 10.1007/978-1-4939-7477-1_1.
36. Rabindran SK, Wisniewski J, Li LG, Li GC, Wu C. Interaction between Heat-Shock Factor and Hsp70 Is Insufficient to Suppress Induction of DNA-Binding Activity in-Vivo. *Molecular and Cellular Biology* (1994) 14(10):6552-60. doi: Doi 10.1128/Mcb.14.10.6552.
37. Zou JY, Guo YL, Guettouche T, Smith DF, Voellmy R. Repression of heat shock transcription factor HSF1 activation by HSP90 (HSP90 complex) that forms a stress-sensitive complex with HSF1. *Cell* (1998) 94(4):471-80. doi: Doi 10.1016/S0092-8674(00)81588-3.
38. Wieten L, van der Zee R, Goedemans R, Sijtsma J, Serafini M, Lubsen NH, et al. Hsp70 expression and induction as a readout for detection of immune modulatory components in food. *Cell Stress Chaperones* (2010) 15(1):25-37. Epub 2009/05/28. doi: 10.1007/s12192-009-0119-8.
39. Westerheide SD, Bosman JD, Mbadugha BNA, Kawahara TLA, Matsumoto G, Kim SJ, et al. Celastrols as inducers of the heat shock response and cytoprotection. *Journal of Biological Chemistry* (2004) 279(53):56053-60. doi: 10.1074/jbc.M409267200.
40. Ohtsuka K, Kawashima D, Gu Y, Saito K. Inducers and co-inducers of molecular chaperones. *Int J Hyperthermia* (2005) 21(8):703-11. Epub 2005/12/13. doi: 10.1080/02656730500384248.
41. Otaka M, Yamamoto S, Ogasawara K, Takaoka Y, Noguchi S, Miyazaki T, et al. The induction mechanism of the molecular chaperone HSP70 in the gastric mucosa by Geranylgeranylacetone (HSP-inducer). *Biochem Biophys Res Commun* (2007) 353(2):399-404. Epub 2006/12/22. doi: 10.1016/j.bbrc.2006.12.031.
42. Hehir MP, Morrison JJ. Paeoniflorin, a novel heat-shock protein inducing compound, and human myometrial contractility in vitro. *J Obstet Gynaecol Res* (2016) 42(3):302-6. Epub 2015/12/09. doi: 10.1111/jog.12895.
43. Ross M, Kaye G, Pawlina III W. Digestive System III: Liver, Gallbladder, and Pancreas'. *Histology a text and atlas, 4th edition Philadelphia, PA: Lippincott Williams & Wilkins* (2003):532-67.

44. Streilein JW, Ma N, Wenkel H, Ng TF, Zamiri P. Immunobiology and privilege of neuronal retina and pigment epithelium transplants. *Vision Res* (2002) 42(4):487-95. Epub 2002/02/21. doi: 10.1016/s0042-6989(01)00185-7.
45. Cunha-Vaz J, Bernardes R, Lobo C. Blood-retinal barrier. *Eur J Ophthalmol* (2011) 21 Suppl 6(6_suppl):S3-9. Epub 2011/01/01. doi: 10.5301/EJO.2010.6049.
46. Chuang JZ, Chou SY, Sung CH. Chloride Intracellular Channel 4 Is Critical for the Epithelial Morphogenesis of RPE Cells and Retinal Attachment. *Molecular Biology of the Cell* (2010) 21(17):3017-28. doi: 10.1091/mbc.E09-10-0907.
47. van Soest S, Westerveld A, de Jong PT, Bleeker-Wagemakers EM, Bergen AA. Retinitis pigmentosa: defined from a molecular point of view. *Surv Ophthalmol* (1999) 43(4):321-34. Epub 1999/02/20. doi: 10.1016/s0039-6257(98)00046-0.
48. Hughes B, Gallemore R, Miller S. Transport mechanisms in the retinal pigment epithelium. *The retinal pigment epithelium* (1998):103-34.
49. Palanova A. The genetics of inherited retinal disorders in dogs: implications for diagnosis and management. *Vet Med (Auckl)* (2016) 7:41-51. Epub 2016/03/15. doi: 10.2147/VMRR.S63537.
50. Mellersh CS. The genetics of eye disorders in the dog. *Canine Genet Epidemiol* (2014) 1(1):3. Epub 2014/01/01. doi: 10.1186/2052-6687-1-3.
51. Beatty S, Koh H, Phil M, Henson D, Boulton M. The role of oxidative stress in the pathogenesis of age-related macular degeneration. *Surv Ophthalmol* (2000) 45(2):115-34. Epub 2000/10/18. doi: 10.1016/s0039-6257(00)00140-5.
52. Kaarniranta K, Sinha D, Blasiak J, Kauppinen A, Vereb Z, Salminen A, et al. Autophagy and heterophagy dysregulation leads to retinal pigment epithelium dysfunction and development of age-related macular degeneration. *Autophagy* (2013) 9(7):973-84. Epub 2013/04/18. doi: 10.4161/auto.24546.
53. Barak A, Morse LS, Goldkorn T. Ceramide: a potential mediator of apoptosis in human retinal pigment epithelial cells. *Invest Ophthalmol Vis Sci* (2001) 42(1):247-54. Epub 2001/01/03.
54. Yang P, Peairs JJ, Tano R, Zhang N, Tyrell J, Jaffe GJ. Caspase-8-mediated apoptosis in human RPE cells. *Invest Ophthalmol Vis Sci* (2007) 48(7):3341-9. Epub 2007/06/27. doi: 10.1167/iovs.06-1340.
55. Liang YG, Jorgensen AG, Kaestel CG, Wiencke AK, Lui GM, la Cour MH, et al. Bcl-2, Bax, and c-Fos expression correlates to RPE cell apoptosis induced by UV-light and daunorubicin. *Curr Eye Res* (2000) 20(1):25-34. Epub 1999/12/28.
56. Ho TC, Yang YC, Cheng HC, Wu AC, Chen SL, Chen HK, et al. Activation of mitogen-activated protein kinases is essential for hydrogen peroxide-induced apoptosis in retinal pigment epithelial cells. *Apoptosis* (2006) 11(11):1899-908. doi: 10.1007/s10495-006-9403-6.
57. Garrido C, Brunet M, Didelot C, Zermati Y, Schmitt E, Kroemer G. Heat shock proteins 27 and 70: anti-apoptotic proteins with tumorigenic properties. *Cell Cycle* (2006) 5(22):2592-601. Epub 2006/11/16. doi: 10.4161/cc.5.22.3448.
58. Stankiewicz AR, Lachapelle G, Foo CP, Radicioni SM, Mosser DD. Hsp70 inhibits heat-induced apoptosis upstream of mitochondria by preventing Bax translocation. *J Biol Chem* (2005) 280(46):38729-39. Epub 2005/09/21. doi: 10.1074/jbc.M509497200.

59. Kaarniranta K, Ryhanen T, Sironen RK, Suuronen T, Elo MA, Karjalainen HM, et al. Geldanamycin activates Hsp70 response and attenuates okadaic acid-induced cytotoxicity in human retinal pigment epithelial cells. *Brain Res Mol Brain Res* (2005) 137(1-2):126-31. Epub 2005/06/14. doi: 10.1016/j.molbrainres.2005.02.027.
60. Kayama M, Nakazawa T, Thanos A, Morizane Y, Murakami Y, Theodoropoulou S, et al. Heat Shock Protein 70 (HSP70) Is Critical for the Photoreceptor Stress Response after Retinal Detachment via Modulating Anti-Apoptotic Akt Kinase. *American Journal of Pathology* (2011) 178(3):1080-91. doi: 10.1016/j.ajpath.2010.11.072.
61. Creagh EM, Carmody RJ, Cotter TG. Heat shock protein 70 inhibits caspase-dependent and -independent apoptosis in Jurkat T cells. *Exp Cell Res* (2000) 257(1):58-66. Epub 2000/06/15. doi: 10.1006/excr.2000.4856.
62. Ravagnan L, Gurbuxani S, Susin SA, Maise C, Daugas E, Zamzami N, et al. Heat-shock protein 70 antagonizes apoptosis-inducing factor. *Nat Cell Biol* (2001) 3(9):839-43. Epub 2001/09/05. doi: 10.1038/ncb0901-839.
63. Zhang CX, Baffi J, Cousins SW, Csaky KG. Oxidant-induced cell death in retinal pigment epithelium cells mediated through the release of apoptosis-inducing factor. *Journal of Cell Science* (2003) 116(10):1915-23. doi: 10.1242/jcs.00390.
64. Paimela T, Hyttinen JM, Viiri J, Ryhanen T, Salminen A, Kaarniranta K. Celastrol Regulates Innate Immunity Response Via Nf-B And Hsp70 In Human Retinal Pigment Epithelial Cells. *Investigative Ophthalmology & Visual Science* (2011) 52(14):864-.
65. Yang HJ, Hu R, Sun H, Bo C, Li X, Chen JB. 4-HNE induces proinflammatory cytokines of human retinal pigment epithelial cells by promoting extracellular efflux of HSP70. *Exp Eye Res* (2019) 188:107792. Epub 2019/09/10. doi: 10.1016/j.exer.2019.107792.
66. Yenari MA, Liu J, Zheng Z, Vexler ZS, Lee JE, Giffard RG. Antiapoptotic and anti-inflammatory mechanisms of heat-shock protein protection. *Ann N Y Acad Sci* (2005) 1053(1):74-83. Epub 2005/09/24. doi: 10.1196/annals.1344.007.
67. Subrizi A, Toropainen E, Ramsay E, Airaksinen AJ, Kaarniranta K, Urtti A. Oxidative stress protection by exogenous delivery of rhHsp70 chaperone to the retinal pigment epithelium (RPE), a possible therapeutic strategy against RPE degeneration. *Pharm Res* (2015) 32(1):211-21. Epub 2014/07/18. doi: 10.1007/s11095-014-1456-6.
68. Lavinsky D, Wang J, Huie P, Dalal R, Lee SJ, Lee DY, et al. Nondamaging Retinal Laser Therapy: Rationale and Applications to the Macula. *Invest Ophthalmol Vis Sci* (2016) 57(6):2488-500. Epub 2016/05/10. doi: 10.1167/iovs.15-18981.
69. Brader HS, Young LH. Subthreshold Diode Micropulse Laser: A Review. *Semin Ophthalmol* (2016) 31(1-2):30-9. Epub 2016/03/10. doi: 10.3109/08820538.2015.1114837.
70. Inagaki K, Shuo T, Katakura K, Ebihara N, Murakami A, Ohkoshi K. Sublethal Photothermal Stimulation with a Micropulse Laser Induces Heat Shock Protein Expression in ARPE-19 Cells. *J Ophthalmol* (2015) 2015:729792. Epub 2015/12/24. doi: 10.1155/2015/729792.

71. Amirkavei M, Pitkänen M, Kaikkonen O, Kaarniranta K, André H, Koskelainen A. Induction of Heat Shock Protein 70 in Mouse RPE as an In Vivo Model of Transpupillary Thermal Stimulation. *Int J Mol Sci* (2020) 21(6). Epub 2020/03/21. doi: 10.3390/ijms21062063.
72. Iwami H, Pruessner J, Shiraki K, Brinkmann R, Miura Y. Protective effect of a laser-induced sub-lethal temperature rise on RPE cells from oxidative stress. *Exp Eye Res* (2014) 124:37-47. Epub 2014/05/08. doi: 10.1016/j.exer.2014.04.014.
73. Wang J, Quan Y, Dalal R, Palanker D. Comparison of Continuous-Wave and Micropulse Modulation in Retinal Laser Therapy. *Invest Ophthalmol Vis Sci* (2017) 58(11):4722-32. Epub 2017/09/15. doi: 10.1167/iovs.17-21610.
74. Du S, Zhang Q, Zhang S, Wang L, Lian J. Heat shock protein 70 expression induced by diode laser irradiation on choroid-retinal endothelial cells in vitro. *Mol Vis* (2012) 18:2380-7. Epub 2012/10/11.
75. Roider J, Michaud NA, Flotte TJ, Birngruber R. Response of the retinal pigment epithelium to selective photocoagulation. *Arch Ophthalmol* (1992) 110(12):1786-92. Epub 1992/12/01. doi: 10.1001/archophth.1992.01080240126045.
76. Wang J, Huie P, Dalal R, Lee S, Tan G, Lee D, et al., editors. Heat shock protein expression as guidance for the therapeutic window of retinal laser therapy. *Ophthalmic Technologies XXVI*; 2016: International Society for Optics and Photonics.
77. Song Q, Uygun B, Banerjee I, Nahmias Y, Zhang Q, Berthiaume F, et al. Low Power Laser Irradiation Stimulates the Proliferation of Adult Human Retinal Pigment Epithelial Cells in Culture. *Cell Mol Bioeng* (2009) 2(1):87-103. Epub 2009/03/01. doi: 10.1007/s12195-008-0041-7.
78. Fog CK, Zago P, Malini E, Solanko LM, Peruzzo P, Bornaes C, et al. The heat shock protein amplifier arimoclomol improves refolding, maturation and lysosomal activity of glucocerebrosidase. *EBioMedicine* (2018) 38:142-53. Epub 2018/12/01. doi: 10.1016/j.ebiom.2018.11.037.
79. Endo S, Hiramatsu N, Hayakawa K, Okamura M, Kasai A, Tagawa Y, et al. Geranylgeranylacetone, an inducer of the 70-kDa heat shock protein (HSP70), elicits unfolded protein response and coordinates cellular fate independently of HSP70. *Mol Pharmacol* (2007) 72(5):1337-48. Epub 2007/08/19. doi: 10.1124/mol.107.039164.
80. Gordon S, Taylor PR. Monocyte and macrophage heterogeneity. *Nat Rev Immunol* (2005) 5(12):953-64. Epub 2005/12/03. doi: 10.1038/nri1733.
81. Chamberlain CS, Leiferman EM, Frisch KE, Wang S, Yang X, van Rooijen N, et al. The influence of macrophage depletion on ligament healing. *Connect Tissue Res* (2011) 52(3):203-11. Epub 2010/12/02. doi: 10.3109/03008207.2010.511355.
82. Biswas SK, Mantovani A. Macrophage plasticity and interaction with lymphocyte subsets: cancer as a paradigm. *Nature Immunology* (2010) 11(10):889-96. doi: 10.1038/ni.1937.
83. Zimmerer JM, Liu XL, Blaszczyk A, Avila CL, Pham TA, Warren RT, et al. Critical Role of Macrophage FcγR Signaling and Reactive Oxygen Species in Alloantibody-Mediated Hepatocyte Rejection. *J Immunol* (2018) 201(12):3731-40. Epub 2018/11/07. doi: 10.4049/jimmunol.1800333.

84. Chawla A, Nguyen KD, Goh YP. Macrophage-mediated inflammation in metabolic disease. *Nat Rev Immunol* (2011) 11(11):738-49. Epub 2011/10/11. doi: 10.1038/nri3071.
85. Durafourt BA, Moore CS, Zammit DA, Johnson TA, Zaguia F, Guiot MC, et al. Comparison of polarization properties of human adult microglia and blood-derived macrophages. *Glia* (2012) 60(5):717-27. Epub 2012/02/01. doi: 10.1002/glia.22298.
86. Fraternali A, Brundu S, Magnani M. Polarization and repolarization of macrophages. *J Clin Cell Immunol* (2015) 6(319):2.
87. Murray PJ, Allen JE, Biswas SK, Fisher EA, Gilroy DW, Goerdt S, et al. Macrophage activation and polarization: nomenclature and experimental guidelines. *Immunity* (2014) 41(1):14-20. Epub 2014/07/19. doi: 10.1016/j.immuni.2014.06.008.
88. Ferrante CJ, Leibovich SJ. Regulation of Macrophage Polarization and Wound Healing. *Adv Wound Care (New Rochelle)* (2012) 1(1):10-6. Epub 2012/02/01. doi: 10.1089/wound.2011.0307.
89. Krzyszczyk P, Schloss R, Palmer A, Berthiaume F. The Role of Macrophages in Acute and Chronic Wound Healing and Interventions to Promote Pro-wound Healing Phenotypes. *Front Physiol* (2018) 9:419. Epub 2018/05/17. doi: 10.3389/fphys.2018.00419.
90. Iqbal S, Kumar A. Characterization of in vitro generated human polarized macrophages. *J Clin Cell Immunol* (2015) 6(380.10):4172.
91. Garash R, Bajpai A, Marcinkiewicz BM, Spiller KL. Drug delivery strategies to control macrophages for tissue repair and regeneration. *Exp Biol Med (Maywood)* (2016) 241(10):1054-63. Epub 2016/05/18. doi: 10.1177/1535370216649444.
92. Murray PJ, Wynn TA. Protective and pathogenic functions of macrophage subsets. *Nat Rev Immunol* (2011) 11(11):723-37. Epub 2011/10/15. doi: 10.1038/nri3073.
93. Lurier EB, Dalton D, Dampier W, Raman P, Nassiri S, Ferraro NM, et al. Transcriptome analysis of IL-10-stimulated (M2c) macrophages by next-generation sequencing. *Immunobiology* (2017) 222(7):847-56. Epub 2017/03/21. doi: 10.1016/j.imbio.2017.02.006.
94. Spiller KL, Wrona EA, Romero-Torres S, Pallotta I, Graney PL, Witherel CE, et al. Differential gene expression in human, murine, and cell line-derived macrophages upon polarization. *Experimental Cell Research* (2016) 347(1):1-13. doi: 10.1016/j.yexcr.2015.10.017.
95. Ogle ME, Segar CE, Sridhar S, Botchwey EA. Monocytes and macrophages in tissue repair: Implications for immunoregenerative biomaterial design. *Exp Biol Med (Maywood)* (2016) 241(10):1084-97. Epub 2016/05/28. doi: 10.1177/1535370216650293.
96. Wang Q, Ni H, Lan L, Wei X, Xiang R, Wang Y. Fra-1 protooncogene regulates IL-6 expression in macrophages and promotes the generation of M2d macrophages. *Cell Res* (2010) 20(6):701-12. Epub 2010/04/14. doi: 10.1038/cr.2010.52.
97. Sunakawa Y, Stintzing S, Cao S, Heinemann V, Cremolini C, Falcone A, et al. Variations in genes regulating tumor-associated macrophages (TAMs) to predict outcomes of bevacizumab-based treatment in patients with metastatic

- colorectal cancer: results from TRIBE and FIRE3 trials. *Ann Oncol* (2015) 26(12):2450-6. Epub 2015/09/30. doi: 10.1093/annonc/mdv474.
98. Gao J, Scheenstra MR, van Dijk A, Veldhuizen EJA, Haagsman HP. A new and efficient culture method for porcine bone marrow-derived M1- and M2-polarized macrophages. *Vet Immunol Immunopathol* (2018) 200:7-15. Epub 2018/05/20. doi: 10.1016/j.vetimm.2018.04.002.
 99. Sylvestre M, Crane CA, Pun SH. Progress on Modulating Tumor-Associated Macrophages with Biomaterials. *Adv Mater* (2020) 32(13):e1902007. Epub 2019/09/29. doi: 10.1002/adma.201902007.
 100. MacMicking J, Xie QW, Nathan C. Nitric oxide and macrophage function. *Annu Rev Immunol* (1997) 15(1):323-50. Epub 1997/01/01. doi: 10.1146/annurev.immunol.15.1.323.
 101. Martinez FO, Gordon S, Locati M, Mantovani A. Transcriptional profiling of the human monocyte-to-macrophage differentiation and polarization: new molecules and patterns of gene expression. *J Immunol* (2006) 177(10):7303-11. Epub 2006/11/04. doi: 10.4049/jimmunol.177.10.7303.
 102. Yao Y, Xu XH, Jin L. Macrophage Polarization in Physiological and Pathological Pregnancy. *Front Immunol* (2019) 10:792. Epub 2019/05/01. doi: 10.3389/fimmu.2019.00792.
 103. Fumagalli S, Perego C, Pischiutta F, Zanier ER, De Simoni MG. The ischemic environment drives microglia and macrophage function. *Front Neurol* (2015) 6:81. Epub 2015/04/24. doi: 10.3389/fneur.2015.00081.
 104. Anders CB, Lawton TMW, Smith H, Garret J, Ammons MCB. Metabolic Immunomodulation, Transcriptional Regulation, and Signal Protein Expression Define the Metabotype and Effector Functions of Five Polarized Macrophage Phenotypes. *bioRxiv* (2020):2020.03.10.985788. doi: 10.1101/2020.03.10.985788.
 105. Weisser SB, McLaren KW, Kuroda E, Sly LM. Generation and characterization of murine alternatively activated macrophages. *Basic Cell Culture Protocols*. Springer (2013). p. 225-39.
 106. Wang C, Yu X, Cao Q, Wang Y, Zheng G, Tan TK, et al. Characterization of murine macrophages from bone marrow, spleen and peritoneum. *BMC Immunol* (2013) 14(1):6. Epub 2013/02/07. doi: 10.1186/1471-2172-14-6.
 107. Cassado AD, Lima MRD, Bortoluci KR. Revisiting mouse peritoneal macrophages: heterogeneity, development, and function. *Frontiers in Immunology* (2015) 6:225. doi: 10.3389/fimmu.2015.00225.
 108. Chanput W, Mes JJ, Wichers HJ. THP-1 cell line: an in vitro cell model for immune modulation approach. *Int Immunopharmacol* (2014) 23(1):37-45. Epub 2014/08/19. doi: 10.1016/j.intimp.2014.08.002.
 109. Wellman ML, Krakowka S, Jacobs RM, Kociba GJ. A macrophage-monocyte cell line from a dog with malignant histiocytosis. *In Vitro Cell Dev Biol* (1988) 24(3):223-9. Epub 1988/03/01. doi: 10.1007/bf02623551.
 110. Gebhard D, Levy M, Ley D, editors. Isolation and characterization of functionally and phenotypically distinct continuous monocytoid cell lines from a canine malignant histiocytosis. *Proceedings of the Fourth International Veterinary Immunology Symposium, Davis, CA, USA; 1995*.
 111. Schwende H, Fitzke E, Ambs P, Dieter P. Differences in the state of differentiation of THP-1 cells induced by phorbol ester and 1,25-dihydroxyvitamin D3. *J Leukoc Biol* (1996) 59(4):555-61. Epub 1996/04/01.

112. Lv R, Bao Q, Li Y. Regulation of M1-type and M2-type macrophage polarization in RAW264.7 cells by Galectin-9. *Mol Med Rep* (2017) 16(6):9111-9. Epub 2017/10/11. doi: 10.3892/mmr.2017.7719.
113. Mezouar S, Mege J, editors. *New Tools for Studying Macrophage Polarization: Application to Bacterial Infections*. 2020.
114. Mosser DD, Caron AW, Bourget L, Meriin AB, Sherman MY, Morimoto RI, et al. The chaperone function of hsp70 is required for protection against stress-induced apoptosis. *Molecular and Cellular Biology* (2000) 20(19):7146-59. doi: Doi 10.1128/Mcb.20.19.7146-7159.2000.
115. Pockley AG. Heat shock proteins as regulators of the immune response. *Lancet* (2003) 362(9382):469-76. doi: Doi 10.1016/S0140-6736(03)14075-5.
116. Nollen EA, Morimoto RI. Chaperoning signaling pathways: molecular chaperones as stress-sensing heat shock proteins. *Journal of cell science* (2002) 115(14):2809-16.
117. Hagiwara S, Iwasaka H, Matsumoto S, Noguchi T. Changes in cell culture temperature alter release of inflammatory mediators in murine macrophagic RAW264.7 cells. *Inflamm Res* (2007) 56(7):297-303. Epub 2007/07/31. doi: 10.1007/s00011-007-6161-z.
118. Polla BS, Cossarizza A. Stress proteins in inflammation. *EXS* (1996) 77:375-91. Epub 1996/01/01. doi: 10.1007/978-3-0348-9088-5_25.
119. Fincato G, Polentarutti N, Sica A, Mantovani A, Colotta F. Expression of a heat-inducible gene of the HSP70 family in human myelomonocytic cells: regulation by bacterial products and cytokines. *Blood* (1991) 77(3):579-86. Epub 1991/02/01.
120. Ding XZ, Fernandez-Prada CM, Bhattacharjee AK, Hoover DL. Over-expression of hsp-70 inhibits bacterial lipopolysaccharide-induced production of cytokines in human monocyte-derived macrophages. *Cytokine* (2001) 16(6):210-9. Epub 2002/03/09. doi: 10.1006/cyto.2001.0959.
121. Snyder YM, Guthrie L, Evans GF, Zuckerman SH. Transcriptional inhibition of endotoxin-induced monokine synthesis following heat shock in murine peritoneal macrophages. *Journal of leukocyte biology* (1992) 51(2):181-7.
122. Chen H, Wu Y, Zhang Y, Jin L, Luo L, Xue B, et al. Hsp70 inhibits lipopolysaccharide-induced NF- κ B activation by interacting with TRAF6 and inhibiting its ubiquitination. *FEBS letters* (2006) 580(13):3145-52.
123. Tang D, Kang R, Xiao W, Wang H, Calderwood SK, Xiao X. The anti-inflammatory effects of heat shock protein 72 involve inhibition of high-mobility-group box 1 release and proinflammatory function in macrophages. *J Immunol* (2007) 179(2):1236-44. Epub 2007/07/10. doi: 10.4049/jimmunol.179.2.1236.
124. Cooper ZA, Ghosh A, Gupta A, Maity T, Benjamin IJ, Vogel SN, et al. Febrile-range temperature modifies cytokine gene expression in LPS-stimulated macrophages by differentially modifying NF-kappa B recruitment to cytokine gene promoters. *Am J Physiol Cell Physiol* (2010) 298(1):C171-81. Epub 2009/10/23. doi: 10.1152/ajpcell.00346.2009.
125. Muralidharan S, Ambade A, Fulham MA, Deshpande J, Catalano D, Mandrekar P. Moderate alcohol induces stress proteins HSF1 and hsp70 and inhibits proinflammatory cytokines resulting in endotoxin tolerance. *J Immunol* (2014) 193(4):1975-87. Epub 2014/07/16. doi: 10.4049/jimmunol.1303468.

126. Ryan AJ, Flanagan SW, Moseley PL, Gisolfi CV. Acute heat stress protects rats against endotoxin shock. *J Appl Physiol* (1985) (1992) 73(4):1517-22. Epub 1992/10/01. doi: 10.1152/jappl.1992.73.4.1517.
127. Kluger MJ, Rudolph K, Soszynski D, Conn CA, Leon LR, Kozak W, et al. Effect of heat stress on LPS-induced fever and tumor necrosis factor. *Am J Physiol* (1997) 273(3 Pt 2):R858-63. Epub 1997/10/10. doi: 10.1152/ajpregu.1997.273.3.R858.
128. Dokladny K, Kozak A, Wachulec M, Wallen ES, Menache MG, Kozak W, et al. Effect of heat stress on LPS-induced febrile response ind-galactosamine-sensitized rats. *American Journal of Physiology-Regulatory, Integrative and Comparative Physiology* (2001) 280(2):R338-R44. doi: 10.1152/ajpregu.2001.280.2.R338.
129. Dokladny K, Lobb R, Wharton W, Ma TY, Moseley PL. LPS-induced cytokine levels are repressed by elevated expression of HSP70 in rats: possible role of NF- κ B. *Cell Stress and Chaperones* (2010) 15(2):153-63.
130. Villar J, Ribeiro SP, Mullen JB, Kuliszewski M, Post M, Slutsky AS. Induction of the heat shock response reduces mortality rate and organ damage in a sepsis-induced acute lung injury model. *Crit Care Med* (1994) 22(6):914-21. Epub 1994/06/01.
131. Ganter MT, Ware LB, Howard M, Roux J, Gartland B, Matthay MA, et al. Extracellular heat shock protein 72 is a marker of the stress protein response in acute lung injury. *American Journal of Physiology-Lung Cellular and Molecular Physiology* (2006) 291(3):L354-L61. doi: 10.1152/ajplung.00405.2005.
132. van Eden W, van der Zee R, Prakken B. Heat-shock proteins induce T-cell regulation of chronic inflammation. *Nat Rev Immunol* (2005) 5(4):318-30. Epub 2005/04/02. doi: 10.1038/nri1593.
133. Detanico T, Rodrigues L, Sabritto AC, Keisermann M, Bauer ME, Zwickey H, et al. Mycobacterial heat shock protein 70 induces interleukin-10 production: immunomodulation of synovial cell cytokine profile and dendritic cell maturation. *Clin Exp Immunol* (2004) 135(2):336-42. Epub 2004/01/24. doi: 10.1111/j.1365-2249.2004.02351.x.
134. Gao B, Tsan MF. Endotoxin contamination in recombinant human heat shock protein 70 (Hsp70) preparation is responsible for the induction of tumor necrosis factor alpha release by murine macrophages. *J Biol Chem* (2003) 278(1):174-9. Epub 2002/10/31. doi: 10.1074/jbc.M208742200.
135. Triantafilou K, Triantafilou M, Dedrick RL. A CD14-independent LPS receptor cluster. *Nat Immunol* (2001) 2(4):338-45. Epub 2001/03/29. doi: 10.1038/86342.
136. Triantafilou M, Triantafilou K. Heat-shock protein 70 and heat-shock protein 90 associate with Toll-like receptor 4 in response to bacterial lipopolysaccharide. *Biochem Soc Trans* (2004) 32(Pt 4):636-9. Epub 2004/07/24. doi: 10.1042/bst0320636.
137. Theriault JR, Adachi H, Calderwood SK. Role of scavenger receptors in the binding and internalization of heat shock protein 70. *J Immunol* (2006) 177(12):8604-11. Epub 2006/12/05. doi: 10.4049/jimmunol.177.12.8604.
138. Vega VL, Rodriguez-Silva M, Frey T, Gehrman M, Diaz JC, Steinem C, et al. Hsp70 translocates into the plasma membrane after stress and is released into the extracellular environment in a membrane-associated form that

- activates macrophages. *Journal of Immunology* (2008) 180(6):4299-307. doi: DOI 10.4049/jimmunol.180.6.4299.
139. Gautam PK, Kumar S, Deepak P, Acharya A. Morphological effects of autologous hsp70 on peritoneal macrophages in a murine T cell lymphoma. *Tumour Biol* (2013) 34(6):3407-15. Epub 2013/06/21. doi: 10.1007/s13277-013-0913-x.
 140. Motta A, Schmitz C, Rodrigues L, Ribeiro F, Teixeira C, Detanico T, et al. Mycobacterium tuberculosis heat - shock protein 70 impairs maturation of dendritic cells from bone marrow precursors, induces interleukin - 10 production and inhibits T - cell proliferation in vitro. *Immunology* (2007) 121(4):462-72.
 141. Stocki P, Wang XN, Dickinson AM. Inducible heat shock protein 70 reduces T cell responses and stimulatory capacity of monocyte-derived dendritic cells. *J Biol Chem* (2012) 287(15):12387-94. Epub 2012/02/16. doi: 10.1074/jbc.M111.307579.
 142. Wang R, Kovalchin JT, Muhlenkamp P, Chandawarkar RY. Exogenous heat shock protein 70 binds macrophage lipid raft microdomain and stimulates phagocytosis, processing, and MHC-II presentation of antigens. *Blood* (2006) 107(4):1636-42. Epub 2005/11/03. doi: 10.1182/blood-2005-06-2559.
 143. Wang R, Town T, Gokarn V, Flavell RA, Chandawarkar RY. HSP70 enhances macrophage phagocytosis by interaction with lipid raft-associated TLR-7 and upregulating p38 MAPK and PI3K pathways. *J Surg Res* (2006) 136(1):58-69. Epub 2006/09/19. doi: 10.1016/j.jss.2006.06.003.

2



The anti-inflammatory properties of heat shock proteins and therapeutic tolerance induction in chronic inflammatory diseases

Ariana Barbera Betancourt^{1*}, Qingkang Lyu², Femke Broere², Alice Sijts², Victor Rutten² and Willem van Eden²

¹ Department of Medicine, University of Cambridge, United Kingdom

² Department of Infectious Diseases & Immunology, Faculty of Veterinary Medicine, Utrecht University, Utrecht, The Netherlands

Frontiers in immunology 8 (2017): 1408.

Abstract

Failing immunological tolerance for critical self-antigens is the problem underlying most chronic inflammatory diseases of humans. Despite the success of novel immuno-suppressive biological drugs, the so-called biologics, in the treatment of diseases such as rheumatoid arthritis (RA) and type 1 diabetes (T1D), none of these approaches does lead to a permanent state of medicine free disease remission. Therefore, there is a need for therapies that restore physiological mechanisms of self-tolerance. Heat shock proteins (HSPs) have shown disease suppressive activities in many models of experimental autoimmune diseases through the induction of regulatory T cells (Tregs). Also, in first clinical trials with HSP-based peptides in RA and diabetes the induction of Tregs was noted. Due to their exceptionally high degree of evolutionary conservation, HSP protein sequences (peptides) are shared between the microbiota-associated bacterial species and the self-HSP in the tissues. Therefore, Treg mechanisms, such as those induced and maintained by gut mucosal tolerance for the microbiota, can play a role by targeting the more conserved HSP peptide sequences in the inflamed tissues. In addition, the stress upregulated presence of HSP in these tissues may well assist the targeting of the HSP induced Treg specifically to the sites of inflammation.

Keywords: heat shock proteins, tolerance, T regulatory cells, rheumatoid arthritis, inflammatory eye diseases, diabetes mellitus, type 1

Introduction

In many cases, chronic inflammatory diseases are autoimmune diseases that are caused by a loss of tolerance to self-antigens due to inappropriate activation of the immune system. Collectively, autoimmune diseases affect 4–5% of the population, being females affected with a higher incidence than males (3:1 ratio) (1).

Genome-wide association studies (GWAS) have underscored the genetic association of the major histocompatibility complex (MHC) region with autoimmune diseases, in which case various predisposing alleles have been found (2, 3). The main function of MHC molecules is to present processed peptides for the recognition of antigen-specific T cells. And such T cells have the capacity to damage healthy tissues when they are not tightly controlled. The exact mechanisms triggering autoimmune diseases are unknown, but the presence of pro-inflammatory T cells in target organs as well as the strong link with MHC loci highlights the important role for adaptive immune responses in their development. The most accepted hypothesis proposes that for the initiation of an autoimmune disease, an immune response with pro-inflammatory characteristics needs to be directed against specific tissue antigens in genetically susceptible individuals. Regulatory mechanisms exist in the periphery to control such effector responses to avoid excessive tissue damage (4). Mechanisms include the following: regulatory T cells (Tregs), direct inactivation of effector T (Teff) cells by induction of anergy or apoptosis and activities mediated by tolerogenic antigen presenting cells (APCs). However, there is an increasing understanding that pro-inflammatory responses directed to self-antigens become chronic in autoimmune diseases because regulatory mechanisms fail to control them.

Peripheral tolerance mechanisms

CD4+CD25^{high} FoxP3+ Tregs

CD4+CD25^{high} FoxP3+ Tregs can prevent autoimmune diseases by maintaining the tolerance to self-antigens. FoxP3 constitutes the most specific marker for these cells and is to some extent indispensable to develop a Treg phenotype and for their suppressive function (5). The development of autoimmune diseases when CD4+CD25+ cells are depleted in normal rodents or when rodents and humans have mutated FoxP3 genes highlights the role of Tregs in the prevention of such diseases (6, 7). As illustrated in Figure 1, when activated by their cognate antigen, Treg cells display a broad range of suppressive mechanisms, which endow them with the ability to control immune responses. The potential of controlling T- and B-

cell responses with different specificities as well as the modulation of the maturation status of APCs by Tregs makes them attractive targets for the development of therapeutic strategies. Apart from CD4+CD25^{high} Foxp3+ Tregs, there are several subsets of CD8+ T cells that are able to downregulate CD4+ T-cell effector responses by different mechanisms including the induction of anergy in APCs and T cells as well as the secretion of anti-inflammatory cytokines (8). CD8+CD28⁻Foxp3+ Treg cells are probably the subset best characterized (9). The activation of these cells is antigen-specific [major histocompatibility complex (MHC)-I class-restricted], and their suppressor mechanism involves the induction of a tolerogenic phenotype in APCs by the increased expression of immunoglobulin-like transcript 3 (ILT3) and ILT4. ILT3 and ILT4 suppress the activation of nuclear factor- κ B mediated by CD40, which in turn reduces the transcription of co-stimulatory molecules such as CD80 and CD86 (9-11). These tolerogenic APCs in turn promote an anergic phenotype on naive CD4+ and CD8+ T cells, which could acquire similar regulatory functions spreading the induction of tolerance (10).

However, some studies have shown that patients with autoimmune diseases have less effective or fewer CD4+CD25^{high} Foxp3+ Treg cells compared with healthy individuals (reviewed in Ref. (12)). Numbers and/or function of CD8+ Tregs have been also found to be defective in animal models of autoimmunity and in patients (13). Defects in the capacity of T effector cells to be controlled by Tregs have also been found in the context of autoimmune diseases (12). Collectively, these findings suggest that Treg malfunction might be a factor promoting the development or chronicity of autoimmune diseases. Therefore, approaches to expand regulatory populations in autoimmune diseases have therapeutic potential (14, 15).

Anergy

T cells are activated when their T-cell receptors (TCR) recognize antigenic peptides presented by MHC molecules expressed on the surface of APCs. Secondary signals like the one provided by CD28 expressed by T cells and B7.1 (CD80) or B7.2 (CD86) expressed by APCs are essential to initiate IL-2 production and T-cell proliferation. However, the activation of T cells without second signals induces a state of anergy where these clones are not able to respond to antigenic stimulus because they cannot produce IL-2. Cytotoxic T lymphocyte-associated molecule-4 (CTLA4) is a cell surface molecule related to CD28 that has the ability to block CD28-dependent T cell activation (16). The critical role of this molecule in controlling T-cell activation and maintaining peripheral tolerance was supported by the development of a massive lymphoproliferative disorder and autoimmune disease being fatal by 3-4 weeks of age in CTLA-4-deficient mice (17). Activated T cells transiently increase the expression of CTLA4, which is important to limit the

expansion of activated T cells during an immune response. This cell surface molecule is expressed constitutively by Tregs endowing them with the potential to control T-cell activation through CD28 blockade (**Figure 1**). The inhibition of the CD28-dependent T cell activation has been used as a therapeutic tool for several autoimmune diseases. The blockade of the CD28 pathway with CTLA-Ig in animal models of autoimmune diseases prevented the progression of the disease [reviewed in Ref. (18)]. Abatacept (CTLA4-Ig) has been approved by the FDA for use in rheumatoid arthritis (RA) patients with an inadequate response to one or more of the disease-modifying antirheumatic drugs.

Apoptosis

Apoptotic cell death is another important regulatory mechanism operating in the thymus and periphery to delete self-reactive T cells or activated pathogenic T-cell clones, respectively. During the development of T cells in the thymus, clones bearing autoreactive TCRs are eliminated by apoptosis in a process known as negative selection. However, T cells with potential autoreactive receptors escape to the periphery where these clones should be kept in check by regulatory mechanisms such as Tregs, anergy or deletion. In the periphery, activated T cells express death receptors belonging to the tumor necrosis factor (TNF) family (e.g., Fas/Fas-ligand) making them susceptible to activation-induced cell death (AICD) (19, 20). Memory T cells, Tregs and Th2 cells are less susceptible than Th1 cells to AICD (21, 22), allowing the polarization of the immune response to protective responses (Th2/Treg) in the periphery. On the other hand, by inducing IL-2 deprivation and secreting perforins and granzymes, Tregs at the site of inflammation increase the susceptibility of Teff cells and other cells such as B cells and monocytes to cell death (23, 24).

Tolerogenic APC

Tolerogenic APCs present antigens to T cells but since they display low numbers of co-stimulatory molecules such as CD80, CD86 and CD40, antigen presentation leads to T-cell anergy (25). Tolerogenic APCs can be induced and enhanced using different compounds such as rapamycin, corticosteroids, interleukin-10 (IL-10) and transforming growth factor beta 1 (TGF β -1) (26). Several studies have shown the therapeutic effect of tolerogenic APCs induced *ex vivo* in experimental animal models (reviewed in Ref. (27, 28)). Treg cells can also modulate the maturation status of APCs. For example, these cells can decrease the expression of co-stimulatory molecules on APC affecting their capacity to activate T cells (29). In addition, ligation of CTLA4 to CD80 and CD86 induces APC to express an immunosuppressive molecule (indoleamine 2,3-dioxygenase) which is able to

abolish T-cell activation (30, 31). Lymphocyte activation gene 3 (LAG-3) is another molecule expressed by Tregs that could affect APC function. This is a CD4 homolog with a high affinity for MHC class II molecules. The binding of LAG3 to MHC class II induces an inhibitory signaling pathway, which leads to the inhibition of APC maturation (**Figure 1**) (32).

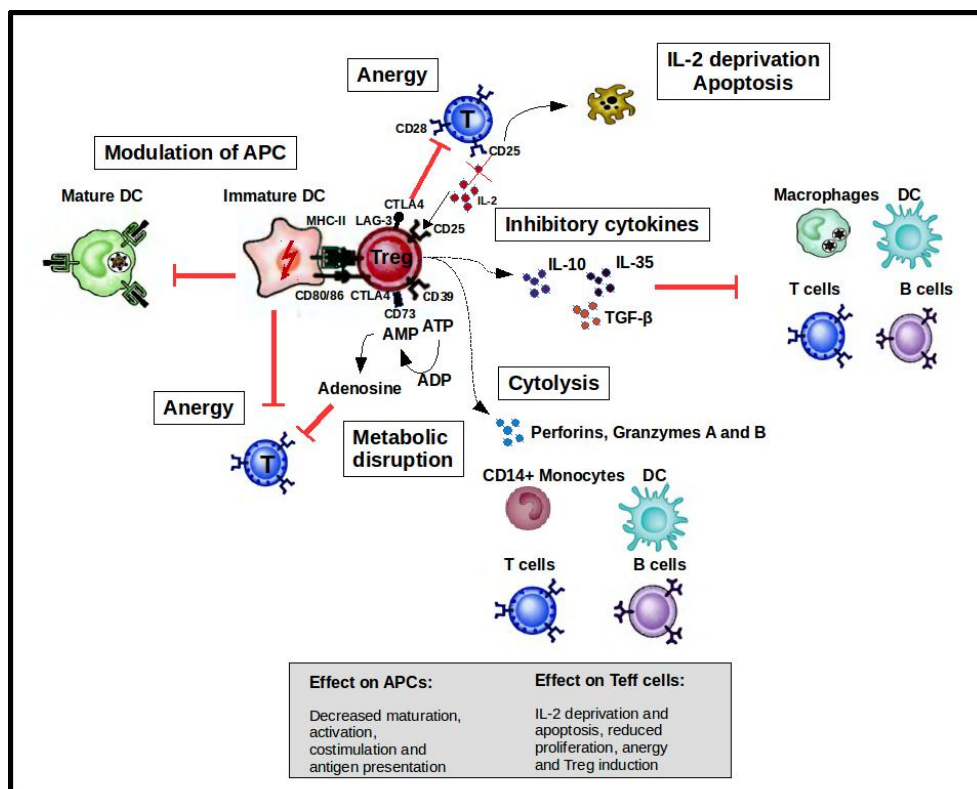


Figure 1. Mechanisms of suppression by Treg cells to control immune responses. A broad range of molecular mechanisms contribute to the suppressive function of Tregs. Mechanisms include the following: apoptosis/cytolysis (IL-2 deprivation, granzyme A/B, perforins); antigen-presenting cell (APC) modulation (CTLA4, LAG-3); inhibitory cytokines (IL-10, IL-35, and TGF- β); and metabolic disruption (CD73/39 and ATP/adenosine mechanism). Abbreviations: CTLA4, cytotoxic T lymphocyte-associated antigen-4; DC, dendritic cell; CD, cluster of differentiation; IL-, interleukin; LAG3, lymphocyte activation gene 3; TGF, transforming growth factor; MHC, major histocompatibility complex.

MHC associated diseases are T-cell mediated and possible targets for induction of heat shock protein (HSP) driven therapeutic tolerance

The strong link of autoimmune diseases with MHC loci and the presence of pro-inflammatory T cells in target organs highlight the important role for adaptive immune responses in their development. In such cases, therapeutic tolerance may become established through the induction of Tregs with bystander regulatory activities leading to the inhibition or modulatory skewing of these pro-inflammatory self-antigen-specific T cells. Examples of MHC-associated, primarily T-cell driven autoimmune diseases are RA, type 1 diabetes (T1D), and several eye diseases.

Rheumatoid Arthritis

Rheumatoid arthritis is a chronic inflammatory disease characterized by joint inflammation and synovial hyperplasia, which leads to cartilage and bone destruction (33).

The HLA-DRB1 gene has been associated with the susceptibility of this disease, especially with the shared epitope (SE) coding alleles (HLA-DRB1*0401, *0404, *0405, *0408, *0101, *0102, *1402 and *1001). The SE is a five amino-acid sequence motif found in residues 70–74 of the HLA-DR β chain that encodes a conserved positively charged residue at position 71 (34). The latter seems to guide the nature of the amino acid that can be accommodated in the P4 pocket of these HLA-DR molecules. Although the susceptibility of this disease appears to be determined genetically, the onset might depend on other factors such as environmental, epigenetic or posttranslational events factors (35).

As expected by the strong association of HLA-DRB1 and RA, CD4⁺ T cells are enriched in synovia of these patients and seem to play a critical role in the perpetuation of inflammation [reviewed in Ref. (36)]. Susceptibility to RA has also been linked to other pathways implicated in the activation of T cells, such as PTPN22, PTPN2, CTLA4, IL2RA, IL-2RB, among others [reviewed in Ref. (29)]. Specifically, a CD4⁺ T cell subset that produces IL-17, 21, 22 and TNF- α has been in the center of the attention in recent years. Emerging data have suggested that active RA might result from an imbalance between defective Tregs and pro-inflammatory Th17 cells (37-39). Nevertheless, the mechanisms governing such imbalance that could contribute to RA chronicity have remained unclear.

Tumor necrosis factor- α has been shown to be the master element of inflammation

in RA (40). Consequently, the blockade of this cytokine has emerged as the main tool for its treatment. Although the exact mechanism underlying clinical effects of anti-TNF- α therapy in patients is not completely understood it is apparent that it can have an effect on other pathways associated with tolerance (41). For instance, it has been reported that the treatment with infliximab increases the percentage of CD4+CD25+ Tregs in RA patients who responded to therapy (42). Further studies showed that infliximab induced a distinct Treg population in vitro that could compensate the compromised Tregs detected in RA (43). Despite excellent results in patients responding to anti-TNF- α therapy, there is an increased susceptibility to serious adverse effects including: infectious diseases, malignancies and demyelination (44). In addition, only partial responses are achieved with this treatment and a continuous treatment is required.

Diabetes mellitus type 1

Pancreatic β cells producing insulin are the targets for antigen-specific T cells in T1D. Epidemiologic studies suggest that the incidence of this disease is rising (45). The updated estimates of the incidence (20.04 per 100,000 per year) and prevalent cases (129,350) of T1D in children 0–14 years old in Europe for 2013 (46) reflect an increasing trend of 3–4% per annum during the past 20 years (47).

HLA-DRB1*0401-DQB1*0302 and HLA-DRB1*0301-DQB1*0201 have been associated with T1D susceptibility whereas the haplotypes HLA-DRB1*1501 and HLA-DQA1*0102-DQB1*0602 confer resistance (48). However, most people bearing the haplotypes associated with the greatest susceptibility do not develop the disease. In addition, despite the finding of islet-specific T cells in the blood of healthy individuals, one study showed that these cells secrete IL-10 instead of interferon gamma (IFN- γ) (49), indicating that regulatory mechanisms should fail to develop T1D. Indeed, there is evidence supporting that regulation is impaired in this disease, where patients seem to have a decreased Treg suppressive functionality compared with non-diabetic controls (50, 51).

The exact mechanism by which β cells are destroyed in the pancreas is not fully understood, but genetic and environmental factors appear to predispose individuals with defective regulatory mechanisms to develop the disease. Similar to other chronic inflammatory diseases, T1D onset requires CD4+ and CD8+ T cells [reviewed in Ref. (52)]. The latter has been demonstrated in experiments in which the precipitation or prevention of diabetes was achieved in the non-obese mice model by transfer or elimination of CD4+ or CD8+ T cells, respectively. Both cell types are able to infiltrate the pancreatic islets in mice and humans and are considered to be the final executors of the destruction of insulin-producing β cells

(52). CD4+ and CD8+ T cells can induce the death of pancreatic β cells. However, as β cells only express HLA class I, direct cytotoxicity can be only mediated by CD8+ T cells able to recognize appropriated peptides displayed on β -cell class I molecules. CD8+ T cells are able to kill β cells through different mechanisms including granzyme B and perforins, pro-inflammatory cytokines and/or Fas/FasL interactions (52).

No drugs have been approved to halt the autoimmune process that causes the destruction of β cells in T1D (53). The main goals are the induction of a residual β -cell function. Different approaches to treat this disease have been used so far [reviewed in Ref. (54)]. One of the therapeutic approaches showing promise in T1D is the use of anti-CD3 monoclonal antibodies which have been shown to interfere antigen-specific T cell activation. However, after promising clinical trials (phase 1 and 2) in T1D patients with a recent onset, phase 3 trials fail to meet primary endpoints (55, 56).

MHC associated inflammatory eye diseases

Various studies have confirmed that eye diseases, such as idiopathic uveitis (57), birdshot retinochoroidopathy (BSR) (58), and sympathetic ophthalmia (59), have an association with MHC. Uveitis is the most common form of inflammatory eye disease and one of the leading causes of visual impairment and blindness. The association of the MHC class I molecule HLA-B27 with uveitis was first noted in 1973 (60). The precise molecular and pathogenic mechanisms behind the association between Uveitis and HLA-B27 have remained unclear. HLA-B27 encompasses around 105 known subtypes (HLA-B*27:01 to HLA-B*27:106 thus far identified) that are encoded by 132 alleles (61). HLA-B27 subtypes have a varied prevalence in different races and regions of the world. HLA-B*2705 and B*2702 are the main HLA-B27 subtypes in northern Europe, while HLA-B*2704 and B*2706 are the most widespread subtype among Asian populations (62). A study from China found that among northern Chinese people, Ankylosing Spondylitis (AS) patients with B*2704 have a stronger risk of developing uveitis than those with B*2705 in Ref. (63). Conversely, a Japanese study showed that HLA-B27 anterior uveitis (AAU) patients with the B*2704 subtype seemed to be less susceptible than patients with B*2705 (64). This suggests that HLA-B*2704 and HLA-B*2705 may be the most prevalent HLA-B27 subtypes, with observed conflicting results on the role of this molecule in AAU caused by different races and regions, genetic background, or environmental factors. Remarkably, the majority of individuals who carry susceptibility conferring HLA subtypes never develop uveitis or other systemic autoimmune disease, implying that HLA-B27 is a genetically predisposing factor for uveitis but that other genetic or environmental factors contribute to the

development of uveitis. HLA-B27-associated uveitis is also closely related to other systemic autoimmune syndromes, such as AS and systemic sarcoidosis. Several studies have shown that HLA-B27 positive AS patients are more susceptible to uveitis than HLA-B27 negative patients (65, 66). 20-30% of patients with sarcoidosis were affected by uveitis (67).

Except for uveitis, also specific other ocular inflammatory diseases show a strong association with HLA. BSR and idiopathic retinal vasculitis are associated with HLA-A29 (68), with HLA-A*29.01 and HLA-A*29.02 representing the most common A29 subtypes found in BSR patients (69). The HLA-A*29.01 subtype is more frequent among Asians, while HLA-A*29.02 is more common among Caucasians (70). In addition, Behcet's disease (BD) is an inflammatory disease affecting multiple organs that also includes a relapsing and remitting pan-uveitis, which is strongly associated with HLA-B*51 (71). HLA-B5101 is the predominant subtype associated with BD in Japanese and Iranian patients. The association of HLA-B*5108 and BD was also found in Greek and Spanish patients. A study of Israeli showed that HLA-B*52 may also be associated with BD (72).

In humans, more and more evidence reveal that cytokines produced by autoreactive T cell play a pivotal role in the pathogenesis of autoimmune uveitis. Early studies suggested that the imbalance of anti- and pro-inflammatory Th2 and Th1 subsets is responsible for the pathology of uveitis. However, in recent studies emphasis was laid on Th17 and CD4+CD25+FoxP3+ T regulatory cells, which produce IL-17 and IL-10, respectively. The ratio of Th17/Treg was distinctly increased at the progression of uveitis in patients and in experimental autoimmune uveitis (EAU) disease models (73, 74), and imbalance of Treg cells over Th17 cells was observed at the recovery phase of EAU (73). Th1 cells play central roles in early phase of uveitis, whereas Th17 cells act in the late phase of uveitis (75), Treg and inducible Treg cells suppress both Th1 and Th17 cell responses by counterbalancing pro-inflammatory activities of these T cells. This implies that increasing the number of Treg cells may be a promising and safe way to control MHC-associated eye diseases.

HSP and the induction of therapeutic tolerance

HSP proteins or peptides as inducers of regulatory T cells

Initial studies reported that several HSP families were able to induce both pro-inflammatory and anti-inflammatory effects. Pro-inflammatory cytokine production mediated by HSP70 appears to be linked to the activation of toll-like receptor 2 (TLR2) and TLR4 signaling pathways on innate immune cells (76, 77). Pathogen-

associated molecular patterns such as lipopolysaccharide (LPS) or other proteins present in recombinant HSP produced in bacteria have been suggested to be responsible for the observed pro-inflammatory effects [reviewed in Ref. (78)]. In line with this idea, HSPs often fail to induce an inflammatory effector response in highly purified preparations (79, 80). On the contrary, other studies using non-recombinant Hsp70, boiling treatments (which cause the degradation of HSP) or antibiotics have led to the conclusion that HSPs are responsible for the activation of innate immune cells as well as T cells through TLR signaling pathways (81, 82). It seems that whether these proteins have an activating or immunosuppressive role depends on several factors including their local concentration, the nature of the HSP itself (self or microbial), among others [reviewed in Ref. (83)]. In the context of autoimmune diseases, HSP proteins have been considered as target molecules involved in their pathogenesis in part because they become highly available at sites of inflammation (83). The other main reason is the high homology between species whereby microbial HSPs can active immune responses that can be cross-reactive with self-HSPs which in theory could provoke autoimmunity. However, autoreactivity to self-HSPs has been also found in healthy individuals (84, 85), which means that these proteins are under a tight regulation network. The latter also means that autoreactivity to self-HSPs is not a synonym of autoimmunity. In fact, self-HSP reactivity appears to be a physiological mechanism for controlling the inflammatory process (86). In this regard, several studies in mice and humans support the fact that HSP, and specially conserved epitopes have the potential for attenuating rather than triggering inflammatory responses (87, 88).

The initial indication of a possible role of HSP in the induction of therapeutic tolerance was obtained in the model of adjuvant arthritis in rats. T cells collected from diseased animals were found to respond to mycobacterial HSP60 (89). When the recombinant mycobacterial HSP60 protein was used for immunizations, no arthritis was seen to develop. Interestingly, induction of adjuvant arthritis in these immunized animals appeared not to be possible anymore. Subsequent experiments revealed that the same protection against adjuvant arthritis induction was obtained by immunizing the animals with only a conserved sequence (peptide) of mycobacterial HSP60 (90). On the basis of these latter experiments, it was concluded that the conserved peptide induced T cells that were cross-reactive with self (mammalian) HSP upregulated at the site of inflammation. In various additional studies, the regulatory nature of these cross-reactive T cells was recognized, since they were producing regulatory cytokines such as IL-10.

More recent studies have shown the HSP mediated induction of T cells with regulatory potential, which showed the actual phenotypic characteristics of the currently known Tregs (91). This was amongst others the case for a HSP70

derived conserved mycobacterial peptide called B29. When BALB/c mice were immunized with B29, responding T cells were collected on the basis of CD25 expression and transferred into naïve syngeneic recipient mice. Subsequently, these T cells were found to inhibit disease activity after induction of arthritis and to persist in various organs, including the joints, for more than 50 days. When during this time period, the presence of these cells was interrupted by infusion of a Treg depleting antibody, disease returned, which showed the actual disease suppressive activity of these HSP70 specific Tregs. When B29 specific T cells were selected on the basis of LAG-3 expression, it sufficed to transfer only 4000 of these T cells to fully inhibit arthritis. Several explanations are possible for the capacity of conserved microbial HSP peptides to induce Tregs. An obvious explanation can be found in the contact of the immune system with microbiota in the gut. It is known that APCs lining the gut mucosa ingest bacteria from the microbiota. This causes transport to mesenteric lymph nodes, where the derivative microbial antigens are presented to T cells, a phenomenon that must contribute to mucosal tolerance. Since ingestion of bacteria will lead to a stress response, both in bacteria and in the APC of the host, MHC molecules will be loaded with HSP fragments in this process. By these mechanisms, both microbial and the self-cross-reactive T cells will be activated. And since such events happen in the environment of the tolerance promoting mucosa, induction of peripheral Tregs seems a direct and physiological consequence. Given the evolutionary conservation of the HSP molecules present in the complete kingdom of prokaryotes, it seems unavoidable that through the repeated contacts with bacteria, the immune system develops a focus on the conserved parts of the molecules. And by this same focus on the shared sequences between bacterial and mammalian HSPs, Tregs induced by bacterial HSP may easily cross-respond to self-HSP (over-)expressed in the inflamed tissues. Herewith the regulation, which is of a bystander nature, will be targeted towards the sites of inflammation.

Endogenous HSP loaded MHC molecules

Apart from the possibility that mucosal tolerance creates a repertoire of HSP specific Treg, there is also reason to think that HSPs are a default antigen for Tregs in the context of healthy tolerogenic APCs in the absence of co-stimulation activating micro-organisms. In various studies HSP70 has been found to belong to the most frequent cytosolic/nuclear MHC class II natural ligand sources (92). In other words, MHC elution studies have revealed that sequences of HSP70 family members are relatively often present in the proteome obtained from the antigen-binding clefts of human and mouse MHC II molecules. And especially in the case of cell-stress, such as the stress caused by inflammatory mediators, HSP70 fragments have been seen to become preferentially uploaded into MHCII

molecules [reviewed in Ref. (87)]. Dengjel et al. (93) have analyzed the sequences eluted from human B cell derived HLA-DR4 molecules under amino-acid deprivation as the cell-stress factor. It was shown that under such conditions chaperone-mediated autophagy became operative, which led to involvement of HSP70, which is one of the molecular participants in the process of chaperone mediated autophagy. In general terms, it was seen that under stress the presentation of peptides from intracellular and lysosomal source proteins was strongly increased on MHC-II in contrast to peptides from membrane and secreted proteins. For these reasons, it was concluded that their study illustrated a profound influence of autophagy on the class II peptide repertoire and suggested that this finding had implications for the regulation of CD4(+) T cell-mediated processes. Interestingly, also the mammalian homologs of our earlier defined HSP70 derived B29 peptide were eluted from this HLA-DR4 molecule (HLA DRB1*0401). Knowing this, it seems reasonable to think that HSPs, and HSP70 family members in particular are frequently seen by Tregs in the context of MHCII molecules. In this manner, they could well serve as a default antigen for Tregs, especially when presented by tolerogenic APC.

Given the stress inducible nature of various HSP70 family members, we have attempted to raise the abundance of HSP70 fragments in MHCII molecules of APCs by administering a so-called HSP co-inducing compound (94, 95). And indeed, in the experimental model of proteoglycan induced arthritis (PGIA) in mice, we have seen such an intervention with an HSP co-inducer to lead to a T cell mediated resistance against arthritis. The experiments were carried out with carvacrol, an essential oil obtained from Oregano plants. Initial studies in vitro had indicated that incubation of cells before further exposure to classical stressors, such as raised temperature or arsenite, caused a raised expression of endogenous HSP70. When given orally, carvacrol was found to lead to a raised expression of HSP70 family members in the Peyer's patches, the lymphoid organs of the gut. In addition, when analyzing the T cell responses to HSP70, it was found that oral carvacrol had raised the frequency of HSP70-specific T cells and that such cells showed to an enhanced degree the CD4+CD25+Foxp3+ phenotype of Tregs. Transfer of these cells into naïve recipients inhibited subsequently induced PGIA. Thus, the experiments with carvacrol have indicated that for the purpose of generating therapeutic tolerance, the co-induction of HSPs, even by dietary measures, may be a possible and attractive strategy.

How to induce HSP based therapeutic tolerance in T-cell mediated autoimmune diseases

Effective interventions in animal models are usually based on disease inhibition by

administering therapeutics before disease induction. In other words, effective interventions are mostly preventive and not therapeutic. Successful therapeutic interventions, when overt disease has been established, are notoriously difficult to reach. The reason for this is that established inflammation is known to cause a relative resistance to therapy, amongst others by a supposed resistance of effector cells to the regulation by Tregs (96). For these reasons, it seems essential for therapeutic tolerance to become an effective intervention, to treat chronic inflammatory diseases in an early phase of the disease.

Initial clinical studies in patients with autoimmune diseases with a recent diagnosis using peptides derived from HSP have shown that the treatment is safe and also the possibility to skew the pro-inflammatory profile of pathogenic T-cell clones has been noted [reviewed in Ref. (97-99)]. For example, dnaJP1 is a 15 mer peptide, derived from bacterial HSP40, that shares homology with the “shared epitope” sequence present in some HLA-class II molecules associated with RA, which confers susceptibility to develop the disease. The peptide was identified as a pro-inflammatory T cell epitope in patients with active RA (100, 101), and authors hypothesized that it could be involved in the amplification of the inflammation due to the loss of regulatory mechanisms. In the double blind, placebo-controlled phase II trial, dnaJP1 was administered to active RA patients (< 5 years of diagnosis) with the aim of inducing mucosal tolerance to this pro-inflammatory epitope. The treatment consisted in the administration of 25 mg of the peptide by oral route daily for 6 months. A decreased percentage of CD3+ T cells producing TNF- α in response to restimulation *in vitro* with dnaJP1 was observed in patients treated with the peptide but not with placebo. A trend towards increased levels of IL-10 was seen only in clinical responders. The expression of certain molecules associated with the downregulation of the immune response before the therapy was found necessary for successfully tolerization using this peptide. Finally, authors reported significant differences between treatment groups on day 140 for both American College of Rheumatology (ACR)20 and ACR50 responses (102).

More recently, a randomized placebo-controlled double-blind phase I/IIA trial was performed in patients with unresponsive active RA using binding immunoglobulin protein (BiP). BiP is an endoplasmic reticulum resident chaperone and stress protein with strong tolerogenic effects in the collagen induced arthritis model (103). A single *i.v.* infusion of BiP (1, 5 or 15 mg) was well tolerated. The efficacy in this study was confounded by a high clinical response in the placebo group. However, at the end of the follow up period (12 weeks), remission was only achieved by some patients receiving 5 and 15 mg of BiP. Decreased C-reactive protein levels, VEGF and IL-8 were decreased in patients receiving BiP compared with placebo at that time point (104). Finally, it was concluded that a large study is required to find

the optimum dose and frequency of BiP administration.

Antigen-specific tolerance using HSP-derived peptides has also been explored in T1D. DiaPep277 is a 24-amino acid peptide derived from the 437–460 sequence of HSP60. The treatment of newly diagnosed diabetic patients with DiaPep277 was well tolerated. In some patients, the treatment may delay the loss of the C-peptide production thereby decreasing the demand for exogenous insulin when compared with placebo groups in phase I and II clinical trials (105). The study of the T-cell populations of patients treated with DiaPep277 but not with placebo showed a shift towards a Th2 phenotype characterized by reduced levels of IFN- γ and increased expression of IL-4, IL-10, and IL-13 (106).

In general, immunological effects often correlate with a trend to clinical efficacy compared with placebo groups. However, the clinical efficacy has been less than expected. Therefore, it may turn out necessary to combine various strategies. For example, anti-TNF- α drugs may be combined with HSP peptide-based vaccination to have a synergic effect of inhibition of inflammation in combination with a Treg inducing strategy. A recently probed intervention was utilizing autologous tolerogenic dendritic cells loaded with (autologous) synovial fluids in patients with progressive forms of RA (107). This first phase clinical trial showed the safety and the attainability of the approach. Although in some patients also a beneficial clinical effect was noted, it now seems needed to repeat such an intervention in patients with less advanced forms of the disease. Since it will be less practical to obtain synovial fluids from such patients, an attractive alternative possibility will be the use of HSP70 peptide B29. Besides the fact that B29 has shown a capacity to induce HSP70 specific Tregs, an additional advantage of using a well-defined antigen, such as B29, is that this will provide an opportunity to monitor the effect of the intervention precisely at the level of peptide specific T cells. A clinical trial exploring the effect of B29 in combination with tolerogenic DCs in patients with RA is under development.

Although clearly in its infancy, therapeutic tolerance is expected to become a reality. In the case of RA therapeutic progress has been significant until now. From the first pain killers, such as aspirin that was already available in the end of the nineteenth century, gold preparations since the 30s of the previous century, prednisone since world war II and biologics more recently, a very significant progress was made. The typical anatomical joint aberrations as they were seen frequently in RA patients are fully avoidable these days. Nonetheless, none of these interventions leads to cure. When therapy is halted, disease returns. Knowing this, the real challenge for the coming years will be the development of interventions that lead to a permanent remission based on regained self- tolerance.

Given their supposed physiological role as targets for T cell regulation, HSPs may provide us possibly with the means to achieve true therapeutic tolerance.

AUTHOR CONTRIBUTIONS

AB, QL, and WE did the writing. FB, AS, and VR were involved with the design of the paper.

FUNDING

The authors thank the Dutch Reumafonds for continued support. QL is supported by a grant from the Chinese government (CSC).

CONFLICT OF INTEREST STATEMENT

The authors declare that the research was conducted in the absence of any commercial or financial relationships that could be construed as a potential conflict of interest.

References

1. Vyse TJ, Todd JA. Genetic analysis of autoimmune disease. *Cell* (1996) 85(3):311-8. Epub 1996/05/03. doi: 10.1016/s0092-8674(00)81110-1.
2. Cho JH, Gregersen PK. Genomics and the multifactorial nature of human autoimmune disease. *N Engl J Med* (2011) 365(17):1612-23. Epub 2011/10/28. doi: 10.1056/NEJMra1100030.
3. Parkes M, Cortes A, van Heel DA, Brown MA. Genetic insights into common pathways and complex relationships among immune-mediated diseases. *Nature Reviews Genetics* (2013) 14(9):661-73. doi: 10.1038/nrg3502.
4. Sakaguchi S, Wing K, Onishi Y, Prieto-Martin P, Yamaguchi T. Regulatory T cells: how do they suppress immune responses? *International immunology* (2009) 21(10):1105-11.
5. Fontenot JD, Gavin MA, Rudensky AY. Foxp3 programs the development and function of CD4+CD25+ regulatory T cells. *Nat Immunol* (2003) 4(4):330-6. Epub 2003/03/04. doi: 10.1038/ni904.
6. Sakaguchi S. Naturally arising CD4+ regulatory t cells for immunologic self-tolerance and negative control of immune responses. *Annu Rev Immunol* (2004) 22:531-62. Epub 2004/03/23. doi: 10.1146/annurev.immunol.21.120601.141122.
7. Fontenot JD, Rudensky AY. A well adapted regulatory contrivance: regulatory T cell development and the forkhead family transcription factor Foxp3. *Nat Immunol* (2005) 6(4):331-7. Epub 2005/03/24. doi: 10.1038/ni1179.
8. Strioga M, Pasukoniene V, Characiejus D. CD8+ CD28- and CD8+ CD57+ T cells and their role in health and disease. *Immunology* (2011) 134(1):17-32.
9. Suci-Foca N, Manavalan JS, Scotto L, Kim-Schulze S, Galluzzo S, Naiyer AJ, et al. Molecular characterization of allospecific T suppressor and tolerogenic dendritic cells: review. *Int Immunopharmacol* (2005) 5(1):7-11. Epub 2004/12/14. doi: 10.1016/j.intimp.2004.09.003.
10. Vlad G, Cortesini R, Suci-Foca N. License to heal: bidirectional interaction of antigen-specific regulatory T cells and tolerogenic APC. *J Immunol* (2005) 174(10):5907-14. Epub 2005/05/10. doi: 10.4049/jimmunol.174.10.5907.
11. Vlad G, King J, Chang CC, Liu Z, Friedman RA, Torkamani AA, et al. Gene profile analysis of CD8(+) ILT3-Fc induced T suppressor cells. *Hum Immunol* (2011) 72(2):107-14. Epub 2010/10/27. doi: 10.1016/j.humimm.2010.10.012.
12. Buckner JH. Mechanisms of impaired regulation by CD4(+)CD25(+)FOXP3(+) regulatory T cells in human autoimmune diseases. *Nat Rev Immunol* (2010) 10(12):849-59. Epub 2010/11/26. doi: 10.1038/nri2889.
13. Dinesh RK, Skaggs BJ, La Cava A, Hahn BH, Singh RP. CD8+ Tregs in lupus, autoimmunity, and beyond. *Autoimmun Rev* (2010) 9(8):560-8. Epub 2010/04/14. doi: 10.1016/j.autrev.2010.03.006.
14. Fessler J, Felber A, Duftner C, Dejaco C. Therapeutic potential of regulatory T cells in autoimmune disorders. *BioDrugs* (2013) 27(4):281-91. Epub 2013/04/13. doi: 10.1007/s40259-013-0026-5.

15. Zaccane P, Cooke A. Harnessing CD8(+) regulatory T cells: therapy for type 1 diabetes? *Immunity* (2010) 32(4):504-6. Epub 2010/04/24. doi: 10.1016/j.immuni.2010.04.009.
16. Bluestone JA. Is CTLA-4 a master switch for peripheral T cell tolerance? *The Journal of Immunology* (1997) 158(5):1989-93.
17. Tivol EA, Borriello F, Schweitzer AN, Lynch WP, Bluestone JA, Sharpe AH. Loss of CTLA-4 leads to massive lymphoproliferation and fatal multiorgan tissue destruction, revealing a critical negative regulatory role of CTLA-4. *Immunity* (1995) 3(5):541-7. Epub 1995/11/01. doi: 10.1016/1074-7613(95)90125-6.
18. Kristiansen O, Larsen Z, Pociot F. CTLA-4 in autoimmune diseases—a general susceptibility gene to autoimmunity? *Genes & Immunity* (2000) 1(3):170-84.
19. Aggarwal BB. Signalling pathways of the TNF superfamily: a double-edged sword. *Nat Rev Immunol* (2003) 3(9):745-56. Epub 2003/09/02. doi: 10.1038/nri1184.
20. Bohana-Kashtan O, Civin CI. Fas ligand as a tool for immunosuppression and generation of immune tolerance. *Stem Cells* (2004) 22(6):908-24. doi: DOI 10.1634/stemcells.22-6-908.
21. Zhang X, Brunner T, Carter L, Dutton RW, Rogers P, Bradley L, et al. Unequal death in T helper cell (Th) 1 and Th2 effectors: Th1, but not Th2, effectors undergo rapid Fas/FasL-mediated apoptosis. *The Journal of experimental medicine* (1997) 185(10):1837-49.
22. Varadhachary AS, Perdow SN, Hu C, Ramanarayanan M, Salgame P. Differential ability of T cell subsets to undergo activation-induced cell death. *Proc Natl Acad Sci U S A* (1997) 94(11):5778-83. Epub 1997/05/27. doi: 10.1073/pnas.94.11.5778.
23. Pandiyan P, Zheng L, Ishihara S, Reed J, Lenardo MJ. CD4+ CD25+ Foxp3+ regulatory T cells induce cytokine deprivation-mediated apoptosis of effector CD4+ T cells. *Nature immunology* (2007) 8(12):1353-62.
24. Cao X, Cai SF, Fehniger TA, Song J, Collins LI, Piwnicka-Worms DR, et al. Granzyme B and perforin are important for regulatory T cell-mediated suppression of tumor clearance. *Immunity* (2007) 27(4):635-46. Epub 2007/10/09. doi: 10.1016/j.immuni.2007.08.014.
25. Gallucci S, Lolkema M, Matzinger P. Natural adjuvants: endogenous activators of dendritic cells. *Nat Med* (1999) 5(11):1249-55. Epub 1999/11/05. doi: 10.1038/15200.
26. Morelli AE, Thomson AW. Tolerogenic dendritic cells and the quest for transplant tolerance. *Nat Rev Immunol* (2007) 7(8):610-21. Epub 2007/07/14. doi: 10.1038/nri2132.
27. Stoop JN, Harry RA, von Delwig A, Isaacs JD, Robinson JH, Hilkens CM. Therapeutic effect of tolerogenic dendritic cells in established collagen - induced arthritis is associated with a reduction in Th17 responses. *Arthritis & Rheumatism* (2010) 62(12):3656-65.
28. Thomson AW, Robbins PD. Tolerogenic dendritic cells for autoimmune disease and transplantation. *Ann Rheum Dis* (2008) 67 Suppl 3(Suppl 3):iii90-6. Epub 2008/12/17. doi: 10.1136/ard.2008.099176.
29. Oderup C, Cederbom L, Makowska A, Cilio CM, Ivars F. Cytotoxic T lymphocyte antigen-4-dependent down-modulation of costimulatory

- molecules on dendritic cells in CD4+ CD25+ regulatory T-cell-mediated suppression. *Immunology* (2006) 118(2):240-9. Epub 2006/06/15. doi: 10.1111/j.1365-2567.2006.02362.x.
30. Grohmann U, Orabona C, Fallarino F, Vacca C, Calcinaro F, Falorni A, et al. CTLA-4-Ig regulates tryptophan catabolism in vivo. *Nature immunology* (2002) 3(11):1097-101.
 31. Fallarino F, Grohmann U, Hwang KW, Orabona C, Vacca C, Bianchi R, et al. Modulation of tryptophan catabolism by regulatory T cells. *Nat Immunol* (2003) 4(12):1206-12. Epub 2003/10/28. doi: 10.1038/ni1003.
 32. Liang B, Workman C, Lee J, Chew C, Dale BM, Colonna L, et al. Regulatory T cells inhibit dendritic cells by lymphocyte activation gene-3 engagement of MHC class II. *J Immunol* (2008) 180(9):5916-26. Epub 2008/04/22. doi: 10.4049/jimmunol.180.9.5916.
 33. McInnes IB, Schett G. The pathogenesis of rheumatoid arthritis. *N Engl J Med* (2011) 365(23):2205-19. Epub 2011/12/14. doi: 10.1056/NEJMra1004965.
 34. Gregersen PK, Silver J, Winchester RJ. The shared epitope hypothesis. An approach to understanding the molecular genetics of susceptibility to rheumatoid arthritis. *Arthritis Rheum* (1987) 30(11):1205-13. Epub 1987/11/01. doi: 10.1002/art.1780301102.
 35. Holoshitz J. The rheumatoid arthritis HLA-DRB1 shared epitope. *Curr Opin Rheumatol* (2010) 22(3):293-8. Epub 2010/01/12. doi: 10.1097/BOR.0b013e328336ba63.
 36. Cope AP, Schulze-Koops H, Aringer M. The central role of T cells in rheumatoid arthritis. *Clin Exp Rheumatol* (2007) 25(5 Suppl 46):S4-11. Epub 2007/11/21.
 37. Toh ML, Miossec P. The role of T cells in rheumatoid arthritis: new subsets and new targets. *Curr Opin Rheumatol* (2007) 19(3):284-8. Epub 2007/04/07. doi: 10.1097/BOR.0b013e32805e87e0.
 38. Nistala K, Wedderburn LR. Th17 and regulatory T cells: rebalancing pro- and anti-inflammatory forces in autoimmune arthritis. *Rheumatology (Oxford)* (2009) 48(6):602-6. Epub 2009/03/10. doi: 10.1093/rheumatology/kep028.
 39. Wang W, Shao S, Jiao Z, Guo M, Xu H, Wang S. The Th17/Treg imbalance and cytokine environment in peripheral blood of patients with rheumatoid arthritis. *Rheumatol Int* (2012) 32(4):887-93. Epub 2011/01/12. doi: 10.1007/s00296-010-1710-0.
 40. Davignon JL, Hayder M, Baron M, Boyer JF, Constantin A, Apparailly F, et al. Targeting monocytes/macrophages in the treatment of rheumatoid arthritis. *Rheumatology (Oxford)* (2013) 52(4):590-8. Epub 2012/12/04. doi: 10.1093/rheumatology/kes304.
 41. Albani S, Koffeman EC, Prakken B. Induction of immune tolerance in the treatment of rheumatoid arthritis. *Nat Rev Rheumatol* (2011) 7(5):272-81. Epub 2011/04/07. doi: 10.1038/nrrheum.2011.36.
 42. Ehrenstein MR, Evans JG, Singh A, Moore S, Warnes G, Isenberg DA, et al. Compromised function of regulatory T cells in rheumatoid arthritis and reversal by anti-TNF α therapy. *Journal of Experimental Medicine* (2004) 200(3):277-85.

43. Nadkarni S, Mauri C, Ehrenstein MR. Anti-TNF- α therapy induces a distinct regulatory T cell population in patients with rheumatoid arthritis via TGF- β . *The Journal of experimental medicine* (2007) 204(1):33-9.
44. Rubbert-Roth A. Assessing the safety of biologic agents in patients with rheumatoid arthritis. *Rheumatology (Oxford)* (2012) 51 Suppl 5(suppl_5):v38-47. Epub 2012/06/29. doi: 10.1093/rheumatology/kes114.
45. Maahs DM, West NA, Lawrence JM, Mayer-Davis EJ. Epidemiology of type 1 diabetes. *Endocrinol Metab Clin North Am* (2010) 39(3):481-97. Epub 2010/08/21. doi: 10.1016/j.ecl.2010.05.011.
46. Patterson C, Guariguata L, Dahlquist G, Soltész G, Ogle G, Silink M. Diabetes in the young—a global view and worldwide estimates of numbers of children with type 1 diabetes. *Diabetes research and clinical practice* (2014) 103(2):161-75.
47. Patterson CC, Dahlquist GG, Gyürüs E, Green A, Soltész G, Group ES. Incidence trends for childhood type 1 diabetes in Europe during 1989–2003 and predicted new cases 2005–20: a multicentre prospective registration study. *The Lancet* (2009) 373(9680):2027-33.
48. Erlich H, Valdes AM, Noble J, Carlson JA, Varney M, Concannon P, et al. HLA DR-DQ haplotypes and genotypes and type 1 diabetes risk: analysis of the type 1 diabetes genetics consortium families. *Diabetes* (2008) 57(4):1084-92. Epub 2008/02/07. doi: 10.2337/db07-1331.
49. Arif S, Tree TI, Astill TP, Tremble JM, Bishop AJ, Dayan CM, et al. Autoreactive T cell responses show proinflammatory polarization in diabetes but a regulatory phenotype in health. *Journal of Clinical Investigation* (2004) 113(3):451-63. doi: 10.1172/Jci200419585.
50. Lindley S, Dayan CM, Bishop A, Roep BO, Peakman M, Tree TI. Defective suppressor function in CD4(+)CD25(+) T-cells from patients with type 1 diabetes. *Diabetes* (2005) 54(1):92-9. Epub 2004/12/24. doi: 10.2337/diabetes.54.1.92.
51. Haseda F, Imagawa A, Murase - Mishiba Y, Terasaki J, Hanafusa T. CD4(+) CD45RA(-) FoxP3^{high} activated regulatory T cells are functionally impaired and related to residual insulin - secreting capacity in patients with type 1 diabetes. *Clinical & Experimental Immunology* (2013) 173(2):207-16.
52. van Belle TL, Coppieters KT, von Herrath MG. Type 1 diabetes: etiology, immunology, and therapeutic strategies. *Physiol Rev* (2011) 91(1):79-118. Epub 2011/01/21. doi: 10.1152/physrev.00003.2010.
53. Greenbaum C, Atkinson MA. *Persistence is the twin sister of excellence: an important lesson for attempts to prevent and reverse type 1 diabetes*. Am Diabetes Assoc (2011).
54. von Herrath M, Peakman M, Roep B. Progress in immune-based therapies for type 1 diabetes. *Clin Exp Immunol* (2013) 172(2):186-202. Epub 2013/04/12. doi: 10.1111/cei.12085.
55. Sherry N, Hagopian W, Ludvigsson J, Jain SM, Wahlen J, Ferry Jr RJ, et al. Teplizumab for treatment of type 1 diabetes (Protégé study): 1-year results from a randomised, placebo-controlled trial. *The Lancet* (2011) 378(9790):487-97.
56. Bach JF. Anti-CD3 antibodies for type 1 diabetes: beyond expectations. *Lancet* (2011) 378(9790):459-60. Epub 2011/07/02. doi: 10.1016/S0140-6736(11)60980-X.

57. Palmares J, Castro-Correia J, Coutinho MF, Mendes A, Delgado L. HLA and idiopathic uveitis. *Ocul Immunol Inflamm* (1993) 1(1-2):179-85. Epub 1993/01/01. doi: 10.3109/09273949309086557.
58. LeHoang P, Ozdemir N, Benhamou A, Tabary T, Edelson C, Betuel H, et al. HLA-A29.2 subtype associated with birdshot retinochoroidopathy. *Am J Ophthalmol* (1992) 113(1):33-5. Epub 1992/01/15. doi: 10.1016/s0002-9394(14)75749-6.
59. Davis JL, Mittal KK, Freidlin V, Mellow SR, Optican DC, Palestine AG, et al. HLA associations and ancestry in Vogt-Koyanagi-Harada disease and sympathetic ophthalmia. *Ophthalmology* (1990) 97(9):1137-42. Epub 1990/09/01. doi: 10.1016/s0161-6420(90)32446-6.
60. Brewerton D, NICHOLS A, CAFFREY M, Walters D, James D. O. (1973). Acute anterior uveitis and HLA 27. *Lancet* 2:994
61. Khan MA. Polymorphism of HLA-B27: 105 subtypes currently known. *Curr Rheumatol Rep* (2013) 15(10):362. Epub 2013/08/31. doi: 10.1007/s11926-013-0362-y.
62. Chang JH, McCluskey PJ, Wakefield D. Acute anterior uveitis and HLA-B27. *Surv Ophthalmol* (2005) 50(4):364-88. Epub 2005/06/22. doi: 10.1016/j.survophthal.2005.04.003.
63. Li H, Li Q, Ji C, Gu J. Ankylosing Spondylitis Patients with HLA-B*2704 have More Uveitis than Patients with HLA-B*2705 in a North Chinese Population. *Ocul Immunol Inflamm* (2018) 26(1):65-9. Epub 2016/07/19. doi: 10.1080/09273948.2016.1188967.
64. Konno Y, Numaga J, Tsuchiya N, Ogawa A, Islam SM, Mochizuki M, et al. HLA-B27 subtypes and HLA class II alleles in Japanese patients with anterior uveitis. *Invest Ophthalmol Vis Sci* (1999) 40(8):1838-44. Epub 1999/07/07.
65. Linssen A, Meenken C. Outcomes of HLA-B27-positive and HLA-B27-negative acute anterior uveitis. *Am J Ophthalmol* (1995) 120(3):351-61. Epub 1995/09/01. doi: 10.1016/s0002-9394(14)72165-8.
66. Khan MA, Kushner I, Braun WE. Comparison of clinical features in HLA-B27 positive and negative patients with ankylosing spondylitis. *Arthritis Rheum* (1977) 20(4):909-12. Epub 1977/05/01. doi: 10.1002/art.1780200401.
67. Bodaghi B, Touitou V, Fardeau C, Chapelon C, LeHoang P. Ocular sarcoidosis. *Presse Med* (2012) 41(6 Pt 2):e349-54. Epub 2012/05/19. doi: 10.1016/j.lpm.2012.04.004.
68. Bloch-Michel E, Frau E. Birdshot retinochoroidopathy and HLA-A29+ and HLA-A29-idiopathic retinal vasculitis: comparative study of 56 cases. *Canadian journal of ophthalmology Journal canadien d'ophtalmologie* (1991) 26(7):361-6.
69. Holdsworth R, Hurley C, Marsh S, Lau M, Noreen H, Kempenich J, et al. The HLA dictionary 2008: a summary of HLA - A, - B, - C, - DRB1/3/4/5, and - DQB1 alleles and their association with serologically defined HLA - A, - B, - C, - DR, and - DQ antigens. *Tissue antigens* (2009) 73(2):95-170.
70. Cao K, Hollenbach J, Shi XJ, Shi WX, Chopek M, Fernandez-Vina MA. Analysis of the frequencies of HLA-A, B, and C alleles and haplotypes in the five major ethnic groups of the United States reveals high levels of diversity in these loci and contrasting distribution patterns in these populations.

- Human Immunology* (2001) 62(9):1009-30. doi: Doi 10.1016/S0198-8859(01)00298-1.
71. Kaya TI. Genetics of Behçet's disease. *Pathology research international* (2012) 2012.
 72. Arber N, Klein T, Meiner Z, Pras E, Weinberger A. Close association of HLA-B51 and B52 in Israeli patients with Behcet's syndrome. *Ann Rheum Dis* (1991) 50(6):351-3. Epub 1991/06/01. doi: 10.1136/ard.50.6.351.
 73. Zhang L, Wan F, Song J, Tang K, Zheng F, Guo J, et al. Imbalance Between Th17 Cells and Regulatory T Cells During Monophasic Experimental Autoimmune Uveitis. *Inflammation* (2016) 39(1):113-22. Epub 2015/08/25. doi: 10.1007/s10753-015-0229-7.
 74. Zhuang Z, Wang Y, Zhu G, Gu Y, Mao L, Hong M, et al. Imbalance of Th17/Treg cells in pathogenesis of patients with human leukocyte antigen B27 associated acute anterior uveitis. *Sci Rep* (2017) 7(1):40414. Epub 2017/01/17. doi: 10.1038/srep40414.
 75. Takeda A, Sonoda K-H, Ishibashi T. Regulation of Th1 and Th17 cell differentiation in uveitis. *Inflammation and Regeneration* (2013) 33(5):261-8. doi: 10.2492/inflammregen.33.261.
 76. Pockley AG, Muthana M, Calderwood SK. The dual immunoregulatory roles of stress proteins. *Trends Biochem Sci* (2008) 33(2):71-9. Epub 2008/01/10. doi: 10.1016/j.tibs.2007.10.005.
 77. Asea A, Kraeft SK, Kurt-Jones EA, Stevenson MA, Chen LB, Finberg RW, et al. HSP70 stimulates cytokine production through a CD14-dependant pathway, demonstrating its dual role as a chaperone and cytokine. *Nature Medicine* (2000) 6(4):435-42.
 78. van Eden W, Spiering R, Broere F, van der Zee R. A case of mistaken identity: HSPs are no DAMPs but DAMPERs. *Cell Stress and Chaperones* (2012) 17(3):281-92.
 79. Bausinger H, Lipsker D, Ziylan U, Manie S, Briand JP, Cazenave JP, et al. Endotoxin-free heat-shock protein 70 fails to induce APC activation. *Eur J Immunol* (2002) 32(12):3708-13. Epub 2003/01/09. doi: 10.1002/1521-4141(200212)32:12<3708::AID-IMMU3708>3.0.CO;2-C.
 80. Bendz H, Marincek BC, Momburg F, Ellwart JW, Issels RD, Nelson PJ, et al. Calcium signaling in dendritic cells by human or mycobacterial Hsp70 is caused by contamination and is not required for Hsp70-mediated enhancement of cross-presentation. *J Biol Chem* (2008) 283(39):26477-83. Epub 2008/07/29. doi: 10.1074/jbc.M803310200.
 81. Zanin-Zhorov A, Nussbaum G, Franitza S, Cohen IR, Lider O. T cells respond to heat shock protein 60 via TLR2: activation of adhesion and inhibition of chemokine receptors. *FASEB J* (2003) 17(11):1567-9. Epub 2003/06/26. doi: 10.1096/fj.02-1139fje.
 82. Asea A, Rehli M, Kabingu E, Boch JA, Bare O, Auron PE, et al. Novel signal transduction pathway utilized by extracellular HSP70: role of toll-like receptor (TLR) 2 and TLR4. *J Biol Chem* (2002) 277(17):15028-34. Epub 2002/02/12. doi: 10.1074/jbc.M200497200.
 83. Quintana FJ, Cohen IR. The HSP60 immune system network. *Trends Immunol* (2011) 32(2):89-95. Epub 2010/12/15. doi: 10.1016/j.it.2010.11.001.
 84. Munk ME, Schoel B, Modrow S, Karr RW, Young RA, Kaufmann SH. T lymphocytes from healthy individuals with specificity to self-epitopes shared

- by the mycobacterial and human 65-kilodalton heat shock protein. *J Immunol* (1989) 143(9):2844-9. Epub 1989/11/01.
85. Pockley AG, Bulmer J, Hanks BM, Wright BH. Identification of human heat shock protein 60 (Hsp60) and anti-Hsp60 antibodies in the peripheral circulation of normal individuals. *Cell Stress Chaperones* (1999) 4(1):29-35. Epub 1999/09/01. doi: 10.1054/csac.1998.0121.
 86. van Eden W, van der Zee R, Paul AG, Prakken BJ, Wendling U, Anderton SM, et al. Do heat shock proteins control the balance of T-cell regulation in inflammatory diseases? *Immunology today* (1998) 19(7):303-7.
 87. van Eden W, van Herwijnen M, Wagenaar J, van Kooten P, Broere F, van der Zee R. Stress proteins are used by the immune system for cognate interactions with anti-inflammatory regulatory T cells. *FEBS letters* (2013) 587(13):1951-8.
 88. Wieten L, Broere F, van der Zee R, Koerkamp EK, Wagenaar J, van Eden W. Cell stress induced HSP are targets of regulatory T cells: a role for HSP inducing compounds as anti-inflammatory immuno-modulators? *FEBS letters* (2007) 581(19):3716-22.
 89. van Eden W, Thole JE, van der Zee R, Noordzij A, van Embden JD, Hensen EJ, et al. Cloning of the mycobacterial epitope recognized by T lymphocytes in adjuvant arthritis. *Nature* (1988) 331(6152):171-3. Epub 1988/01/14. doi: 10.1038/331171a0.
 90. Anderton SM, van der Zee R, Prakken B, Noordzij A, van Eden W. Activation of T cells recognizing self 60-kD heat shock protein can protect against experimental arthritis. *J Exp Med* (1995) 181(3):943-52. Epub 1995/03/01. doi: 10.1084/jem.181.3.943.
 91. van Herwijnen MJ, Wieten L, van der Zee R, van Kooten PJ, Wagenaar-Hilbers JP, Hoek A, et al. Regulatory T cells that recognize a ubiquitous stress-inducible self-antigen are long-lived suppressors of autoimmune arthritis. *Proceedings of the National Academy of Sciences* (2012) 109(35):14134-9.
 92. Paludan C, Schmid D, Landthaler M, Vockerodt M, Kube D, Tuschl T, et al. Endogenous MHC class II processing of a viral nuclear antigen after autophagy. *Science* (2005) 307(5709):593-6. Epub 2004/12/14. doi: 10.1126/science.1104904.
 93. Dengjel J, Schoor O, Fischer R, Reich M, Kraus M, Muller M, et al. Autophagy promotes MHC class II presentation of peptides from intracellular source proteins. *Proc Natl Acad Sci U S A* (2005) 102(22):7922-7. Epub 2005/05/17. doi: 10.1073/pnas.0501190102.
 94. Wieten L, van der Zee R, Spiering R, Wagenaar-Hilbers J, van Kooten P, Broere F, et al. A novel heat-shock protein coinducer boosts stress protein Hsp70 to activate T cell regulation of inflammation in autoimmune arthritis. *Arthritis Rheum* (2010) 62(4):1026-35. Epub 2010/02/05. doi: 10.1002/art.27344.
 95. Wieten L, van der Zee R, Goedemans R, Sijtsma J, Serafini M, Lubsen NH, et al. Hsp70 expression and induction as a readout for detection of immune modulatory components in food. *Cell Stress Chaperones* (2010) 15(1):25-37. Epub 2009/05/28. doi: 10.1007/s12192-009-0119-8.
 96. van Loosdregt J, Fleskens V, Tiemessen MM, Mokry M, van Boxtel R, Meerding J, et al. Canonical Wnt signaling negatively modulates regulatory T

- cell function. *Immunity* (2013) 39(2):298-310. Epub 2013/08/21. doi: 10.1016/j.immuni.2013.07.019.
97. Spierings J, van Eden W. Heat shock proteins and their immunomodulatory role in inflammatory arthritis. *Rheumatology (Oxford)* (2017) 56(2):198-208. Epub 2016/07/15. doi: 10.1093/rheumatology/kew266.
98. Barbera A, Broereb F, van Eden W. Heat shock proteins as target for the induction of antigen-specific tolerance in rheumatoid arthritis and other chronic inflammatory diseases. *T cell targeted interventions in experimental autoimmunity* (2015):25.
99. Zonneveld-Huijssoon E, Albani S, Prakken BJ, van Wijk F. Heat shock protein bystander antigens for peptide immunotherapy in autoimmune disease. *Clin Exp Immunol* (2013) 171(1):20-9. Epub 2012/12/04. doi: 10.1111/j.1365-2249.2012.04627.x.
100. Albani S, Keystone EC, Nelson JL, Ollier WE, La Cava A, Montemayor AC, et al. Positive selection in autoimmunity: abnormal immune responses to a bacterial dnaJ antigenic determinant in patients with early rheumatoid arthritis. *Nat Med* (1995) 1(5):448-52. Epub 1995/05/01. doi: 10.1038/nm0595-448.
101. Albani S, Tuckwell JE, Esparza L, Carson DA, Roudier J. The susceptibility sequence to rheumatoid arthritis is a cross-reactive B cell epitope shared by the Escherichia coli heat shock protein dnaJ and the histocompatibility leukocyte antigen DRB10401 molecule. *J Clin Invest* (1992) 89(1):327-31. Epub 1992/01/01. doi: 10.1172/JCI115580.
102. Koffeman EC, Genovese M, Amox D, Keogh E, Santana E, Matteson EL, et al. Epitope-specific immunotherapy of rheumatoid arthritis: clinical responsiveness occurs with immune deviation and relies on the expression of a cluster of molecules associated with T cell tolerance in a double-blind, placebo-controlled, pilot phase II trial. *Arthritis Rheum* (2009) 60(11):3207-16. Epub 2009/10/31. doi: 10.1002/art.24916.
103. Shields AM, Panayi GS, Corrigall VM. A New-Age for Biologic Therapies: Long-Term Drug-Free Therapy with BiP? *Front Immunol* (2012) 3:17. Epub 2012/05/09. doi: 10.3389/fimmu.2012.00017.
104. Kirkham B, Chaabo K, Hall C, Garrood T, Mant T, Allen E, et al. Safety and patient response as indicated by biomarker changes to binding immunoglobulin protein in the phase I/IIA RAGULA clinical trial in rheumatoid arthritis. *Rheumatology (Oxford)* (2016) 55(11):1993-2000. Epub 2016/08/09. doi: 10.1093/rheumatology/kew287.
105. Schloot NC, Cohen IR. DiaPep277® and immune intervention for treatment of type 1 diabetes. *Clinical Immunology* (2013) 149(3):307-16.
106. Raz I, Elias D, Avron A, Tamir M, Metzger M, Cohen IR. Beta-cell function in new-onset type 1 diabetes and immunomodulation with a heat-shock protein peptide (DiaPep277): a randomised, double-blind, phase II trial. *Lancet* (2001) 358(9295):1749-53. Epub 2001/12/06. doi: 10.1016/S0140-6736(01)06801-5.
107. Bell GM, Anderson AE, Diboll J, Reece R, Eltherington O, Harry RA, et al. Autologous tolerogenic dendritic cells for rheumatoid and inflammatory arthritis. *Ann Rheum Dis* (2017) 76(1):227-34. Epub 2016/04/28. doi: 10.1136/annrheumdis-2015-208456.

3



Leucinostatin acts as a co-inducer for Heat Shock Protein 70 in cultured canine retinal pigment epithelial cells

Qingkang Lyu, Irene S. Ludwig, Peter J. S. Kooten, Alice J. A. M. Sijts, Victor P. M. G. Rutten[†], Willem van Eden, Femke Broere*

Department of Infectious Diseases and Immunology, Faculty of Veterinary Medicine, Utrecht University; Yalelaan 1, Utrecht, The Netherlands

[†]Department of Veterinary Tropical Diseases, Faculty of Veterinary Science, Pretoria University, South Africa

*Corresponding author: f.broere@uu.nl.

Cell Stress and Chaperones 25.2 (2020): 235-243

Abstract

Dysregulation of retinal pigment epithelium (RPE) cells is the main cause of a variety of ocular diseases. Potentially heat shock proteins, by preventing molecular and cellular damage and modulating inflammatory disease, may exert a protective role in eye disease. In particular, the inducible form of heat shock protein 70 (Hsp70) is widely upregulated in inflamed tissues, and in vivo upregulation of Hsp70 expression by HSP co-inducing compounds has been shown to be a potential therapeutic strategy for inflammatory diseases. In order to gain further understanding of the potential protective effects of Hsp70 in RPE cells, we developed a method for isolation and culture of canine RPE cells. Identity of RPE cells was confirmed by detection of its specific marker, RPE65, in qPCR, flow cytometry and immunocytochemistry analysis. The ability of RPE cells to express Hsp70 upon experimental induction of cell stress, by arsenite, was analyzed by flow cytometry. Finally, in search of a potential Hsp70 co-inducer, we investigated whether the compound leucinostatin could enhance Hsp70 expression in stressed RPE cells. Canine RPE cells were isolated and cultured successfully. Purity of cells that strongly expressed RPE65 was over 90%. Arsenite-induced stress led to a time- and dose-dependent increase in Hsp70 expression in canine RPE cells in vitro. In addition, leucinostatin, which enhanced heat shock factor-1-induced transcription from the heat shock promoter in DNAJB1-luc-O23 reporter cell line, also enhanced Hsp70 expression in arsenite-stressed RPE cells, in a dose-dependent fashion. These findings demonstrate that leucinostatin can boost Hsp70 expression in canine RPE cells, most likely by activating heat shock factor-1, suggesting that leucinostatin might be applied as a new co-inducer for Hsp70 expression.

Keywords: Retinal pigment epithelial cell, Leucinostatin, Heat shock protein 70, Canine

Introduction

The retinal pigment epithelium (RPE) is a single layer of polarized pigmented cells, in between the retina and the choroid, which originated from the neural ectoderm (1). RPE cells play a critical role in the protection of retina function and vision of the eye: they nourish photoreceptors, absorb stray light, and engulf and degrade shed photoreceptor outer segments. As part of the blood-retina barrier, RPE cells also have a crucial role in maintaining the immune privilege of the eye, and in modulating local immune responses. Dysregulation and death of RPE cells is thought to contribute to a number of ocular disorders, such as age related macular degeneration (AMD) (2), diabetic retinopathy (3) and uveitis (4). Eye diseases detected in dogs, in veterinary clinics, are quite similar to those found in human patients. Therefore, diseased dogs may serve as an excellent model to study potential treatments, also for human diseases. So far, there are no effective strategies to cure these eye diseases, in neither humans nor dogs. Therefore, a search for novel and effective agents to modulate and regenerate RPE cell functionality is needed.

Heat shock protein 70 (HSPA1A, HSPA1B), which is a member of a major heat shock protein family, is highly conserved, and ubiquitously expressed during cell stress. Hsp70 has been implicated in T cell regulation of various chronic inflammatory diseases, including Rheumatoid arthritis (5), colitis (6), neurodegenerative diseases (7) and experimental autoimmune uveoretinitis (8), which makes the molecule a potential therapeutic target in chronic inflammations. Moreover, over-expression of Hsp70 was reported to play an essential role in regulation of apoptosis (9, 10) and protection against inflammation (11).

In clinical ophthalmology, retinal laser therapy such as laser photocoagulation and non-damaging retinal laser therapy (NRT) are widely used, to treat various retinal diseases. Studies on therapeutic mechanisms of retinal laser therapy showed that Hsp70 was substantially induced in laser target sites of ARPE cells (12) and the RPE layer of the rabbit model (13, 14). Such upregulated Hsp70 may be involved in the improvement of the physiological function of RPE cells. Consequently, boosting of Hsp70 expression in RPE cells has been proposed as a possible therapeutic strategy in eye diseases. Currently, pharmacological co-induction of Hsp70 by food- or herb-derived compounds shows great promise in the battle against chronic inflammatory diseases, by enhancing the physiological Hsp70 response. It has been reported that HSP co-inducers, such as Bimoclolmol, Geranylgeranylacetone (GGA) and celastrol, have a beneficial effect in the treatment of various inflammatory diseases by boosting HSP expression in experimental animal models, such as cerebrovascular disorders (15), neurodegenerative diseases (16), and uveitis (8).

Transcription of HSPs is regulated by the heat shock transcription factor 1 (HSF1). Under normal conditions, HSF1 is in an inactive state in the cytoplasm where it stays bound to Hsp70, Hsp90 and Hsp40. Upon stress, HSF1 undergoes nuclear translocation, binds to heat shock promoter elements, and induces transcription of heat shock genes (HSE). So far, compounds that increase HSP expression in canine RPE cells and the mechanisms involved have not been studied.

Aiming at a potential model for modulating HSP70 expression in dogs, as a target and model species, we successfully isolated and cultured canine RPE. We observed that arsenite-stress induced a time and dose-dependent increase in Hsp70 expression in RPE cells in vitro, and that leucinostatin, an antimicrobial and antitumor antibiotic produced by the fungus *Paecilomyces lilacinus*, enhanced Hsp70 expression in arsenite-stressed cells in a dose-dependent fashion. In the present study, we thus identify a novel compound, leucinostatin, that can boost Hsp70 expression by activating heat shock factor-1.

Materials and methods

Animals

All dogs used in the experiments were owned by the Department of Clinical Science of Companion Animals of the Faculty of Veterinary Medicine, Utrecht University. The breeds of dogs included beagle and mongrel dogs. Eyes were isolated from healthy dogs, without any eye diseases, that were euthanized for unrelated purposes. This study was approved by the Utrecht University animal experiments committee (approval number: AVD115002016531).

Dog RPE isolation and culture

To purify primary RPE cells from dogs, eyes were taken out and placed in DMEM medium with penicillin-streptomycin and 10% bovine serum, and connective tissue was removed. Then, eyes were washed successively with 70% ethanol, penicillin-streptomycin, and PBS. Afterwards, the anterior segment of the eye was removed along the ora serrata. Vitreous in the eye cup was pushed out as much as possible and the eye cup was filled with 2 ml of PBS with 1 mM EDTA (pre-warmed to 37 °C), placed in a well of a 12-well tissue culture plate, and put in the incubator (37 °C and 5% CO₂) for 20-30 min, to loosen the neural retina. Then the retina was peeled off gently and the eye cup was refilled with 3 ml of pre-warmed 0.05% trypsin (Gibco), and incubated for another 30-40 min at 37 °C. RPE cells were harvested by gentle pipetting. Cells were seeded in T-75 tissue culture flasks and expanded at 37 °C with 5% CO₂ in DMEM (Gibco, Cat. No.: 31966021) containing 10% FBS, 100 units/mL

penicillin and 100 µg/ml streptomycin, non-essential amino acids and 1 ng/mL epidermal growth factor (SIGMA-ALDRICH, Cat. No.: E417). Cells were passaged at 80% confluency.

The DNAJB1-Luc-O23 reporter cell line and luciferase assays

The DNAJB1-Luc-O23 cell line, a generous gift of Kampinga HH (17, 18), was grown in DMEM supplemented with 10% FBS, 100 units/mL penicillin and 100 µg/mL streptomycin, and 1 mg/mL hygromycin (Roche Diagnostics GmbH), in an 37 °C incubator with 5% CO₂.

After trypsinization, DNAJB-Luc-O23 cells were seeded into the wells of a white µClear 96-well plate (Greiner Bio-one, 1.5×10⁴ cells/well), and placed in DMEM medium with 10% FBS, 100 U/ml penicillin and 100 µg/ml streptomycin. After 24 h, leucinostatin and sodium arsenite were added at specified concentrations (Fig. 7) and after o/n incubation, luciferase activity was measured with a Promega Steady-Glo Luciferase Assay System using a LB960 Microplate Luminometer (Berthold Technologies), according to manufacturer's instruction.

Quantitative real time PCR

RPE cells were harvested at passage 1, 2, 3 and 4. Total RNA was isolated using an RNeasy kit (Qiagen, Venlo, the Netherlands), according to the manufacturer's instructions, followed by DNase treatment. RNA concentrations were measured using a Nano-drop-1000 spectrophotometer, and mRNA was reverse-transcribed to cDNA using an iScript™ cDNA Synthesis Kit (Bio-Rad) and Bio-Rad Thermal Cycler, according to manufacturer's instructions.

Primers for RPE65 were synthesized by Invitrogen (Forward primer: 5'-GCC TCG TCA AGC CTT TGA GT-3'. Reverse primer: 5'-CTG ATG GGT ATG AGT CGG GC-3'). Quantitative PCR to detect RPE65 expression in RPE cells was performed using iQ™ SYBR Green Supermix (Bio-Rad) and 0.4 µM of RPE65 primers, applying the following cycle parameters: 3 min at 95 °C, followed by 40 cycles of 20 s at 95 °C and 45 s at 60 °C (Bio-Rad CFX Connect real time system). Relative expression of mRNA was calculated by the Pfaffl-method using the housekeeping gene RPS19, encoding the Ribosomal Protein S19, as a reference (Forward primer: 5'-CCT TCC TCA AAA AGT CTG GG-3' Reverse primer: 5'-GTT CTC ATC GTA GGG AGC AAG-3').

Hsp70 induction in RPE cells

RPE cells were seeded in 12-well plates ($2 - 4 \times 10^5$ cells/well) and cultured at 37 °C o/n. At the second day, the medium was refreshed, and cells were incubated with carvacrol (SIGMA-ALDRICH, Cat. No. 499-75-2) or leucinoastatin (SIGMA-ALDRICH, Cat. No: SML1566) dissolved in vehicle (ethanol and DMSO respectively) at the concentrations indicated in the figures (Fig 4, 5, 6, and 7). Control cultures were incubated with medium or vehicle alone. After 2 h, sodium arsenite was added to the cultures, at the concentrations indicated in the Figs. 4, 5, 6, and 7. Cells were collected after time intervals of 4, 8, 16, or 32 h, and Hsp70 expression was analyzed as described below.

Flow cytometric analysis of Hsp70 and RPE 65 expression

For analysis of intracellular Hsp70 expression, cells were fixed and permeabilized for 30 min in Cytofix/Cytoperm solution (BD Pharmingen), washed, and then incubated with either a fluorescein isothiocyanate-labeled monoclonal antibody (SPA-810; Stressgen) to specifically detect inducible Hsp70 (HSPA1A/HSPA1B), or with the corresponding isotype control antibody, in Perm/Wash (BD Pharmingen) supplemented with 2% normal mouse serum. For analysis of intracellular RPE65 expression, cells were collected at passage 1, 2, or 3, and fixed and permeabilized as above. Then RPE cells were stained with an RPE65 monoclonal antibody for 30 min. Afterwards, cells were washed two times and incubated with Goat anti-mouse IgG(H+L)-PE. For final analysis of fluorescence, a FACS Canto (BD Pharmingen) flow cytometer was used.

Immunocytochemistry

Cells (1×10^5 cells/well) were grown on Lab-Tek II chamber slides overnight to let them attach, and then fixed in 4% paraformaldehyde (PFA) in PBS for 10 min at room temperature. After that, cells were washed three times with ice-cold PBS and permeabilized with Perm/Wash (BD Pharmingen) for 30 min. Subsequently, cells were blocked with 3% dog serum in prewash at room temperature for 60 min. Then cells were incubated with anti-mouse RPE65 (1:100, Invitrogen, Cat. No. MA1-16578) overnight at 4 °C. Cells were washed three times, 5 min each, with Perm/Wash to remove unbound antibodies and incubated for 30 min at room temperature with anti-mouse AlexaFluor 488 (life technologies, Cat. No. A21121) 1:400 diluted in Perm/Wash. Afterwards, cells were washed three times and mounted with 40, 60-diamino-2-phenylindole (DAPI) mounting medium to stain the cell nuclei. Finally, cells were imaged with a fluorescence microscope.

Statistical analysis

GraphPad Prism 7.04 (GraphPad Software, La Jolla, CA, USA) was used for statistical analyses and graphical display of the data. For multiple comparisons, one-way or two-way ANOVA tests with Bonferroni correction were used. *P* values below 0.05 were considered statistically significant.

Results

Characterization of cultured dog RPE cells

Although most studies describe the isolation of RPE cells by peeling the RPE sheet from the choroid (19, 20), it has proven to be challenging to obtain pure populations of RPE cells, due to firm attachment to the Bruch's membrane and choroid. Therefore, we developed a method that does not rely on peeling off the RPE layer. To this end, the eye anterior segment and neural retina were removed, and then trypsin was added directly into the remaining posterior eye cup to digest the RPE layer, as described in "Materials and Methods." A few hours after seeding into the flasks, most of the RPE cells had attached (Fig. 1, day 1). Primary cultures of dog RPE cells grew as hexagonal, pigmented cells, and reached confluency after 8 days of culture. However, RPE cell pigmentation reduced with the number of cell divisions (Fig. 1, day 3 and day 8).

To test the RPE cell cultures for expression of the RPE cell-specific marker RPE65, primary cells in passage 1 were harvested and allowed to adhere to a coverslip. Then, cells were fixed and stained for immunofluorescence analysis. As shown in Fig. 2c, over 90% of canine RPE cells expressed the cytoplasmic RPE65 protein, in contrast to control, primary canine fibroblasts (Fig. 2b).

To assess RPE65 expression in dog primary RPE cells, at different passages, we collected cells at passage 1, 2, 3, and 4 and measured RPE65 expression at protein and mRNA levels (Fig. 3). The percentage of RPE65 positive cells detected by flow cytometry (Fig. 3a, b) was approximately 95% in passage 1, and then decreased with increasing number of cell passage, which was in line with RPE65 mRNA expression in the different passages (Fig. 3c).

Hence it was shown that the alternative RPE cell isolation method employed yielded a highly homogenous population of canine RPE cells, expressing RPE65 protein in passage 1. RPE65 expression however was gradually lost over time of culture, to approximately 10% of initial expression level in passage 4.

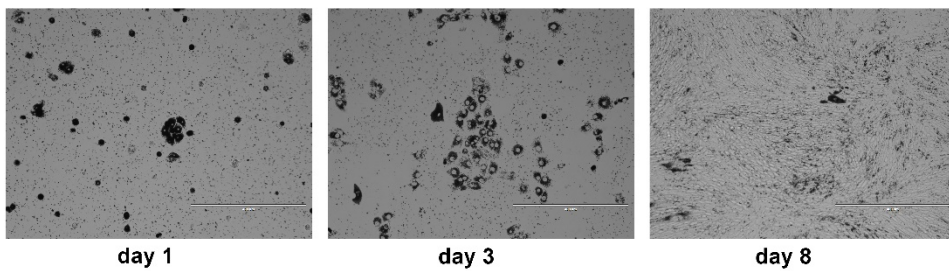


Fig. 1 Isolation of primary RPE cells from dog eyes. Light micrographs of RPE cells at 1, 3, and 8 days after plating. Scale bar: 400 μ m

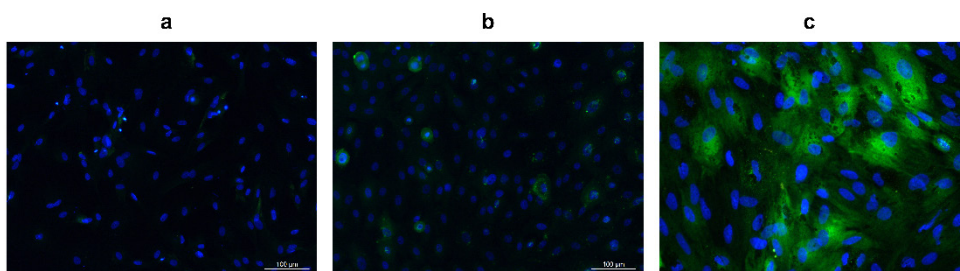


Fig. 2 Expression of RPE65 protein in cultured dog RPE cells. Cells (in passage 1) were fixed and stained with RPE65 antibody to label RPE65 protein (green) and DAPI to label nuclei (blue). **a**, DAPI was used to visualize cell nuclei in RPE cells; **b**, RPE65 expression in canine epidermal keratinocytes (MSECK), as control group; **c**, RPE65 expression in dog primary RPE cells.

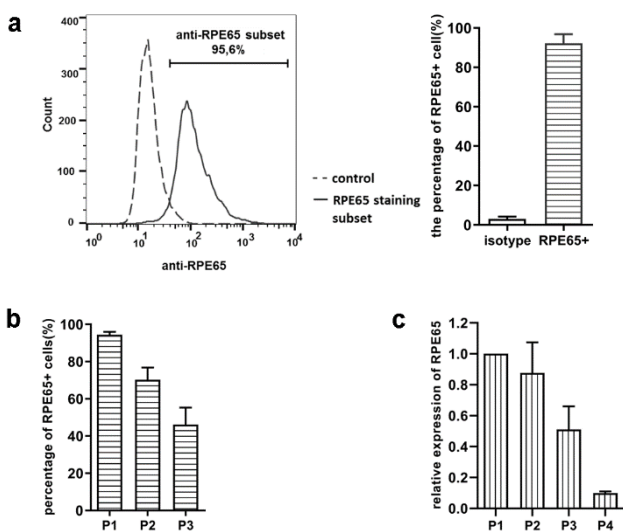


Fig. 3 RPE65 protein expression analysis in different passages of dog primary RPE cells. RPE cells were stained with anti-RPE65 MoAb and analyzed by flow cytometry. **a**, Representative histogram (left) of the percentage of RPE65 expressing cells in dog RPE cell cultures in passage 1; the bar-graph (right) shows the mean of three independent experiments; **b**, Percentage of RPE65 protein expressing cells in passages 1, 2, and 3; **c**, gene expression comparison among different passages of cultured RPE cells (passage 1, 2, 3, and 4). RPE65 expression in passage 1 was regarded as maximum expression. Representative results from three separate experiments.

Hsp70 production is induced in arsenite-stressed canine RPE cells

To study whether stress upregulated Hsp70 production in RPE cells, the well-known stressor arsenite was chosen. Primary canine RPE cells were exposed to different concentrations of arsenite (0, 2.5, 5, 10, 20, and 40 μ M) for 4, 8, 16, and 32 h, and Hsp70 protein expression was measured by flow cytometry (Fig. 4). We found that arsenite when applied at concentrations ranging from 5 μ M to 40 μ M, induced a dose-dependent increase in Hsp70 expression. The most significant differences were observed following a 16 h incubation, at different arsenite concentrations. These data indicate that arsenite-stress induces a time and dose-dependent increase in expression of Hsp70 in cultured canine RPE cells.

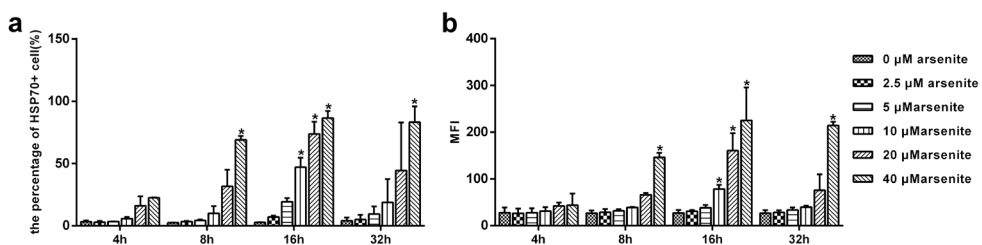


Fig. 4 Sodium arsenite stimulation induces production of Hsp70 in dog primary RPE cells. RPE cells were incubated with sodium arsenite at the indicated concentrations, for 4, 8, 16, and 32 h at 37 °C. **a**, Percentage of Hsp70 positive cells, detected by immunofluorescence staining with a MoAb, specific for inducible Hsp70, and flow cytometry. **b**, Mean fluorescence intensity (MFI) of Hsp70+ cells. Data are representative of three independent experiments. $P < 0.05$ was considered statistically significant.

Effect of carvacrol and leucinostatin on the induction of Hsp70 in stressed canine RPE cells

To determine whether Hsp70 could be co-induced in canine RPE cells, carvacrol, known to co-induce Hsp70 in various cell types (21, 22) was used. RPE cells were incubated for 16 h with arsenite and the indicated concentrations of carvacrol (Fig. 5). We found that carvacrol up-regulated Hsp70 expression dose-dependently in cells stressed by 5, 10, and 20 μM arsenite, even at doses $<5 \mu\text{M}$ at which arsenite alone failed to upregulate Hsp70 (Fig. 5). Thus, indeed carvacrol enhanced the stress response in arsenite-treated RPE cells, but failed to induce Hsp70 expression in the absence of a stressor. These data show that carvacrol functions as a co-inducer of Hsp70 expression in the canine RPE cell culture, which is in line with previous results in mouse and human cells (21, 22).

Next, leucinostatin, an antimicrobial and antitumor antibiotic with potential immunomodulating capacities that is produced by the fungus *Paecilomyces lilacinus*, was tested for its ability to enhance Hsp70 expression. First, we determined Hsp70 expression in leucinostatin-treated cells in the presence or absence of arsenite by flow cytometry. As shown in Fig. 6, leucinostatin enhanced Hsp70 expression in arsenite-stressed cells in a dose-dependent fashion. Thus, these data identify leucinostatin as a new co-inducer of Hsp70 in RPE cells.

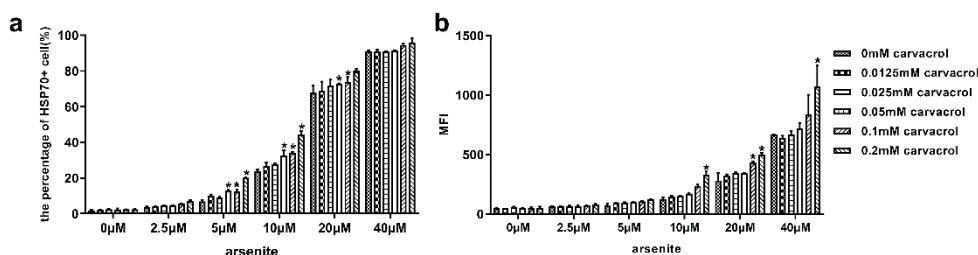


Fig. 5 Carvacrol co-induced Hsp70 expression in dog primary RPE cell (passage 2-4). RPE cells were incubated with the indicated concentration of carvacrol for 2 h at 37 $^{\circ}\text{C}$, followed by incubation with sodium arsenite at the indicated concentrations. After 16 h, Hsp70 expression in RPE cells was detected by immunofluorescence staining and flow cytometry. a, Mean percentages of sodium arsenite and/or carvacrol treated RPE cells, expressing Hsp70; b, Mean Fluorescence Intensity (MFI) of Hsp70-expression, detected in treated, cultured RPE cells. Data are representative of three independent experiments. $P < 0.05$ was considered statistically significant.

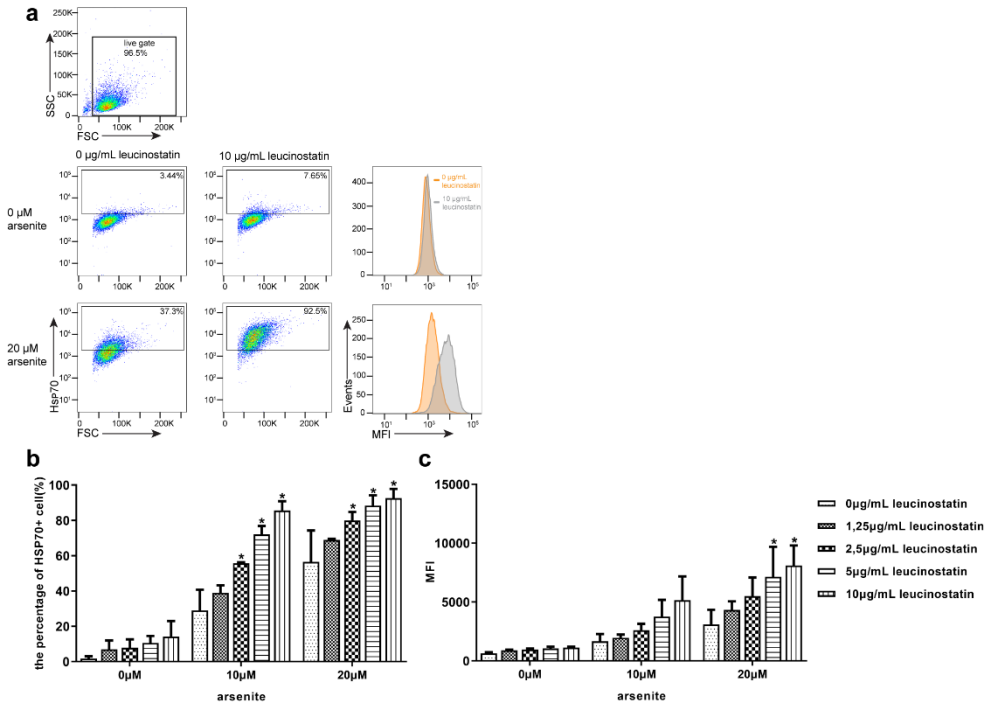


Fig. 6 Leucinostatin co-induced Hsp70 expression in dog primary RPE cells (passage 2-4). RPE cells were incubated with the indicated concentrations of leucinostatin for 2 h at 37 °C, followed by incubation with sodium arsenite at indicated concentrations. After 16 h, Hsp70 expression in RPE cells was detected by immunofluorescence staining and flow cytometry. **a**, Gating strategy and representative FACS plots, showing Hsp70 expression in sodium arsenite and/or leucinostatin-treated RPE cells; **b**, Mean percentage of arsenite- and/or leucinostatin-treated RPE cells expressing Hsp70; **c**, Mean Fluorescence Intensity (MFI) of Hsp70-expression, detected in treated, cultured RPE cells. Data are representative of three independent experiments. $P < 0.05$ was considered statistically significant.

Activation of HSF1 by leucinostatin

Induction of HSPs is regulated by translocated HSF1. Wieten et al. (2010b) have shown that carvacrol can enhance heat shock responses via activation of HSF1. To further examine if the HSP co-stimulatory effect of leucinostatin is mediated via HSF1, a reporter system was used (17). O23 cells carrying a luciferase reporter gene driven by the DNAJB1 (Hsp40) promoter were stressed by arsenite in the presence or absence of leucinostatin, as described previously for carvacrol. After 16 h,

luciferase activity was measured with the Promega Steady-Glo Luciferase Assay System (Fig. 7). We found that treatment with 5 $\mu\text{g}/\text{ml}$ leucinostatin in the presence of 30 μM arsenite, and 1, 2, or 5 $\mu\text{g}/\text{ml}$ leucinostatin in the presence 40 μM arsenite, activated transcription of the reporter from the Hsp40 promoter, which was in line with the postulated co-inducing effect. These results indicated that leucinostatin is able to promote the activation of HSF1.

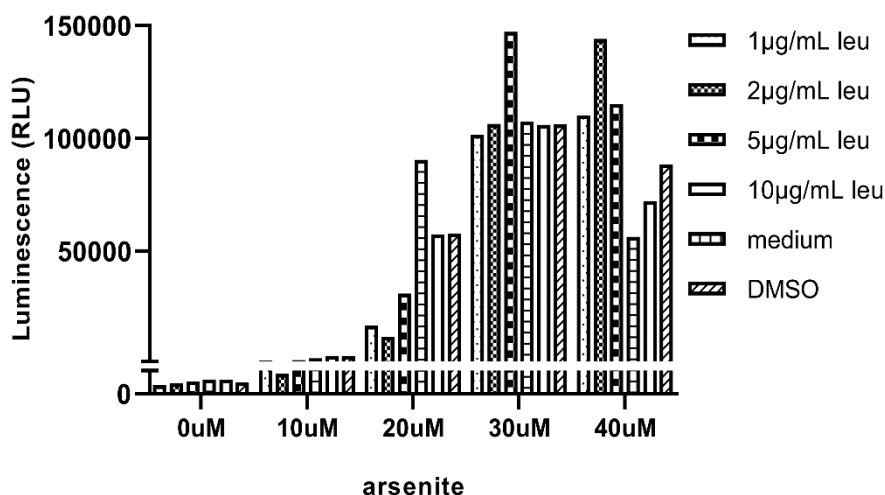


Fig. 7 HSF1 activated by leucinostatin in DNAJB1-luc-O23 reporter cells. Stable human DNAJB1-luc-O23 cells were treated with indicated concentrations of leucinostatin and sodium arsenite at 37 °C. Luciferase activity was measured after overnight incubation.

Discussion

Due to their many functions, RPE cells are a crucial cellular target during inflammation in a variety of ocular disorders. Various studies have shown that the morphology and functionality of RPE cells is changed in age-related macular degeneration (AMD) (23) and in retinitis pigmentosa (24). Therefore, modulation and regeneration of RPE cell functionality is becoming a promising therapeutic target for multiple eye diseases. Human ophthalmologists have endeavored in upregulating Hsp70 expression in RPE cells to improve RPE health and function by sublethal thermal irradiation (12, 13, 25), thus ameliorating ocular diseases. However, the damage threshold caused by sublethal thermal irradiation is difficult to define. Recently, compounds derived from food, herb, or approved drugs, such as carvacrol (21), celastrol (26) and geranyl geranyl acetone, (GGA) (27) that pharmacologically elevate the level of Hsp70 expression have gained more attention. In our study, we found that leucinostatin enhanced Hsp70 expression in arsenite-stressed canine

RPE cells in a dose-dependent fashion. Furthermore, leucinostatin increased the transcriptional activation of a heat shock promoter, heat shock factor-1.

Although, the isolation of RPE cells has been described decades ago, there is no published protocol for isolation and culture canine RPE cells. Here, in order to find a reliable, effective, and reproducible approach for canine RPE cell isolation, we tried several published protocols used in other species (20, 28, 29). In our experience, it was very hard to just peel off the RPE sheet from canine choroid, which is a crucial step in isolation. When harvesting RPE cells by digesting choroid/RPE sheets, the RPE cells will be contaminated with fibroblasts or other melanocytes (data not shown). Also, the detachment of the RPE cells by dispase took a long time, which is not good for the viability of RPE cells. Therefore, our method was based on Toops et al., in which the eye cup is incubated with 0.05% trypsin to loosen RPE cells from choroid.

Purity of human RPE primary cell cultures was determined by flow cytometric detection of the RPE cell specific protein, RPE65 (30). In our study, over 90% of canine RPE cells in passage 1 expressed the cytoplasmic RPE65 protein, as shown by both flow cytometry and immunocytochemistry. Furthermore, a decreasing expression of RPE65 and decreasing pigment production was seen in the following passages in longitudinal culture, which is in line with studies of human and bovine RPE cells (31-34). In our cultures, beginning at passage 4, primary canine RPE cells underwent a phenotypic change, from epithelial to mesenchymal morphology. Higher seeding densities of canine RPE cells contributed to maintenance of hexagonal morphology, RPE65 expression, and pigment production (data not shown).

Therapeutic enhancement of HSP expression may facilitate refolding of proteins in cell stress situations and restore cellular stress resistance (35). In addition, such enhanced expression may lead to modulation of the immune response due to induction of HSP specific regulatory T cells (5). Interestingly, different studies show that enhanced expression of Hsp70 in the eye not only normalizes the physiology of RPE cells (8), but also modulates the T cell immune response (15), suggesting the therapeutic potential of Hsp70 (co-)induction in curing ocular diseases. In our study we chose arsenite as a stressor and we determined if arsenite was capable of inducing Hsp70 expression in canine RPE cells. We found that in vitro arsenite stress induced a time- and dose-dependent increase in expression of Hsp70 in canine RPE cells, which is in line with our previous work (17). Interestingly, this increase of Hsp70 expression was further augmented in RPE cells by carvacrol administration which has been found to act as HSP co-inducer in various murine and human models (21). Using the same system, we found that leucinostatin, a candidate co-inducer, dose-

dependently enhanced Hsp70 expression in arsenite-stressed cells, thus confirming that leucinostatin acts as a novel HSP co-inducer.

The expression of inducible HSPs is initiated by the nuclear translocation of HSF1. HSP inducers or co-inducers can activate HSF and induce HSPs in different ways. Otaka et al showed that GGA could release HSF1 by binding to the C-terminus of Hsp70, resulting in induction of Hsp70 (27); geldanamycin binds to Hsp90 to dissociate HSF1, leading to HSP induction (36); and boosting of Hsp70 by celastrol (26) and paeoniflorin (37) is mediated by HSF1 activation. In view of this, we set out to further elucidate the HSP co-induction mechanism of leucinostatin, using the luciferase reporter O23-line. Leucinostatin appeared to be able to promote the activation of HSF1 to induce HSP expression in the O23 reporter cell line, which provides a mechanistic basis for therapeutic strategies aimed at upregulating Hsp70 expression in RPE cells.

In summary, we successfully isolated and cultured canine RPE cells, and obtained a pure primary RPE cell culture. We proved that arsenite stress induced a time- and dose-dependent increase in Hsp70 expression in canine RPE cells *in vitro*. We investigated leucinostatin as a novel HSP co-inducer and explored its Hsp70 enhancing effects in arsenite-stressed RPE cells in a dose-dependent fashion. In addition, its Hsp70 inducing role in an HSF-1 dependent reporter system was shown. The present findings suggest that Hsp70 co-inducers like carvacrol and leucinostatin might be applied as (new) enhancers of induced Hsp70 expression, with a possible therapeutic application in inflammatory diseases of the eye.

Acknowledgements

Qingkang Lyu was supported by a fellowship of the China Scholarship Council (CSC).

References

1. Hartnett ME. *Pediatric retina*: Lippincott Williams & Wilkins (2005).
2. Heller JP, Martin KR. Enhancing RPE Cell-Based Therapy Outcomes for AMD: The Role of Bruch's Membrane. *Transl Vis Sci Technol* (2014) 3(3):11. Epub 2014/07/30. doi: 10.1167/tvst.3.3.11.
3. Cai J, Nelson KC, Wu M, Sternberg P, Jr., Jones DP. Oxidative damage and protection of the RPE. *Prog Retin Eye Res* (2000) 19(2):205-21. Epub 2000/02/16. doi: 10.1016/s1350-9462(99)00009-9.
4. Konda BR, Pararajasegaram G, Wu GS, Stanforth D, Rao NA. Role of retinal pigment epithelium in the development of experimental autoimmune uveitis. *Invest Ophthalmol Vis Sci* (1994) 35(1):40-7. Epub 1994/01/01.
5. van Eden W, van der Zee R, Prakken B. Heat-shock proteins induce T-cell regulation of chronic inflammation. *Nat Rev Immunol* (2005) 5(4):318-30. Epub 2005/04/02. doi: 10.1038/nri1593.
6. Tanaka K, Namba T, Arai Y, Fujimoto M, Adachi H, Sobue G, et al. Genetic evidence for a protective role for heat shock factor 1 and heat shock protein 70 against colitis. *J Biol Chem* (2007) 282(32):23240-52. Epub 2007/06/09. doi: 10.1074/jbc.M704081200.
7. van Noort JM. Stress proteins in CNS inflammation. *J Pathol* (2008) 214(2):267-75. Epub 2007/12/29. doi: 10.1002/path.2273.
8. Kitamei H, Kitaichi N, Yoshida K, Nakai A, Fujimoto M, Kitamura M, et al. Association of heat shock protein 70 induction and the amelioration of experimental autoimmune uveoretinitis in mice. *Immunobiology* (2007) 212(1):11-8. Epub 2007/02/03. doi: 10.1016/j.imbio.2006.08.004.
9. Beere HM, Wolf BB, Cain K, Mosser DD, Mahboubi A, Kuwana T, et al. Heat-shock protein 70 inhibits apoptosis by preventing recruitment of procaspase-9 to the Apaf-1 apoptosome. *Nat Cell Biol* (2000) 2(8):469-75. Epub 2000/08/10. doi: 10.1038/35019501.
10. Saleh A, Srinivasula SM, Balkir L, Robbins PD, Alnemri ES. Negative regulation of the Apaf-1 apoptosome by Hsp70. *Nat Cell Biol* (2000) 2(8):476-83. Epub 2000/08/10. doi: 10.1038/35019510.
11. Wang LC, Liao LX, Lv HN, Liu D, Dong W, Zhu J, et al. Highly Selective Activation of Heat Shock Protein 70 by Allosteric Regulation Provides an Insight into Efficient Neuroinflammation Inhibition. *Ebiomedicine* (2017) 23:160-72. doi: 10.1016/j.ebiom.2017.08.011.
12. Inagaki K, Shuo T, Katakura K, Ebihara N, Murakami A, Ohkoshi K. Sublethal Photothermal Stimulation with a Micropulse Laser Induces Heat Shock Protein Expression in ARPE-19 Cells. *J Ophthalmol* (2015) 2015:729792. Epub 2015/12/24. doi: 10.1155/2015/729792.
13. Wang J, Huie P, Dalal R, Lee S, Tan G, Lee D, et al., editors. Heat shock protein expression as guidance for the therapeutic window of retinal laser therapy. *Ophthalmic Technologies XXVI*; 2016: International Society for Optics and Photonics.
14. Desmettre T, Muraige CA, Mordon S. Heat shock protein hyperexpression on chorioretinal layers after transpupillary thermotherapy. *Invest Ophthalmol Vis Sci* (2001) 42(12):2976-80. Epub 2001/11/01.

15. Erdo F, Erdo SL. Bimoclolmol protects against vascular consequences of experimental subarachnoid hemorrhage in rats. *Brain Res Bull* (1998) 45(2):163-6. Epub 1998/01/27. doi: 10.1016/s0361-9230(97)00333-x.
16. Chow AM, Brown IR. Induction of heat shock proteins in differentiated human and rodent neurons by celastrol. *Cell Stress Chaperones* (2007) 12(3):237-44. Epub 2007/10/06. doi: 10.1379/csc-269.1.
17. Wieten L, van der Zee R, Goedemans R, Sijtsma J, Serafini M, Lubsen NH, et al. Hsp70 expression and induction as a readout for detection of immune modulatory components in food. *Cell Stress & Chaperones* (2010) 15(1):25-37. doi: 10.1007/s12192-009-0119-8.
18. Kampinga HH, Hageman J, Vos MJ, Kubota H, Tanguay RM, Bruford EA, et al. Guidelines for the nomenclature of the human heat shock proteins. *Cell Stress Chaperones* (2009) 14(1):105-11. Epub 2008/07/30. doi: 10.1007/s12192-008-0068-7.
19. Heller JP, Kwok JC, Vecino E, Martin KR, Fawcett JW. A Method for the Isolation and Culture of Adult Rat Retinal Pigment Epithelial (RPE) Cells to Study Retinal Diseases. *Front Cell Neurosci* (2015) 9:449. Epub 2015/12/05. doi: 10.3389/fncel.2015.00449.
20. Amirpour N, Karamali F, Razavi S, Esfandiari E, Nasr-Esfahani MH. A proper protocol for isolation of retinal pigment epithelium from rabbit eyes. *Adv Biomed Res* (2014) 3:4. Epub 2014/03/05. doi: 10.4103/2277-9175.124630.
21. Wieten L, van der Zee R, Spiering R, Wagenaar-Hilbers J, van Kooten P, Broere F, et al. A novel heat-shock protein coinducer boosts stress protein Hsp70 to activate T cell regulation of inflammation in autoimmune arthritis. *Arthritis Rheum* (2010) 62(4):1026-35. Epub 2010/02/05. doi: 10.1002/art.27344.
22. Burt SA, van der Zee R, Koets AP, de Graaff AM, van Knapen F, Gaastra W, et al. Carvacrol induces heat shock protein 60 and inhibits synthesis of flagellin in Escherichia coli O157:H7. *Appl Environ Microbiol* (2007) 73(14):4484-90. Epub 2007/05/29. doi: 10.1128/AEM.00340-07.
23. Golestaneh N, Chu Y, Xiao YY, Stoleru GL, Theos AC. Dysfunctional autophagy in RPE, a contributing factor in age-related macular degeneration. *Cell Death Dis* (2017) 8(1):e2537. Epub 2017/01/06. doi: 10.1038/cddis.2016.453.
24. Mitamura Y, Mitamura-Aizawa S, Nagasawa T, Katome T, Eguchi H, Naito T. Diagnostic imaging in patients with retinitis pigmentosa. *J Med Invest* (2012) 59(1-2):1-11. Epub 2012/03/28. doi: 10.2152/jmi.59.1.
25. Iwami H, Pruessner J, Shiraki K, Brinkmann R, Miura Y. Protective effect of a laser-induced sub-lethal temperature rise on RPE cells from oxidative stress. *Exp Eye Res* (2014) 124:37-47. Epub 2014/05/08. doi: 10.1016/j.exer.2014.04.014.
26. Westerheide SD, Bosman JD, Mbadugha BNA, Kawahara TLA, Matsumoto G, Kim SJ, et al. Celastrols as inducers of the heat shock response and cytoprotection. *Journal of Biological Chemistry* (2004) 279(53):56053-60. doi: 10.1074/jbc.M409267200.
27. Otaka M, Yamamoto S, Ogasawara K, Takaoka Y, Noguchi S, Miyazaki T, et al. The induction mechanism of the molecular chaperone HSP70 in the gastric mucosa by Geranylgeranylacetone (HSP-inducer). *Biochem Biophys Res*

- Commun* (2007) 353(2):399-404. Epub 2006/12/22. doi: 10.1016/j.bbrc.2006.12.031.
28. Fernandez-Godino R, Garland DL, Pierce EA. Isolation, culture and characterization of primary mouse RPE cells. *Nat Protoc* (2016) 11(7):1206-18. Epub 2016/06/10. doi: 10.1038/nprot.2016.065.
 29. Toops KA, Tan LX, Lakkaraju A. A detailed three-step protocol for live imaging of intracellular traffic in polarized primary porcine RPE monolayers. *Exp Eye Res* (2014) 124:74-85. Epub 2014/05/28. doi: 10.1016/j.exer.2014.05.003.
 30. Srivastava GK, Reinoso R, Singh AK, Fernandez-Bueno I, Martino M, Garcia-Gutierrez MT, et al. Flow cytometry assessment of the purity of human retinal pigment epithelial primary cell cultures. *J Immunol Methods* (2013) 389(1-2):61-8. Epub 2013/01/16. doi: 10.1016/j.jim.2013.01.003.
 31. Tamiya S, Liu LH, Kaplan HJ. Epithelial-Mesenchymal Transition and Proliferation of Retinal Pigment Epithelial Cells Initiated upon Loss of Cell-Cell Contact. *Investigative Ophthalmology & Visual Science* (2010) 51(5):2755-63. doi: 10.1167/iovs.09-4725.
 32. Liggett TE, Griffiths TD, Gaillard ER. Isolation and characterization of a spontaneously immortalized bovine retinal pigmented epithelial cell line. *BMC Cell Biol* (2009) 10(1):33. Epub 2009/05/06. doi: 10.1186/1471-2121-10-33.
 33. Alge CS, Suppmann S, Priglinger SG, Neubauer AS, May CA, Hauck S, et al. Comparative proteome analysis of native differentiated and cultured dedifferentiated human RPE cells. *Invest Ophthalmol Vis Sci* (2003) 44(8):3629-41. Epub 2003/07/29. doi: 10.1167/iovs.02-1225.
 34. Hunt RC, Davis AA. Altered expression of keratin and vimentin in human retinal pigment epithelial cells in vivo and in vitro. *J Cell Physiol* (1990) 145(2):187-99. Epub 1990/11/01. doi: 10.1002/jcp.1041450202.
 35. Georgopoulos C, Welch WJ. Role of the Major Heat-Shock Proteins as Molecular Chaperones. *Annual Review of Cell Biology* (1993) 9(1):601-34. doi: DOI 10.1146/annurev.cb.09.110193.003125.
 36. Zou JY, Guo YL, Guettouche T, Smith DF, Voellmy R. Repression of heat shock transcription factor HSF1 activation by HSP90 (HSP90 complex) that forms a stress-sensitive complex with HSF1. *Cell* (1998) 94(4):471-80. doi: Doi 10.1016/S0092-8674(00)81588-3.
 37. Hehir MP, Morrison JJ. Paeoniflorin, a novel heat-shock protein inducing compound, and human myometrial contractility in vitro. *J Obstet Gynaecol Res* (2016) 42(3):302-6. Epub 2015/12/09. doi: 10.1111/jog.12895.

4



Hsp70 and NF- κ B mediated control of innate inflammatory responses in a canine macrophage cell line

Qingkang Lyu¹, Magdalena Wawrzyniuk¹, Victor P. M. G. Rutten^{1,2}, Willem van Eden¹, Alice J. A. M. Sijts¹ and Femke Broere^{1,*}

¹Department of Infectious diseases and Immunology, Faculty of Veterinary Medicine, Utrecht University; 3584 CL, Utrecht, The Netherlands

²Department of Veterinary Tropical diseases, Faculty of Veterinary Science, Pretoria University, South Africa

*Correspondence: f.broere@uu.nl

International journal of molecular sciences 21.18 (2020): 6464.

Abstract

The pathogenesis of many inflammatory diseases is associated with the uncontrolled activation of nuclear factor kappa B (NF- κ B) in macrophages. Previous studies have shown that in various cell types, heat shock protein 70 (Hsp70) plays a crucial role in controlling NF- κ B activity. So far, little is known about the role of Hsp70 in canine inflammatory processes. In this study we investigated the potential anti-inflammatory effects of Hsp70 in canine macrophages as well as the mechanisms underlying these effects. To this end, a canine macrophage cell line was stressed with arsenite, a chemical stressor, which upregulated Hsp70 expression as detected by flow cytometry and qPCR. A gene-edited version of this macrophage cell line lacking inducible Hsp70 was generated using CRISPR-Cas9 technology. To determine the effects of Hsp70 on macrophage inflammatory properties, arsenite-stressed wild-type and Hsp70 knockout macrophages were exposed to lipopolysaccharide (LPS), and the expression of the inflammatory cytokines IL-6, IL-1 β and TNF- α and levels of phosphorylated NF- κ B were determined by qPCR and Western Blotting, respectively. Our results show that non-toxic concentrations of arsenite induced Hsp70 expression in canine macrophages; Hsp70 upregulation significantly inhibited the LPS-induced expression of the pro-inflammatory mediators TNF- α and IL-6, as well as NF- κ B activation in canine macrophages. Furthermore, the gene editing of inducible Hsp70 by CRISPR-Cas9-mediated gene editing neutralized this inhibitory effect of cell stress on NF- κ B activation and pro-inflammatory cytokine expression. Collectively, our study reveals that Hsp70 may regulate inflammatory responses through NF- κ B activation and cytokine expression in canine macrophages.

Keywords: macrophages; heat shock protein; NF- κ B; cytokines

Introduction

Macrophages constitute a major component of the innate immune response. They are originally derived from myeloid progenitors (1) and ubiquitously distributed throughout the body tissues, including lung, liver, gut and brain, comprising the innate defense against pathogen invasion and tissue damage. The cytokines produced by macrophages are initiators of inflammation. Macrophages are highly heterogeneous cells, showing high plasticity; their phenotype may change rapidly (2) in response to stimuli such as lipopolysaccharide (LPS) or interferon- γ (IFN- γ). Macrophage activation, which is associated with an inflammatory response, induces the production and secretion of a variety of inflammatory mediators, including interleukin-6 (IL-6), IL-1 β , tumor necrosis factor- α (TNF- α) and nitric oxide (NO) (3, 4). Under physiological conditions, the release of those inflammatory mediators tunes the immune response, facilitates the resolution of inflammation, and finally protects the organism from pathogen invasion. However, if the inflammatory response is out of control, the excessive release of those inflammatory mediators may result in chronic inflammatory diseases, including atopic dermatitis (5), inflammatory bowel disease (6), rheumatoid arthritis (7), diabetes (8), and even cancer (9). Thus, the modulation of those inflammatory mediators may have a potentially therapeutic effect on severe disease-associated inflammation.

Nuclear factor kappa B (NF- κ B) is the major regulator of pro-inflammatory gene expression in many cell types contributing to both acute and chronic inflammation. The NF- κ B family is composed of five NF- κ B subtypes, including RelA (p65), c-Rel, RelB, NF- κ B1 (p50) and NF- κ B2 (p52), of which p50/p65 forms the most abundant heterodimer. In resting cells, NF- κ B is in an inactive state, bound by the inhibitor of the nuclear factor kappa B (I κ B) inhibitory protein in the cytoplasm. Upon exposure to stimuli, the activation of I κ B kinase (IKK) triggers the phosphorylation of I κ B, resulting in I κ B degradation by the ubiquitin proteasome system. Subsequently, the NF- κ B complex, predominantly p50/p65, is released and phosphorylated, facilitating the nuclear translocation of NF- κ B and binding to specific promoter sites, in order to induce pro-inflammatory gene expression (10, 11). It is well-established that NF- κ B signaling plays a key role in the LPS-mediated induction of inflammatory cytokine expression in macrophages (12, 13). Sakai et al. showed that the stimulation of RAW264.7 cell-expressed toll-like receptor 4 (TLR4) by LPS initiated NF- κ B translocation in a MyD88-dependent fashion (14). As macrophages express multiple TLRs, each of them recognizing different pathogen components, but all triggering the activation of NF- κ B and inducing the secretion of cytokines and chemokines, e.g., IL-1 β or IL-6 (15), NF- κ B may be a suitable target to control macrophage-induced inflammatory responses.

Heat shock proteins (HSPs) are a group of well-conserved stress proteins maintaining protein homeostasis by counteracting protein denaturation, preventing protein misfolding and assisting assembly. Recently, HSPs have been found to be associated with anti-inflammatory effects. Inducible Hsp70 is a representative member of the family of HSPs, and has been largely examined for its functions in stressed human and murine macrophages (16-18). The upregulation of Hsp70 by inducers such as celastrol was shown to inhibit the production of pro-inflammatory cytokines, such as TNF- α , IL-6 and IL-1 β in BV2 cells (19), human retinal pigment epithelial cells (20), and human alveolar macrophages (21). Similarly, the overexpression of Hsp70 attenuates LPS-induced cytokine expression in macrophages (22) and microglia cells (23). An increasing number of studies have shown that the inflammation-inhibitory effects of Hsp70 may involve the regulation of NF- κ B activity. For instance, Bhagat et al. have shown that Hsp70 protects against acute pancreatitis by preventing NF- κ B activation (24). In addition, the overexpression of Hsp72 reduced NF- κ B DNA binding activity (23). Some researchers also reported an interaction between Hsp70 and TRAF6, an essential activator of the NF- κ B pathway (19, 25), thereby disturbing NF- κ B activation and translocation. Those findings suggest that Hsp70 modulates NF- κ B activity.

So far, little is known about the role of Hsp70 in canine inflammatory processes. In this study, we demonstrated that the chemical stressor sodium arsenite dose-dependently induced Hsp70 expression in a canine macrophage cell line. The upregulation of Hsp70 by arsenite decreased LPS-induced NF- κ B phosphorylation and pro-inflammatory cytokine expression. Furthermore, the suppressive effects on NF- κ B p65 activation and cytokine expression were abolished in Hsp70-deficient canine macrophages. Our results suggest that Hsp70 inducers are promising therapeutics for the treatment of inflammatory disease in dogs.

Results

Induction of Hsp70 in Arsenite-Stressed 030D Cells

To investigate whether Hsp70 production can be induced in 030D cells, arsenite, as a known stressor that induces the cellular stress-response, was used (26, 27). The 030D cells were incubated with various concentrations of arsenite, and the effects on Hsp70 expression were measured by flow cytometry and qPCR (Figure 1A, B and C). An upregulation of Hsp70 production was observed to occur in a dose-dependent manner, with a significant upregulation at arsenite concentrations ranging from 0.625 μ M to 10 μ M. In contrast, LPS (1 μ g/mL) only failed to induce Hsp70 expression.

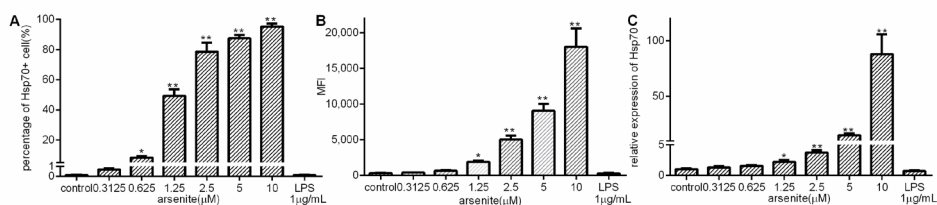


Figure 1. The induction of Hsp70 production in arsenite-stressed 030D cells. 030D cells were either left untreated, or exposed to the indicated concentrations of arsenite or LPS (1 μ g/mL) for 16 h. **(A)** The percentages of Hsp70-positive cells detected by flow cytometry using FITC-labeled Hsp70 specific antibody. **(B)** Mean fluorescence intensities (MFI) of Hsp70 positive cells. **(C)** The mRNA expression of Hsp70 was measured by qPCR. Data are shown as the mean \pm SD and are representative of three independent experiments. * $p < 0.05$, ** $p < 0.01$, vs. control group.

Inhibition of Expression of LPS-Induced Pro-inflammatory Cytokines in Stressed 030D Cells

Next, we tested the effect of cell stress on LPS-induced pro-inflammatory cytokine expression in 030D cells. The cells were pre-treated with arsenite at concentrations ranging from 1.25 μ M to 10 μ M for 16 h to induce Hsp70, and then stimulated with 1 μ g/mL LPS for 6 h. The expression of inducible Hsp70 was detected by qPCR. In line with our previous results in Figure 1, Hsp70 expression was dose-dependently induced regardless of LPS (Figure S2). The mRNA expression of three major pro-inflammatory cytokines, IL-6, TNF- α and IL-1 β , was assessed by qPCR. As shown in Figure 2, cells stressed with 1.25–10 μ M arsenite showed a significantly reduced IL-6 and TNF- α expression compared to cells treated with LPS alone (Figure 2A and B). In contrast, the lower concentrations of arsenite failed to lower LPS-induced IL-1 β expression. IL-1 β expression was only reduced in cells pre-treated with higher concentrations of arsenite (Figure 2C).

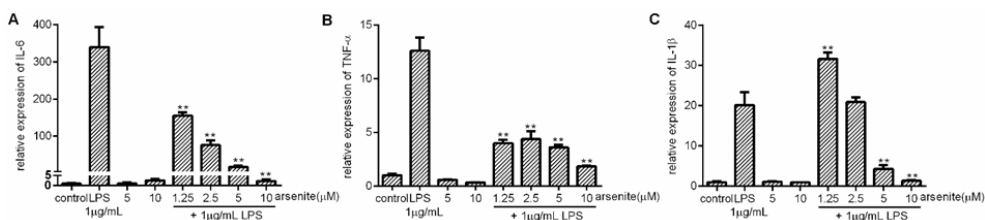


Figure 2. The inhibition of expression of LPS-induced pro-inflammatory cytokines by cell stress in 030D cells. 030D cells were treated with various concentration of arsenite (1.25 μ M to 10 μ M) for 16 h as indicated. Next, left unstimulated or stimulated with 1 μ g/mL LPS for 6 h. mRNA expression of IL-6 **(A)**, TNF- α **(B)** and

IL-1 β (C) was measured by qPCR. Data are shown as the mean \pm SD and are representative of three independent experiments. * $p < 0.05$, ** $p < 0.01$, vs. LPS alone group.

Effect of Arsenite on 030D Cell Viability

To exclude the possibility that the observed cell stress-associated reduction in cytokine expression in LPS-treated 030D cells is due to the toxic effects of arsenite treatment, we assessed the metabolic activity of 030D exposed to arsenite in an MTT assay (Figure 3). While 030D's metabolic activity was impaired at the higher concentrations, arsenite at concentrations ranging from 0.3125 to 2.5 μ M did not have any effect on the ability of these cells to reduce MTT into formazan crystals. A similar result was found by cell counting after arsenite treatment (Figure S3). Thus, at concentrations of 2.5 μ M and lower, arsenite is not cytotoxic for 030D cells, and was used for further experimentation.

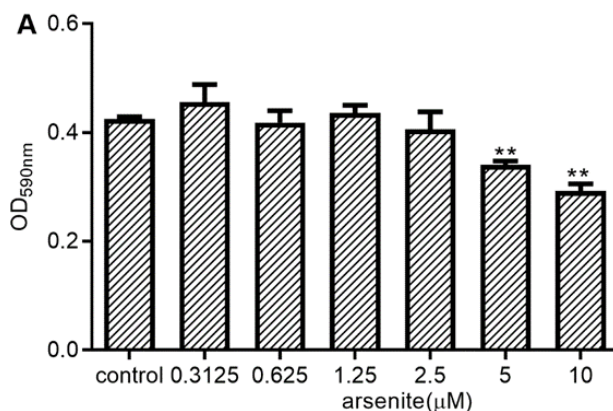


Figure 3. Effects of arsenite on the metabolic activity of 030D cells. 030D cells were incubated with the indicated concentrations of arsenite for 24 h. Metabolic activity, representative of cell viability, was evaluated in an MTT assay. Untreated cells were used as control. Y-axis: OD590, reflecting MTT reduction into purple colored formazan crystals which were solubilized before measurement (see *Materials and Methods*). Data are shown as the mean \pm SD and representative of three independent experiments. * $p < 0.05$, ** $p < 0.01$, vs. control group.

Effects of Cell Stress on NF- κ B Phosphorylation in LPS-Stimulated 030D Cells

To examine whether the cell stress-induced downregulation of LPS-induced IL-6 and IL-1 β or TNF- α expression is due to downregulation of NF- κ B activity, 030D cells were treated with different concentrations of arsenite or left untreated for 16 h.

Subsequently, they were exposed to LPS and harvested after 5, 15, 30 and 60 min. The NF-κB p65 phosphorylation levels at Ser 536 were analyzed by Western Blotting. As shown in Figure 4, LPS treatment induced an increase in the levels of phosphorylated NF-κB p65 at Ser 536 detected in the whole cell lysates. In comparison, the levels of phosphorylated NF-κB p65 at Ser 536 were significantly lower in arsenite-treated cells at any time point tested, suggesting that cell stress inhibits cytosolic NF-κB p65 phosphorylation.

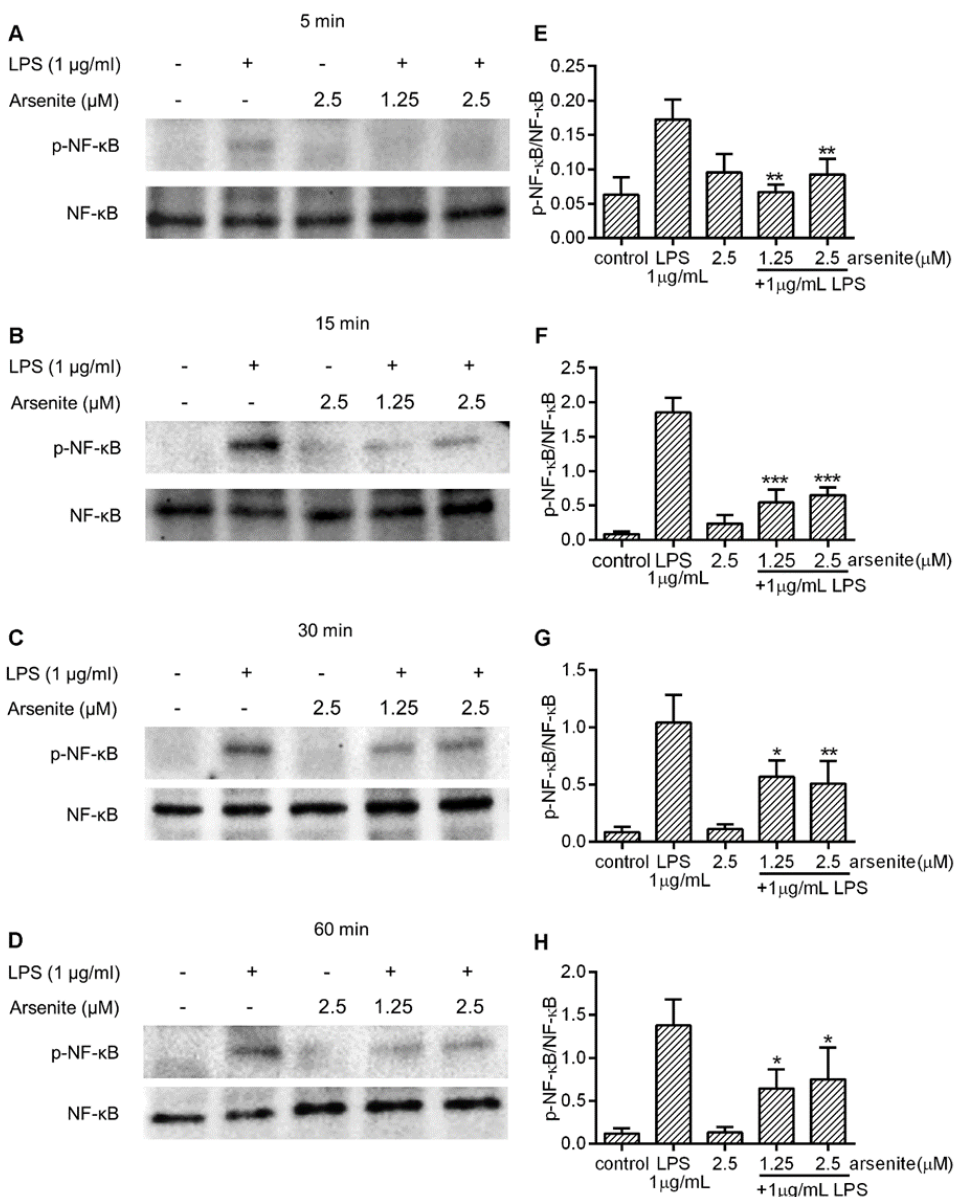


Figure 4. The effect of cell stress on NF- κ B phosphorylation in LPS-stimulated 030D cells. The 030D cells were incubated with different concentrations (1.25 and 2.5 μ M) of arsenite, or without, for 16 h, after which the cells were exposed to LPS and harvested at 5 min (A, E), 15 min (B, F), 30 min (C, G) and 60 min (D, H). Whole cell lysates were extracted and analyzed by Western Blotting. Control: untreated cells. Phosphorylated NF- κ B and total NF- κ B were detected with rabbit monoclonal anti-phospho-NF- κ B p65 and HRP-labeled swine-anti rabbit IgG, and mouse monoclonal anti- NF- κ B p65 and HRP-labeled rabbit anti-mouse IgG, respectively. The densitometry of the protein bands was scanned and quantitated with Image labTM software 6.0.1 (E, F, G and H). The total NF- κ B levels were used as an internal control. Data are shown as the mean \pm SD and are representative of three independent experiments. * $p < 0.05$, ** $p < 0.01$, and *** $p < 0.001$, vs. LPS alone group.

Generation and Validation of Hsp70 Knockout of a 030D Cell Line

To further confirm that cell stress-induced Hsp70 inhibited pro-inflammatory cytokine expression and NF- κ B phosphorylation, gene-edited 030D cells were generated by targeting inducible Hsp70 with the CRISPR/Cas9 gene editing system (Figure 5A), as detailed in the Materials and Methods section. To validate the successful inactivation of the inducible Hsp70 gene, target site sequencing (Figure 5B, S4 and S5) and flow cytometry analysis (Figure 5C) were performed. As shown in Figure 5C, arsenite stress induced Hsp70 expression in approximately 50% of wild-type 030D cells, and most single cell colonies that had been subjected to gene editing lacked the expression of Hsp70 under these conditions (Figure S6). Among those colonies, clone 2 was selected for target site sequencing. We found that clone 2 has a 214 bp deletion (#2.1) between two gRNA targeting sites in one allele (#2.1), and the other allele has a 74 bp deletion and a 1 bp insertion (#2.2), compared to wild-type 030D cells.

The Effect of Hsp70 on Pro-inflammatory Cytokine Expression and NF- κ B Phosphorylation

To further confirm the role of cell stress-induced Hsp70 in attenuation of pro-inflammatory cytokine expression and NF- κ B phosphorylation, Hsp70 knockout 030D cells (clone 2) were treated with arsenite and LPS, and then examined by qPCR for pro-inflammatory cytokine expression and Western Blotting for NF- κ B activation. In contrast to our observations in wild-type 030D cells (Figure 2 and Figure S7D, E, F), arsenite treatment at non-toxic concentrations did not decrease LPS-induced IL-6 or TNF- α expression in Hsp70 knockout cells (Figure 6A, B and Figure S7A, B). As expected, LPS-induced IL-1 β mRNA expression was also not

reduced (Figure 6C and Figure S7C). In agreement with these findings, arsenite-treated Hsp70 knockout cells did not exhibit a decrease in the levels of LPS-induced NF- κ B p65 phosphorylation at Ser 536. These data suggest that inducible Hsp70 plays a pivotal role in the NF- κ B signaling pathway.

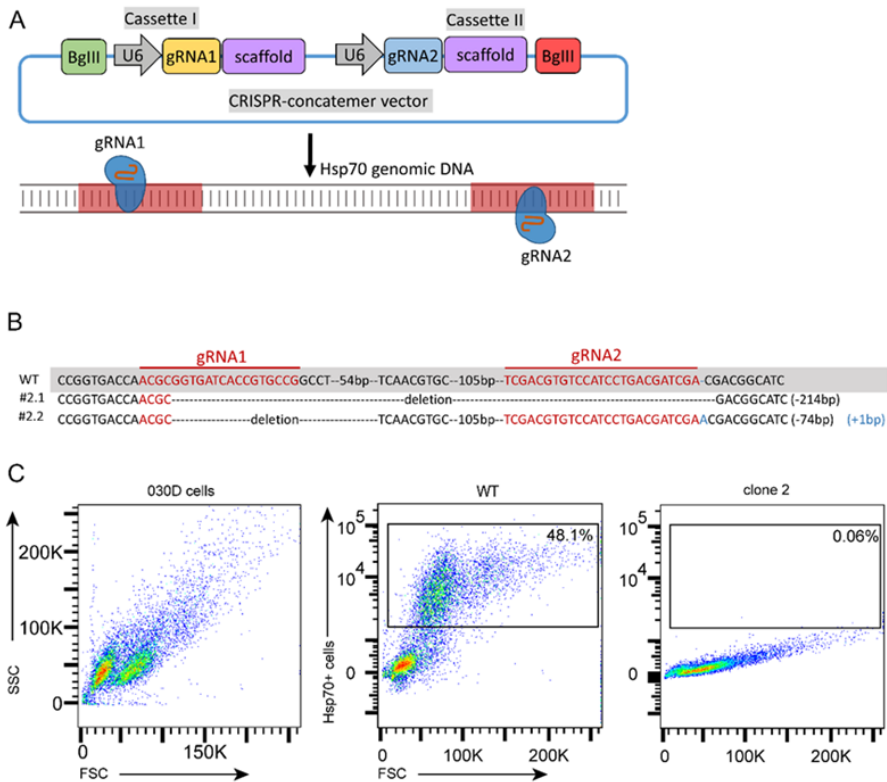


Figure 5. Generation and validation of Hsp70 knockout in cells of the 030D cell line. (A) schematic diagram of the CRISPR-concatemer with 2 gRNAs and the targeting site of Hsp70 by guide RNAs (see Figure S4). (B) Sanger sequencing results of clone 2 (including two alleles) and alignment with wild-type 030D cell (-: deleted bases; +: inserted bases). (C) Flow cytometry analysis of knockout cell clones to evaluate the expression of Hsp70 in 030D cells under arsenite stress. Wild-type 030D cells under arsenite stress were used as positive control.

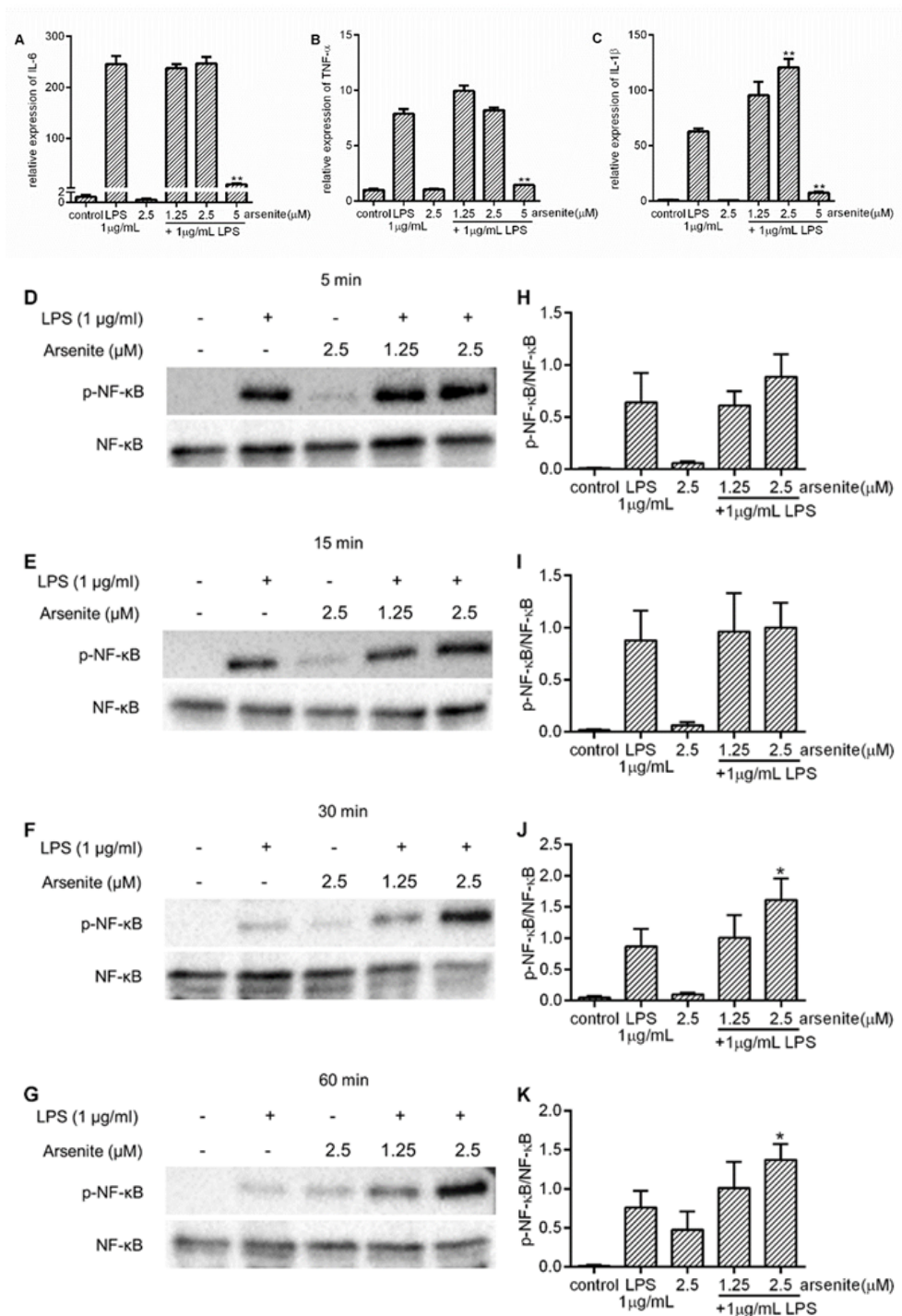


Figure 6. The effect of a deficiency of inducible Hsp70 on pro-inflammatory cytokine expression and NF- κ B phosphorylation. Hsp70 knockout 030D cells were treated with different concentrations (1.25, 2.5 or 5 μ M) of arsenite, or without, for 16 h, and then exposed to LPS. The cells were harvested after 6 h (**A**, **B** and **C**) of LPS exposure. qPCR was performed to detect the expression of IL-6 (**A**), IL-1 β (**B**) and TNF- α (**C**). For Western Blotting, the cells were harvested after 5 (**D** and **H**), 15 (**E** and **I**), 30 (**F** and **J**) and 60 (**G** and **K**) min of LPS exposure. Western Blotting was performed to detect levels of phosphorylated NF- κ B and total NF- κ B at certain time points. The densitometry of the protein bands was scanned and quantitated with Image lab™ software 6.0.1. (**H**, **I**, **J** and **K**). The total NF- κ B levels were used as an internal control. Data are shown as the mean \pm SD and are representative of three independent experiments. * $p < 0.05$, ** $p < 0.01$ and *** $p < 0.001$ vs. LPS alone group.

Discussion

The abnormal activation of NF- κ B in macrophages leads to excessive pro-inflammatory cytokine expression, as can be seen in many inflammatory diseases, such as rheumatoid arthritis (11), neurodegenerative diseases (28), inflammatory bowel disease (29) and type I diabetes (30). Previous studies showed that Hsp70 was implicated in inflammatory responses by modulating NF- κ B activity (31-33). However, the potential anti-inflammatory effects of inducible Hsp70 in canine cell systems have remained unknown. In the present study, using arsenite as a chemical stressor to induce Hsp70, we showed that Hsp70 upregulation significantly inhibited the LPS-induced expression of the pro-inflammatory mediators TNF- α and IL-6, as well as NF- κ B activation, in a canine macrophage cell line. Furthermore, the inactivation of inducible Hsp70 by CRISPR-Cas9-mediated gene editing neutralized this inhibitory effect of cell stress on NF- κ B activation and pro-inflammatory cytokine expression. Taken together, our results indicate that the upregulation of Hsp70 plays a critical role in modulating LPS-induced NF- κ B activation and cytokine expression.

Although the inhibitory effects of Hsp70 on pro-inflammatory cytokines have been described in other cell types and animals, the profile of the cytokines suppressed by Hsp70 has remained controversial. A preceding study has indicated that the pro-inflammatory cytokines TNF- α and IL-1 β were significantly downregulated in brain ischemia and microglia by the overexpression of Hsp70 (34). Similarly, in murine Kupffer cells, the upregulation of Hsp70 induced by sodium arsenite not only inhibited the production of LPS-induced pro-inflammatory cytokines TNF- α and IL-1 β , but also anti-inflammatory cytokine IL-10 (35). Human monocyte-derived macrophages transfected with Hsp70 followed by exposure to LPS expressed less TNF- α , IL-1 β , IL-12 and IL-10 at mRNA level, but not IL-6, compared to

macrophages transfected with Hsp70 anti-sense DNA (22). Nevertheless, in the murine microglial cell line BV-2, the pharmacological activation of Hsp70 by handelin significantly blocked the secretion of the pro-inflammatory cytokines TNF- α , IL-1 β and IL-6 (19). In our study of canine macrophage cells, we found that the LPS-induced upregulation of TNF- α and IL-6 mRNA was dramatically diminished upon cell stress. The reduction in pro-inflammatory cytokine transcription correlated with an increase in Hsp70 levels, and the levels of TNF- α and IL-6 mRNA remained intact when gene-edited Hsp70-deficient macrophages were used. The expression of IL-1 β mRNA was not inhibited in wild-type canine macrophage cells or in Hsp70-deficient cells. IL-1 β differs from other cytokines, as IL-1 β expression depends on transcriptional and post-transcriptional processes (36). IL-1 β levels are regulated by different signals, such as the cAMP-PKA pathway (37). In line with our data, the overexpression of Hsp70 significantly prevented TNF- α and IL-6 release and mRNA expression in rat macrophages (38) and tuberculosis patient's macrophages (21). In view of the above studies, we speculate that the differences in the spectrum of regulation of the cytokines profile by Hsp70 may be caused by the differences in species and methods applied for Hsp70 induction.

The activation of p65 leads to the transactivation of a variety of target genes, such as those coding for inflammatory cytokines, cell adhesion molecules and chemokines (39). The activation of p65, and thus NF- κ B function, is controlled in part by phosphorylation. The p65 subunit of NF- κ B possesses multiple serine (Ser) and threonine (Thr) residues that may be the subject of phosphorylation. Previous studies have shown that the phosphorylation of p65 on Ser 276, 529 and 536 enhances the NF- κ B-mediated transcription of inflammatory genes (40, 41); however, the phosphorylation of p65 on Thr 254 suppresses p65 activity (42). Yang et al. (43) found that LPS could induce the phosphorylation of p65 on Ser 536, which potentiated its translocation and enhanced the transcription of IL-6 and IL-1 β in macrophages (44). Our results show that after exposure to LPS, canine macrophages exhibited a significant increase in p65 phosphorylated at Ser 536, while pre-treatment with non-toxic levels of arsenite attenuated this effect. These results suggest that the cell stress-induced upregulation of Hsp70 suppresses p65 activation, thus inhibiting LPS-induced IL-6 and TNF- α expression in canine macrophages.

Other studies have also shown that inducible Hsp70 may dampen the activation of NF- κ B complexes. In the rat, the overexpression of Hsp70 blocked the LPS-induced increase in the production of IL-6 and TNF- α by preventing I κ B α degradation and NF- κ B p65 nuclear translocation (38). Similarly, in Hela cells (45) and human retinal pigment epithelial cells (20), Hsp70 upregulation reduced the phosphorylation of NF- κ B p65 and subsequent p65 DNA binding. Furthermore, in the first part of our

studies, we found that cell stress reduces LPS-induced NF- κ B activation and pro-inflammatory cytokine expression. To directly demonstrate that this occurs via elevation of the expression levels of Hsp70, we established a canine macrophage cell clone, lacking inducible Hsp70. Consistent with previous data, we found that in the absence of induced Hsp70, cell stress failed to attenuate the LPS-induced activation of NF- κ B p65, and IL-6 and TNF- α expression. The specific molecular mechanism of interaction between Hsp70 and the NF- κ B complex is still unclear.

Previous studies indicated that Hsp70 recognizes short hydrophobic stretches within a protein sequence (46, 47). Bernd Bukau's lab investigated in detail its substrate recognition principle, as a result providing a scoring matrix for determining possible binding sites within a protein sequence. A vast majority of proteins carry (multiple) Hsp70 binding sites (47, 48), and as such hydrophobic peptides are required for holding the 3D fold of a protein, constituting the hydrophobic core of a globular protein. Meanwhile, Hsp70 requires the extended conformation of its substrate in order to bind (49). We mapped the potential Hsp70 binding sites within the sequence of the p65 (RELA) protein as a model NF- κ B member, and compared the localization of the binding peptides with known phosphorylation sites on p65 (see Figure S8). We found that the phosphorylation sites are located in proximity to the accessible chaperone binding peptides. Apart from p65, an interaction between Hsp70 and p50 has also been reported (50). In addition, an earlier study by Bao et al. indicated that Hsp27 and Hsp70 interacted with IKK α and I κ B α respectively in mice with liver injury, thereby inhibiting I κ B degradation and NF- κ B activation (51). A study by Chen et al. (25) showed that Hsp70 blocked IKK α / β phosphorylation by binding TNF receptor-associated factor 6 (TRAF6), and thus inhibited LPS-induced NF- κ B activation, but a direct interaction between Hsp70 and IKK α / β was not detected. Conversely, Ran et al. (52) reported that Hsp70 can decrease NF- κ B activity by binding to IKK γ . In microglia subjected to treatment with TNF- α , the overexpression of Hsp70 not only reduced NF- κ B DNA binding activity, but also the activity of IKK kinase and the phosphorylation level of I κ B α (23). These different results suggest that Hsp70 may modulate the NF- κ B pathway at different levels, but the reason for these differences requires further study.

Taken together, the chemical stressor arsenite dose-dependently induced Hsp70 expression in the canine macrophage cell line, and this increase in Hsp70 levels was sufficient to repress LPS-induced NF- κ B p65 phosphorylation and pro-inflammatory cytokine expression. Moreover, the repressive effects on cytokine (IL-6 and TNF- α) expression and NF- κ B p65 activation were abolished in the Hsp70-deficient canine macrophage. These data indicate that Hsp70 upregulation by cell stress can suppress the LPS-induced inflammatory response in canine macrophages by downregulating NF- κ B p65 nuclear translocation and subsequent pro-inflammatory

cytokine expression (IL-6 and TNF- α). Our study suggests that Hsp70 could be a promising target for the development of anti-inflammatory therapeutics, and that the use of such therapeutics may extend to animal species such as the dog.

Materials and Methods

Cell Culture

A canine histiocytic cell line 030D characterized as macrophages was used (53). Cells were grown in RPMI 1640 (Gibco, Cat. No. 72400) supplemented with 10% fetal bovine serum (BODINCO B. V., The Netherlands), 1% penicillin/streptomycin (Gibco, Cat. No. 15140122) at 37 °C and 5% CO₂.

Analysis of Hsp70 Expression in 030D Cells by Flow Cytometry

The 030D cells were seeded into the wells of 12-well culture plates at a density of 1×10^6 cells/well. After 6 h, non-adherent cells were removed and the adherent cells were incubated with or without various amounts (0.3125, 0.625, 1.25, 2.5, 5 and 10 μ M) of arsenite for 16 h. At different timepoints, the cells were washed twice with PBS and collected by treatment with 0.5 M EDTA (Invitrogen, Cat. No.15575020). To analyze inducible Hsp70 produced by 030D cells, the cells were fixed and permeabilized with Cytotfix/Cytoperm solution (BD Pharmingen) for 30 min at 4 °C, followed by washing with Perm/Wash (BD Pharmingen) and blocking with 5% normal mouse serum. Then, cells were stained with either a fluorescein isothiocyanate (FITC) labeled Hsp70 specific monoclonal antibody (SPA-810; Stressgen) or with a corresponding isotype control, in Perm/Wash supplemented with 2% normal mouse serum. After washing, the cells were re-suspended in FACS buffer (2% BSA in PBS) and fluorescence was measured using a FACS Canto (BD Pharmingen) flow cytometer. Data were analyzed using FlowJo v10 Software.

Analysis of IL-6, IL-1 β , TNF- α and Hsp70 Expression by Real-Time PCR

The 030D cells (1×10^6 cells/well) were incubated with or without various amounts (1.25, 2.5, 5 or 10 μ M) of arsenite. After 16 h, the cells were exposed or unexposed to 1 μ g/mL LPS (Sigma-Aldrich, *Escherichia coli* 0111:B4, Cat. No. L2630) for 6 h. The cells were harvested and total RNA was isolated using RNeasy kit (Qiagen, Venlo, The Netherlands), according to the manufacturer's instructions. RNA was treated with DNase I (Qiagen, Cat. No. 79254) for 15 min to avoid DNA contamination. RNA concentration and quality were assessed by the measurement

of 260/280 ratio using a Nano-drop-1000 spectrophotometer. For reverse transcription to cDNA with an iScript™ cDNA Synthesis Kit (Bio-Rad) according to manufacturer's instructions, 1 μ g mRNA was used.

Real time PCR for IL-6, TNF- α , IL-1 β and Hsp70 mRNA detection was performed on a CFX Connect™ Real-Time System using iQ™ SYBR Green Supermix (Bio-Rad), applying the following cycle parameters: 3 min at 95 °C, followed by 40 cycles of 20 s at 95 °C and 45 s at 60 °C. Canine IL-6, TNF- α , IL-1 β and Hsp70 primers were synthesized by Invitrogen. The primer sequences were the following: IL-6, forward primer 5'-TCCTGGTGATGGCTACTGCTT-3', reverse primer 5'-GAC TAT TTG AAG TGG CAT CAT CCT T-3'; IL-1 β , forward primer 5'- TCT CCC ACC AGC TCT GTA ACA A-3', reverse primer 5'- GCA GGG CTT CTT CAG CTT CTC-3'; TNF- α , forward primer 5'-CCC CGG GCT CCA GAA GGT G-3', reverse primer 5'- GCA GCA GGC AGA AGA GTG TGG TG-3'; and Hsp70, forward primer 5'-TTC TTT AAC GGC CGC GAT CT-3', reverse primer 5'-GGT TGT CCG AGT AGG TGG TG-3'. The Ribosomal Protein S19 (RPS19) gene was used as a reference gene (forward primer: 5'-CCT TCC TCA AAA AGT CTG GG-3', reverse primer: 5'-GTT CTC ATC GTA GGG AGC AAG-3'). Relative expression of mRNA was calculated by the Pfaffl-method.

Cell Viability Assay

In order to evaluate the potential toxicity of arsenite for O30D cells, a 3-(4, 5-dimethylthiazol-2-yl)-2, 5-diphenyltetrazolium bromide (MTT) assay was used to assess cell metabolism. Briefly, 1×10^4 cells/well O30D cells were placed in a 96-well plate. After 6 h of incubation, non-adherent cells were removed. Adherent cells were placed in various concentrations of arsenite (0.3125, 0.625, 1.25, 2.5, 5 and 10 μ M) and incubated for 24 h at 37 °C and 5% CO₂. Then, 100 μ L 1 mg/mL MTT (Abcam, Cat. No. ab146345) was added to each well and after 4 h the medium was aspirated. Formazan crystals that had formed through cell respiration were dissolved in 150 μ L dimethyl sulfoxide (DMSO). Absorbance was read at 595 nm using a Model 550 Microplate Reader (Bio-Rad, The Netherlands). Cells cultured in medium only were used as control. Each treatment was performed in triplicate and all assays were performed 3 times at least.

Assessment of NF- κ B Activation by Western Blot

The O30D cells were seeded into a 6-well plate at a density of 2×10^6 cells/well. After 6 h, non-adherent cells were removed, and the adherent cells were incubated with or without various amounts (1.25 and 2.5 μ M) of arsenite. After 16 h, cells were exposed to 1 μ g/mL LPS (Sigma-Aldrich, *Escherichia coli* 0111:B4, Cat. No. L2630) for 5, 15, 30 and 60 min. Subsequently the cells were washed twice with cold PBS

and harvested by treatment with 0.5 M EDTA following centrifugation at 3000× *g* for 10 min. Pelleted cells were lysed with Pierce™ RIPA Buffer (Thermo Scientific, Cat. No. 89900) with protease inhibitors (Roche, Cat. No. 11826170001) for 20–30 min on ice and then centrifuged at 14,000× *g* for 15 min at 4 °C. The protein contents in the lysates were measured using a Micro BCA™ Protein Assay Kit (Thermo Scientific, Cat. No. 23235) according to manufacturer's instructions. Proteins were denatured in laemmli buffer with 10% β-Mercaptoethanol at 60 °C for 30 min, and aliquots were stored at –70 °C prior to analysis.

For Western Blot analysis, protein samples (30 µg) were subjected to PAGE using 4–20% Mini-PROTEAN® TGX™ Gels (Bio-Rad, Cat. No. 456-1095) and then transferred onto the PVDF membrane. This membrane was blocked for 2 h at room temperature with 0.2% gelatin (Sigma-Aldrich, Cat. No. G7765) in PBS with 0.01% Tween-20, and then incubated with rabbit monoclonal anti-phospho-NF-κB p65 (Ser 536) (1:1000; Thermo Scientific, Cat. No. MA5-15160) or mouse monoclonal anti-NF-κB p65 (Ser 536) (1:4000; Thermo Scientific, Cat. No. 436700) overnight at 4 °C. After four repetitions of rinsing in PBST, the membrane was incubated with HRP-labeled swine-anti rabbit IgG (1:2000; Dako, Cat. No. P0399) or rabbit anti-mouse IgG (1:5000; Dako, Cat. No. P0260) for 2 h at room temperature. The HRP signal was enhanced using SuperSignal™ West Pico PLUS Chemiluminescent Substrate (Thermo Scientific, Cat. No. 34580) according to the manufacturer's instructions, and visualized using a Gel Doc™ XR+ Molecular Imager (Bio-Rad). The density of bands was analyzed by Image Lab Software (Bio-Rad).

Design of Guide RNA for Hsp70 Knockout and Cloning

The guide RNAs for targeting Canine Hsp70 (Gene ID: 403612) were designed using the website <http://www.benchling.com> (Benchling, San Francisco, CA, USA) and synthesized by Invitrogen. To enhance the chance of knockout, two gRNAs were designed, and the overhangs of a specific CRISPR-concatemer vector (54) were added to each gRNA oligo. The sequences are shown in Table 1. The gRNAs were cloned into a CRISPR-concatemer vector (Figure 5A) (kind gift from Dr. Merenda) as described by Merenda, Alessandra, et al. (54). Briefly, 5' ends of gRNA oligos (10 µM) were phosphorylated and annealed with T4 PNK (Biolabs, Cat. No. M0201S) using the following cycle parameters: 30 min at 37 °C, 5 min at 95 °C, then ramp down to 25 °C at 0.3 °C/min and 4 °C. Subsequently, the annealed gRNAs were ligated into the CRISPR-concatemer vector using 100 ng CRISPR-concatemer vector, 10.0 µL oligo mixture, 1.0 µL BSA-containing restriction enzyme buffer (10×), 1.0 µL DTT (10 mM), 1.0 µL ATP (10 mM), 1.0 µL *Bbs*I, 1.0 µL T7 ligase, 5.0 µL H₂O, and the following cycle parameters: 25 cycles of 5 min at 37 °C and 5 min at 21 °C, hold for 15 min at 37 °C and then 4 °C forever. Ligated CRISPR-concatemer

Hsp70 and NF- κ B mediated inflammatory responses in canine macrophages

vectors were transformed into DH5 α . Clones were grown overnight at 37 °C in a shaking incubator and DNA was extracted using Zyppy™ Plasmid Miniprep kit (Cat. No. D4020). A quantity of 200 ng DNA was digested with 10 U *EcoRI* and 5 U *BglII* at 37 °C for 3 h, and run on 1% agarose gel to select CRISPR-concatemer vectors containing gRNA. Single digests with *BbsI* were used as control. Sequences of selected constructs were confirmed by Sanger sequencing.

Table 1. Hsp70 guide RNA ([gRNA]) and overhangs (guide RNA cassette).

	Cassette 1	Cassette 2
Forward sequence (5'-3')	CACCGG[TCCATCCTG ACGATCGACGA]GT	ACCGG[CGGCACGGT GATCACCGCGT]G
Reverse sequence (5'-3')	TAAAAC[TCGTGATC GTCAGGATGGA]CC	AAAAC[ACGCGGTGAT CACCGTGCCG]C

4

Establishment of a Hsp70 Knockout 030D Cell Line and Validation

A Hsp70 knockout 030D cell line was generated as previously described (55). Briefly, 2×10^7 cells were harvested and incubated with 10 μ g cas9 and 5 μ g Hsp70 gRNA for 10 min at room temperature. Cells were then transferred into a 0.4 cm gap electroporation cuvette (Bio-Rad, Cat. No. 1652081) and electroporated using a Gene Pulser® II Electroporation System (Bio-Rad) with settings: 250 V, 975 μ F, resistance set to infinity. Cells were seeded in a 6 cm dish with warm medium, and 48 h later 5 μ g/mL puromycin (Sigma-Aldrich, Cat. No. P9620) was added to the culture medium for another 48 h, to select gene-edited cells. Five days after selection, single cell sorting was performed using a BD Influx™ cell sorter (BD Biosciences, USA), and cells were seeded in a 96-well plate. After 2 weeks expansion of individual colonies, Hsp70 expression was analyzed by flow cytometry to detect clones lacking the expression of inducible Hsp70. Genomic DNA from these cells was isolated using the PureLink™ Genomic DNA Mini Kit (Cat. No. K182002) according to the manufacturer's instructions. PCR was performed using Hsp70 primers (forward: 5'-TGA GCT ACA AGG GGG AGA-3', reverse: 5'-TGG TGA TGG ACG TGT AGA-3') that cover the restriction sites, and PCR products were sent to Macrogen (The Netherlands) for sequencing, to confirm Hsp70 gene editing.

Statistical Analysis

The statistical analysis and graphical display were performed using GraphPad Prism 8.3.0. Data are shown as the mean \pm SD. Comparison among groups was performed by one-way ANOVA test with Bonferroni correction. *p*-values below 0.05 were regarded as statistically significant.

Supplementary Materials: Supplementary Materials can be found at <http://www.mdpi.com/1422-0067/21/18/6464/s1>.

Author Contributions: Conceptualization, Qingkang Lyu, Alice Sijts and Femke Broere; Investigation, Qingkang Lyu and Magdalena Wawrzyniuk; Project administration, Alice Sijts and Femke Broere; Supervision, Victor P.M.G. Rutten, Willem van Eden, Alice Sijts and Femke Broere; Writing—original draft, Qingkang Lyu; Writing—review and editing, Victor P.M.G. Rutten, Willem van Eden, Alice Sijts and Femke Broere.

Funding: This research received no external funding.

Conflicts of Interest: The authors declare no conflict of interest.

Acknowledgments: Qingkang Lyu was supported by a fellowship of the China Scholarship Council (CSC).

Abbreviations

Hsp70	Heat shock protein70
NF- κ B	nuclear factor kappa light chain enhancer of activated B cells
TNF- α	Tumor necrosis factor α
CRISPR	Clustered regularly interspaced short palindromic repeat
Cas	CRISPR-associated
LPS	Lipopolysaccharide
qPCR	Quantitative polymerase chain reaction
IL-6	Interleukin 6
gRNA	Guide ribonucleic acid
I κ B	Inhibitor of nuclear factor kappa B
TLR	toll-like receptor
NO	Nitric oxide

Supplementary materials

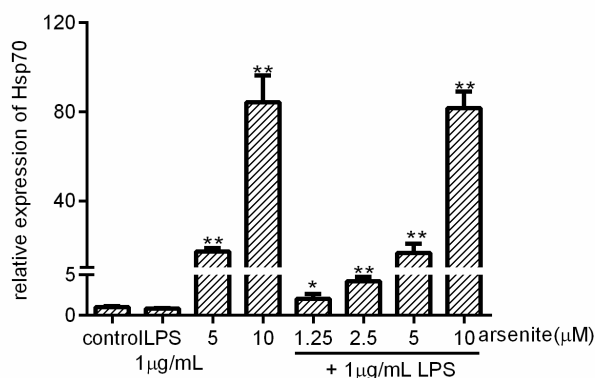


Figure S2. The expression of Hsp70 by 030D cells after arsenite and LPS stimulation. 030D cells were treated with various concentration of arsenite (1.25 μM to 10 μM) for 16 h as indicated. Then they were left unstimulated or stimulated with 1 $\mu\text{g}/\text{mL}$ LPS for 6 h. mRNA expression of Hsp70 was measured by qPCR. Data are shown as the mean \pm SD and are representative of three independent experiments. * $p < 0.05$, ** $p < 0.01$, vs LPS alone group.

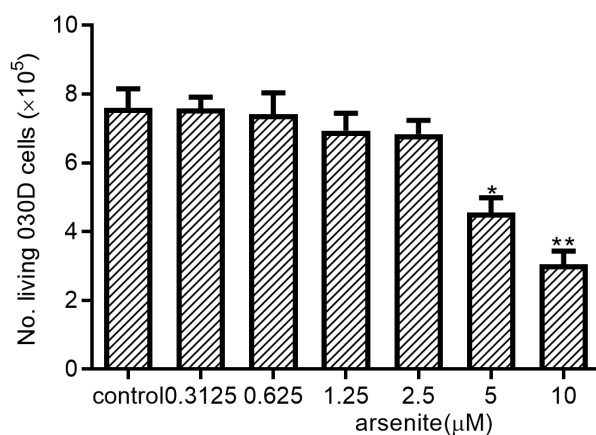


Figure S3. Effects of arsenite on the metabolic activity of 030D cells. 030D cells (2×10^5 cells/well) were incubated with the indicated concentrations of arsenite for 24 h.

Hsp70 and NF- κ B mediated inflammatory responses in canine macrophages

Living 030D cells were counted. Untreated cells were used as control. Data are shown as the mean \pm SD and representative of three independent experiments. * $p < 0.05$, ** $p < 0.01$, vs control group.

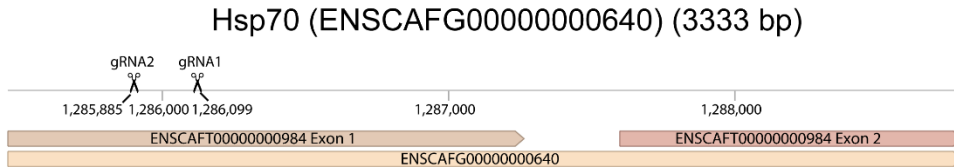


Figure S4. Targeting sites of gRNA

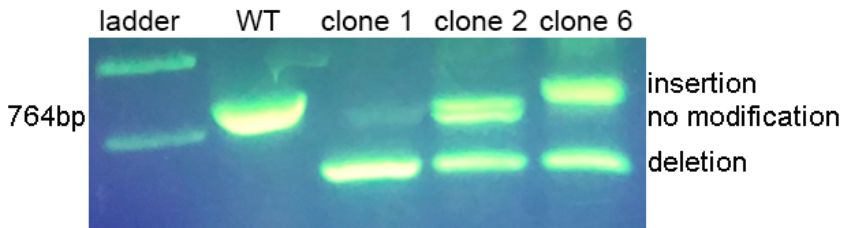


Figure S5. Validation of Hsp70 gene modification in 030D cell clones. Genomic DNA from these cells was isolated. PCR was performed using Hsp70 primers that cover the restriction sites and PCR products were visualized by gel electrophoresis on 1% agarose gel. Clone 1, clone 2 and clone 6 are gene-modified. WT = wild type

Chapter 4

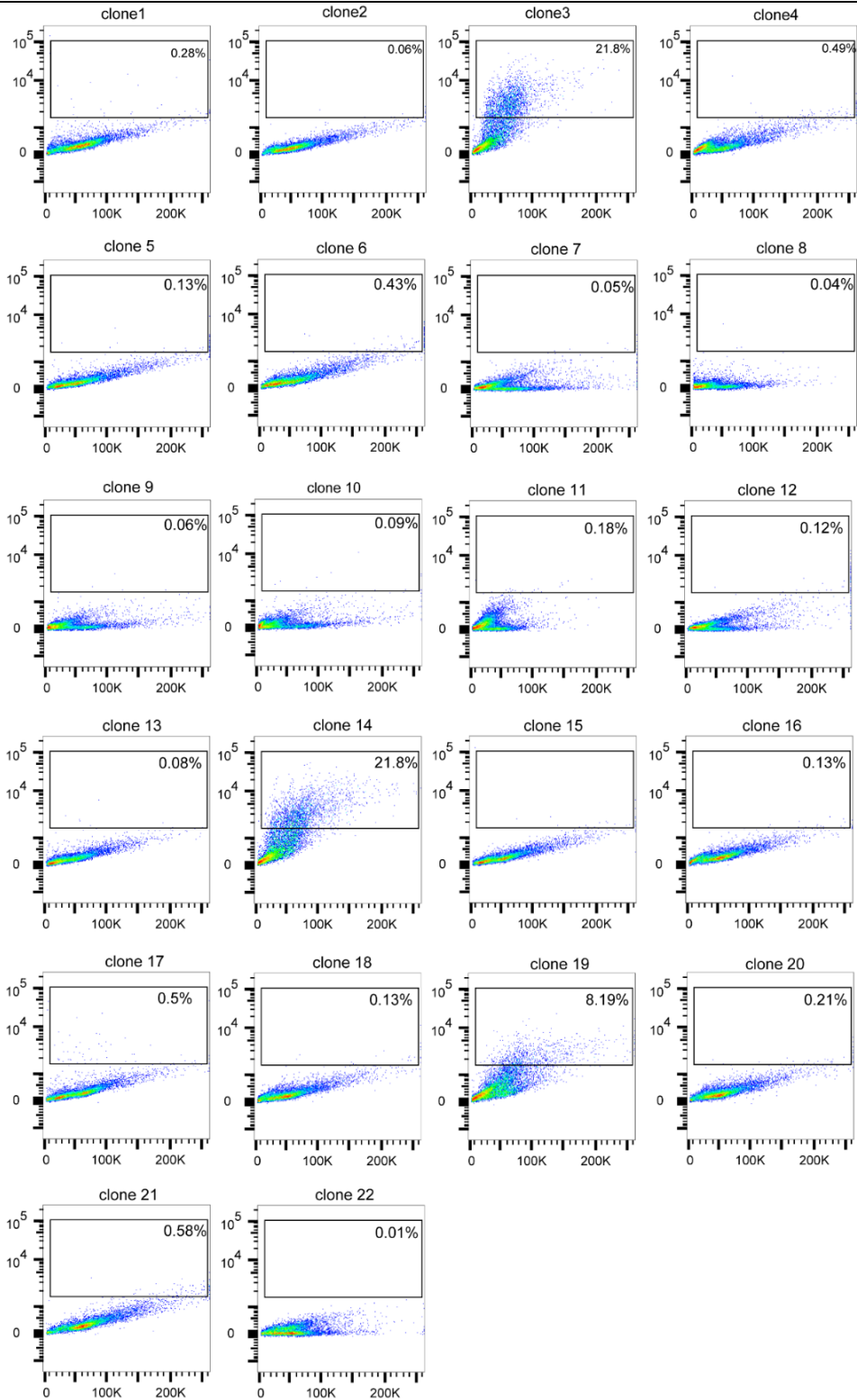


Figure S6. Flow cytometry analysis of gene-modified cell clones (1-22) to evaluate the expression of Hsp70 in 030D cells

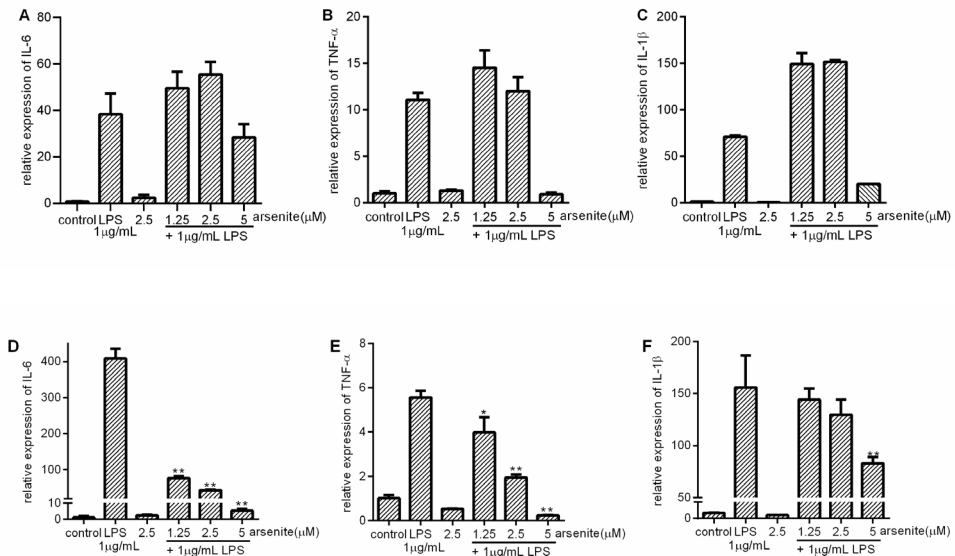


Figure S7. The effect of inducible Hsp70 on pro-inflammatory cytokine expression. A second Hsp70 knockout 030D clone, clone5 (**A, B, C**) and corresponding CRISPER/Cas9-treated wild type-like clones, clone 3 (**D, E, F**) were treated with different concentrations (1.25, 2.5 or 5 μ M) of arsenite or without for 16 h and then exposed to LPS. The cells were harvested after 6 h of LPS exposure. qPCR were performed to detect the expression of IL-6 (**A**), IL-1 β (**B**) and TNF- α (**C**) on clone 5 and clone 3 (**D, E, and F, respectively**). Data are shown as the mean \pm SD and are representative of three independent experiments. * $p < 0.05$, ** $p < 0.01$, and *** $p < 0.001$, vs LPS alone group

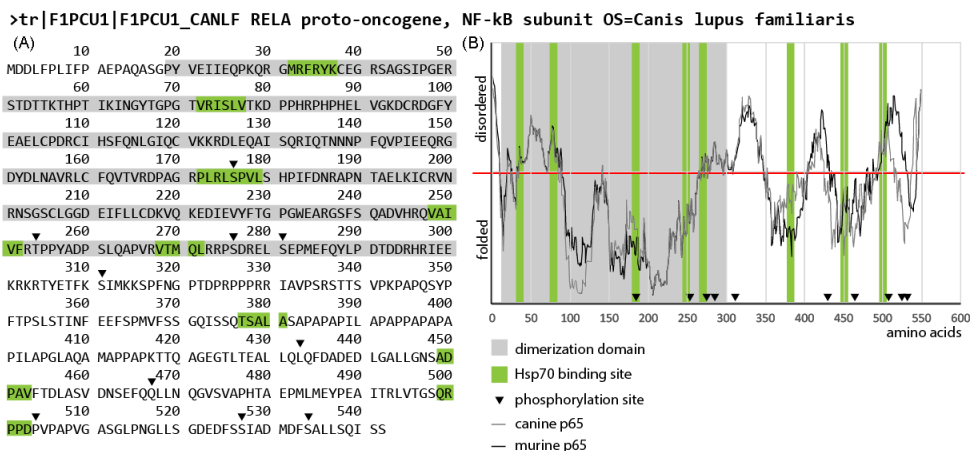


Figure S8. The prediction of the Hsp70 binding sites on p65 (RELA) protein. **(A)** shows the amino acid sequence of canine p65. **(B)** shows that the amino acid sequence of murine p65 (UniProt ID: Q04207) is strongly similar to canine p65 (UniProt ID: F1PCU1). Black triangle representative reported phosphorylation sites; green: predicted Hsp70 binding sites on p65.

References

1. Perdiguero EG, Klapproth K, Schulz C, Busch K, Azzoni E, Crozet L, et al. Tissue-resident macrophages originate from yolk-sac-derived erythro-myeloid progenitors. *Nature* (2015) 518(7540):547-51.
2. Orecchioni M, Ghosheh Y, Pramod AB, Ley K. Macrophage polarization: different gene signatures in M1 (LPS+) vs. classically and M2 (LPS-) vs. alternatively activated macrophages. *Frontiers in immunology* (2019) 10:1084.
3. David S, Kroner A. Repertoire of microglial and macrophage responses after spinal cord injury. *Nature Reviews Neuroscience* (2011) 12(7):388-99.
4. Hume DA, Freeman TC. Transcriptomic analysis of mononuclear phagocyte differentiation and activation. *Immunological reviews* (2014) 262(1):74-84.
5. Kasraie S, Werfel T. Role of macrophages in the pathogenesis of atopic dermatitis. *Mediators of inflammation* (2013) 2013.
6. Na YR, Stakenborg M, Seok SH, Matteoli G. Macrophages in intestinal inflammation and resolution: a potential therapeutic target in IBD. *Nature Reviews Gastroenterology & Hepatology* (2019):1.
7. Udalova IA, Mantovani A, Feldmann M. Macrophage heterogeneity in the context of rheumatoid arthritis. *Nature Reviews Rheumatology* (2016) 12(8):472.
8. He W, Yuan T, Maedler K. Macrophage-associated pro-inflammatory state in human islets from obese individuals. *Nutrition & diabetes* (2019) 9(1):1-4.
9. Ta W, Chawla A, Pollard J. Origins and hallmarks of macrophages: development, homeostasis, and disease. *Nature* (2013) 496:445-55.
10. SC BSL. Functions of NF- κ B1 and NF- κ B2 in immune cell biology. *Biochemical Journal* (2004) 382:393-409.
11. Liu T, Zhang L, Joo D, Sun S-C. NF- κ B signaling in inflammation. *Signal transduction and targeted therapy* (2017) 2(1):1-9.
12. Hambleton J, Weinstein SL, Lem L, DeFranco AL. Activation of c-Jun N-terminal kinase in bacterial lipopolysaccharide-stimulated macrophages. *Proceedings of the National Academy of Sciences* (1996) 93(7):2774-8.
13. Scherle PA, Jones EA, Favata MF, Daulerio AJ, Covington MB, Nurnberg SA, et al. Inhibition of MAP kinase kinase prevents cytokine and prostaglandin E2 production in lipopolysaccharide-stimulated monocytes. *The Journal of Immunology* (1998) 161(10):5681-6.
14. Sakai J, Cammarota E, Wright JA, Cicuta P, Gottschalk RA, Li N, et al. Lipopolysaccharide-induced NF- κ B nuclear translocation is primarily dependent on MyD88, but TNF α expression requires TRIF and MyD88. *Scientific reports* (2017) 7(1):1-9.
15. Murray PJ, Allen JE, Biswas SK, Fisher EA, Gilroy DW, Goerdts S, et al. Macrophage activation and polarization: nomenclature and experimental guidelines. *Immunity* (2014) 41(1):14-20.
16. Köller M, Hensler T, König B, Prévost G, Alouf J, König W. Induction of heat-shock proteins by bacterial toxins, lipid mediators and cytokines in human leukocytes. *Zentralblatt für Bakteriologie* (1993) 278(2-3):365-76.
17. TESHIMA S, ROKUTAN K, TAKAHASHI M, NIKAWA T, KISHI K. Induction of heat shock proteins and their possible roles in macrophages during activation

- by macrophage colony-stimulating factor. *Biochemical Journal* (1996) 315(2):497-504.
18. Jiang B, Xiao W, Shi Y, Liu M, Xiao X. Heat shock pretreatment inhibited the release of Smac/DIABLO from mitochondria and apoptosis induced by hydrogen peroxide in cardiomyocytes and C2C12 myogenic cells. *Cell stress & chaperones* (2005) 10(3):252.
 19. Wang L-C, Liao L-X, Lv H-N, Liu D, Dong W, Zhu J, et al. Highly selective activation of heat shock protein 70 by allosteric regulation provides an insight into efficient neuroinflammation inhibition. *EBioMedicine* (2017) 23:160-72.
 20. Paimela T, Hyttinen JM, Viiri J, Ryhanen T, Salminen A, Kaarniranta K. Celastrol Regulates Innate Immunity Response Via Nf-B And Hsp70 In Human Retinal Pigment Epithelial Cells. *Investigative Ophthalmology & Visual Science* (2011) 52(14):864-.
 21. Wang C-H, Chou P-C, Chung F-T, Lin H-C, Huang K-H, Kuo H-P. Heat shock protein70 is implicated in modulating NF-κB activation in alveolar macrophages of patients with active pulmonary tuberculosis. *Scientific reports* (2017) 7(1):1-9.
 22. Ding XZ, Fernandez-Prada CM, Bhattacharjee AK, Hoover DL. Overexpression of hsp-70 inhibits bacterial lipopolysaccharide-induced production of cytokines in human monocyte-derived macrophages. *Cytokine* (2001) 16(6):210-9.
 23. Sheppard PW, Sun X, Khammash M, Giffard RG. Overexpression of heat shock protein 72 attenuates NF-κB activation using a combination of regulatory mechanisms in microglia. *PLoS Comput Biol* (2014) 10(2):e1003471.
 24. Bhagat L, Singh VP, Dawra RK, Saluja AK. Sodium arsenite induces heat shock protein 70 expression and protects against secretagogue-induced trypsinogen and NF-κB activation. *Journal of cellular physiology* (2008) 215(1):37-46.
 25. Chen H, Wu Y, Zhang Y, Jin L, Luo L, Xue B, et al. Hsp70 inhibits lipopolysaccharide-induced NF-κB activation by interacting with TRAF6 and inhibiting its ubiquitination. *FEBS letters* (2006) 580(13):3145-52.
 26. Lyu Q, Ludwig IS, Kooten PJ, Sijts AJ, Rutten VP, Van Eden W, et al. Leucinoastatin acts as a co-inducer for heat shock protein 70 in cultured canine retinal pigment epithelial cells. *Cell Stress and Chaperones* (2020) 25(2):235-43.
 27. Lin L, Stringfield TM, Shi X, Chen Y. Arsenite induces a cell stress-response gene, RTP801, through reactive oxygen species and transcription factors Elk-1 and CCAAT/enhancer-binding protein. *Biochemical Journal* (2005) 392(1):93-102.
 28. Srinivasan M, Lahiri DK. Significance of NF-κB as a pivotal therapeutic target in the neurodegenerative pathologies of Alzheimer's disease and multiple sclerosis. *Expert opinion on therapeutic targets* (2015) 19(4):471-87.
 29. Papoutsopoulou S, Burkitt MD, Bergey F, England H, Hough R, Schmidt L, et al. Macrophage-specific NF-κB activation dynamics can segregate inflammatory bowel disease patients. *Frontiers in immunology* (2019) 10:2168.
 30. Patel S, Santani D. Role of NF-κB in the pathogenesis of diabetes and its associated complications. *Pharmacological Reports* (2009) 61(4):595-603.

31. Lee C-T, Repasky EA. Opposing roles for heat and heat shock proteins in macrophage functions during inflammation: a function of cell activation state? *Frontiers in immunology* (2012) 3:140.
32. Ferat-Osorio E, Sánchez-Anaya A, Gutiérrez-Mendoza M, Boscó-Gárate I, Wong-Baeza I, Pastelin-Palacios R, et al. Heat shock protein 70 down-regulates the production of toll-like receptor-induced pro-inflammatory cytokines by a heat shock factor-1/constitutive heat shock element-binding factor-dependent mechanism. *Journal of Inflammation* (2014) 11(1):1-12.
33. Daneri Becerra CdR, Galigniana MD. Regulatory role of heat-shock proteins in autoimmune and inflammatory diseases. (2016).
34. Zheng Z, Kim JY, Ma H, Lee JE, Yenari MA. Anti-inflammatory effects of the 70 kDa heat shock protein in experimental stroke. *Journal of Cerebral Blood Flow & Metabolism* (2008) 28(1):53-63.
35. Sun D, Chen D, Du B, Pan J. Heat shock response inhibits NF- κ B activation and cytokine production in murine Kupffer cells. *Journal of Surgical Research* (2005) 129(1):114-21.
36. Greten FR, Arkan MC, Bollrath J, Hsu L-C, Goode J, Miething C, et al. NF- κ B is a negative regulator of IL-1 β secretion as revealed by genetic and pharmacological inhibition of IKK β . *Cell* (2007) 130(5):918-31.
37. Zastona Z, Pålsson-McDermott EM, Menon D, Haneklaus M, Flis E, Prendeville H, et al. The induction of pro-IL-1 β by lipopolysaccharide requires endogenous prostaglandin E2 production. *The Journal of Immunology* (2017) 198(9):3558-64.
38. Dokladny K, Lobb R, Wharton W, Ma TY, Moseley PL. LPS-induced cytokine levels are repressed by elevated expression of HSP70 in rats: possible role of NF- κ B. *Cell Stress and Chaperones* (2010) 15(2):153-63.
39. Pahl HL. Activators and target genes of Rel/NF- κ B transcription factors. *Oncogene* (1999) 18(49):6853-66.
40. Perkins ND. Post-translational modifications regulating the activity and function of the nuclear factor kappa B pathway. *Oncogene* (2006) 25(51):6717-30.
41. Giridharan S, Srinivasan M. Mechanisms of NF- κ B p65 and strategies for therapeutic manipulation. *Journal of inflammation research* (2018) 11:407.
42. Ryo A, Suizu F, Yoshida Y, Perrem K, Liou Y-C, Wulf G, et al. Regulation of NF- κ B signaling by Pin1-dependent prolyl isomerization and ubiquitin-mediated proteolysis of p65/RelA. *Molecular cell* (2003) 12(6):1413-26.
43. Yang F, Tang E, Guan K, Wang C-Y. IKK β plays an essential role in the phosphorylation of RelA/p65 on serine 536 induced by lipopolysaccharide. *The Journal of Immunology* (2003) 170(11):5630-5.
44. Hayden M, West A, Ghosh S. NF- κ B and the immune response. *Oncogene* (2006) 25(51):6758-80.
45. Cao X, Yue L, Song J, Wu Q, Li N, Luo L, et al. Inducible HSP70 antagonizes IL-1 β cytotoxic effects through inhibiting NF- κ B activation via destabilizing TAK1 in HeLa cells. *PLoS One* (2012) 7(11):e50059.
46. Rüdiger S, Germeroth L, Schneider-Mergener J, Bukau B. Substrate specificity of the DnaK chaperone determined by screening cellulose-bound peptide libraries. *The EMBO journal* (1997) 16(7):1501-7.

47. Mayer MP, Bukau B. Hsp70 chaperones: cellular functions and molecular mechanism. *Cell Mol Life Sci* (2005) 62(6):670-84. Epub 2005/03/17. doi: 10.1007/s00018-004-4464-6.
48. Srinivasan SR, Gillies AT, Chang L, Thompson AD, Gestwicki JE. Molecular chaperones DnaK and DnaJ share predicted binding sites on most proteins in the E. coli proteome. *Molecular BioSystems* (2012) 8(9):2323-33.
49. Stein KC, Kriel A, Frydman J. Nascent polypeptide domain topology and elongation rate direct the cotranslational hierarchy of Hsp70 and TRiC/CCT. *Molecular cell* (2019) 75(6):1117-30. e5.
50. Guzhova IV, Darieva ZA, Melo AR, Margulis BA. Major stress protein Hsp70 interacts with NF- κ B regulatory complex in human T-lymphoma cells. *Cell stress & chaperones* (1997) 2(2):132.
51. Bao X-Q, Liu G-T. Induction of overexpression of the 27-and 70-kDa heat shock proteins by bicyclol attenuates concanavalin A-induced liver injury through suppression of nuclear factor- κ B in mice. *Molecular pharmacology* (2009) 75(5):1180-8.
52. Ran R, Lu A, Zhang L, Tang Y, Zhu H, Xu H, et al. Hsp70 promotes TNF-mediated apoptosis by binding IKK γ and impairing NF- κ B survival signaling. *Genes & development* (2004) 18(12):1466-81.
53. Gebhard D, Levy M, Ley D, editors. Isolation and characterization of functionally and phenotypically distinct continuous monocytoid cell lines from a canine malignant histiocytosis. *Fourth International Veterinary Immunology Symposium Davis, California, USA*; 1995.
54. Merenda A, Andersson-Rolf A, Mustata RC, Li T, Kim H, Koo B-K. A protocol for multiple gene knockout in mouse small intestinal organoids using a CRISPR-concatemer. *JoVE (Journal of Visualized Experiments)* (2017) (125):e55916.
55. Zhang J, Zhao J, Zheng X, Cai K, Mao Q, Xia H. Establishment of a novel hepatic steatosis cell model by Cas9/sgRNA-mediated DGK θ gene knockout. *Molecular medicine reports* (2018) 17(2):2169-76.

5



Comprehensive characterization of dog monocyte-derived macrophages at different polarization statuses: M1 and M2

Qingkang Lyu¹, Victor P. M. G. Rutten^{1,2}, Willem van Eden¹, Alice J. A. M. Sijts¹ and Femke Broere^{1,3,*}

¹Department of Infectious diseases and Immunology, Faculty of Veterinary Medicine, Utrecht University; 3584 CL, Utrecht, The Netherlands

²Department of Veterinary Tropical diseases, Faculty of Veterinary Science, Pretoria University, South Africa

³Department of Clinical Sciences of Companion Animals, Faculty Veterinary Medicine, Utrecht University, Utrecht, The Netherlands

*Correspondence: f.broere@uu.nl

Abstract

Macrophages can be differentiated into multiple functional subsets under different micro-environment. Identification of macrophage polarization states is valuable for the study of immune-related diseases. However, knowledge about dog monocyte-derived macrophages is still considerably lacking. In this study, we isolated dog monocytes and polarized these with GM-CSF, IFN- γ and LPS towards an M1, or M-CSF and IL-4 towards an M2 phenotype, and with unpolarized M0 as control. Polarized macrophage subsets were thoroughly characterized based on morphology, surface makers feature, gene profiles and functional properties. Our results showed that M1-polarized macrophages appeared as round cells with a dominant amoeboid and “fried-egg” phenotype, while M2-polarized macrophages obtained an elongated spindle morphology. Phenotypically, M1-polarized macrophages expressed high levels of CD40, CD80, CD86 and MHC II, while a significant increase in the expression levels of CD206, CD209, CD163, and CD32 was observed in M2-polarized macrophages. The RNA sequencing results showed that M1 and M2-polarized macrophages have distinct gene profiles, which are closely associated with immune response, cell differentiation and phagocytosis. Functionally, all three polarization states of dog monocyte-derived macrophages can phagocytose latex beads, M2-polarized macrophages exhibited the strongest phagocytic capacity compared to M0- and M1-polarized macrophages. With our work, we contribute to a better understanding on canine macrophage biology and immune system.

Keywords: dog monocyte-derived macrophages, macrophage morphology, surface markers, gene profiles, phagocytosis

Introduction

Macrophages are a group of heterogeneous innate immune cells originated mainly from hematopoietic stem cells (HSCs), yolk sac or fetal liver, acting as sentinel of immune system (1). After birth, monocytes derived from HSCs are the main source of tissue-resident macrophages (2). Macrophages are highlighted by high plasticity and functional diversity, therefore macrophages can be differentiated into multiple functional subsets in different micro-environments (3). Based on phenotypic and functional features, macrophages can be roughly classified into two groups, known as the classically activated macrophage (M1) and the alternatively activated macrophage (M2), which present in different phase of inflammation or infection (4). Classically, during inflammation or infection, inflamed tissues are stimulated and start to express recruitment-related cytokines, chemokines and adhesion molecules, such as IL-6, C-C Motif Chemokine Ligand 2 (CCL2), and Intercellular Adhesion Molecule 1 (ICAM1), which recruit circulating monocytes to infiltrate and migrate to the inflammatory site (5, 6). There, monocytes are differentiated into M1 macrophages in response to pathogens, cytokines, or chemokines in the local environment. Activated M1 cells become bigger with ruffling of the plasma membrane and stretched out pseudopods, which help macrophages phagocytize and digest pathogens (7). Activated M1 macrophages secrete a variety of cytokines and chemokines to recruit other immune cells, such as B cells and T cells. Simultaneously, co-stimulatory molecules CD40, CD80, CD86, and MHC II, MHC I are upregulated, which contribute to the interaction between macrophages and T, B cells (8). In the later phase of inflammation, M1 cells undergo apoptosis, and the inflammatory response is then dominated by M2 cells. The M2 phenotype mitigates the inflammatory process and starts the resolution of inflammation and tissue repair by releasing anti-inflammatory cytokines, like IL-10 or TGF- β (9). Phagocytosis-related molecules, such as CD206, CD209 and CD163, are expressed by M2 cells, which help to clean pathogens, apoptotic cells and debris (10). Besides, the expression of Fc receptors, such as Fc γ R I, II and III, also enhance phagocytosis of M1 and M2 macrophages (11). Combined, M1 and M2 macrophages show noticeable differences during polarization in morphology, surface markers expression, cytokines secretion and phagocytic capacity. These differences offer a powerful tool to characterize macrophages subsets in *in vitro* studies.

In vitro, monocytes from peripheral blood mononuclear cells (PBMCs) can be polarized into various macrophage subsets such as M1, M2a, M2b and M2c by different stimuli. In the presence of granulocyte-macrophage colony-stimulating factor (GM-CSF), monocytes are differentiated toward the M1 subsets by microbial component such as lipopolysaccharide (LPS) in combination with Th1 cytokines, like

IFN- γ , or TNF- α (12). M1 cells exhibit pro-inflammatory properties by secreting cytokines like IL-6, IL-12, IL-23, IL-1 β and TNF- α (12). In contrast, M2 cells are oriented by Th2-type cytokines, such as IL-4, IL-10, and IL-13. In the presence of macrophage-colony stimulating factor (M-CSF), M2a and M2c subsets can be induced by incubation with IL-4/IL-13 and IL-10, respectively; M2b subsets are generated by exposure to immune complexes and TLR agonists (13-15). M2 cells dominantly secrete IL-10 and TGF- β , displaying an anti-inflammatory role (14). Thus, the functions and phenotypes of macrophages can shift along with micro-environment (16, 17). Previous studies have shown that dysfunction of macrophage polarization is involved in many immune diseases, such as autoimmune diseases, cancers, and chronic inflammatory diseases (18-20). Consequently, exploring the function of macrophages plays an important role in studying the onset and progression of many diseases.

Dogs are considered as an attractive animal model due to natural development of many immunological diseases. So far, hundreds of spontaneous inherited diseases have been characterized in dogs, most of which have clinically and genetically similarity to human diseases (21-23), including lymphomas, osteosarcoma, autoimmune haemolytic anemia and atopic dermatitis (24-26). Considering the importance of macrophages in these diseases, well-characterized dog macrophages are a valuable tool for canine immunological studies as well as for human studies using as a translation animal model. However, specific phenotypic M1 and M2 markers have not been identified in dog. Compared to studies on human and mouse macrophages, the knowledge about the characterization of dog monocyte-derived macrophages (MDMs) is considerably lacking.

In this study, we successfully cultured and polarized dog macrophages with a modified protocol. Subsequently, we described morphological differences between polarized dog MDMs. Then, we evaluated the expression of surface markers and differences in transcriptomics in M1 and M2 MDMs by flow cytometry and mRNA sequencing, respectively. Finally, we assessed phagocytosis of polarized dog MDMs.

Materials and methods

Dog PBMCs and monocytes isolation

Collection of dog blood samples, buffy coats, was conducted by professional veterinarians in the department of clinical Sciences of Companion Animals of Utrecht University. The use of buffy coat was approved for these experiments by the Utrecht University animal experiments committee.

Peripheral blood mononuclear cells (PBMCs) were isolated from dog buffy coats by gradient centrifugation using Histopaque-1077 (Sigma Aldrich, Gillingham, United Kingdom). Briefly, buffy coats from dog donors were diluted 1:1 in phosphate buffered saline (PBS) and gently layered over 1 volume of Histopaque-1077. The mixture was centrifuged for 30 min at 800 ×g at room temperature without braking. The layer of PBMCs located between plasma and Histopaque-1077 was collected using a Pasteur pipette and washed three times with PBS containing 0.5% fetal calf serum (FCS) and 2 mM EDTA (MACS buffer). Subsequently, monocytes were enriched by MACS column and a MACS separator using an anti-CD14 antibody (see table 1) and anti-mouse IgG Microbeads (Miltenyi Biotec GmbH, Bergisch Gladbach, Germany). Briefly, harvested dog PBMCs were incubated with anti-CD14 antibody (1:100) on ice for 30 min. After washing with MACS buffer, cells were incubated with anti-mouse IgG Microbeads for 30 min on ice, according to the manufacturers' instructions. Afterwards, labeled cells were washed using MACS buffer and then placed in a LS magnetic column (Miltenyi Biotec GmbH, Bergisch Gladbach, Germany) which was fixed on a MACS separator. CD14 labeled cells were retained in the column after 3 times rinsing with MACS buffer. Then the column was moved away from magnetic field, followed by the elution and collection of CD14⁺ cells.

Culture and polarization of dog monocyte-derived macrophages

Newly isolated CD14⁺ monocytes were seeded in a 24-well plate at a density of 7.5×10^5 cells/well. Cells were cultured in RPMI-1640 GultaMAX (Life Technologies™ Ltd., Paisley, Scotland, UK) supplemented with 5% fetal bovine serum (BODINCO B.V., The Netherlands), and 1% penicillin/streptomycin (Life Technologies™ Ltd., Paisley, Scotland, UK) at 37 °C and 5% CO₂. To generate monocyte-derived macrophages (MDMs), dog CD14⁺ monocytes were treated with canine recombinant GM-CSF (R&D systems, Abingdon, United Kingdom) and recombinant human macrophage colony stimulating factor (M-CSF) (Gibco™, Thermo Fisher Scientific, Carlsbad, USA) for 7 days to differentiate M1 and M2 macrophages, respectively. The medium was refreshed every 2 days. On day 5, GM-CSF treated monocytes were classically activated with 20 ng/ml recombinant canine IFN-γ (R&D system, Abingdon, United Kingdom) and 100 ng/ml LPS from *Escherichia coli* O111:B4 (Sigma-Aldrich, Saint Louis, MO, USA) for M1 polarization; M-CSF treated monocytes were alternatively activated with 40 ng/ml recombinant canine IL-4 (R&D system, Abingdon, United Kingdom) for M2 polarization. Monocytes without any stimulation were cultured in the same conditions serving as controls (M0 macrophages). Cells were harvested on day 7 for phenotype assay, mRNA isolation and phagocytosis assay.

Morphological characterization of dog monocyte-derived macrophages by Phase-contrast microscopy

After 3, 5, and 7 days culture, the morphology of polarized cells and control were examined using a phase-contrast microscope, Nikon eclipse TS100 inverted microscope (Nikon Instruments Europe B.V., Amstelveen, The Netherlands) and ImageFocus v3.0.0.2. Pictures were processed using Fiji ImageJ.

Phenotypic Analysis of dog monocyte-derived macrophages (MDMs) by flow cytometry

After 7 days of polarization, adherent macrophages were rinsed with cold PBS and collected using a cell scraper. Cells were counted and washed, followed by placing on a round-bottom 96-well plate at a concentration of 2×10^5 cells/well. After 30 min blocking with 10% autologous dog serum, surface marker expression of M0, M1 and M2 macrophages was examined with a panel of surface markers including CD14, CD40, CD80, MHC II, CD206, CD209, CD83, CD163, CD86, CD32, CD11b (all antibodies are listed in Table 1). For fluorochrome-conjugated antibodies, cells were incubated on ice for 30 min, followed by washing three times, after which the cells were measured. Corresponding secondary antibodies and streptavidin conjugates (see Table 1) were used to stain unconjugated or biotin-conjugated antibodies. Dog MDMs were washed three times with FACS buffer (2% FCS in PBS) between staining steps. Isotype control for each antibody was included. ViaKrome 808 Fixable Viability Dye (Beckman Coulter, Woerden, Netherlands) was used for the discrimination of live and dead macrophages. Surface marker expression on macrophages was measured by CytoFLEX LX flow cytometer (Beckman Coulter Inc., Brea, CA, USA). FlowJo Software v. 10.5 (FlowJo LCC, Ashland, OR, USA) was used to analyze FACS data.

RNA isolation, library preparation and RNA sequencing for dog MDMs

After 7 days polarization as described above, the Qiagen RNeasy mini kit was used to extract total RNA from M0, M1 and M2 macrophages. In addition, newly isolated CD14⁺ cell and CD14 depletion (CD14D) population were also included. RNA concentration was measured using a NanoDrop-1000 Spectrophotometer (Isogen Lifescience B.V., Utrecht, The Netherlands). RNA quality, library preparation and RNA sequencing were done by Novogene Co., Ltd. More specifically, RNA samples were analyzed on a 1% agarose gels and a NanoPhotometer spectrophotometer (IMPLEN, CA, USA) to monitor RNA degradation, contamination, and purity. The

RNA Nano 6000 Assay Kit from the bioanalyzer 2100 system (Afilent Technologies, CA, USA) was used to assess RNA integrity and quantitation. RNA samples with RNA Integrity Number (RIN) ≥ 8 were included in the following analysis.

Following quality control of RNA, up to 1 μg RNA per sample was used for library preparation using NEBNext[®] UltraTM RNA Library Prep Kit for Illumina[®] (NEB, USA) according to manufacturer's instructions. Briefly, PolyA-containing mRNA was enriched from total RNA using poly-T oligo-attached magnetic beads. RNA fragmentation was performed using divalent cations under elevated temperature in NEBNext First Strand Synthesis Reaction Buffer (5 \times). First-strand cDNA was synthesized using M-MuLV Reverse Transcriptase (RNase H-) with random hexamer primer. Second-strand cDNA was synthesized using DNA Polymerase I and RNase H. Next, 3' end adenylation and adaptor ligation were carried out. 150-200 bp cDNA fragments were purified with AMPure XP system (Beckman Coulter, Beverly, USA) for library fragments, which further amplified with PCR process. Library quality was evaluated using the Agilent Bioanalyzer 2100 system. Subsequently, cluster generation was carried out on a cBot Cluster Generation System using PE Cluster Kit cBot-HS (Illumina). Finally, the sequencing was performed on a NovaSeq 6000 System (Illumina, San Diego, CA) with paired-end read configuration.

Reads processing and Differential expression analysis from RNA-seq data

In order to get clean reads, reads meeting the following conditions were filtered out from the sequenced/raw reads: 1) containing adapters, 2) the quality value of over 50% bases of the read is less than or equal to 5, 3) percentage of non-determined bases is over 10%. Clean reads were mapped to the *Canis familiaris*.canfam 3.1 reference genome using HISAT2 software v2.0.5 (27, 28).

Differential gene expression between groups was calculated using DESeq2 package from Bioconductor with default parameters in R program. Transcripts with read counts < 2 were filtered out from DEG testing. Genes with $|\log_2(\text{fold change})| \geq 1$ and adjusted p value < 0.05 were considered as differentially expressed genes (DEGs). DEGs were assessed through 6 group comparisons: M0 vs M1, M0 vs M2, M1 vs M2, CD14 vs M0, CD14 vs M1, and CD14 vs M2. Heat map generation and cluster analysis were performed using R package "pheatmap". Volcano plots generating with "ggplot2" in R packages displayed DEGs for each comparison. Principal component analysis (PCA) was conducted based on normalized Fragments Per Kilobase Million (FPKM) to show the similarity and difference of M0, M1, M2, CD14 and CD14D populations.

Gene Ontology (GO) enrichment analysis and Kyoto Encyclopedia of Genes and Genomes (KEGG) Pathway enrichment analysis

The annotation of sorted DEGs were performed using the GO and KEGG database. DEGs from each group comparison were used for GO and KEGG enrichment analysis using the R package ClusterProfiler v3.8.1. GO terms enriched within Biological Process (BP), Cellular Component (CC), and Molecular Function (MF) were assessed. In addition, the enrichment of DEGs within KEGG pathways were explored. The difference between compared groups was evaluated using Gene Set Enrichment Analysis (GSEA). Go terms and KEGG pathways with corrected p value < 0.05 were determined as statistically significantly enrichment. The top 20 most enriched GO terms and KEGG pathways in DEGs were shown.

Flow cytometry to assess Non-specific phagocytosis of dog MDMs

Dog CD14⁺ monocytes were polarized and activated as described above. one μm crimson carboxylate-modified FluoSpheres fluorescent beads (Life Technologies Corporation, Eugene, USA) were used to assess phagocytic ability of MDMs. Briefly, MDMs were co-cultured with FluoSpheres fluorescent beads at a ratio of 1:10 (bead : cell) for 4 h on day 7. To exclude unengulfed beads, MDMs were washed three times with PBS and harvested by scraping. Then MDMs were placed in a U-bottom 96-well plate, followed by staining of the cells for viability with ViaKrome 808 Fixable Viability Dye (Beckman Coulter, Woerden, Netherlands) on ice. After 30 min, MDMs were washed twice with FACS buffer and fixed in 4% paraformaldehyde (Alfa Aesar, Kandel, Germany) for 15 min at room temperature. Next, MDMs were washed and resuspended in FACS buffer. Internalization of beads by MDMs was analyzed on CytoFLEX LX flow cytometer (Beckman Coulter Inc., CA, USA) using 638 nm laser and 660/10 fluorescent channel. Results were processed with FlowJo Software v.10.5 (FlowJo LCC, Ashland, USA) and GraphPad Prism 8.3.0 (Graphpad Software LLC., San Diego, USA). The first positive peak present in the histogram was regarded as cells containing a single bead. M0 macrophages were considered as control. Data are expressed as the percentage of phagocytic cells, geometric mean fluorescence intensity (gMFI) and fold change in bead uptake, which were calculated using the following formula (29):

$$\text{Bead/cell} = \frac{\text{MFI}_{\text{total}}}{\text{MFI}_{\text{1bead/cell}}} \text{ and fold change} = \frac{\text{beads/cell}_{\text{M1 or M2}}}{\text{beads/cell}_{\text{M0}}}$$

Confocal microscopy to evaluate non-specific phagocytosis of MDMs

To confirm the internalization of MDMs, CD14⁺ monocytes were grown on sterilized 12 mm coverslips in a 24-well plate. After 7 days of polarization and activation, 1 μ m crimson carboxylate-modified FluoSpheres fluorescent beads (Life Technologies Corporation, Eugene, USA) were added into the 24-well plate at a ratio of 1:10 (beads : cells), and incubated for 4 h at 37 °C. Then unengulfed beads were washed away from the plate using cold Hank's balanced salt solution (HBSS) (Gibco, Paisley, UK). MDMs were subsequently stained with 2 μ g/ml Alexa Fluor 488 conjugated Wheat germ agglutinin (WGA) (Life Technologies Corporation, Eugene, USA) in HBSS at 37 °C. 10 min later, MDMs were rinsed twice with cold HBSS and fixed in 4% paraformaldehyde, for 15 min at room temperature. The cover slips containing the MDMs were washed twice again before mounting on polysine slides (Thermo Scientific, Braunschweig, Germany). FluorSave Reagent (Millipore, San Diego, USA) was used as mounting reagent. Finally, the phagocytosis of MDMs was visualized using Leica TCS SPE-II and LAS-AF software (Leica Microsystems B.V., Amsterdam, The Netherlands) with 488 and 638 nm laser. In order to determine successful beads uptake, z-stacks was performed during imaging. Microscopic images analysis and 3D construction were performed using Fiji ImageJ.

Statistical Analysis

GraphPad Prism 8.3.0 (Graphpad Software LLC., San Diego, USA) was used to evaluate statistical significance. Statistical significance among M0, M1 and M2 cells was analyzed using one-way ANOVA test with multiple comparisons. If there were missing values, a mixed effects model was used. Data are reported as mean \pm SD. mRNA sequencing data was analyzed using R program and appropriate R packages as indicated above. Data were harvested from at least three donors and repeated at least three times. Statistical significance was defined as significant difference when $*p < 0.05$ and highly significant when $**p < 0.01$.

Chapter 5

Table 1. list of antibodies used for flow cytometry

Antigen	Target species	Clone	Isotype	Dilution	Source
CD14, vioblue	Mouse anti-human	TÜK4	Mouse IgG2a, κ	1:100	Miltenyi Biotec
CD11b, biotin	Mouse anti-dog	CA16.3E10	Mouse IgG1	1:100	P. Moore
CD32B+CD32 A biotin	Mouse anti-human	AT10	Mouse IgG1	1:50	Abcam
CD40, R-PE	Mouse anti-human	LOB7/6	Mouse IgG2a	1:25	BIO-RAD
CD80, FITC	Hamster anti-mouse	16-10A1	Hamster IgG2	1:100	BD Biosciences
CD86, unconjugated	Mouse anti-dog	CA24.3E4	Mouse IgG1	1:50	P. Moore
CD83, APC	Mouse anti-human	HB15e	Mouse IgG1, κ	1:50	Biogend
CD163 unconjugated	Mouse anti-canine	AM-3K	Mouse IgG1	1:50	COSMO BIO Co., LTD.
CD206, APC/Cyanine7	Mouse anti-human	15-2	Mouse IgG1, κ	1:50	Biogend
CD209, APC	Mouse Anti-human	102E11.06	Murine IgG1	1:50	Fisher scientific
MHC II, APC	Rat anti-canine	YKIX334.2	Rat IgG2a, κ	1:50	eBioscience™
GaM-IgG1- PerCP	Mouse IgG	-	IgG	1:100	Santa Cruz Biotechnology
streptavidin - PE	-	-	-	1:2000	BD Biosciences
CD14, unconjugated	Mouse anti-human	TÜK4	Mouse IgG2a, κ	1:100	Bio-RAD

Peter Moore, university of Davis, CA, USA

Results

Morphologic characterization of dog monocyte-derived macrophages

In order to obtain dog macrophages in vitro, CD14⁺ cells, derived from dog PBMC, were cultured in the presence of GM-CSF (M1) or M-CSF (M2) for 7 days. At day 5, M1- and M2-polarized macrophages were activated with IFN- γ + LPS and with IL-4 for 2 days, respectively. The morphologic features were monitored by phase contrast microscopy during the cultivation period (Figure 1A). The size of macrophages was quantitated by flow cytometry on the basis of forward scatter and side scatter (Figure 1B). Microscopic analysis showed that distinct morphologic differences are seen at day 5 and 7 (Figure 1). However, there are no obvious morphologic differences among M0, M1 and M2 macrophages at day 3. At day 3 of polarization, both M1- and M2-polarized macrophages showed a small and roundish shape, which is similar to M0 macrophages. At day 5, M1-polarized macrophages displayed certain morphological changes such as increased size, flat, roundish, and amoeboid shape (Figure 1A). Some M1 cells adopted a typical well-spread “fried-egg” phenotype (red arrow) (Figure 1A). A small portion of stretched, spindle-like cells were presented in M2-polarized macrophages at day 5 (blue arrow) (Figure 1A). At day 7, M1-polarized macrophages were differentiated into homogenous round cells with a dominant amoeboid and “fried-egg” phenotype (Figure 1A), while a large portion of M2-polarized macrophages obtained an elongated spindle morphology. Flow cytometry analysis show that M1-polarized macrophages are bigger and more granular than M0- and M2-polarized macrophages (Figure 1B and C). The size of M1 cells is significantly increased compared to M0 and M2 cells (Figure 1C). This indicates that polarized dog MDMs can be clearly distinguished under phase contrast microscope.

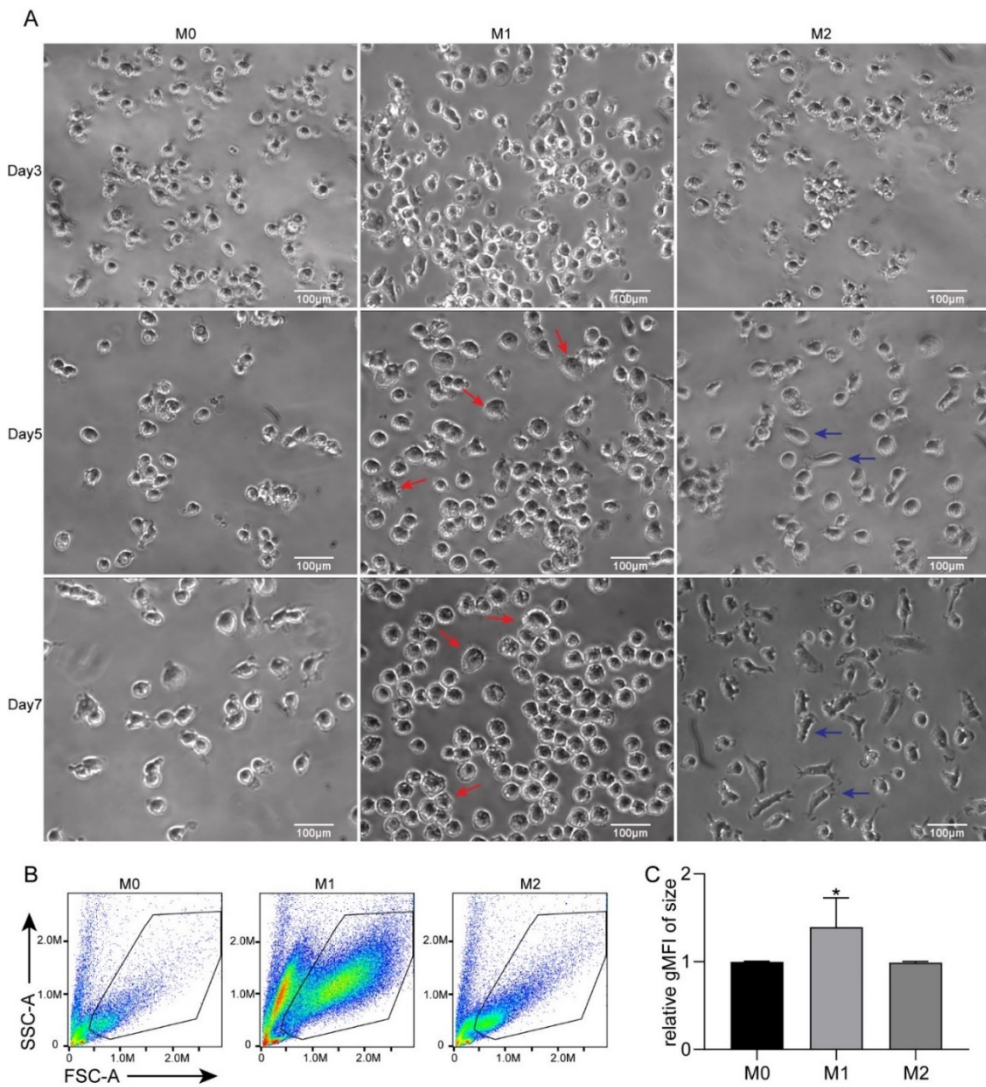


Figure 1 The morphology of dog monocyte-derived macrophages (MDMs). Isolated CD14⁺ monocytes were cultured in the presence of 5 ng/ml GM-CSF (M1) or 25 ng/ml M-CSF (M2) for 7 days. At day 5, macrophages were activated with 20 ng/ml IFN- γ and 100 ng/ml LPS for M1 or 20 ng/ml IL-4 for M2. M0 macrophages were cultured with complete medium only. **(A)** Characteristics of MDMs (M0, M1 and M2) were recorded by phase contrast light microscopy with 20 \times magnification at day 3, 5 and 7. M1 (GM-CSF + IFN- γ + LPS) macrophages exhibit large and round shape with amoeboid and flat morphology (red arrow), while M2 (M-CSF + IL-4)

macrophages exhibit a stretched and spindle-like morphology (blue arrow). Scale bar=100 μm . **(B and C)** Flow cytometry was performed to assess the differences in forward scatter (FSC) profiles indicative of size. FSC profiles of MDMs at day 7 are exhibited in **(B)**. FSC based size difference between M0, M1 and M2 is summarized in **(C)** with $n=3$. Representative images and flow cytometry plots of at least three independent donors are shown. Relative gMFI of size is shown as the mean of the geometric fluorescence intensity of M1 and M2 relative to M0, namely, relative gMFI of size = (gMFI of M0, M1 or M2)/(gMFI of M0). Data are reported as mean \pm SD. * $p < 0.05$; ** $p < 0.01$. Scale bar=100 μm . gMFI: geometric mean of fluorescence intensity, SSC: side scatter, FSC: forward scatter.

Phenotypic Characterization of dog MDMs by Flow Cytometry

In order to further phenotypically characterize *in vitro* polarized dog MDMs (M0, M1 and M2), a phenotypic analysis of the dog MDMs culture by flow cytometry was performed after 7 days of polarization and activation. A set of surface markers related to macrophage activation was selected based on previous studies (30, 31) including CD14, CD11b, CD40, CD80, CD206, MHC II, CD209, CD163, CD32, and CD83. As shown in Figure 2, both CD14 and CD11b were expressed by polarized M0, M1 and M2 macrophages, which are regarded as pan-macrophages markers (32-34) (Figure 2A and B). No significant difference was seen in CD14 expression among M0, M1 and M2 macrophages on day 7. However, CD11b expression was significantly increased on M1 and M2 macrophages, compared to M0 macrophages. Interestingly, M1-polarized MDMs expressed high levels of CD40, CD80, CD86 and MHC II (Figure 2A and B), which are used as M1 marker in human and mouse studies. In contrast, M0- and M2-polarized macrophages expressed comparable levels of CD40, CD80 and CD86, which were significantly lower than those on M1-polarized macrophages (Figure 2A and B). While both M1 and M2 cells expressed a higher level of MHC II than M0 macrophages, the expression of MHC II was significantly higher on M1 than on M2 cells (Figure 2A and B). In contrast, a significant increase in the expression levels of CD206, CD209, CD163, and CD32 was observed in M2-polarized macrophages, but not in M1-polarized macrophages. A decrease of CD83 expression was detected in M1-polarized macrophages, compared to M0 and M2 macrophages. Thus, dog M1-polarized MDMs are characterized by high expression of CD40, CD80, CD86 and MHC II, dog M2-polarized MDMs are identified by an increase of CD206, CD209, CD163 and CD32.

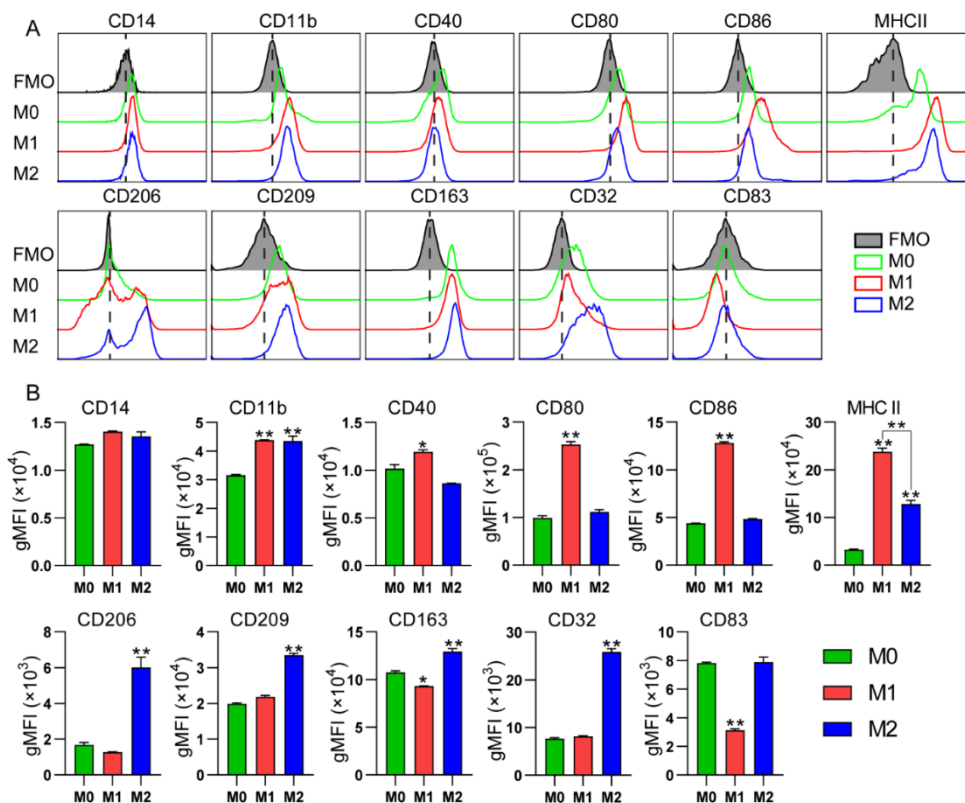


Figure 2 Expression of surface markers on dog MDMs was determined by flow cytometry. Polarized dog MDMs (M0, M1 and M2) were collected on day 7. Harvested MDMs were stained with a set of macrophages surface markers (see table 1) and subsequently analyzed by flow cytometry. (A) Histograms depict the results obtained in one representative donor out of 3 different donors. Each overlaid histograms represent an overlay of the respective monoclonal antibody and fluorescence-minus-one (FMO) controls (shaded black lines) for the indicated marker. Green line: M0, red line: M1, blue line: M2. (B) The bar graphs represent the means of geometric fluorescence intensity (MFI) \pm SD of positive cells in 3 different donors. *p* values of M1 and M2 are relative to M0. **p* < 0.05; ***p* < 0.01.

Differentially expressed genes between M0-, M1-, and M2-polarized macrophages

To investigate gene expression profiles of M0-, M1- and M2-polarized macrophages, mRNA sequencing was performed. After filtering out genes with read counts < 2,

17929 genes in total were identified from 5 groups, M0, M1, M2, CD14 and CD14D (supplementary table S1). Figure 3A shows the distribution of genes among the different subsets in a Venn diagram: M1- and M2-polarized macrophages displayed 10030 genes in common and 440 versus 816 specific genes in M1 versus M2 macrophages, respectively. In M0 vs M1 vs M2 group, 9895 genes were co-expressed by both M0, M1 and M2 macrophages. There were 244 specific genes in M0 macrophages, 272 specific genes in M1 macrophages and 246 specific genes in M2 macrophages (Figure 3A). Comparison of genes between M0, M1, M2, CD14 and CD14D determined 9222 co-expressed genes. The number of specific genes for each group is 89 genes for M0, 120 genes for M1, 109 genes for M2, 118 genes for CD14 and 845 genes for CD14D.

To identify DEGs from different groups, $p < 0.05$ and $|\log_2(\text{FC})| > 1$ were set as criteria. Based on the criteria, 13052 differentially expressed genes (DEGs) were sorted (supplementary Table S2). A heat map was plotted to show the expression levels of sorted DEGs of each sample, from which the expression trend of DEGs can be clearly seen (Figure 3B). Compared to M0, 3199 DEGs were observed in the M1 group, with 1649 upregulated and 1550 downregulated genes (Figure 4A), and 1882 DEGs in the M2 group, with 901 upregulated and 981 downregulated genes (Figure 4B). A total of 3124 DEGs were found in the M1 vs M2 comparison, with 1688 upregulated and 1436 downregulated genes (Figure 4C). In other pairwise comparisons, there were 6092 DEGs between CD14 and M0, 6283 DEGs between CD14 and M1, 6330 DEGs between CD14 and M2 (Figure S1). Among the DEGs, the number of up- and down-regulated genes was almost evenly distributed, i.e. we detected 3192 upregulated and 2900 downregulated genes in CD14 vs M0, 3235 upregulated and 3048 downregulated genes in CD14 vs M1, and 3270 upregulated and 3060 downregulated genes in CD14 vs M2 (Figure S1). The top 10 up- and down-regulated genes were labeled in each pairwise comparison. The top 50 up- and down-regulated genes were listed in supplementary Table S3-S8. To further evaluate clustering of gene profiles, principal component analysis (PCA) was performed. Our results showed that M2 macrophages clustered with M0 macrophages rather than M1 macrophages, CD14 and CD14D populations (Figure 4D). In contrast, M1 macrophages showed a clear separation from other groups, including M0, M2, CD14 and CD14D, indicating that each cluster (M0-M2, M1, CD14 and CD14D) has a unique gene expression profile. Principal component analysis revealed that M1 and M2 macrophages are distinct populations. Overall, the transcriptomic data confirmed that monocyte-derived M1 and M2 macrophages show significantly different gene profile and activation patterns.

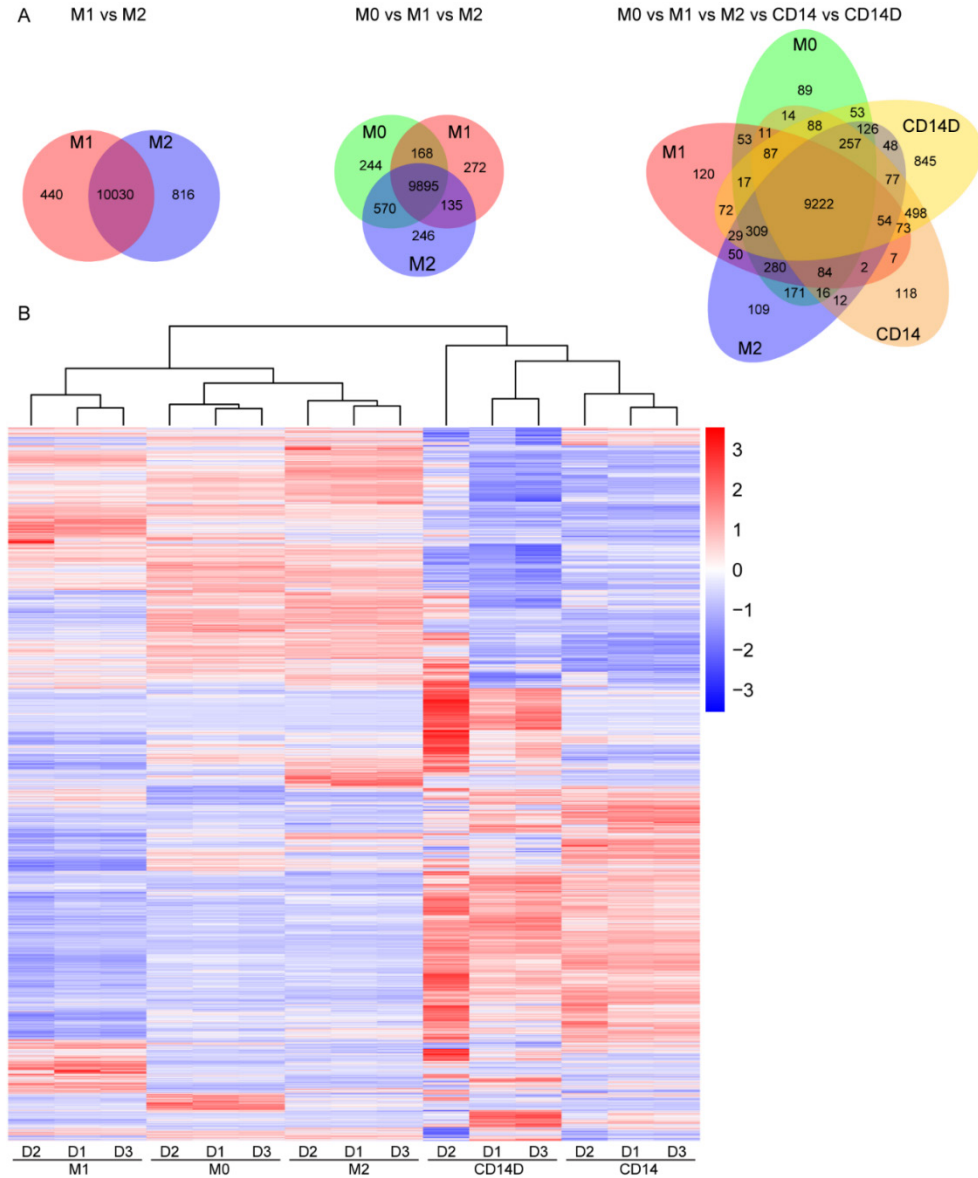


Figure 3 Gene expression profiles of M0, M1, M2, CD14 and CD14D were shown by Venn diagram and heat map. **(A)** Co-expression Venn diagram showing the distribution of expressed genes in 3 compared groups, including M1 vs M2, M0 vs M1 vs M2, and M0 vs M1 vs M2 vs CD14 vs CD14D. The number of uniquely expressed genes was shown in each group. The overlapping regions indicated the

number of co-expressed genes in two or more samples. M0, M1 and M2 represent different polarization states of macrophages. CD14 are freshly isolated CD14⁺ cells from PBMC. CD14D indicate the CD14⁺ depleted population of PBMC. **(B)** Heat map with cluster analysis showing differential expression genes within all comparison groups. Each column indicates one sample. Each row indicates a single gene. The color ranges from red to blue represents the expression level of genes from high to low. The $\log_2(\text{FPKM}+1)$ value was used for cluster analysis. FPKM: Fragments Per Kilobase Million.

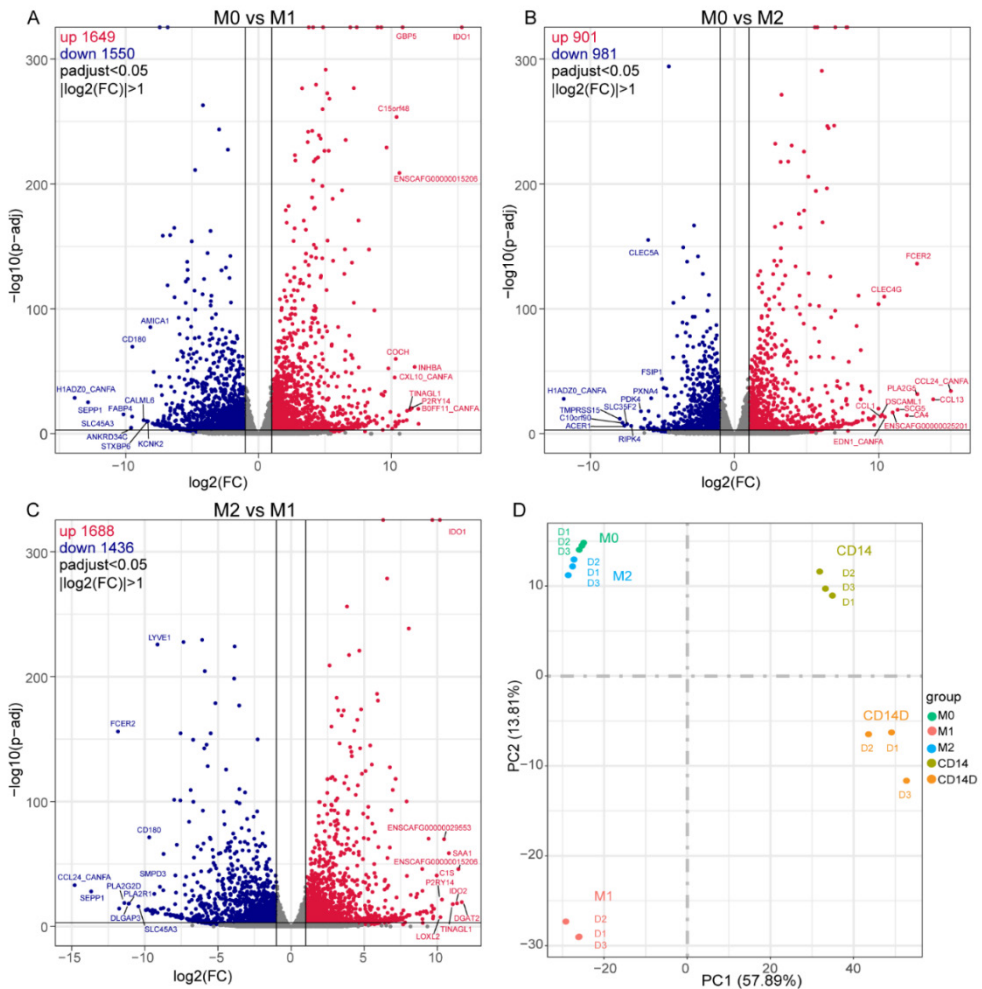


Figure 4 Polarized macrophage subsets show distinct gene expression profiles. Volcano plots depicting differentially expressed genes in different comparison

groups, namely **(A)** comparison between M0 and M1, **(B)** M0 and M2, and **(C)** M1 vs M2. Each volcano plot was shown as \log_2 (fold change) (x-axis) vs $-\log_{10}(p\text{-adj})$ (y-axis). M0 macrophages are considered as control in **(A)** and **(B)**. M2 macrophages are considered as control in **(C)**. Genes with adjusted p value < 0.05 and $|\log_2(\text{FC})| > 1$ are regarded as statistically significantly different. The horizontal line at $y \approx 1.303$ indicates $p = 0.05$. Vertical lines at $x = 1$ or -1 indicate $\log_2(\text{FC}) = 1$ or -1 . Red dots, blue dots and gray dots represent up-regulated, down-regulated, and non-significant DEGs, respectively. The name of top 10 DEGs with $p < 0.001$ and $|\log_2(\text{FC})| \geq 8$ were labeled out. FC: fold change; DEGs: differentially expressed genes. **(D)** Principal-component (PC) analysis of all genes expressed in M0, M1, M2, CD14 and CD14D. Dots with the same color represent sample replicates.

GO and KEGG enrichment analysis of DEGs between M0-, M1 and M2-polarized macrophages

To determine the main changes in biological processes during polarization of macrophages, GO and KEGG enrichment analysis of all DEGs was performed using the “clusterProfiler” package in R. The top 20 of most enriched GO terms and KEGG pathways are shown in Figure 5. GO analysis of all DEGs for M0 vs M1 comparison showed that only two GO terms, “immune system process” and “immune response”, were significantly enriched within biological process (BP) (Figure 5A and supplementary Table S9). Upregulated DEGs in M0 vs M1 comparison were significantly enriched in 3 GO terms of biological processes (BP), 3 GO terms of cellular components (CC) and 7 GO terms of molecular functions (MF) (supplementary Figure S2, S3 and Table S15). All downregulated DEGs in M0-M1 comparison were significantly enriched in 7 GO terms of BP (supplementary Figure S2, S3 and Table S16). KEGG analysis showed that DEGs between M0 and M1 were enriched in 80 KEGG pathways, such as Th17 cell differentiation, TNF signaling pathway and Toll-like receptor signaling pathway (Figure 5D and supplementary Table S12). Up- and down-regulated DEGs were enriched in 87 and 10 pathways, respectively (supplementary Table S17 and S18).

In the M0 vs M2 comparison, enriched DEGs are mainly associated with “GTPase activator activity” and “G-protein coupled receptor binding” in MF (Figure 5B and supplementary Table S10). Upregulated DEGs in M2 were assigned to 7 GO terms of BP and 7 GO terms of MF, such as immune response, cytokine, and chemokine activity. Downregulated DEGs in M2 were significantly associated with “transferase activity” and “hydrolase activity” in MF. Furthermore, 26 significant enriched pathways were found in the M0 vs M2 group, such as the phagosome and chemokine signaling pathway (Figure 5E and supplementary Table S13). Specifically, 34 pathways enriched with upregulated DEGs and 4 pathways enriched

with downregulated DEGs were identified (supplementary Table S19 and 20).

In the M1 vs M2 comparison, GO analysis revealed that GO terms, “immune system process” and “immune response”, were the most enriched. Among all the DEGs, upregulated DEGs were distributed over 15 GO terms with 14 in BP and 1 in MF, and downregulated DEGs over 22 GO terms with 15 in BP, 2 in CC, 5 in MF (Figure 5C, Table S11, S21 and S22). KEGG analysis showed that 39 pathways were enriched in all DEGs such as Th1 and Th2 cell differentiation, Th17 cell differentiation, C-type lectin receptor signaling pathway and IL-17 signaling pathway (Figure 5F and supplementary Table S14). There are 61 pathways in upregulated DEGs, including Th1 and Th2 cell differentiation, and 5 pathways in downregulated DEGs, such as cell cycle, DNA replication and ribosome (supplementary Table S23 and S24). However, only a few DEGs were found enriched in CC in all three pairwise comparisons.

In summary, the enrichment analysis showed that upregulated DEGs in M1 and M2 cells were enriched in many GO terms and pathways, of which the majority of GO terms and pathways were associated with the immune response, such as immune system processes, Th1 and Th2 cell differentiation, Th17 cell differentiation and the Toll-like receptor signaling pathway, suggesting that monocyte-derived M1 and M2 macrophages are associated with Th1, Th2 and Th17 responses. In addition, the comparison between M1 and M2 indicated that the DEGs of M1 and M2 were enriched in different GO terms and KEGG pathways.

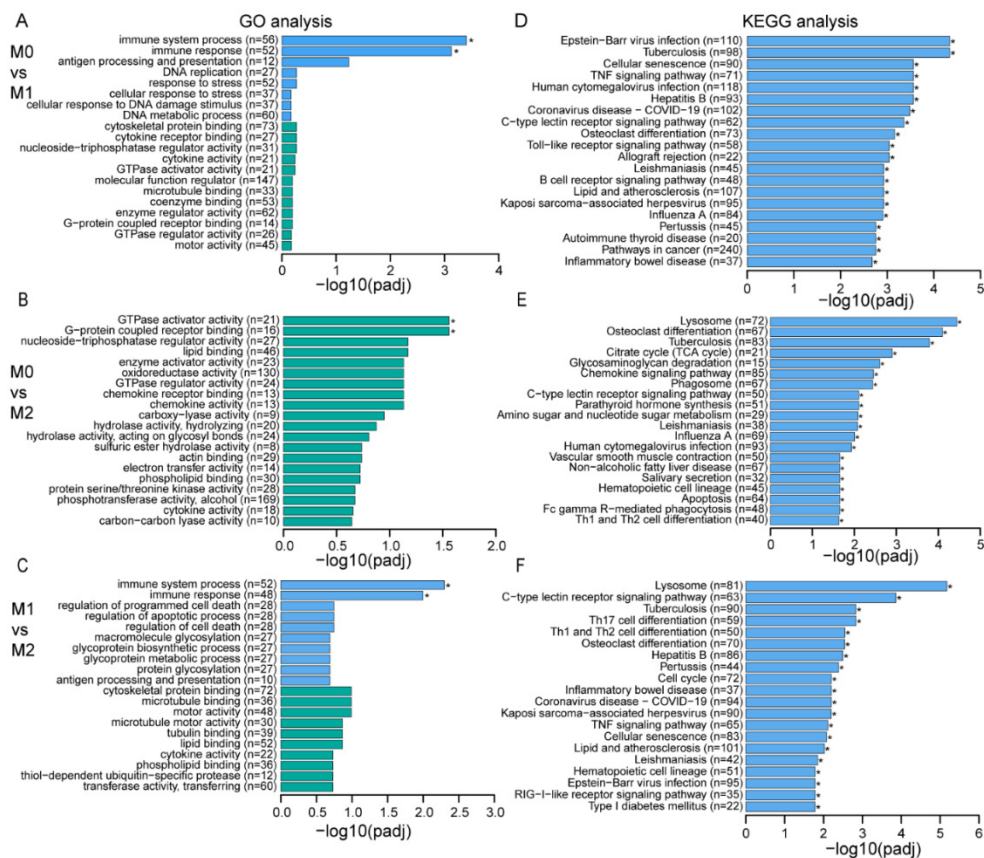


Figure 5 The GO terms and KEGG pathway enrichment analysis of DEGs between M0, M1 and M2 macrophages. DEGs including both up- and down-regulated genes from each compared group were subjected to GO and KEGG analysis. The top 20 most enriched GO terms (including BP, CC, and MF) and KEGG pathways of DEGs are shown by compared groups, (A, D) M0 vs M1, (B, E) M0 vs M2, and (C, F) M1 vs M2. Blue and green in (A, B, and C) represent BP and MF, respectively.

M2-polarized dog MDMs have a higher non-specific phagocytic capacity compared to M0- and M1-polarized dog MDMs

The polarization of macrophages is associated with changes in functional characteristics, such as phagocytic capacity. To investigate whether *in vitro* polarization affects phagocytosis by M0-, M1- and M2-polarized dog MDMs, a functional analysis of the MDMs was performed by examining the non-specific phagocytic capacity of MDMs using crimson carboxylate-modified FluoSpheres fluorescent beads. Our results showed that all MDMs were able to take up

fluorescent beads (Figure 6), while control MDMs co-cultured with beads at 4 °C were failed to engulf any beads (data not shown). M0- and M2-polarized MDMs displayed a significantly higher bead-uptake than M1 cells ($p < 0.05$) (Figure 6A and B). On average, M2-polarized MDMs (1.5 times fold change relative to M0) contained around 3 times more beads than M1-polarized MDMS (0.5 times fold change relative to M0) (Figure 6C). This observation was further confirmed by confocal microscopy (Figure 6D). Clearly, we could see more beads in each cell in M0- and M2- than in M1-polarized MDMs, especially in M2-polarized MDMs with spindle-like shape, suggesting the higher phagocytic ability of individual M2-polarized MDMs. Next, the location of fluorescent beads was visualized by re-constructing a 3D model of MDMs with z-stacks, which confirm beads internalization by MDMs (Supplementary Materials Video S1A, B and C).

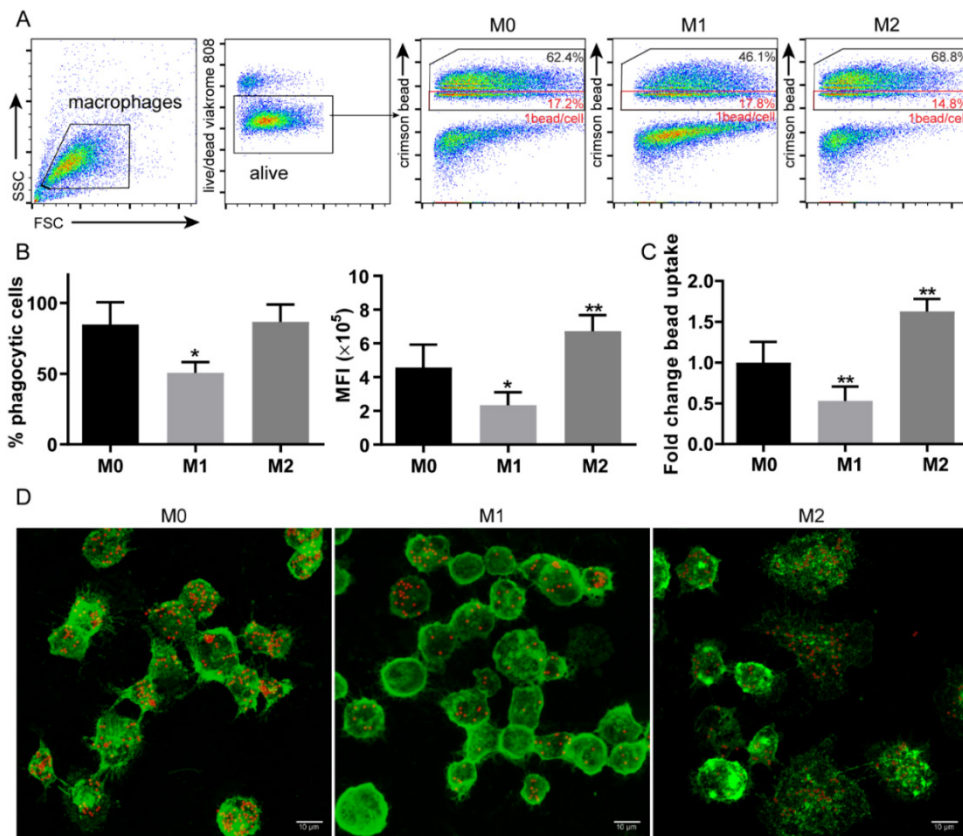


Figure 6 M0, M1 and M2-polarized dog MDMs show different non-specific phagocytic capabilities. Dog CD14⁺ monocytes were polarized and activated for 7

days and incubated with crimson carboxylate-modified FluoSpheres fluorescent beads for 4 h. M0, M1 and M2-polarized dog MDMs were harvested. **(A)** Dog MDMs were gated based on their scatter profile (FSC/SSC) and viability (viakrome). The bead content was analyzed quantitatively by flow cytometry for dog MDMs. Dog MDMs containing beads (black square) and 1 beads/cell (red square) were gated out, from which the average beads/cell and fold change were calculated. Representative flow cytometry plots are shown of one out of three independent donors. **(B)** MDMs containing beads were depicted and shown as the percentage of phagocytic cells and median fluorescence intensity (MFI). **(C)** The fold change of M1- and M2-polarized MDMs in bead uptake was calculated as described in materials and methods and compared to M0 MDMs. **(D)** Confocal microscopy was performed to confirm non-specific phagocytosis by dog MDMs. Cell membrane was stained by WGA-Alexa Fluor 488 shown in green and FluoSpheres fluorescent beads are shown in red. A 3D model of internalization by MDMs was reconstructed from z-stacks. The corresponding video showing 3D structure can be found in Supplementary Materials Video S1A, B and C. Data reflect at least three independent experiments from three independent donors. Data are reported as mean \pm SD. * $p < 0.05$; ** $p < 0.01$. Scale bar=10 μ m.

Discussion

Dogs have become an increasingly important alternative translational animal models for inflammatory and immunological diseases due to similarity of human and canine in many diseases (23, 24). Macrophages play a crucial role in most immune-associated diseases. In countless studies, monocyte-derived macrophages (MDMs) are utilized to understand the biology and differentiation of macrophages. So far, most studies have focused on MDMs from human and mouse, knowledge about dog MDMs is still scarce. Therefore, well-characterized dog macrophage subsets are urgent for a better understanding of the biological functions of dog macrophages. Here, we present a systematic study of dog monocyte-derived M1 and M2 macrophages by showing their morphology, surface markers, differentially expressed genes and functional activity.

In the present study, M1- and M2-polarized MDMs showed substantial differences in morphology. After 7 days of polarization, M1-polarized MDMs (GM-CSF + IFN- γ + LPS) dominantly displayed a round and amoeboid shape, as visible under a light microscope. Also, a small portion of M0 MDMs showed an amoeboid shape, but was smaller in size than M1-polarized MDMs. Among M2-polarized MDMs (M-CSF + IL-4), both populations with small round morphology and with elongated spindle morphology existed. M1- and M2-polarized MDMs but not M0 MDMs largely proliferated during polarization. In addition, M1-polarized MDMs were both larger

and more granular than M0- and M2-polarized MDMs. Thus, this morphology analysis indicated that dog M1- and M2-polarized MDMs can be easily distinguished under a light microscope. Similar to other species, typical M1 and M2 macrophages were also described for pig, ovine, mouse and human MDMs (35-39). In other studies on canine MDMs, except for spindle-like cells, also large/flat shaped cells and multinucleated giant cells were found among M2-polarized MDMs (40, 41). This may be due to the use of PBMC, which contain mononuclear cells as well as dendritic cells and granulocytes. In our study, macrophages were polarized from selected CD14⁺ monocytes, probably leading to a higher purity.

With respect to surface markers, flow cytometry analysis showed that M1- and M2-polarized dog MDMs expressed comparable level of CD14 and CD11b. CD11b was significantly increased on M1- and M2-polarized MDMs compared to M0 MDMs. CD14 and CD11b have been identified as pan-macrophage markers (42), and the expression of these markers suggests these cells indeed maintain macrophage properties during polarization (43). Co-stimulatory molecules CD40, CD80 and CD86 together with MHC II are essential for antigen presentation and T cell activation by macrophages, and are considered as M1 macrophage markers in many species (8, 43-45). C-type mannose receptor 1, CD206 and hemoglobin-haptoglobin scavenger receptor, CD163, were validated as M2 macrophages markers in both mouse and human studies, mainly expressed on IL-4 polarized monocytes and resident macrophages (46, 47). Previous studies reported that the expression of CD206 and CD163 was found in canine cutaneous Langerhans cells and colon resident macrophages (48, 49), both of which are related to phagocytosis of macrophages (50). CD209 was also expressed by tissue resident macrophages such as mucosal macrophages and alveolar macrophages (51, 52), and was increased by treatment with M-CSF and IL-4 (36). In agreement with our study, dog M1-polarized MDMs expressed a markedly higher level of CD40, CD80, CD86 and MHC II than M0- and M2-polarized MDMs. CD163, CD206 and CD209 were significantly increased in M2-polarized MDMs. Notably, both M1- and M2-polarized MDMs highly expressed MHC II, whereas the expression of MHC II is significantly higher in M1- than in M2-polarized MDMs. A similar observation was made by Heinrich, et al. in immunocytochemistry (41). Unfortunately, semi-quantitative results obtained by immunocytochemistry were unable to distinguish differences in expression levels of MHC II between M1 and M2 macrophages. CD32, known as FCγRII, is one of the phagocytic receptors, which was shown to be highly expressed by M2-polarized dog MDMs in our study. However, the discussion on CD32 expression level between M1 and M2 macrophages varies. A variety of studies described CD32 as a M1 macrophage marker (53, 54). On the contrary, other studies showed that CD32 are highly induced in M2 macrophages (55, 56). It is also reported that the expression of CD32 by human macrophages was not changed after polarization (30). By

comparing different literatures, we speculate that the different description on CD32 may cause by difference among species or the use of different stimulus.

Next, we compared the global gene expression profiles of M0, M1 and M2-polarized macrophages, using the CD14⁺ and CD14D populations as control. We found that most of genes were shared by these groups, while each group also expressed subset-specific genes (Figure 3). Principal component analysis showed that M0 and M2 clustered together, while a clear separation was observed between other pairwise compared macrophage populations. This result suggested that M0 and M2 may have similar gene profiles, whereas M1 is a distinct population from M0 and M2. However, a previous transcriptome study for rat bone marrow-derived macrophages showed that the variance of M0, M1 and M2 was low (57). Moreover, a greater distance between M0, M1 and M2 was observed in a microarray-based Gene Expression study on human monocyte-derived macrophages (58). By comparing these group, we detected over a thousand of DEGs in M0 vs M1, M0 vs M2 and M1 vs M2, specifically 3199 for M0 vs M1, 1882 for M0 vs M2, and 3124 for M1 vs M2. Those DEGs were subjected to GO and KEGG enrichment analysis. Our results showed that upregulated DEGs in M1 and M2 were mostly enriched in immune-related GO terms and pathways compared to M0. For example, significantly enriched GO terms included immune system processes, cytokine and chemokine activity, antigen processing and presentation, G-protein coupled receptor binding, proteasome complexes, etc. They further included signaling pathways, like Epstein-Barr virus infection, tuberculosis, TNF signaling pathway, Th1 and Th2 cell differentiation, the TNF signaling pathway, Th17 cell differentiation, and chemokine signaling pathway, etc. Interestingly, in the M1 vs M2 comparison, DEGs were the most enriched in GO terms including immune system processes, immune responses, antigen processing and presentation, regulation of programmed cell death, etc, and pathway, including the lysosome, the C-type lectin receptor signaling pathway, tuberculosis, Th17 cell differentiation, and Th1 and Th2 cell differentiation, etc. However, in our study, in cellular components the GO terms only enriched a few DEGs, which may be due to the shared origin of polarized macrophages. In addition, the enrichment of phagosome- and lectin receptor-related genes in M1 and M2 cells may contribute to their mutual phagocytic function (supplementary Table S12, S13 and S14). These results suggested that dog monocyte-derived M1 and M2 cells *in vitro* displayed some crucial differences at the mRNA levels, which are closely related to Th1 and Th2 responses.

The change of phenotypes and gene profiles is often accompanied by a change of functional activity (59). Phagocytosis is one of the main functions of macrophages, which is modulated by a variety of phagocytic receptors. Using latex beads, we measured a change in phagocytosis by dog MDMs following polarization. Although

all three polarization states of dog MDMs could phagocytose latex beads, M2-polarized MDMs exhibited the strongest phagocytic capacity when compared to M0- and M1-polarized MDMs. This is different from our previous study on canine 030D macrophage cell line in which M1 macrophages displayed the strongest phagocytic capacity (chapter 6). Such differences between a cell line and primary monocytes were observed also in a human macrophage study (60). In addition, the induction of phagocytosis-related markers such as CD32, CD163, CD206 and CD209 may contribute to phagocytic capacity of M2-polarized dog MDMs. Nitric oxide (NO) production is another important function for activated macrophages in mouse study. Unfortunately, no detectable NO production was found in dog MDMs (data not shown).

In conclusion, in the present study, we showed that *in vitro* polarized dog M1 and M2 MDMs have a distinct morphology, surface markers features, gene profiles and phagocytotic capacity. M1-polarized dog MDMs were characterized by a large/round morphology, high CD40, CD80, CD86 and MHC II, and weak phagocytosis, whereas M2-polarized dog MDMs showed a spindle-like shape, increased CD163, CD209, CD206 and CD32 expression, and strong phagocytosis. In transcriptomics, 3199 DEGs for M1 and 1882 DEGs for M2 were identified compared to M0 cells, which are significantly associated with immune response, cell differentiation and phagocytosis. Thus, with this study, we contribute to a better understanding of canine macrophage biology and immune system.

ACKNOWLEDGEMENTS

The authors thank China Scholarship Council (CSC) for offering scholarship. The authors also thank Evieke Ruijsink for collecting flow cytometry data from one of dog donors. All fluorescent microscopy images have been acquired at the Center of Cellular Imaging, Faculty of Veterinary Medicine, Utrecht University. All the flow cytometry data were collected using the Flow Cytometry and Cell Sorting Facility at the department of Infectious Diseases & Immunology in Utrecht University.

FUNDING

This research received no external funding

CONFLICTS OF INTEREST

The authors declare no conflict of interest.

Supplementary materials

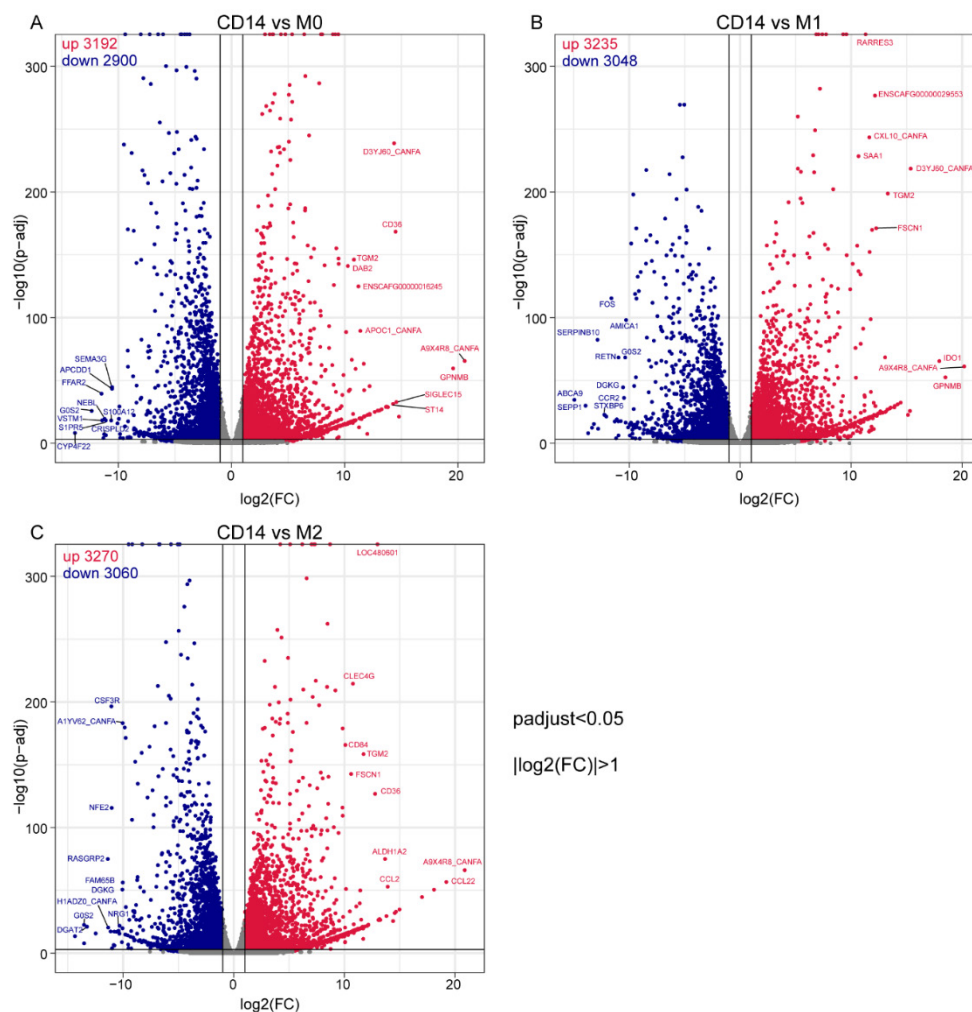


Figure S1 Polarized macrophage subsets show distinct gene expression profiles. Volcano plots depicting differentially expressed genes in different comparison groups, namely **(A)** comparison between CD14 and M0, **(B)** CD14 and M1, and **(C)** CD14 vs M2. Each volcano plot was shown as $\log_2(\text{fold change})$ (x-axis) vs $-\log_{10}(p\text{-adj})$ (y-axis). CD14 population is considered as control. Genes with adjust p value < 0.05 and $|\log_2(FC)| > 1$ are regarded as statistically significant difference. The horizontal line at $y \approx 1.303$ indicates $p = 0.05$. Vertical lines at $x = 1$ or -1 indicate $\log_2(FC) = 1$ or -1 . Red dots, blue dots and gray dots represent up-regulated, down-regulated, and non-significant DEGs, respectively. The name of top 10 DEGs were labeled out. FC: fold change; DEGs: differentially expressed genes.

Comprehensive characterization of dog monocyte-derived macrophages

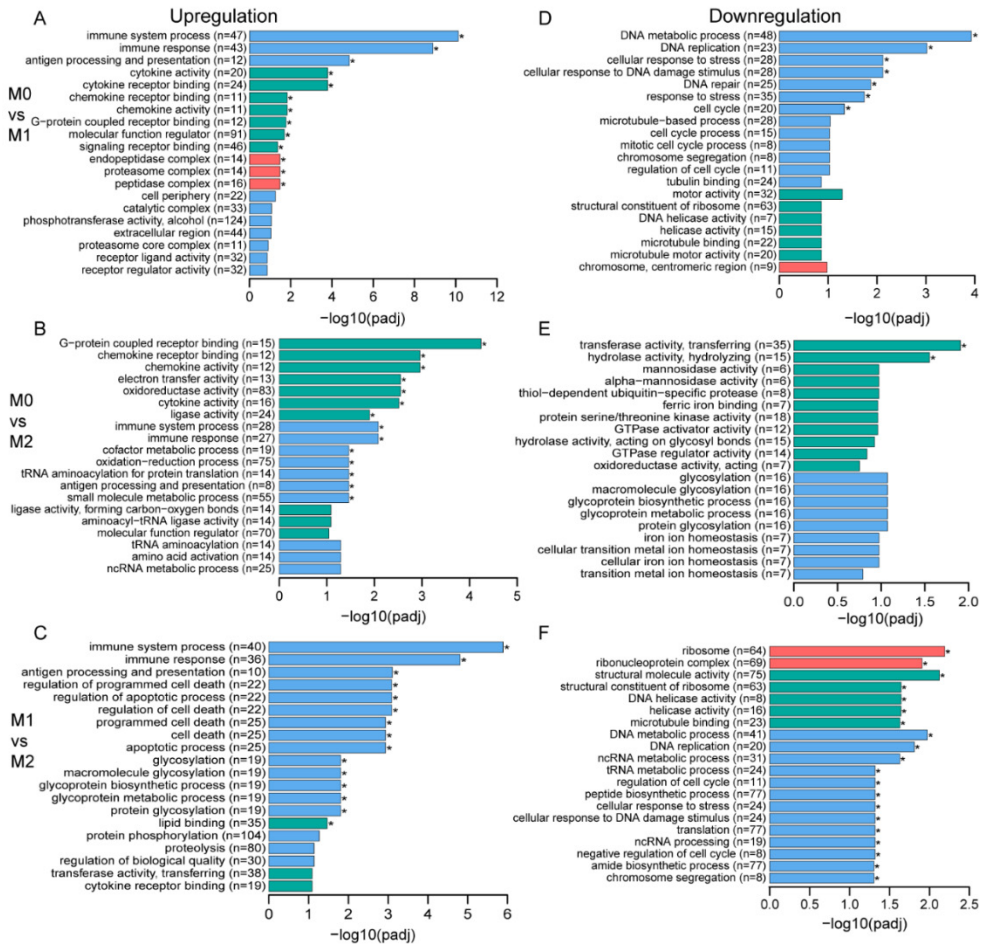


Figure S2 The GO terms enrichment analysis of DEGs between M0, M1 and M2 macrophages. DEGs including both up- and down-regulated genes from each compared group were subjected to GO and KEGG analysis. The top 20 most enriched GO terms (including BP, CC, and MF) and KEGG pathways of DEGs are shown by compared groups, **(A, D)** M0 vs M1, **(B, E)** M0 vs M2, and **(C, F)** M1 vs M2. Blue, red, and green in **(A, B, and C)** represent BP, CC and MF, respectively. **(A, B, and C)** represent upregulated genes. **(D, E, and F)** represent downregulated genes.

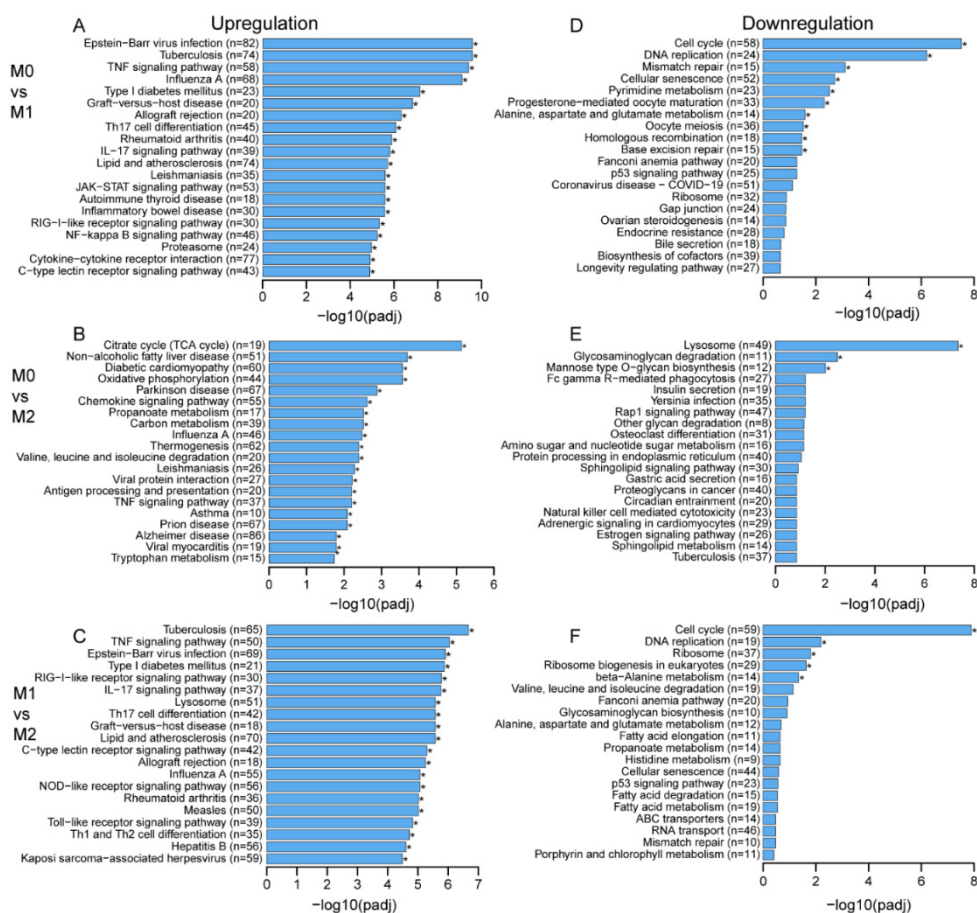


Figure S3 The KEGG pathway enrichment analysis of DEGs between M0, M1 and M2 macrophages. DEGs including both up- and down-regulated genes from each compared group were subjected to GO and KEGG analysis. The top 20 most enriched GO terms (including BP, CC, and MF) and KEGG pathways of DEGs are shown by compared groups, **(A, D)** M0 vs M1, **(B, E)** M0 vs M2, and **(C, F)** M1 vs M2. Blue, red, and green in **(A, B, and C)** represent BP, CC, and MF, respectively. **(A, B, and C)** represent upregulated genes. **(D, E, and F)** represent downregulated genes.

References

1. Hoeffel G, Wang Y, Greter M, See P, Teo P, Malleret B, et al. Adult Langerhans cells derive predominantly from embryonic fetal liver monocytes with a minor contribution of yolk sac-derived macrophages. *J Exp Med* (2012) 209(6):1167-81. Epub 2012/05/09. doi: 10.1084/jem.20120340.
2. Italiani P, Boraschi D. From Monocytes to M1/M2 Macrophages: Phenotypical vs. Functional Differentiation. *Frontiers in Immunology* (2014) 5(514). doi: 10.3389/fimmu.2014.00514.
3. Gharib SA, McMahan RS, Eddy WE, Long ME, Parks WC, Aitken ML, et al. Transcriptional and functional diversity of human macrophage repolarization. *J Allergy Clin Immunol* (2019) 143(4):1536-48. Epub 2018/11/18. doi: 10.1016/j.jaci.2018.10.046.
4. Martin P, Leibovich SJ. Inflammatory cells during wound repair: the good, the bad and the ugly. *Trends in Cell Biology* (2005) 15(11):599-607. doi: <https://doi.org/10.1016/j.tcb.2005.09.002>.
5. Shi C, Pamer EG. Monocyte recruitment during infection and inflammation. *Nature Reviews Immunology* (2011) 11(11):762-74. doi: 10.1038/nri3070.
6. Kratofil RM, Kubes P, Deniset JF. Monocyte Conversion During Inflammation and Injury. *Arterioscler Thromb Vasc Biol* (2017) 37(1):35-42. Epub 2016/10/22. doi: 10.1161/atvbaha.116.308198.
7. Krysko DV, Denecker G, Festjens N, Gabriels S, Parthoens E, D'Herde K, et al. Macrophages use different internalization mechanisms to clear apoptotic and necrotic cells. *Cell Death Differ* (2006) 13(12):2011-22. Epub 2006/04/22. doi: 10.1038/sj.cdd.4401900.
8. Leuti A, Talamonti E, Gentile A, Tiberi M, Matteocci A, Freseigna D, et al. Macrophage Plasticity and Polarization Are Altered in the Experimental Model of Multiple Sclerosis. *Biomolecules* (2021) 11(6). doi: 10.3390/biom11060837.
9. Komai T, Inoue M, Okamura T, Morita K, Iwasaki Y, Sumitomo S, et al. Transforming Growth Factor- β and Interleukin-10 Synergistically Regulate Humoral Immunity via Modulating Metabolic Signals. *Front Immunol* (2018) 9:1364. Epub 2018/07/03. doi: 10.3389/fimmu.2018.01364.
10. Yao Y, Xu XH, Jin L. Macrophage Polarization in Physiological and Pathological Pregnancy. *Front Immunol* (2019) 10:792. Epub 2019/05/01. doi: 10.3389/fimmu.2019.00792.
11. Restrepo BI, Twahirwa M, Rahbar MH, Schlesinger LS. Phagocytosis via complement or Fc-gamma receptors is compromised in monocytes from type 2 diabetes patients with chronic hyperglycemia. *PLoS One* (2014) 9(3):e92977. Epub 2014/03/29. doi: 10.1371/journal.pone.0092977.
12. Atri C, Guerfali FZ, Laouini D. Role of Human Macrophage Polarization in Inflammation during Infectious Diseases. *Int J Mol Sci* (2018) 19(6). Epub 2018/06/21. doi: 10.3390/ijms19061801.
13. Wang LX, Zhang SX, Wu HJ, Rong XL, Guo J. M2b macrophage polarization and its roles in diseases. *J Leukoc Biol* (2019) 106(2):345-58. Epub 2018/12/24. doi: 10.1002/jlb.3ru1018-378rr.

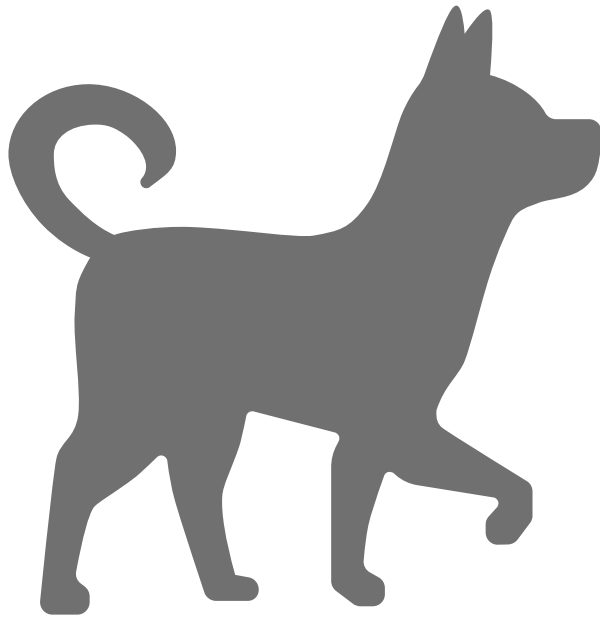
14. Martinez FO, Gordon S. The M1 and M2 paradigm of macrophage activation: time for reassessment. *F1000Prime Rep* (2014) 6:13. Epub 2014/03/29. doi: 10.12703/P6-13.
15. Edwards JP, Zhang X, Frauwirth KA, Mosser DM. Biochemical and functional characterization of three activated macrophage populations. *J Leukoc Biol* (2006) 80(6):1298-307. Epub 2006/08/15. doi: 10.1189/jlb.0406249.
16. Stout RD, Jiang C, Matta B, Tietzel I, Watkins SK, Suttles J. Macrophages sequentially change their functional phenotype in response to changes in microenvironmental influences. *J Immunol* (2005) 175(1):342-9. Epub 2005/06/24. doi: 10.4049/jimmunol.175.1.342.
17. Davis MJ, Tsang TM, Qiu Y, Dayrit JK, Freij JB, Huffnagle GB, et al. Macrophage M1/M2 polarization dynamically adapts to changes in cytokine microenvironments in *Cryptococcus neoformans* infection. *mBio* (2013) 4(3):e00264-13. Epub 2013/06/20. doi: 10.1128/mBio.00264-13.
18. Mosser DM, Edwards JP. Exploring the full spectrum of macrophage activation. *Nat Rev Immunol* (2008) 8(12):958-69. Epub 2008/11/26. doi: 10.1038/nri2448.
19. Zeyda M, Farmer D, Todoric J, Aszmann O, Speiser M, Györi G, et al. Human adipose tissue macrophages are of an anti-inflammatory phenotype but capable of excessive pro-inflammatory mediator production. *Int J Obes (Lond)* (2007) 31(9):1420-8. Epub 2007/06/28. doi: 10.1038/sj.ijo.0803632.
20. Crowther M, Brown NJ, Bishop ET, Lewis CE. Microenvironmental influence on macrophage regulation of angiogenesis in wounds and malignant tumors. *J Leukoc Biol* (2001) 70(4):478-90. Epub 2001/10/09.
21. Sargan DR. IDID: inherited diseases in dogs: web-based information for canine inherited disease genetics. *Mamm Genome* (2004) 15(6):503-6. Epub 2004/06/08. doi: 10.1007/s00335-004-3047-z.
22. Parker HG, Shearin AL, Ostrander EA. Man's best friend becomes biology's best in show: genome analyses in the domestic dog. *Annu Rev Genet* (2010) 44:309-36. Epub 2010/11/05. doi: 10.1146/annurev-genet-102808-115200.
23. Hytönen MK, Lohi H. Canine models of human rare disorders. *Rare Dis* (2016) 4(1):e1241362. Epub 2016/11/03. doi: 10.1080/21675511.2016.1241362.
24. Rowell JL, McCarthy DO, Alvarez CE. Dog models of naturally occurring cancer. *Trends Mol Med* (2011) 17(7):380-8. Epub 2011/03/29. doi: 10.1016/j.molmed.2011.02.004.
25. Day MJ. Antigen specificity in canine autoimmune haemolytic anaemia. *Vet Immunol Immunopathol* (1999) 69(2-4):215-24. Epub 1999/10/03. doi: 10.1016/s0165-2427(99)00055-0.
26. Sinke JD, Rutten VPMG, Willemse T. Immune dysregulation in atopic dermatitis. *Veterinary Immunology and Immunopathology* (2002) 87(3):351-6. doi: [https://doi.org/10.1016/S0165-2427\(02\)00066-1](https://doi.org/10.1016/S0165-2427(02)00066-1).
27. Lindblad-Toh K, Wade CM, Mikkelsen TS, Karlsson EK, Jaffe DB, Kamal M, et al. Genome sequence, comparative analysis and haplotype structure of the domestic dog. *Nature* (2005) 438(7069):803-19. Epub 2005/12/13. doi: 10.1038/nature04338.
28. Kim KS, Lee SE, Jeong HW, Ha JH. The complete nucleotide sequence of the domestic dog (*Canis familiaris*) mitochondrial genome. *Mol Phylogenet Evol* (1998) 10(2):210-20. Epub 1999/01/08. doi: 10.1006/mphev.1998.0513.

29. van den Biggelaar RH, van Eden W, Rutten VP, Jansen CA. Nitric Oxide Production and Fc Receptor-Mediated Phagocytosis as Functional Readouts of Macrophage Activity upon Stimulation with Inactivated Poultry Vaccines In Vitro. *Vaccines (Basel)* (2020) 8(2). Epub 2020/06/26. doi: 10.3390/vaccines8020332.
30. Mendoza-Coronel E, Ortega E. Macrophage Polarization Modulates FcγR- and CD13-Mediated Phagocytosis and Reactive Oxygen Species Production, Independently of Receptor Membrane Expression. *Front Immunol* (2017) 8:303. Epub 2017/04/12. doi: 10.3389/fimmu.2017.00303.
31. Helft J, Böttcher J, Chakravarty P, Zelenay S, Huotari J, Schraml BU, et al. GM-CSF Mouse Bone Marrow Cultures Comprise a Heterogeneous Population of CD11c(+)MHCII(+) Macrophages and Dendritic Cells. *Immunity* (2015) 42(6):1197-211. Epub 2015/06/18. doi: 10.1016/j.immuni.2015.05.018.
32. Antonios JK, Yao Z, Li C, Rao AJ, Goodman SB. Macrophage polarization in response to wear particles in vitro. *Cell Mol Immunol* (2013) 10(6):471-82. Epub 2013/09/10. doi: 10.1038/cmi.2013.39.
33. Noordenbos T. The role of innate immune cells in tissue inflammation in spondyloarthritis (2017).
34. Frafjord A, Skarshaug R, Hammarstrom C, Stankovic B, Dorg LT, Aamodt H, et al. Antibody combinations for optimized staining of macrophages in human lung tumours. *Scand J Immunol* (2020) 92(1):e12889. Epub 2020/04/17. doi: 10.1111/sji.12889.
35. Gao J, Scheenstra MR, van Dijk A, Veldhuizen EJA, Haagsman HP. A new and efficient culture method for porcine bone marrow-derived M1- and M2-polarized macrophages. *Vet Immunol Immunopathol* (2018) 200:7-15. Epub 2018/05/20. doi: 10.1016/j.vetimm.2018.04.002.
36. Durafourt BA, Moore CS, Zammit DA, Johnson TA, Zaguia F, Guiot MC, et al. Comparison of polarization properties of human adult microglia and blood-derived macrophages. *Glia* (2012) 60(5):717-27. Epub 2012/02/01. doi: 10.1002/glia.22298.
37. Shiratori H, Feinweber C, Luckhardt S, Linke B, Resch E, Geisslinger G, et al. THP-1 and human peripheral blood mononuclear cell-derived macrophages differ in their capacity to polarize in vitro. *Molecular Immunology* (2017) 88:58-68. doi: 10.1016/j.molimm.2017.05.027.
38. Liu Y, Yang D, Wei S, Nie Y, Zhang X, Lian Z, et al. Isolation and characterization of ovine monocyte-derived macrophages from peripheral blood. *Veterinary Immunology and Immunopathology* (2018) 205:83-92. doi: https://doi.org/10.1016/j.vetimm.2018.11.004.
39. Sridharan R, Cameron AR, Kelly DJ, Kearney CJ, O'Brien FJ. Biomaterial based modulation of macrophage polarization: a review and suggested design principles. *Materials Today* (2015) 18(6):313-25. doi: https://doi.org/10.1016/j.mattod.2015.01.019.
40. Herrmann I, Gotovina J, Fazekas-Singer J, Fischer MB, Hufnagl K, Bianchini R, et al. Canine macrophages can like human macrophages be in vitro activated toward the M2a subtype relevant in allergy. *Developmental and Comparative Immunology* (2018) 82:118-27. doi: 10.1016/j.dci.2018.01.005.
41. Heinrich F, Lehmbecker A, Raddatz BB, Kegler K, Tipold A, Stein VM, et al. Morphologic, phenotypic, and transcriptomic characterization of classically and alternatively activated canine blood-derived macrophages in vitro. *PLoS*

- One* (2017) 12(8):e0183572. Epub 2017/08/18. doi: 10.1371/journal.pone.0183572.
42. Kosmac K, Peck BD, Walton RG, Mula J, Kern PA, Bamman MM, et al. Immunohistochemical Identification of Human Skeletal Muscle Macrophages. *Bio Protoc* (2018) 8(12). Epub 2018/08/28. doi: 10.21769/BioProtoc.2883.
 43. Raggi F, Pelassa S, Pierobon D, Penco F, Gattorno M, Novelli F, et al. Regulation of Human Macrophage M1-M2 Polarization Balance by Hypoxia and the Triggering Receptor Expressed on Myeloid Cells-1. *Front Immunol* (2017) 8:1097. Epub 2017/09/25. doi: 10.3389/fimmu.2017.01097.
 44. Qu X, Cinar MU, Fan H, Pröll M, Tesfaye D, Tholen E, et al. Comparison of the innate immune responses of porcine monocyte-derived dendritic cells and splenic dendritic cells stimulated with LPS. *Innate Immun* (2015) 21(3):242-54. Epub 2014/03/22. doi: 10.1177/1753425914526266.
 45. Milhau N, Almouazen E, Bouteille S, Hellel-Bourtal I, Azzouz-Maache S, Benavides U, et al. In vitro evaluations on canine monocyte-derived dendritic cells of a nanoparticles delivery system for vaccine antigen against *Echinococcus granulosus*. *PLoS One* (2020) 15(2):e0229121. Epub 2020/02/27. doi: 10.1371/journal.pone.0229121.
 46. Murray PJ, Allen JE, Biswas SK, Fisher EA, Gilroy DW, Goerdts S, et al. Macrophage activation and polarization: nomenclature and experimental guidelines. *Immunity* (2014) 41(1):14-20. Epub 2014/07/19. doi: 10.1016/j.immuni.2014.06.008.
 47. Porcheray F, Viaud S, Rimaniol AC, Léone C, Samah B, Dereuddre-Bosquet N, et al. Macrophage activation switching: an asset for the resolution of inflammation. *Clin Exp Immunol* (2005) 142(3):481-9. Epub 2005/11/22. doi: 10.1111/j.1365-2249.2005.02934.x.
 48. Belluco S, Sammarco A, Sapin P, Lurier T, Marchal T. FOXP3, CD208, and CD206 Expression in Canine Cutaneous Histiocytoma. *Veterinary Pathology* (2020) 57(5):599-607. doi: 10.1177/0300985820941818.
 49. Nolte A, Junginger J, Baum B, Hewicker-Trautwein M. Heterogeneity of macrophages in canine histiocytic ulcerative colitis. *Innate Immunity* (2017) 23(3):228-39. doi: 10.1177/1753425916686170.
 50. Röszer T. Understanding the Mysterious M2 Macrophage through Activation Markers and Effector Mechanisms. *Mediators Inflamm* (2015) 2015:816460. Epub 2015/06/20. doi: 10.1155/2015/816460.
 51. Preza GC, Tanner K, Elliott J, Yang OO, Anton PA, Ochoa MT. Antigen-presenting cell candidates for HIV-1 transmission in human distal colonic mucosa defined by CD207 dendritic cells and CD209 macrophages. *AIDS Res Hum Retroviruses* (2014) 30(3):241-9. Epub 2013/10/19. doi: 10.1089/aid.2013.0145.
 52. Gibbings SL, Thomas SM, Atif SM, McCubbrey AL, Desch AN, Danhorn T, et al. Three Unique Interstitial Macrophages in the Murine Lung at Steady State. *Am J Respir Cell Mol Biol* (2017) 57(1):66-76. Epub 2017/03/04. doi: 10.1165/rcmb.2016-0361OC.
 53. Saqib U, Sarkar S, Suk K, Mohammad O, Baig MS, Savai R. Phytochemicals as modulators of M1-M2 macrophages in inflammation. *Oncotarget* (2018) 9(25):17937-50. Epub 2018/05/01. doi: 10.18632/oncotarget.24788.
 54. Peng H, Geil Nickell CR, Chen KY, McClain JA, Nixon K. Increased expression of M1 and M2 phenotypic markers in isolated microglia after four-

- day binge alcohol exposure in male rats. *Alcohol* (2017) 62:29-40. Epub 2017/08/02. doi: 10.1016/j.alcohol.2017.02.175.
55. Sironi M, Martinez FO, D'Ambrosio D, Gattorno M, Polentarutti N, Locati M, et al. Differential regulation of chemokine production by Fc γ receptor engagement in human monocytes: association of CCL1 with a distinct form of M2 monocyte activation (M2b, Type 2). *J Leukoc Biol* (2006) 80(2):342-9. Epub 2006/06/01. doi: 10.1189/jlb.1005586.
 56. Pahl JH, Kwappenberg KM, Varypataki EM, Santos SJ, Kuijjer ML, Mohamed S, et al. Macrophages inhibit human osteosarcoma cell growth after activation with the bacterial cell wall derivative liposomal muramyl tripeptide in combination with interferon- γ . *J Exp Clin Cancer Res* (2014) 33(1):27. Epub 2014/03/13. doi: 10.1186/1756-9966-33-27.
 57. Guo X-Y, Wang S-N, Wu Y, Lin Y-H, Tang J, Ding S-Q, et al. Transcriptome profile of rat genes in bone marrow-derived macrophages at different activation statuses by RNA-sequencing. *Genomics* (2019) 111(4):986-96. doi: <https://doi.org/10.1016/j.ygeno.2018.06.006>.
 58. Beyer M, Mallmann MR, Xue J, Staratschek-Jox A, Vorholt D, Krebs W, et al. High-resolution transcriptome of human macrophages. *PLoS One* (2012) 7(9):e45466. Epub 2012/10/03. doi: 10.1371/journal.pone.0045466.
 59. Wallner S, Grandl M, Konovalova T, Sigrüner A, Kopf T, Peer M, et al. Monocyte to macrophage differentiation goes along with modulation of the plasmalogen pattern through transcriptional regulation. *PLoS One* (2014) 9(4):e94102. Epub 2014/04/10. doi: 10.1371/journal.pone.0094102.
 60. Vaddi K, Newton RC. Comparison of biological responses of human monocytes and THP-1 cells to chemokines of the intercrine-beta family. *J Leukoc Biol* (1994) 55(6):756-62. Epub 1994/06/01. doi: 10.1002/jlb.55.6.756.

6



A canine macrophage cell line that can be polarized into classically activated M1 and alternatively activated M2 macrophages provides a model for the study of canine macrophage differentiation

Qingkang Lyu¹, Victor P. M. G. Rutten^{1,2}, Willem van Eden¹, Alice J. A. M. Sijts¹ and Femke Broere^{1,3,*}

¹Department of Infectious diseases and Immunology, Faculty of Veterinary Medicine, Utrecht University; 3584 CL, Utrecht, The Netherlands

²Department of Veterinary Tropical diseases, Faculty of Veterinary Science, Pretoria University, South Africa

³Department of Clinical Sciences of Companion Animals, Faculty Veterinary Medicine, Utrecht University, Utrecht, The Netherlands

*Correspondence: f.broere@uu.nl

Abstract

Monocyte-like cell lines have been widely used as surrogates of monocytes to study macrophage biology. However, an appropriate macrophage cell line for canine species is still lacking. The canine 030D cell line is a monocyte-like cell line derived from canine malignant histiocytosis. To determine if 030D cells can be polarized into M1 and M2 macrophages, 030D cells were stimulated for three days with either IFN- γ + LPS for M1 or IL-4 for M2. We further comprehensively characterized 030D-derived M0, M1 and M2 macrophages on each day for morphology, phenotypic characteristics, marker genes expression and phagocytosis. Our result showed that 030D-derived M1 macrophages appeared to obtain a bigger, roundish, and amoeboid shape, showing as “fried-egg” morphology, whereas some of the M2 macrophages adopted an elongated morphology. All three polarization states expressed the pan-macrophage markers CD14 and CD11b. Flow cytometry analysis showed that 030D-derived M1 macrophages upregulated the expression of CD32, CD40, CD80, CD83, CD86 and MHC II, while M2 macrophages expressed a higher level of CD206 relative to M1 macrophages. 030D-derived M1 macrophages highly upregulated the expression of pro-inflammatory cytokines and chemokines, including IL-6, IL-1 β , TNF- α , IL-12p35/40, IL-23p19, COX2, CCL2, CCR7, TGF- β , and IL-10, while the novel identified M2 marker MS4A2 was significantly upregulated in M2 macrophages relative to M1 macrophages. Besides, qPCR analysis showed that mRNA levels of CD16, CD32, CD40, CD64, LOX-1, LXN, MHC I, MHC II, CIITA and arginase-1 were upregulated in M1 macrophages compared to M2 macrophages. Functionally, we found that M1 macrophages had a stronger phagocytic capacity than M0 and M2 macrophages. Taken together, in our study it became evident that canine 030D-derived M1 and M2 macrophages showed many similarities to M1 and M2 macrophages derived from other species, such as human, mouse, pig and ovine. Thus, the 030D-derived macrophage can be a powerful cell model for canine immunological studies.

Keywords: 030D macrophage cell line, macrophages surface marker, phagocytosis, M1 and M2 macrophages

Introduction

The macrophage is a main member of the monocyte/macrophage phagocytotic system (MPS), playing a crucial role in probably all immune responses, including the regulation of inflammation, homeostasis, and tissue repair (1). As a group of important antigen-presenting cells, macrophages serve as regulators between innate and adaptive immune responses, poising anti- and pro-inflammatory responses (2). During infection, activated macrophages recognize and engulf invaders by pattern-recognition receptors, produce inflammatory cytokines and chemokines, and subsequently initiate adaptive immune responses. In this process, macrophages respond to stimuli and signals in the local microenvironment, and polarize into distinct functional subsets (3). So far, according to the local cytokine milieu produced by Th1/Th2 cells, two main macrophage subsets have been identified, namely, classically activated (M1) and alternatively activated (M2) macrophages (4, 5). M1 macrophages produce pro-inflammatory cytokines, participate in pathogen presentation and removal, and promote Th1 responses. In contrast, M2 macrophages produce anti-inflammatory cytokines, develop potent phagocytic capacity, tissue repair and wound healing, and promote Th2 responses (6).

Mimicking the *in vivo* process, M1 macrophages are polarized by administration of Th1 cytokines (such as IFN- γ or TNF- α) and lipopolysaccharide (LPS) *in vitro*. Polarized M1 cells express a variety of cytokines and chemokines, such as IL-6, IL-1 β , TNF- α , IL-23, IL-12, CCL2 and CCR7, which have an extensive pro-inflammatory role (7). These cells also express high levels of the surface markers such as CD40, CD80, CD86 and MHC II, which increases their antigen-presenting ability. On the other hand, M2 cells consist of different subsets, M2a, M2b and M2c, which can be polarized in response to Th2 cytokines, such as IL-4, IL-13, IL-10 or TGF- β (8). M2a macrophages are activated by IL-4 or IL-13; M2b macrophages are polarized by LPS and immune complexes; M2c macrophages are promoted by IL-10 and TGF- β (9). M2 macrophages are characterized by increased CD206, CD209 and CD163 expression on the cell surface (10). Inflammatory responses are relieved by upregulation of anti-inflammatory cytokines like IL-10 and TGF- β . In addition, phagocytosis is one of the essential functions of macrophages, which is regulated by phagocytic receptors such as CD64, CD32 and CD16. Phagocytosis plays an important role in removal of pathogens, dead cells, and debris.

To date, *in vitro* cultures of macrophages from different sources such as bone marrow, peripheral blood mononuclear cells, peritoneum and spleen have been studied in the mouse (11). However, the difficulty to collect, isolate and grow primary macrophages of other animals like dog is huge. Monocyte-derived macrophages

could serve as an alternative source of macrophages but need 7 days of culture in most protocols (12, 13). As an alternative, monocyte-like cell lines have been widely applied as a powerful model for the investigation of immune responses *in vitro* (14). Compared to primary macrophages, monocyte-like cells have notable advantages, for example creating unlimited sources of cells, easy acquisition and culturing, and high homogeneity (15). The canine monocyte-like cell line 030D, was established by Gebhard, et al. in 1995 from a dog suffering from malignant histiocytosis (16). 030D cells have been widely used in many studies of canine immunology and infection (17-20). However, the differentiation potential and characteristics of 030D cells have not been fully investigated up to now. Hence, for further canine immunological studies it is necessary to define the polarization states and immunological and functional characteristics of this cell line.

The purpose of this study was to determine if the canine macrophage cell line 030D, can be polarized into M1 and M2 macrophages. To this end, 030D cells were stimulated with either IFN- γ + LPS for M1 or IL-4 for M2 for three days. The morphological changes between 030D-derived M1 and M2 macrophages were observed on each day. The expression of M1 and M2 markers, like surface markers and cytokines expression, was analyzed in polarized 030D macrophages. Furthermore, non-specific phagocytosis of latex beads was assessed in 030D-derived M0, M1 and M2 macrophages. We found that 030D-derived macrophages provided a good model for canine macrophage studies.

Materials and methods

Cell culture

A canine monocytoid cell line derived from canine malignant histiocytosis, known as 030D, which is a kind gift from Ley, D., was used in this study. 030D cells were cultured in RPMI-1640 GlutaMAX (Life Technologies™ Ltd., Paisley, Scotland, UK) supplemented with 5% fetal bovine serum (BODINCO B.V., The Netherlands), and 1% penicillin/streptomycin (Life Technologies™ Ltd., Paisley, Scotland, UK) at 37 °C and 5% CO₂.

030D Macrophage polarization

030D cells were plated on 6-well plates at a density of 8×10^5 cells/well. After 2 h, the medium was gently refreshed to remove non-adherent cells. In order to differentiate 030D cells into different subsets of macrophages, 030D cells were stimulated with 20 ng/ml recombinant canine IFN- γ (R&D system, Abingdon, United Kingdom) for 6 hours, after which 100 ng/ml LPS from *Escherichia coli* O111:B4 (Sigma-Aldrich,

Saint Louis, MO, USA) was added for M1 polarization. M2 polarization was obtained by incubating cells with 40 ng/ml recombinant canine IL-4 (R&D system, Abingdon, United Kingdom). 030D cells cultured with only complete medium were included and regarded as M0. Cells were harvested by pipetting for analyses after 24, 48, or 72 h incubation in all three conditions.

The morphology observation of macrophages by Phase-contrast microscopy

030D cells were grown and polarized as described above. After 24, 48 and 72 h of culture, the morphology of M0, M1 and M2 macrophages was recorded by Phase-contrast light microscopy using a Nikon eclipse TS100 inverted microscope (Nikon Instruments Europe B.V., Amstelveen, The Netherlands) and ImageFocus v3.0.0.2. Data were processed using Fiji imageJ.

Phenotypic characterization of polarized 030D cell by flow cytometry

For flow cytometry analysis, 030D cell-derived M0, M1 and M2 cells were detached by gentle scraping at day1, day2 and day3. After washing with cold PBS, cells were transferred to a round-bottom 96-well plate at a density of 2×10^5 cells/well. Fc receptors were blocked with 10% autologous dog serum for 30 min to avoid non-specific antibody binding. To determine the phenotype of macrophages, cells were stained for 30 min on ice using antibodies specific for CD14, CD40, CD80, MHC II, CD206, CD83, CD86, CD32, CD11b (see Table 1). Matched isotype controls were used with the same concentration of corresponding antibodies. Cells then were washed 3 times with FACS buffer (2% FCS in FBS) and either directly analyzed when labeled with fluorochrome-conjugated antibodies, or first incubated with secondary or streptavidin conjugated antibodies for a further 30 min on ice, washed and then analyzed using a CytoFLEX LX flow cytometer (Beckman Coulter Inc., CA, USA). In order to gate out dead cells ViaKrome 808 Fixable Viability Dye (Beckman Coulter, Woerden, Netherlands) was used. Acquired data were analyzed with FlowJo Software v.10.5 (FlowJo LCC, Ashland, USA).

Gene Expression of M0, M1 and M2 030D-derived macrophages by real-time qPCR

030D-derived macrophages (M0, M1 and M2) were harvested in 350 μ l of RLT lysis buffer provided by Qiagen RNeasy mini kit at day1, 2 and 3. Total RNA was isolated using a Qiagen RNeasy mini kit (Qiagen, Venlo, The Netherlands) following

manufacturer's instructions and then treated with DNase I. RNA samples were dissolved in RNase-free water and concentrations were measured using a NanoDrop-1000 Spectrophotometer (Isogen Lifescience B.V., Utrecht, the Netherlands). cDNA was generated from 1 µg total RNA using an iScript cDNA Synthesis Kit (Bio-Rad Laboratories B.V., California, USA) following the manufacturer's instructions.

RT-qPCR was conducted using a CFX connect real-time system (Bio-Rad Laboratories B.V., Veenendaal, The Netherlands) with iQ SYBR Green Supermix (Bio-Rad Laboratories B.V., California, USA). The specificity of PCR products was confirmed by melting curve analysis. Data were recorded and analyzed by CFX Maestro 1.1 software. All primers used in this paper were purchased from Invitrogen (Life Technologies Ltd, Paisley, UK). The sequence of primers is listed in Table 2. GAPDH and RPS19 genes were used as reference genes to normalize target gene expression. Relative expression of mRNA was calculated using the Pfaffl-method.

Non-specific phagocytosis assay by flow cytometry

Non-specific phagocytic capacity of 030D-derived M0, M1 and M2 macrophages was evaluated using 1 µm crimson carboxylate-modified FluoSpheres fluorescent beads (Life Technologies Corporation, Eugene, USA). Specifically, 24, 48, 72 h polarized macrophages were incubated with FluoSpheres fluorescent beads at a 1:10 bead-to-cell ratio for 4 h. Then cells were washed three times to remove non-phagocytosed beads. Harvested cells at each time point were washed 2 times with PBS containing 5 mM EDTA and transferred into a 96-well U-bottom plate. Next, the cells were stained with ViaKrome 808 Fixable Viability Dye (Beckman Coulter, Woerden, The Netherlands) for 30 min on ice to exclude dead cells. Afterwards, the cells were washed twice and fixed in 4% paraformaldehyde (Alfa Aesar, Kandel, Germany) for 15 min at room temperature. Finally, the cells were measured on a CytoFLEX LX flow cytometer (Beckman Coulter Inc., CA, USA) using the 638 nm laser and the 660/10 fluorescent channel. Data were analyzed using FlowJo Software v.10.5 (FlowJo LCC, Ashland, USA) and GraphPad Prism 8.3.0 (Graphpad Software LLC., San Diego, USA). The first fluorescent peak showing in histogram was considered as cells with single bead. The average bead uptake and the fold change of beads in each cell was calculated using formulas described in literature (21).

$$\text{Bead/cell} = \frac{\text{MFI}_{\text{total}}}{\text{MFI}_{\text{bead/cell}}} \quad \text{and} \quad \text{fold change} = \frac{\text{beads/cell}_{\text{M1 or M2}}}{\text{beads/cell}_{\text{M0}}}$$

Assessment of internalization by Confocal Microscopy

030D cells were placed at 2×10^5 cells/well in a 24-well plate containing sterilized 12

mm coverslips. Cells were differentiated into M0, M1 and M2 as described above. Macrophages were activated for 24, 48 and 72 h and then co-cultured with FluoSpheres fluorescent beads for 4 h at 1:10 bead-to-cell ratio. Macrophages were washed three times with cold Hank's balanced salt solution (HBSS) (Gibco, Paisley, UK) to remove non-phagocytosed beads, followed by staining macrophages with 2 µg/ml Alexa Fluor 488 conjugated Wheat germ agglutinin (WGA) (Life Technologies Corporation, Eugene, USA) in HBSS for 10 min at 37 °C. When labeling was complete, WGA was removed and macrophages were washed twice with HBSS and fixed with 4% paraformaldehyde for 15 min at room temperature. After washing twice, coverslips with macrophages were mounted on polysine slides (Thermo Scientific, Braunschweig, Germany) with FluorSave Reagent (Millipore, San Diego, USA). Finally, uptake and internalization were confirmed using Leica TCS SPE-II and LAS-AF software (Leica Microsystems B.V., Amsterdam, The Netherlands). Z-stacks was included to determine whether beads were completely internalized. The images from confocal microscopy were analyzed using Fiji ImageJ.

Statistical Analysis

Statistical analysis was conducted using GraphPad Prism 8.3.0 (Graphpad Software LLC., San Diego, USA). Two-way ANOVA tests with multiple comparisons were used to determine statistical differences. The mixed effects model was used when missing values existed. Data are presented as mean ± SD. All independent experiments were repeated at least three times. Each *p* value is adjusted to account for multiple comparisons. **p* < 0.05 and ***p* < 0.01 were considered as significant difference and highly significant, respectively.

Results

Morphological changes of 030D-derived macrophages during polarization

In order to investigate whether the canine macrophage cell line 030D, can be polarized into the classically activated M1 and the alternatively activated M2 macrophage phenotypes, 030D cells were stimulated with IFN- γ + LPS or IL-4 for 3 days. As an initial means to investigate macrophage polarization, the morphology of the cells was observed each day. As shown in Figure 1, M0 macrophages showed a small round morphology (Figure 1A) and did not show any obvious change in morphology or size within 3 days of culture (Figure 1B, 1C and Figure S1). In comparison, M1-polarized macrophages appeared to adopt a well-spread, rounded, large and flat shape (Figure 1A). Some M1-polarized cells showed an amoeboid and typical “fried-egg” morphology (red arrows) (Figure 1A). To quantitate the size changes of cells during polarization, flow cytometry analysis was performed to record the FCS of M0, M1 and M2 cells. As shown in Figure S1 and Figure 1B and C, M1-polarized cells became bigger and more granular than M0- and M2-polarized macrophages since day 2. In contrast with M1 cells, M2-polarized macrophages kept a morphology similar to M0 cells at days 1 and 2, showing a small and round shape. At day 3, M2-polarized macrophages started to obtain an elongated spindle-like morphology (blue arrows) (Figure 1A). No significant size changes of M2 cells were observed, compared to M0 cells. These observations indicated that 030D-derived M1 and M2 macrophages share some of the morphological features of M1 and M2 macrophages.

Cell surface markers expression profiles for canine 030D-derived macrophages

CD14 and CD11b are commonly used pan-macrophage markers to define macrophages (22-24). To confirm macrophage differentiation and maintenance thereof during polarization, the expression of CD14 and CD11b on 030D-derived macrophages was determined by flow cytometry. Our results showed that both CD14 and CD11b were highly expressed on 030D-derived M0, M1 and M2 macrophages at day1, 2 and 3 (Figure 2A and Supplementary Figure S2A). CD14 and CD11b expression was markedly increased on M1-polarized (IFN- γ + LPS) macrophages especially at day 2, whereas their expression on M2-polarized (IL-4) macrophages was decreased (Figure 2B and Supplementary Figure S2B). CD115, colony-stimulating factor-1 receptor, is one of most important antigens for macrophage identification (25, 26). Mer tyrosine kinase (MerTK) is mainly expressed on

macrophages and monocytes, which is responsible for phagocytosis and internalization of apoptotic cells (27, 28). Both CD115 and MerTK can be considered as potential pan-macrophage markers (29, 30). Therefore, CD115 and MerTK were analyzed on canine O30D-derived macrophages by qPCR. As shown in Figure 2, M0-, M1-, and M2-polarized macrophages widely expressed MerTK during polarization (Figure 2C). While M0- and M2-polarized macrophages expressed comparable levels of CD115 at day1 and 2, the expression of CD115 was reduced in M2-polarized macrophages at day3 (Figure 2C). Conversely, CD115 expression in M1-polarized macrophages was gradually and significantly decreased during polarization (Figure 2C).

To define M1 (IFN- γ + LPS) and M2 (IL-4) polarization states, a range of putative polarization markers for M1 and M2 subsets was analyzed over time. As expected, M1-polarized macrophages (IFN- γ + LPS) showed a clear profile of enhanced M1 markers at day2 and day3 in response to IFN- γ + LPS polarization, including elevation of CD32, CD40, CD80, CD83, CD86 and MHC II (Figure 3A and B). It is noteworthy that MHC II expression was elevated in both M1- and M2-polarized macrophages from day 1 (supplementary Figure S2), but its expression on M1 macrophages was significantly higher than on M2 macrophages (Figure 3A and B). CD206 expression, as a M2 marker in multiple species (13, 31, 32), was reduced on both M1 and M2 macrophages during polarization, while the decrease of CD206 on M1 was significantly higher than that of M2 (supplementary Figure S2, and Figure 3A and B). Besides, CD40 and CD86 were observed to increase in M1 macrophages at day 1, but CD32, CD80 and CD83 were not (Figure S2).

To further confirm M1 and M2 polarization states, more macrophage surface markers were analyzed by qPCR. In line with our results obtained by flow cytometry, a similar expression pattern for CD32, CD40, MHC II and CD206 was observed in both M1- and M2-polarized macrophages (Figure 4). More specifically, the expression of CD16, CD32, CD40 and CD64 was dramatically upregulated in M1-polarized macrophages at day 1 compared to M0 and M2 macrophages ($p < 0.01$) (Figure 4), subsequently their expression in M1-polarized macrophages gradually decreased over time. No significant changes in the expression of CD16, CD32, CD40 and CD64 were observed in M2-polarized macrophages. In contrast, the expression of MHC I, MHC II and CIITA was gradually upregulated in M1-polarized macrophages during polarization compared to M0 and M2-polarized macrophages ($p < 0.01$) (Figure 4). Similar to our previous results, MHC II and CIITA were upregulated in both M1 and M2-polarized macrophages relative to their expression in M0 macrophages. On the contrary, a significantly higher level of CD206, CD209 and CD163 was observed in M2 and not M1 macrophages ($p < 0.01$) (Figure 4).

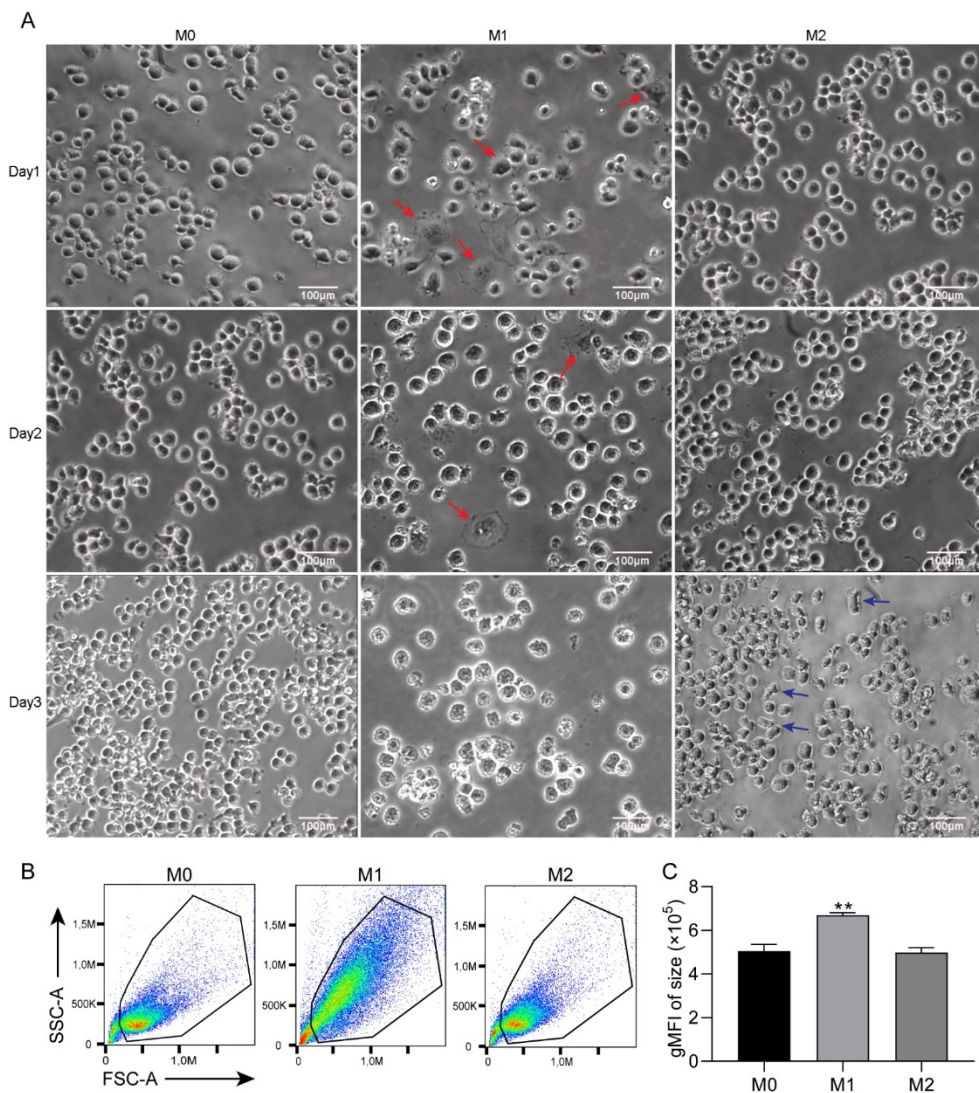


Figure 1 Morphological changes in canine 030D-derived M0, M1 and M2 macrophages. 030D cells were treated with M1 (20 ng/ml IFN- γ + 100 ng/ml LPS) and M2 (40 ng/ml IL-4) polarizing conditions for 24, 48 and 72 h. M0 macrophages were cultured with complete medium only. **(A)** The morphological changes were directly observed by phase contrast microscopy with 20 \times magnification after 24 (Day1), 48 (Day2) and 72 (Day3) h culture. Representative images are shown from at least three independent experiments. M1-polarized macrophages showed a large and rounded morphology (red arrows), whereas M2-polarized macrophages showed an elongated shape at day 3 (blue arrows). M2-polarized macrophages showed a

similar morphology to M0 macrophages at day 1 and day 2. Scale bar=100 μm . **(B and C)** Polarized macrophages at day 1, 2 (see supplementary materials) and 3 were subjected to flow cytometry analysis. Comparison of size between M0, M1 and M2 macrophages at day 3 was evaluated based on forward scatter (FSC) in **(B and C)**. Representative flow cytometry plots were shown in **(B)**, and geometric mean (gMFI) FSC values of M0, M1 and M2 macrophages are shown in **(C)**. Data are presented as mean \pm SD, with $n \geq 3$ per condition. * $p < 0.05$; ** $p < 0.01$. gMFI: geometric mean of fluorescence intensity, SSC: side scatter, FSC: forward scatter.

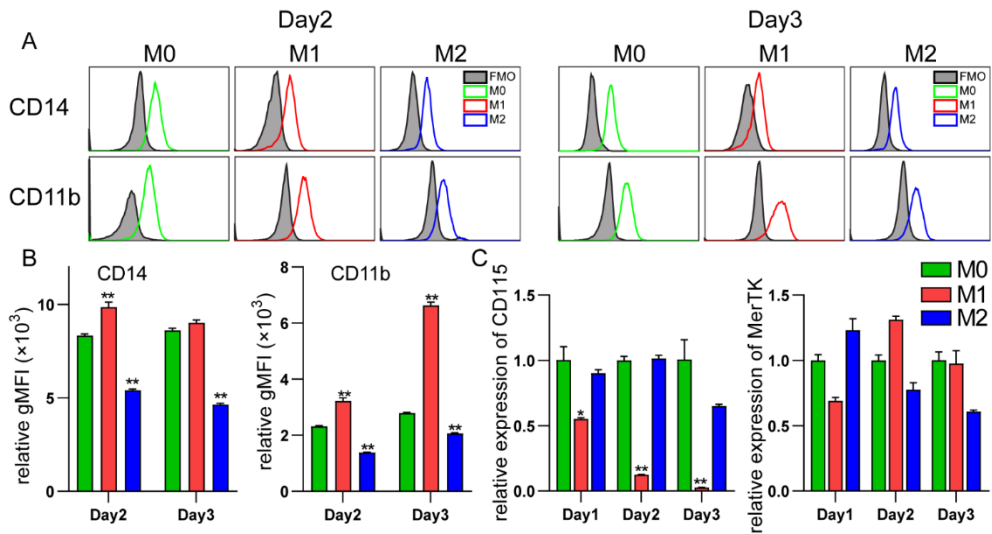


Figure 2 Pan-macrophage marker expression on 030D-derived macrophages. Canine 030D cells were polarized with IFN- γ + LPS (M1) or IL-4 (M2) for 3 days. Polarized cells were harvested at Day1, Day2 and Day3 for the detection of pan-macrophage markers expression using flow cytometry **(A and B)** and qPCR **(C)**. **(A)** Both pan-monocyte markers CD14 and CD11b expression were analyzed by flow cytometry and shown by representative histograms for M0, M1 and M2 cells. Filled gray histograms represent Fluorescence Minus One (FMO) Controls to show the background fluorescence. **(B)** For M0, M1 and M2 macrophages, the expression levels of CD14 and CD11b are expressed as the geometric mean fluorescent intensity (gMFI) for three independent replicates. Shown is the mean of the geometric fluorescence intensity (gMFI) subtracted by gMFI of FMO. **(C)** CD115 and MerTK expression in mRNA level on each day were analyzed by qPCR. Their expression in M1 and M2 is relative to the expression in M0. Data are presented as mean \pm SD, with $n \geq 3$ per condition. * $p < 0.05$; ** $p < 0.01$.

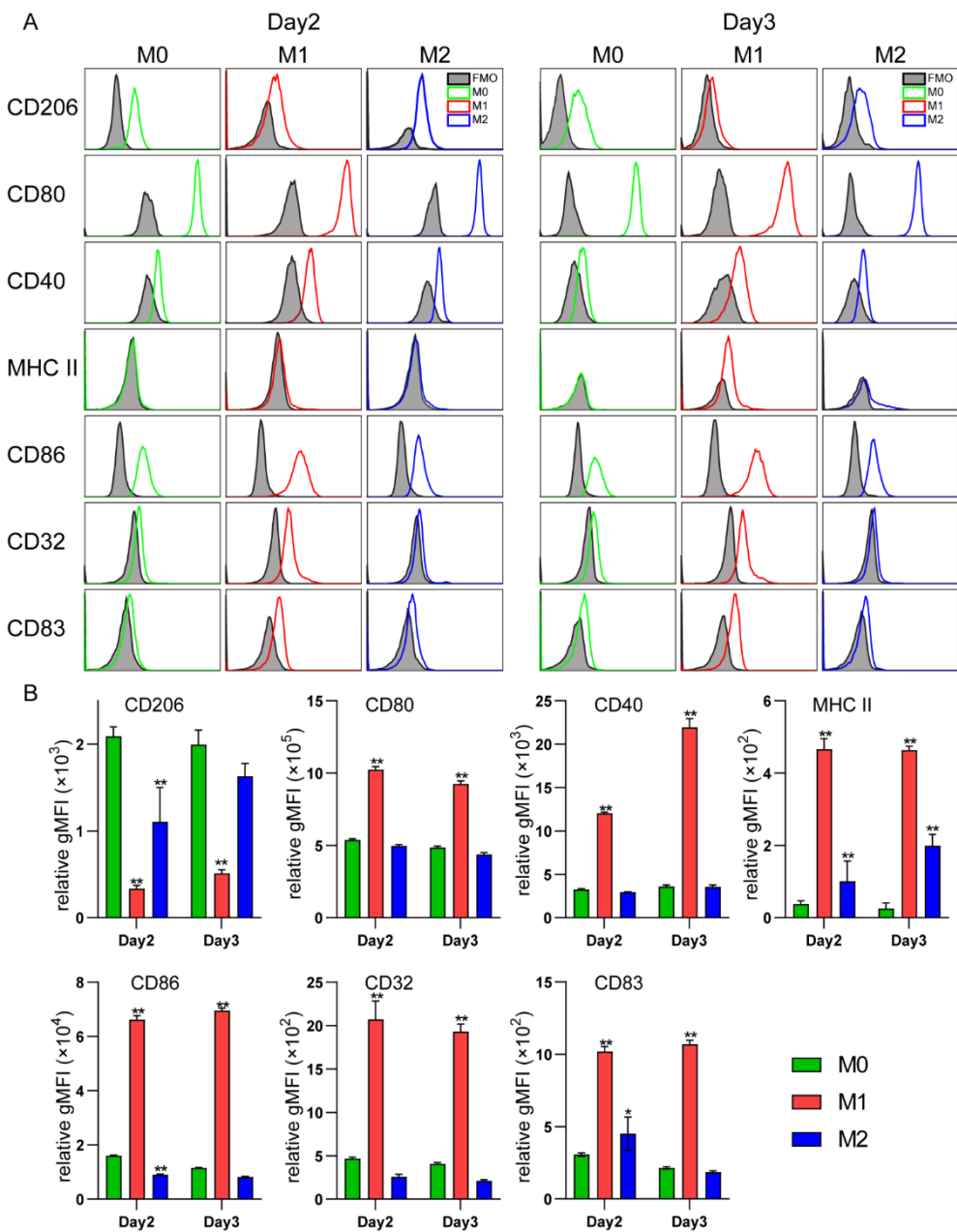


Figure 3 Flow cytometric analysis of surface markers expressed by 030D-derived macrophages. Canine 030D cells were polarized as described in *materials and methods*. Flow cytometry was performed to measure the expression of surface

markers on O30D-derived macrophages at day 1, day 2 and day 3. **(A)** Expression levels of a set of surface markers are presented by representative histograms for M0, M1 and M2 cells. Filled gray histograms represent Fluorescence Minus One (FMO) Controls to show the background fluorescence. **(B)** Relative expression levels of all surface markers are expressed as the geometric mean fluorescent intensity (gMFI) for three independent replicates. Shown is the mean of the geometric fluorescence intensity (gMFI) subtracted by gMFI of FMO. Data are presented as mean \pm SD, with $n \geq 3$ per condition. * $p < 0.05$; ** $p < 0.01$.

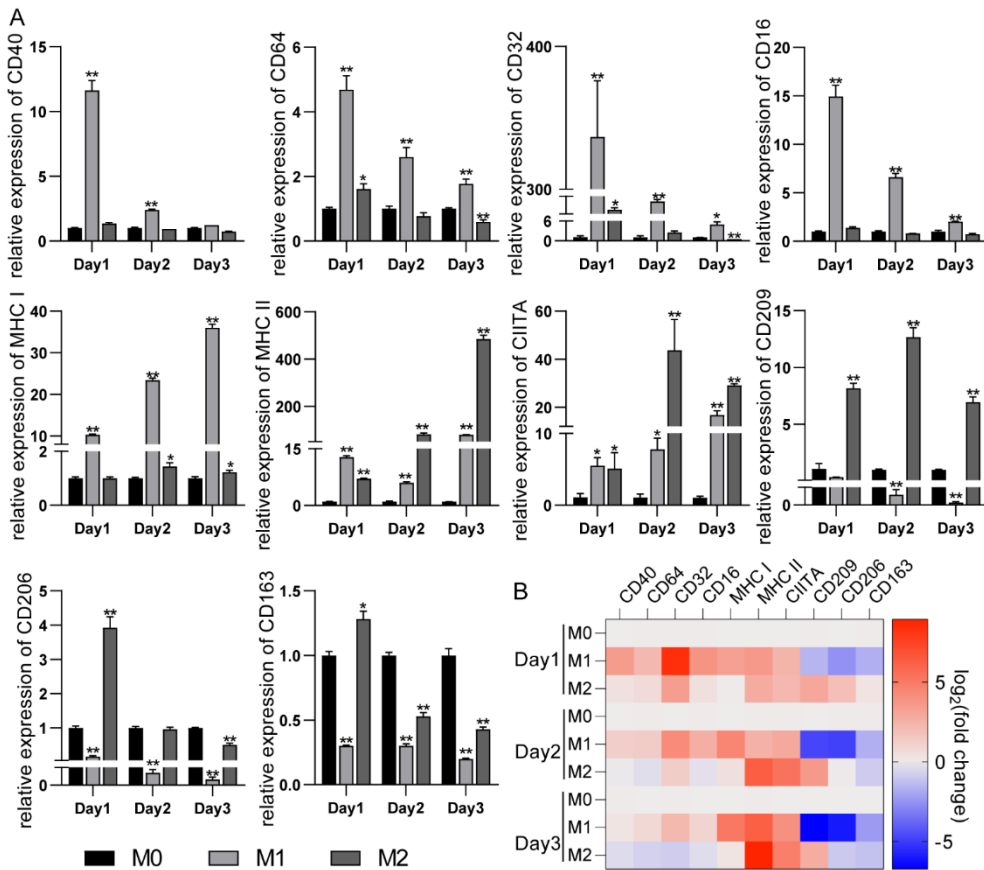


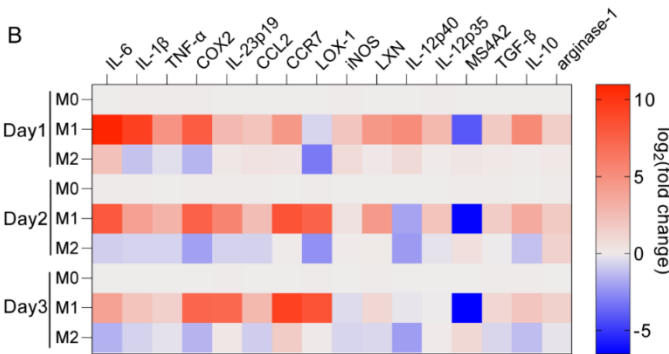
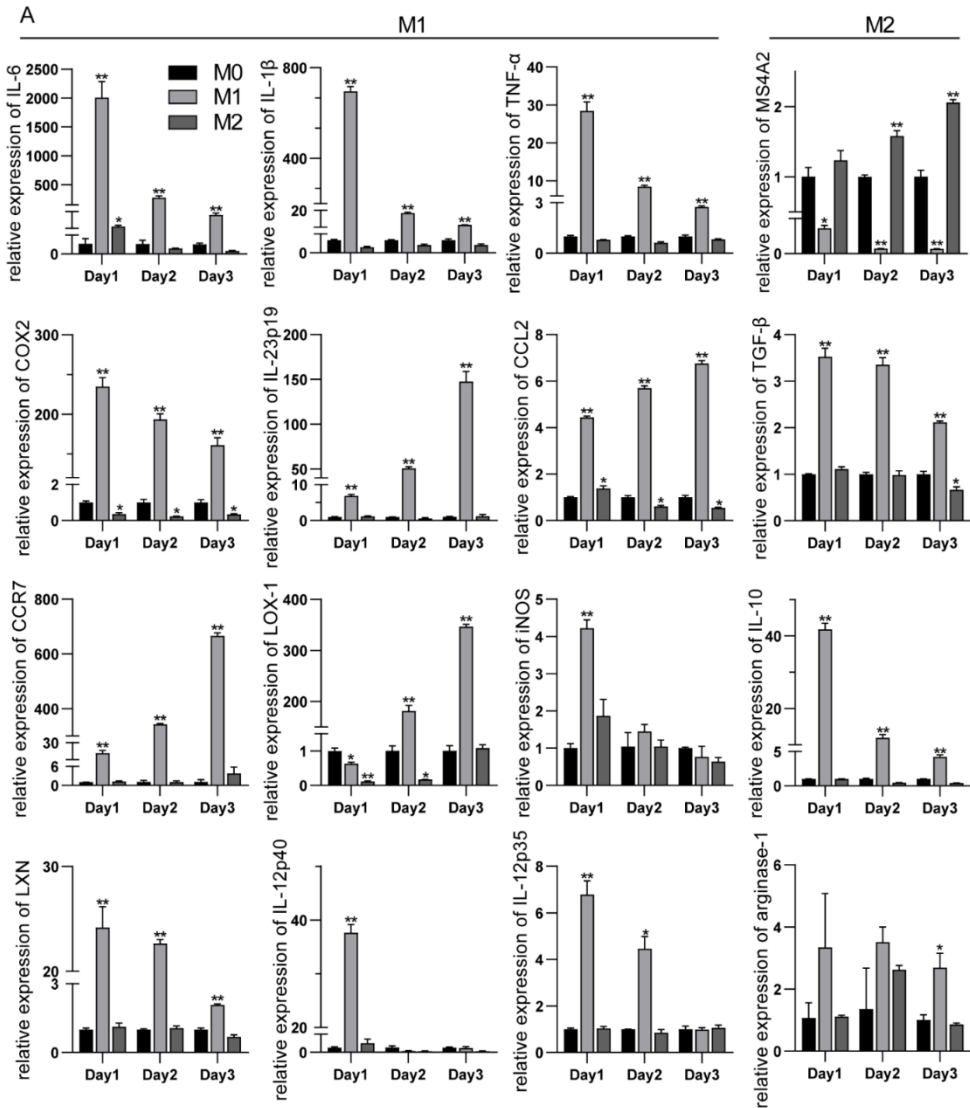
Figure 4 The relative expression of macrophage surface markers associated genes in O30D-derived macrophages. Total mRNA was isolated from M0-, M1-, and M2-polarized macrophages at day 1, day 2 and day 3. **(A)** Subsequently, qPCR was performed on M0, M1 and M2 macrophages to determine the expression surface marker genes, including CD40, CD64, CD32, CD16, MHC I, MHC II, CIITA, CD209, CD206 and CD163. M0 macrophages were used as control. The results were

expressed as relative expression normalized by housekeeping genes RPS19 and GAPDH. **(B)** An overview of gene expression was shown in a heatmap. The color scale of heatmap was shown as $\log_2(\text{fold change})$. MHC I: dog major histocompatibility complex, class I; MHC II: dog major histocompatibility complex, class II; CIITA: class II major histocompatibility complex transactivator. Data are presented as mean \pm SD, with $n \geq 3$ per condition. * $p < 0.05$; ** $p < 0.01$.

Characterization of cytokine and chemokine gene expression in 030D-derived macrophages

To further draw out the characteristics of canine 030D-derived macrophages, we measured the mRNA levels of cytokines and chemokines associated with the activation states of M1 or M2 macrophages. As shown in Figure 5, compared to M0- and M2-polarized macrophages, M1-polarized macrophages strongly expressed M1 marker genes, IL-6, IL-1 β , TNF- α , COX2, iNOS, IL-12p35 and IL-12p40 at day 1 ($p < 0.01$), which gradually declined at day 2 and 3 (Figure 5). The same set of genes was not upregulated in M2-polarized macrophages at the same time point. Other M1 marker genes, IL-23p19, CCL2 and CCR7 were observed to be highly expressed in M1-polarized macrophages at day 1 ($p < 0.01$), and were further upregulated in the following days (Figure 5). The lectin-like oxidized low-density lipoprotein receptor-1 (LOX-1) and Latexin (LXN) are newly proposed M1 markers, which were included in our study (13, 33). Consistent with previous studies (13, 33), the expression levels of both LOX-1 and LXN in M1-polarized macrophages were significantly higher than those in M0- and M2-polarized macrophages. In contrast, as a newly proposed M2 marker (13), Membrane Spanning 4-Domains A2 (MS4A2) expression was significantly upregulated in M2-polarized macrophages and downregulated in M1-polarized macrophages compared to M0 macrophages. Interestingly, other M2 marker genes, TGF- β , IL-10 and arginase-1 were shown to be expressed at a higher level in M1- but not M2-polarized macrophages in our study.

Characterization of canine monocyte-like cell line derived macrophages



6

Figure 5 The expression profile of cytokines and chemokines in 030D-derived macrophages. Canine 030D-derived M0, M1 and M2 macrophages were collected at day 1, day 2 and day 3. Total mRNA was isolated and reverse-transcribed into cDNA. **(A)** Cytokines and chemokines associated with M1 or M2 activation states were determined by qPCR. M0 macrophages were used as control. The results are expressed as relative expression normalized by housekeeping genes RPS19 and GAPDH. **(B)** An overview of the expression level of cytokines and chemokines is shown in a heatmap. The color scale of heatmap is shown as $\log_2(\text{fold change})$. iNOS: inducible nitric oxide synthase; MS4A2: Membrane Spanning 4-Domains A2; LOX-1: the lectin-like oxidized low-density lipoprotein receptor-1; LXN: Latexin. Data are presented as mean \pm SD, with $n \geq 3$ per condition. * $p < 0.05$; ** $p < 0.01$.

Canine 030D-derived macrophages show higher non-specific phagocytosis

Phagocytosis is an important functional characteristic of macrophages. To further characterize the functional properties of canine 030D-derived M0, M1 and M2 macrophages, we assessed the non-specific phagocytic capacity by culturing 030D-derived macrophages with latex beads. As illustrated in Figure 6, a substantial amount of fluorescent beads were engulfed by 030D-derived macrophages with different polarization states (M0, M1 and M2) at day 1, 2 and 3. In comparison to M0- and M2-polarized macrophages, both the percentage of phagocytic cells and MFI in the M1 macrophage population were significantly higher ($p < 0.01$) on each day, indicating the M1 cells displayed the highest phagocytotic capability (Figure 6A, B and C). Compared to day 1 and 3, both M0- and M1-polarized macrophages showed a greater bead uptake at day 2 (Figure 6A, B and C). Within the M2 population, the proportion of phagocytic cells gradually decreased from day 1 to day 3 (Figure 6A), whereas the MFI and fold change of phagocytic M2 macrophages increased (Figure 6 Band C), indicating that the number of beads taken up per M2 macrophage was increased. Compared to bead uptake by M0 macrophages at day 1, all M0-, M1- and M2-polarized macrophages engulfed a significantly higher number of beads at day 2 and day 3, indicating an elevated phagocytic capability. As expected, control 030D-derived macrophages incubated with beads at 4 °C failed to engulf beads (data not shown). The uptake of fluorescent beads by M0-, M1- and M2-polarized macrophages at day 1, 2 and 3 was further confirmed by plasma membrane staining, which showed that the beads were inside the cell membrane (Figure 4D, Supplementary Figure S3 and Video 1, 2 and 3).

Characterization of canine monocyte-like cell line derived macrophages

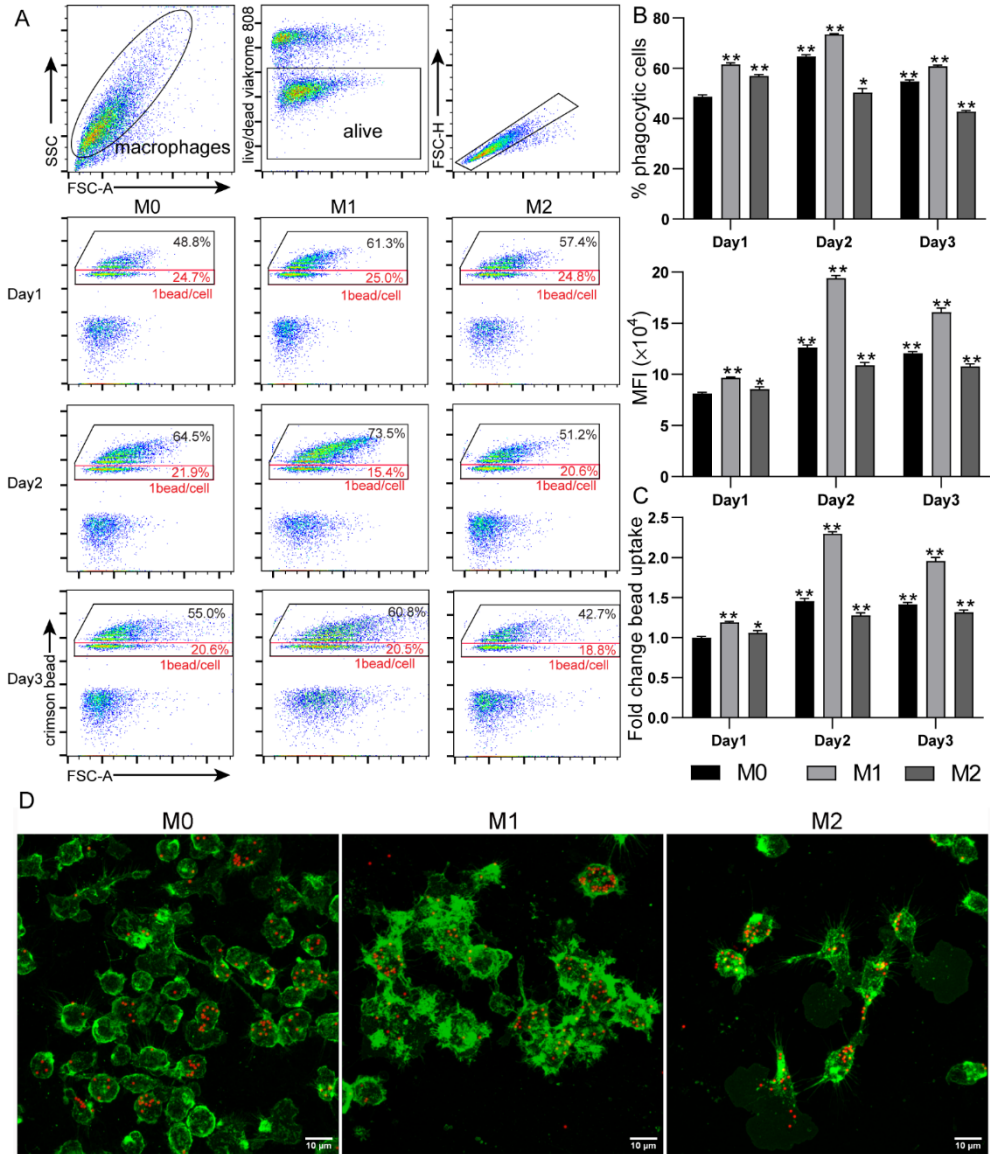


Figure 6 Phagocytosis of canine 030D-derived M0, M1 and M2 macrophages. 030D macrophages were polarized for 1, 2 and 3 days respectively as described in *materials and methods*, followed by incubating with crimson carboxylate-modified FluoSpheres fluorescent beads for 4 h. Flow cytometry analysis was performed to quantify beads uptake. **(A)** Live cells were selected for further analysis after gating for scatter profile (FSC/SSC), viability (viakrome) and singlets. Representative dot plots of a single experiment on each day was shown. Cells with 1 bead/cell were

gated with a red square and cells with multiple beads were gated with a black square, from which the average bead uptake was calculated. **(B)** Cells containing beads were present as the percentage of phagocytic cells and median fluorescent intensity (MFI). **(C)** The fold change of M1- and M2-polarized macrophages in bead uptake was evaluated in comparison to M0 macrophages. **(D)** To further confirm phagocytosis by 030D-derived macrophages, phagocytic cells were visualized in green for plasma membrane staining with wheat germ agglutinin (WGA) and in red for with FluoSpheres fluorescent beads. Representative images are shown as 2 days polarized 030D-derived M0, M1 and M2 macrophages. A reconstructed 3-D model was made based on z-stack to show relative spatial position of fluorescent beads and 030D-derived macrophages (see Supplementary materials Video S2A, B and C). Data are presented as mean \pm SD, with $n \geq 3$ per condition. * $p < 0.05$; ** $p < 0.01$. Scale bar=10 μm .

Discussion

Monocyte-like cell lines have been widely used as surrogates of monocytes to study macrophage biology. Well-characterized macrophage cell lines from different origins are powerful tools for functional and translational studies, for example THP-1, HL-60 and U-937 cells for research on human (14), RAW264.7 and J774.1 cell for research on mouse (34, 35), and HD11 cell for research on chicken macrophages (21). However, an appropriate macrophage cell line for canine is still lacking. Therefore, the aim of this study was to evaluate a macrophage cell line from canine origin as an in vitro model for macrophage polarization. To this end, we first develop a protocol for canine macrophage differentiation from an established canine macrophage cell line, the 030D cell-line. We further comprehensively characterized 030D-derived M0, M1 and M2 macrophages, including cell morphology, phenotypic characteristics, marker gene expression and functional properties. Our results showed that 030D-derived M1 and M2 macrophages showed striking morphological differences, distinct phenotypes and gene expression profiles, and distinguishable phagocytic capacity.

Morphologically, 030D-derived M1 macrophages appeared to obtain a bigger, roundish, and amoeboid shape, showing as “fried-egg” morphology, whereas a low amount of M2 macrophages adopted an elongated morphology. M0 macrophages did not show obvious morphology changes. These findings parallel the observations in other species such as humans, mouse and pig (36-38). However, compared to another well-characterized canine macrophage cell line, DH82 cell, there is no significant morphological difference between DH82-derived M1 and M2 macrophages (39), both of which developed a round, amoeboid and large/flat morphology (39, 40). A flattened, elongated and spindle-like morphology was only observed in the late passages of DH82 cells (passage ≥ 66) (40). This morphology

change present in DH82 cells may be caused by gene loss and functional impairment due to continuous subculturing. Moreover, flow cytometry analysis showed that 030D-derived M1 macrophages were bigger and more granular than M0- and M2-polarized macrophages. This feature obtained by 030D-derived M1 macrophages was also found in porcine and human bone marrow derived macrophages (36). Besides, canine monocyte-derived dendritic cells also gave rise to granular cells (41).

Pan-macrophage markers are widely used to define macrophages (42). So far, several macrophage surface antigens have been validated as pan-macrophage markers including CD14, CD11b, CD68 and F4/80 (known as EGF-like module-containing mucin-like hormone receptor-like 1) (22-24, 43, 44). In our study, CD14 and CD11b were determined. CD14 and CD11b were ubiquitously expressed in 030D-derived M0, M1 and M2 macrophages, which confirmed their macrophage-like properties. Macrophage-colony stimulating factor receptor (CD115) has been proven to play a dominant role in the development of the monocytes/macrophage phagocytotic system (MPS) (25). The expression of CD115 is associated with macrophage differentiation (45). Here, it was found that CD115 expression in 030D-derived M1 macrophages was significantly down-regulated, while 030D-derived M0 and M2 macrophages showed a comparable level of CD115 following polarization. This finding suggested that CD115 might be a potential maker to distinguish M1 and M2 macrophages in canine. Mer tyrosine kinase receptor (MerTK) is another cell surface protein widely expressed by macrophages, which is related to phagocytosis of macrophages (46, 47). Similarly, MerTK was expressed by all polarization states of 030D-derived macrophages, indicating MerTK might be a potential pan-macrophage marker.

Polarization states of macrophages have been shown to be distinguished by the differential expression of surface makers in human and mouse studies (48, 49). CD32, CD40, CD80, CD86 and MHC II were shown to be highly expressed by M1 macrophages, whereas CD163 (scavenger receptor), CD206 (mannose receptor), CD209 (DC-SIGN) were indicated to be specific for M2 macrophages (50-52). Our findings show that 030D-derived M1 macrophages upregulated the expression of CD32, CD40, CD80, CD83, CD86 and MHC II, while 030D-derived M2 macrophages expressed a higher level of CD206 relative to M1 macrophages. Due to the lack of available surface marker antibodies for dog, more surface marker genes were assessed by qPCR. In accordance with previous results, CD40, CD32 and MHC II were highly expressed by 030D-derived M1 macrophages in mRNA level. Moreover, mRNA levels of CD64, CD16, MHC I were increased in M1 macrophages as well. As MHC II transactivator, the expression of CIITA has an expression trend similar to MHC II. Compared to M1 macrophages, the expression of M2 markers, CD209,

CD206 and CD163 were relatively high in M2 macrophages. Based on our present data, 030D-derived macrophages show a distinct phenotypic characteristic between M1 and M2 polarized states. Using the canine cell line DH82, it was previously shown that CD80, CD86 and MHC I were increased in M1 macrophages, which is in line with our results (39, 40). CD206 was expressed slightly higher in M2 than in M1 cells, but this difference was not significant (39). CD14 and MHC II were expressed by DH82 macrophages at a relatively low level (40).

Phenotypic M1 and M2 cells are usually associated with expression of a distinct set of cytokines and chemokines. M1 cells are involved in pro-inflammatory responses, and characterized by increased expression of pro-inflammatory cytokines and chemokines, such as IL-6, IL-1 β , TNF- α , IL-12, IL-23, COX2 and CCL2 (50, 51). M2 cells play an anti-inflammatory role by secreting IL-10 and TGF- β . As expected, 030D-derived M1 macrophages showed a highly upregulated pro-inflammatory cytokine and chemokine expression, including IL-6, IL-1 β , TNF- α , IL-12p35/40, IL-23p19, COX2, CCL2 and CCR7. Newly predicted M1 markers, LOX-1 and LXN, were confirmed as M1-specific in our study by showing enhanced expression in M1 macrophages (13, 33). Interestingly, the anti-inflammatory cytokines TGF- β and IL-10, were expressed at higher levels by M1 than M2 macrophages, but were considered as M2 marker in other studies (53, 54). Similarly, M2 marker arginase-1 was shown to exist at a higher level in M1 macrophages. However, a novel identified M2 marker, MS4A2, known as high affinity IgE Fc ϵ receptor β chain, was significantly upregulated in M2 macrophages relative to M1 macrophages (13). In agreement with studies for human monocyte-derived macrophages, M1 cells produced more IL-10 than M2 cells, indicating an overlap of cytokine profiles between M1 and M2 cells (55, 56). Furthermore, another study reported that macrophages found in the human skeletal muscle displayed a mixed M1/M2 phenotype by expressing CD11b, CD14, CD68, CD86 and CD206, highlighting a phenotype overlap (23). The presence of mixed M1/M2 features blur the boundaries of M1 and M2. Therefore, it is more reasonable to consider diverse polarization states of macrophages as a continuum with overlapping features, such as phenotypes and gene profile. In addition, a slightly higher level of iNOS was expressed by 030D-derived M1 cells. Nevertheless, nitric oxide (NO) production was not detected in any of the three polarization states (data not shown). In line with our studies, DH82 cells (canine macrophage cell line) do not produce nitric oxide after activation (57-59). We speculate that 030D-derived macrophages may produce an undetectable level of nitric oxide.

Macrophages in different activation states or from different origins have shown dramatically different functional properties, such as phagocytic capacity and NO production (11, 60, 61). Our study showed that all 030D-derived M0, M1 and M2 macrophages have the capacity to take up beads. This may be caused by the

expression of pan-macrophage markers, CD14 and MerTK, which are known to mediate phagocytosis (62, 63). 030D-derived M1 macrophages have a stronger phagocytic capacity than M0 and M2 macrophages. The phagocytic capacity of M0 and M2 is comparable. The stronger phagocytic capacity observed in M1 macrophages probably is caused by the administration of LPS, which is known to enhance phagocytosis in macrophages (64). Moreover, higher expression of CD64 (FcγRI), CD32 (FcγRII) and CD16 (FcγRIII) also contribute to enhanced phagocytosis, especially for FcγR-mediated phagocytosis (63, 65). Besides, increased expression of IL-10, TGF-β and chemokines also play crucial roles in phagocytosis (7, 66, 67). The scavenger receptor CD163, mannose receptor CD206 and C-type lectin receptor CD209 are also well-known receptors to facilitate phagocytosis for macrophages (68-71). However, increased phagocytic capacity was not observed in 030D-derived M2 macrophages. In agreement with our results, a lot of previous studies have demonstrated that M1 macrophages showed a higher level of phagocytic activity (60, 72, 73). On the contrary, a large number of studies have shown that M2 macrophages displayed a higher phagocytosis capacity than M1 macrophages (65, 74, 75). We speculate that the paradox of phagocytosis in M1 and M2 macrophages is probably associated with the differential expression of phagocytosis related molecules or different activation states.

In conclusion, this study successfully developed a polarization protocol for canine macrophage cell line 030D cells, which were comprehensively characterized for the first time. 030D-derived M0, M1 and M2 macrophages displayed distinct differences in multiple aspects, including morphology, phenotypic profiles, gene expression profiles and functional properties. As discussed above, this study found that 030D-derived M1 and M2 macrophages showed many similarities to M1 and M2 macrophages derived from other species, such as human, mouse, pig and ovine. As a cell model for macrophages, the 030D-derived macrophage can be a powerful tool for canine immunological studies.

Table 1. list of antibodies used for flow cytometry

Antigen	Target species	Clone	Isotype	Dilution	Source
CD14, vioblue	Mouse anti-human	TÜK4	Mouse IgG2a κ	1:100	Miltenyi Biotec
CD11b, biotin	Mouse anti-dog	CA16.3E10	Mouse IgG1	1:100	P. Moore
CD32B+CD32 A biotin	Mouse anti-human	AT10	Mouse IgG1	1:50	Abcam
CD40, R-PE	Mouse anti-human	LOB7/6	Mouse IgG2a	1:25	BIO-RAD
CD80, FITC	Hamster anti-mouse	16-10A1	Hamster IgG2	1:100	BD Biosciences
CD86, unconjugated	Mouse anti-dog	CA24.3E4	Mouse IgG1	1:50	P. Moore
CD83, APC	Mouse anti-human	HB15e	Mouse IgG1, κ	1:50	Biologend
CD206, APC/Cyanine7	Mouse anti-human	15-2	Mouse IgG1, κ	1:50	Biologend
MHC II, APC	Rat anti-canine	YKIX334.2	Rat IgG2a, κ	1:50	eBioscience™
GaM-IgG1- PerCP	Mouse IgG	-	IgG	1:100	Santa Cruz Biotechnology
streptavidin PE	-	-	-	1:2000	BD Biosciences

Peter Moore, university of Davis, CA, USA

Table 2. Sequences of primers used for quantitative real-time PCR

Gene	Forward primer (5'-3')	Reverse primer (5'-3')	Accession number	Product length (bp)
RPS19	CCTTCCTCAAAAAGTCT GGG	GTTCTCATCGTAGGGAGC AAG	DR103251.1	95
TGF- β	CAAGGATCTGGGCTGG AGTGGA	CCAGGACCTTGCTGTACT GCGTGT	(76)	(76)
TNF- α	CCCCGGGCTCCAGAAG GTG	GCAGCAGGCAGAAGAGT GTGGTG	(77)	(77)
IL-10	CCCGGGCTGAGAACCA CGAC	AAATGCGCTCTTCACCTG CTCCAC	(77)	(77)
IL-1 β	TCTCCCACCAGCTCTGT AACAA	GCAGGGCTTCTTCAGCTT CTC	Z70047	80
IL-6	TCCTGGTGATGGCTACT GCTT	GACTATTTGAAGTGGCAT CATCCTT	U12234	78
GAPDH	CTGAACGGGAAGCTCAC TGG	CGATGCCTGCTTCACTAC CT	AB038240.1	129
Arginase- 1	GCATGAGTTCCACGGCA AAA	CTTTTTCCACCCCTCCTC GT	XM_532053.6	81
iNOS	AATGGAGAGTTGGGCCT TCC	TGGCCCTTAAGAGAAGAC TGG	NM_001313848. 1	227

Characterization of canine monocyte-like cell line derived macrophages

IL-12p40	CAGCAGAGAGGGTCAG AGTGG	ACGACCTCGATGGGTAGG C	AF244915	109
IL-23p19	CAAGGGGAGAAAAACAG CAG	TGCTGTCCGTTCTGTGAG TC	XM_538231	78
CCL2	CCTGCTGCTATACTC A	GCTTCTTTGGGACACTTG	U29653	91
CCR7	TGGTGGTGGCTCTCCTT GTC	AAGTTCCGCACGTCTTTC TTG	XM 548131.2	136
IL-12p35	GTGCCTCAACCACTCCC AA	CAATCTCTTCGGAAGTGC AGG	NM_001003293	100
COX2	TTCCAGACGAGCAGGCT AAT	GCAGCTCTGGGTCAA TC	(77)	112
CD40	GTCTGCCTGCATCCGAA AGGT	GTCCTCCACAGGGTCCTG ATA	NM_001002982. 1	70
MHC II	GATGCTGAGTGAATCG GGG	TGAAGTCCAGAGTGTCCC TTCT	NM_001014768. 1	99
MERTK	GTTCAAGTCCACAACGC GAC	GCAAAATCTACCCAGCCG TG	XM_038691411. 1	119
CD206	TACCCCTCGTCTCCAT CAG	AAATTGCCTAGTGTCAA CAGC	XM_005617093. 4	121
LXN	CAGGGTCAAGCAAGTGC AAAG	CTTCCTTTGGCAGACGGG TA	XM_038432753. 1	164
MS4A2	CTCCCCACCACCCACTT ATG	AACTCAGCTCTCAACCAG CC	XM_038429453. 1	173
CD209	GTGTGACCCCAAGGAGCT C	TGGCGAATCCTGGAGACT TG	NM_001130832. 1	207
LOX-1	CCCAGGAGTCAGAAAGGT GAAC	CCTGGGGACAATGACCT GAA	XM_038439023. 1	157
CD163	ATGTCCAGTGTCCAAAA GGA	CATGTGATCCAGGTCTCC TC	(78)	(78)
CD115	TGCAGTTTGGGAAGACT CTC	TGTGGACTTCAGCATCTT CA	(78)	(78)
CIITA	GCCAAGACTTCTCCCTG GAC	ACAAGGACCGGGCTGAAA TG	XM_014114624. 3	103
CD64	AACAGACCCCGTAAAGG CAG	ATCTGGGGTCAAGGTCT GA	NM_001002976. 2	161
CD32	TTCCAGAAGGGGGAGTCT CAT	TCAGTGACATTGGCTTGG ACA	XM_025420853. 2	236
CD16	CCAGCAGCAACAAGTGA ACA	GTTGATGGAAGCGAAGAA CCTTG	XM_038448606. 1	116
MHC I	CCATCAAGGAGACCGCA CAGA	AACCGTACATGGTCTGGA TGG	LC462830.1	105

MS4A2: Membrane Spanning 4-Domains A2; LOX-1: the lectin-like oxidized low-density lipoprotein receptor-1; LXN: Latexin.

AUTHOR CONTRIBUTIONS

ACKNOWLEDGEMENTS

The authors thank China Scholarship Council (CSC) for offering scholarship. All fluorescent microscopy images have been acquired at the Center of Cellular Imaging, Faculty of Veterinary Medicine, Utrecht University. All the flow cytometry data were collected using the Flow Cytometry and Cell Sorting Facility at the department of Infectious Diseases & Immunology in Utrecht University.

FUNDING

This research received no external funding

CONFLICTS OF INTEREST

The authors declare no conflict of interest.

Supplementary materials

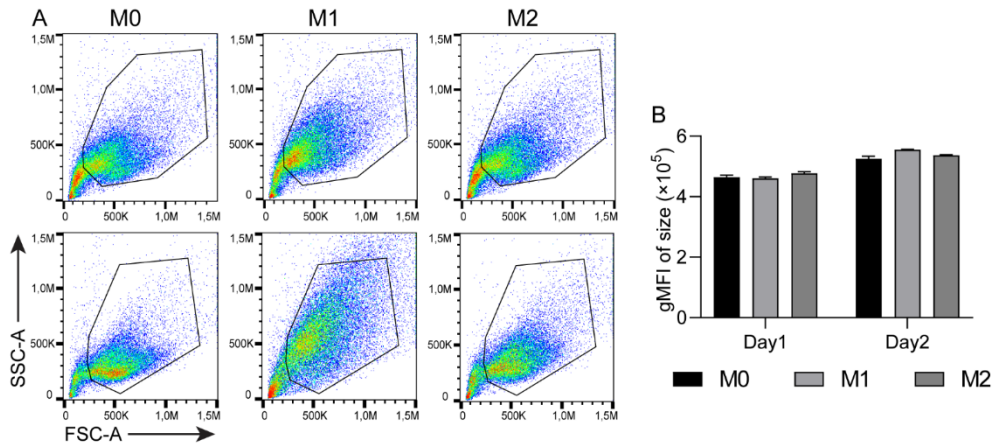


Figure S1 Comparison of size between M0, M1 and M2 macrophages at day 1 and day 2. Polarized macrophages at day 1 and 2 were subjected to flow cytometry analysis. Comparison of size between M0, M1 and M2 macrophages at day 1 and 2 was evaluated based on forward scatter (FSC). Representative flow cytometry plots are shown in (A), and geometric mean (gMFI) FSC values of M0, M1 and M2 macrophages are shown in (B). Data are presented as mean \pm SD, with $n \geq 3$ per condition. * $p < 0.05$; ** $p < 0.01$. gMFI: geometric mean of fluorescence intensity, SSC: side scatter, FSC: forward scatter.

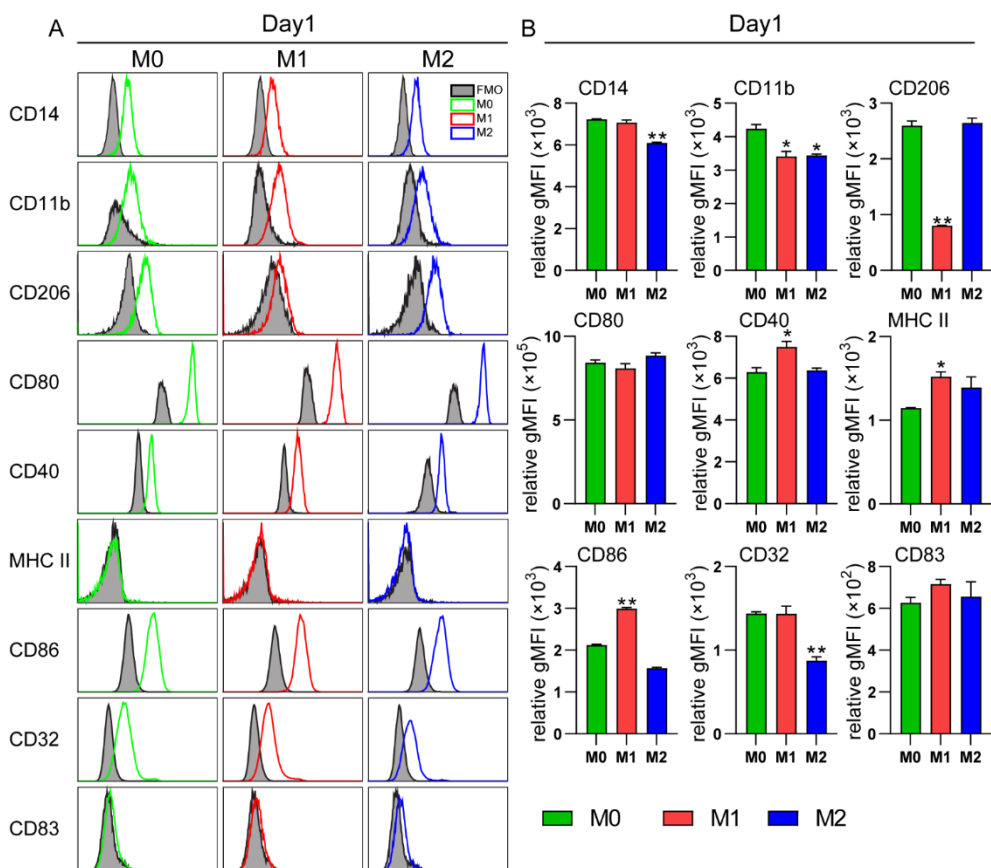


Figure S2 Cell surface marker expressed on 030D-derived macrophages at day1. Canine 030D cells were polarized with IFN- γ + LPS (M1) or IL-4 (M2) for 3 days. Polarized cells were harvested at day 1 for the detection of macrophage surface markers expression using flow cytometry. **(A)** Expression levels of a set of surface markers are presented by representative histograms for M0, M1 and M2 cells at day 1. Filled gray histograms represent Fluorescence Minus One (FMO) Controls to show the background fluorescence. **(B)** Relative expression levels of all surface markers are expressed as the geometric mean fluorescent intensity (gMFI) for three independent replicates. Shown is the mean of the geometric fluorescence intensity (gMFI) subtracted by gMFI of FMO. Data are presented as mean \pm SD, with $n \geq 3$ per condition. * $p < 0.05$; ** $p < 0.01$. gMFI: geometric mean of fluorescence intensity.

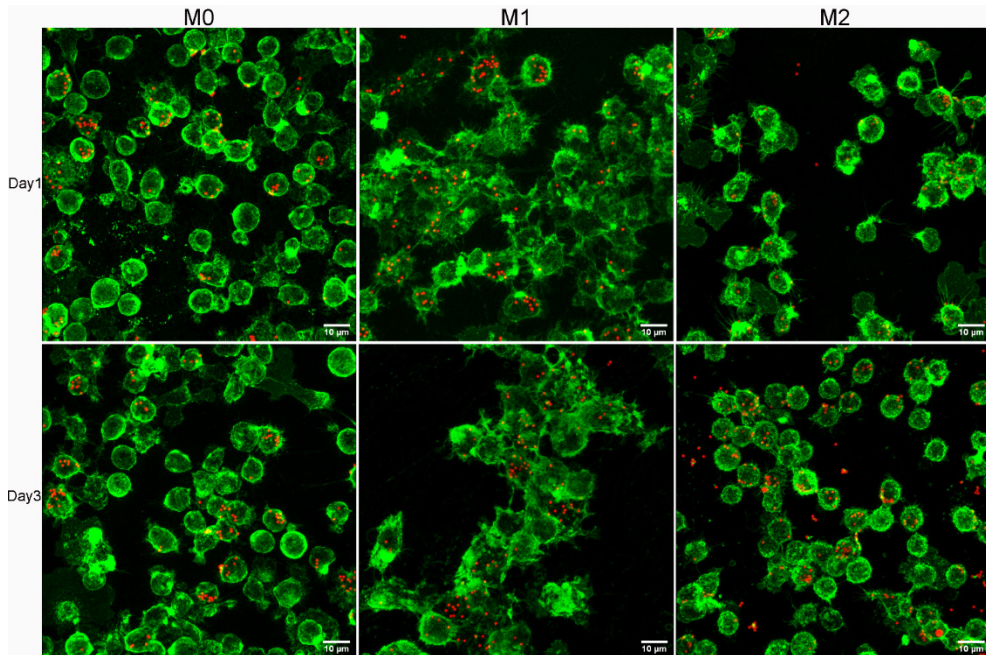


Figure S3 Phagocytosis of canine 030D-derived M0, M1 and M2 macrophages at day 1 and 2. 030D macrophages were polarized for 1, 2 and 3 days respectively as described in materials and methods, followed by incubating with crimson carboxylate-modified FluoSpheres fluorescent beads for 4 h. Phagocytosis by 030D-derived macrophages was confirmed by confocal microscopy. Phagocytic cells were visualized in green for plasma membrane staining with wheat germ agglutinin (WGA) and in red for with FluoSpheres fluorescent beads. Representative images are shown as 1 and 3 days polarized 030D-derived M0, M1 and M2 macrophages. A reconstructed 3-D model was made based on z-stack to show relative spatial position of fluorescent beads and 030D-derived macrophages (see Supplementary materials **Video S1A, B and C** for day 1, and **Video S3A, B and C** for day 3). Scale bar=10 μm.

References

1. Hirayama D, Iida T, Nakase H. The Phagocytic Function of Macrophage-Enforcing Innate Immunity and Tissue Homeostasis. *International Journal of Molecular Sciences* (2018) 19(1):92. doi: 10.3390/ijms19010092.
2. Ito T, Connett JM, Kunkel SL, Matsukawa A. The linkage of innate and adaptive immune response during granulomatous development. *Front Immunol* (2013) 4:10. Epub 2013/02/07. doi: 10.3389/fimmu.2013.00010.
3. Murray PJ, Wynn TA. Protective and pathogenic functions of macrophage subsets. *Nat Rev Immunol* (2011) 11(11):723-37. Epub 2011/10/15. doi: 10.1038/nri3073.
4. Mills CD, Kincaid K, Alt JM, Heilman MJ, Hill AM. M-1/M-2 macrophages and the Th1/Th2 paradigm. *J Immunol* (2000) 164(12):6166-73. Epub 2000/06/08. doi: 10.4049/jimmunol.164.12.6166.
5. Munder M, Eichmann K, Morán JM, Centeno F, Soler G, Modolell M. Th1/Th2-regulated expression of arginase isoforms in murine macrophages and dendritic cells. *J Immunol* (1999) 163(7):3771-7. Epub 1999/09/22.
6. Shapouri-Moghaddam A, Mohammadian S, Vazini H, Taghadosi M, Esmaeili SA, Mardani F, et al. Macrophage plasticity, polarization, and function in health and disease. *J Cell Physiol* (2018) 233(9):6425-40. Epub 2018/01/11. doi: 10.1002/jcp.26429.
7. Yao Y, Xu XH, Jin L. Macrophage Polarization in Physiological and Pathological Pregnancy. *Front Immunol* (2019) 10:792. Epub 2019/05/01. doi: 10.3389/fimmu.2019.00792.
8. Abdelaziz MH, Abdelwahab SF, Wan J, Cai W, Huixuan W, Jianjun C, et al. Alternatively activated macrophages; a double-edged sword in allergic asthma. *J Transl Med* (2020) 18(1):58. Epub 2020/02/07. doi: 10.1186/s12967-020-02251-w.
9. Jiang Z, Zhu L. Update on the role of alternatively activated macrophages in asthma. *J Asthma Allergy* (2016) 9:101-7. Epub 2016/06/29. doi: 10.2147/JAA.S104508.
10. Yao Y, Xu X-H, Jin L. Macrophage polarization in physiological and pathological pregnancy. *Frontiers in immunology* (2019) 10:792.
11. Wang C, Yu X, Cao Q, Wang Y, Zheng G, Tan TK, et al. Characterization of murine macrophages from bone marrow, spleen and peritoneum. *BMC Immunol* (2013) 14(1):6. Epub 2013/02/07. doi: 10.1186/1471-2172-14-6.
12. Tedesco S, Bolego C, Toniolo A, Nassi A, Fadini GP, Locati M, et al. Phenotypic activation and pharmacological outcomes of spontaneously differentiated human monocyte-derived macrophages. *Immunobiology* (2015) 220(5):545-54. Epub 2015/01/15. doi: 10.1016/j.imbio.2014.12.008.
13. Heinrich F, Lehmbecker A, Raddatz BB, Kegler K, Tipold A, Stein VM, et al. Morphologic, phenotypic, and transcriptomic characterization of classically and alternatively activated canine blood-derived macrophages in vitro. *PLoS One* (2017) 12(8):e0183572. Epub 2017/08/18. doi: 10.1371/journal.pone.0183572.
14. Riddy DM, Goy E, Delerive P, Summers RJ, Sexton PM, Langmead CJ. Comparative genotypic and phenotypic analysis of human peripheral blood monocytes and surrogate monocyte-like cell lines commonly used in

- metabolic disease research. *PLoS One* (2018) 13(5):e0197177. Epub 2018/05/11. doi: 10.1371/journal.pone.0197177.
15. Kaur G, Dufour JM. Cell lines: Valuable tools or useless artifacts. *Spermatogenesis* (2012) 2(1):1-5. Epub 2012/05/04. doi: 10.4161/spmg.19885.
 16. Gebhard D, Levy M, Ley D, editors. Isolation and characterization of functionally and phenotypically distinct continuous monocytoid cell lines from a canine malignant histiocytosis. *Proceedings of the Fourth International Veterinary Immunology Symposium, Davis, CA, USA; 1995.*
 17. Lyu Q, Wawrzyniuk M, Rutten V, van Eden W, Sijts A, Broere F. Hsp70 and NF-κB Mediated Control of Innate Inflammatory Responses in a Canine Macrophage Cell Line. *Int J Mol Sci* (2020) 21(18):6464. Epub 2020/09/10. doi: 10.3390/ijms21186464.
 18. Pinelli E, Gebhard D, Mommaas AM, van Hoeij M, Langermans JA, Ruitenbergh EJ, et al. Infection of a canine macrophage cell line with leishmania infantum: determination of nitric oxide production and anti-leishmanial activity. *Vet Parasitol* (2000) 92(3):181-9. Epub 2000/08/30. doi: 10.1016/s0304-4017(00)00312-5.
 19. Rougier S, Vouldoukis I, Fournel S, Pérès S, Woehrlé F. Efficacy of different treatment regimens of marbofloxacin in canine visceral leishmaniosis: a pilot study. *Vet Parasitol* (2008) 153(3-4):244-54. Epub 2008/03/14. doi: 10.1016/j.vetpar.2008.01.041.
 20. Looringh van Beeck FA, Zajonc DM, Moore PF, Schlotter YM, Broere F, Rutten VP, et al. Two canine CD1a proteins are differentially expressed in skin. *Immunogenetics* (2008) 60(6):315-24. Epub 2008/05/20. doi: 10.1007/s00251-008-0297-z.
 21. van den Biggelaar RH, van Eden W, Rutten VP, Jansen CA. Nitric Oxide Production and Fc Receptor-Mediated Phagocytosis as Functional Readouts of Macrophage Activity upon Stimulation with Inactivated Poultry Vaccines In Vitro. *Vaccines (Basel)* (2020) 8(2). Epub 2020/06/26. doi: 10.3390/vaccines8020332.
 22. Frafjord A, Skarshaug R, Hammarstrom C, Stankovic B, Dorg LT, Aamodt H, et al. Antibody combinations for optimized staining of macrophages in human lung tumours. *Scand J Immunol* (2020) 92(1):e12889. Epub 2020/04/17. doi: 10.1111/sji.12889.
 23. Kosmac K, Peck BD, Walton RG, Mula J, Kern PA, Bamman MM, et al. Immunohistochemical Identification of Human Skeletal Muscle Macrophages. *Bio Protoc* (2018) 8(12). Epub 2018/08/28. doi: 10.21769/BioProtoc.2883.
 24. Cao X, van den Hil FE, Mummery CL, Orlova VV. Generation and Functional Characterization of Monocytes and Macrophages Derived from Human Induced Pluripotent Stem Cells. *Curr Protoc Stem Cell Biol* (2020) 52(1):e108. Epub 2020/03/12. doi: 10.1002/cpsc.108.
 25. Francke A, Herold J, Weinert S, Strasser RH, Braun-Dullaeus RC. Generation of Mature Murine Monocytes from Heterogeneous Bone Marrow and Description of Their Properties. *Journal of Histochemistry & Cytochemistry* (2011) 59(9):813-25. doi: 10.1369/0022155411416007.
 26. Dai XM, Ryan GR, Hapel AJ, Dominguez MG, Russell RG, Kapp S, et al. Targeted disruption of the mouse colony-stimulating factor 1 receptor gene results in osteopetrosis, mononuclear phagocyte deficiency, increased

- primitive progenitor cell frequencies, and reproductive defects. *Blood* (2002) 99(1):111-20. Epub 2002/01/05. doi: 10.1182/blood.v99.1.111.
27. Scott RS, McMahon EJ, Pop SM, Reap EA, Caricchio R, Cohen PL, et al. Phagocytosis and clearance of apoptotic cells is mediated by MER. *Nature* (2001) 411(6834):207-11. doi: 10.1038/35075603.
 28. Borgman KJE, Flórez-Grau G, Ricci MA, Manzo C, Lakadamyali M, Cambi A, et al. Membrane receptor MerTK is a newly identified transcriptional regulator that associates to chromatin as nanoclusters during human DC differentiation. *bioRxiv* (2020):2020.04.16.044974. doi: 10.1101/2020.04.16.044974.
 29. Hey YY, Tan JK, O'Neill HC. Redefining Myeloid Cell Subsets in Murine Spleen. *Front Immunol* (2015) 6:652. Epub 2016/01/23. doi: 10.3389/fimmu.2015.00652.
 30. Sasmono RT, Oceandy D, Pollard JW, Tong W, Pavli P, Wainwright BJ, et al. A macrophage colony-stimulating factor receptor-green fluorescent protein transgene is expressed throughout the mononuclear phagocyte system of the mouse. *Blood* (2003) 101(3):1155-63. doi: 10.1182/blood-2002-02-0569.
 31. Murray PJ, Allen JE, Biswas SK, Fisher EA, Gilroy DW, Goerdt S, et al. Macrophage activation and polarization: nomenclature and experimental guidelines. *Immunity* (2014) 41(1):14-20. Epub 2014/07/19. doi: 10.1016/j.immuni.2014.06.008.
 32. Röszer T. Understanding the Mysterious M2 Macrophage through Activation Markers and Effector Mechanisms. *Mediators Inflamm* (2015) 2015:816460. Epub 2015/06/20. doi: 10.1155/2015/816460.
 33. Chanput W, Mes JJ, Savelkoul HF, Wichers HJ. Characterization of polarized THP-1 macrophages and polarizing ability of LPS and food compounds. *Food Funct* (2013) 4(2):266-76. Epub 2012/11/09. doi: 10.1039/c2fo30156c.
 34. Morita H, He F, Fuse T, Ouwehand AC, Hashimoto H, Hosoda M, et al. Cytokine production by the murine macrophage cell line J774.1 after exposure to lactobacilli. *Biosci Biotechnol Biochem* (2002) 66(9):1963-6. Epub 2002/10/29. doi: 10.1271/bbb.66.1963.
 35. Taciak B, Bialasek M, Braniewska A, Sas Z, Sawicka P, Kiraga L, et al. Evaluation of phenotypic and functional stability of RAW 264.7 cell line through serial passages. *PLoS One* (2018) 13(6):e0198943. Epub 2018/06/12. doi: 10.1371/journal.pone.0198943.
 36. Gao J, Scheenstra MR, van Dijk A, Veldhuizen EJ, Haagsman HP. A new and efficient culture method for porcine bone marrow-derived M1-and M2-polarized macrophages. *Veterinary immunology and immunopathology* (2018) 200:7-15.
 37. Banete A, Achita P, Harding K, Mulder R, Basta S. Immortalized murine macrophage cell line as a model for macrophage polarization into classically activated M (IFN γ + LPS) or alternatively activated M (IL-4) macrophages. *J Clin Cell Immunol* (2015) 6(318.10):4172. doi: 10.4172/2155-9899.1000318.
 38. Shiratori H, Feinweber C, Luckhardt S, Linke B, Resch E, Geisslinger G, et al. THP-1 and human peripheral blood mononuclear cell-derived macrophages differ in their capacity to polarize in vitro. *Molecular Immunology* (2017) 88:58-68. doi: 10.1016/j.molimm.2017.05.027.
 39. Herrmann I, Gotovina J, Fazekas-Singer J, Fischer MB, Hufnagl K, Bianchini R, et al. Canine macrophages can like human macrophages be in vitro

- activated toward the M2a subtype relevant in allergy. *Developmental and Comparative Immunology* (2018) 82:118-27. doi: 10.1016/j.dci.2018.01.005.
40. Heinrich F, Contioso VB, Stein VM, Carlson R, Tipold A, Ulrich R, et al. Passage-dependent morphological and phenotypical changes of a canine histiocytic sarcoma cell line (DH82 cells). *Vet Immunol Immunopathol* (2015) 163(1-2):86-92. Epub 2014/12/24. doi: 10.1016/j.vetimm.2014.11.006.
 41. Gutzwiller MER, Moulin HR, Zurbriggen A, Roosje P, Summerfield A. Comparative analysis of canine monocyte- and bone-marrow-derived dendritic cells. *Veterinary Research* (2010) 41(4):40. doi: 10.1051/vetres/2010012.
 42. Raggi F, Blengio F, Eva A, Pende D, Varesio L, Bosco MC. Identification of CD300a as a new hypoxia-inducible gene and a regulator of CCL20 and VEGF production by human monocytes and macrophages. *Innate Immunity* (2014) 20(7):721-34. doi: 10.1177/1753425913507095.
 43. Bertani FR, Mozetic P, Fioramonti M, Iuliani M, Ribelli G, Pantano F, et al. Classification of M1/M2-polarized human macrophages by label-free hyperspectral reflectance confocal microscopy and multivariate analysis. *Sci Rep* (2017) 7(1):8965. Epub 2017/08/23. doi: 10.1038/s41598-017-08121-8.
 44. Antonios JK, Yao Z, Li C, Rao AJ, Goodman SB. Macrophage polarization in response to wear particles in vitro. *Cell Mol Immunol* (2013) 10(6):471-82. Epub 2013/09/10. doi: 10.1038/cmi.2013.39.
 45. Huang B, Pan PY, Li Q, Sato AI, Levy DE, Bromberg J, et al. Gr-1+CD115+ immature myeloid suppressor cells mediate the development of tumor-induced T regulatory cells and T-cell anergy in tumor-bearing host. *Cancer Res* (2006) 66(2):1123-31. Epub 2006/01/21. doi: 10.1158/0008-5472.CAN-05-1299.
 46. Gautier EL, Shay T, Miller J, Greter M, Jakubzick C, Ivanov S, et al. Gene-expression profiles and transcriptional regulatory pathways that underlie the identity and diversity of mouse tissue macrophages. *Nature Immunology* (2012) 13(11):1118-28. doi: 10.1038/ni.2419.
 47. Mohning MP, Thomas SM, Barthel L, Mould KJ, McCubbrey AL, Frasch SC, et al. Phagocytosis of microparticles by alveolar macrophages during acute lung injury requires MerTK. *Am J Physiol Lung Cell Mol Physiol* (2018) 314(1):L69-L82. Epub 2017/09/25. doi: 10.1152/ajplung.00058.2017.
 48. David S, Kroner A. Repertoire of microglial and macrophage responses after spinal cord injury. *Nat Rev Neurosci* (2011) 12(7):388-99. Epub 2011/06/16. doi: 10.1038/nrn3053.
 49. Kigerl KA, Gensel JC, Ankeny DP, Alexander JK, Donnelly DJ, Popovich PG. Identification of Two Distinct Macrophage Subsets with Divergent Effects Causing either Neurotoxicity or Regeneration in the Injured Mouse Spinal Cord. *Journal of Neuroscience* (2009) 29(43):13435-44. doi: 10.1523/Jneurosci.3257-09.2009.
 50. Sylvestre M, Crane CA, Pun SH. Progress on Modulating Tumor-Associated Macrophages with Biomaterials. *Adv Mater* (2020) 32(13):e1902007. Epub 2019/09/29. doi: 10.1002/adma.201902007.
 51. Rey-Giraud F, Hafner M, Ries CH. In Vitro Generation of Monocyte-Derived Macrophages under Serum-Free Conditions Improves Their Tumor Promoting Functions. *Plos One* (2012) 7(8):e42656. doi: 10.1371/journal.pone.0042656.
 52. Saha B, Bruneau JC, Kodys K, Szabo G. Alcohol-induced miR-27a regulates

- differentiation and M2 macrophage polarization of normal human monocytes. *J Immunol* (2015) 194(7):3079-87. Epub 2015/02/27. doi: 10.4049/jimmunol.1402190.
53. Martinez FO, Gordon S. The M1 and M2 paradigm of macrophage activation: time for reassessment. *F1000Prime Rep* (2014) 6:13. Epub 2014/03/29. doi: 10.12703/P6-13.
 54. Edwards JP, Zhang X, Frauwirth KA, Mosser DM. Biochemical and functional characterization of three activated macrophage populations. *J Leukoc Biol* (2006) 80(6):1298-307. Epub 2006/08/15. doi: 10.1189/jlb.0406249.
 55. Raggi F, Pelassa S, Pierobon D, Penco F, Gattorno M, Novelli F, et al. Regulation of Human Macrophage M1-M2 Polarization Balance by Hypoxia and the Triggering Receptor Expressed on Myeloid Cells-1. *Front Immunol* (2017) 8:1097. Epub 2017/09/25. doi: 10.3389/fimmu.2017.01097.
 56. Jaguin M, Houllbert N, Fardel O, Lecureur V. Polarization profiles of human M-CSF-generated macrophages and comparison of M1-markers in classically activated macrophages from GM-CSF and M-CSF origin. *Cell Immunol* (2013) 281(1):51-61. Epub 2013/03/05. doi: 10.1016/j.cellimm.2013.01.010.
 57. Mendonça PHB, da Rocha R, Moraes JBB, LaRocque-de-Freitas IF, Logullo J, Morrot A, et al. Canine Macrophage DH82 Cell Line As a Model to Study Susceptibility to *Trypanosoma cruzi* Infection. *Front Immunol* (2017) 8:604. Epub 2017/06/18. doi: 10.3389/fimmu.2017.00604.
 58. Wasserman J, Diese L, VanGundy Z, London C, Carson WE, Papenfuss TL. Suppression of canine myeloid cells by soluble factors from cultured canine tumor cells. *Vet Immunol Immunopathol* (2012) 145(1-2):420-30. Epub 2012/01/17. doi: 10.1016/j.vetimm.2011.12.018.
 59. Nadaes NR, Silva da Costa L, Santana RC, LaRocque-de-Freitas IF, Vivarini Ádc, Soares DC, et al. DH82 Canine and RAW264.7 Murine Macrophage Cell Lines Display Distinct Activation Profiles Upon Interaction With *Leishmania infantum* and *Leishmania amazonensis*. *Frontiers in Cellular and Infection Microbiology* (2020) 10(247). doi: 10.3389/fcimb.2020.00247.
 60. Tarique AA, Logan J, Thomas E, Holt PG, Sly PD, Fantino E. Phenotypic, functional, and plasticity features of classical and alternatively activated human macrophages. *Am J Respir Cell Mol Biol* (2015) 53(5):676-88. Epub 2015/04/15. doi: 10.1165/rcmb.2015-0012OC.
 61. van den Biggelaar RHGA, Arkesteijn GJA, Rutten VPMG, van Eden W, Jansen CA. In vitro Chicken Bone Marrow-Derived Dendritic Cells Comprise Subsets at Different States of Maturation. *Frontiers in Immunology* (2020) 11(141). doi: 10.3389/fimmu.2020.00141.
 62. Schlegel RA, Krahling S, Callahan MK, Williamson P. CD14 is a component of multiple recognition systems used by macrophages to phagocytose apoptotic lymphocytes. *Cell Death and Differentiation* (1999) 6(6):583-92. doi: 10.1038/sj.cdd.4400529.
 63. Zizzo G, Hilliard BA, Monestier M, Cohen PL. Efficient clearance of early apoptotic cells by human macrophages requires M2c polarization and MerTK induction. *J Immunol* (2012) 189(7):3508-20. Epub 2012/09/04. doi: 10.4049/jimmunol.1200662.
 64. Hess DJ, Henry-Stanley MJ, Bendel CM, Zhang B, Johnson MA, Wells CL. *Escherichia coli* and TNF-alpha modulate macrophage phagocytosis of *Candida glabrata*. *J Surg Res* (2009) 155(2):217-24. Epub 2009/06/02. doi:

- 10.1016/j.jss.2008.07.022.
65. Mendoza-Coronel E, Ortega E. Macrophage Polarization Modulates FcγR- and CD13-Mediated Phagocytosis and Reactive Oxygen Species Production, Independently of Receptor Membrane Expression. *Front Immunol* (2017) 8:303. Epub 2017/04/12. doi: 10.3389/fimmu.2017.00303.
 66. Aldo PB, Racicot K, Craviero V, Guller S, Romero R, Mor G. Trophoblast induces monocyte differentiation into CD14+/CD16+ macrophages. *Am J Reprod Immunol* (2014) 72(3):270-84. Epub 2014/07/06. doi: 10.1111/aji.12288.
 67. Chistiakov DA, Bobryshev YV, Nikiforov NG, Elizova NV, Sobenin IA, Orekhov AN. Macrophage phenotypic plasticity in atherosclerosis: The associated features and the peculiarities of the expression of inflammatory genes. *Int J Cardiol* (2015) 184:436-45. Epub 2015/03/11. doi: 10.1016/j.ijcard.2015.03.055.
 68. Kneidl J, Löffler B, Erat MC, Kalinka J, Peters G, Roth J, et al. Soluble CD163 promotes recognition, phagocytosis and killing of *Staphylococcus aureus* via binding of specific fibronectin peptides. *Cell Microbiol* (2012) 14(6):914-36. Epub 2012/02/09. doi: 10.1111/j.1462-5822.2012.01766.x.
 69. Schulz D, Severin Y, Zanotelli VRT, Bodenmiller B. In-Depth Characterization of Monocyte-Derived Macrophages using a Mass Cytometry-Based Phagocytosis Assay. *Scientific Reports* (2019) 9(1):1-12. doi: 10.1038/s41598-018-38127-9.
 70. Montoya D, Cruz D, Teles RM, Lee DJ, Ochoa MT, Krutzik SR, et al. Divergence of macrophage phagocytic and antimicrobial programs in leprosy. *Cell Host Microbe* (2009) 6(4):343-53. Epub 2009/10/20. doi: 10.1016/j.chom.2009.09.002.
 71. Teles RM, Krutzik SR, Ochoa MT, Oliveira RB, Sarno EN, Modlin RL. Interleukin-4 regulates the expression of CD209 and subsequent uptake of *Mycobacterium leprae* by Schwann cells in human leprosy. *Infect Immun* (2010) 78(11):4634-43. Epub 2010/08/18. doi: 10.1128/IAI.00454-10.
 72. Sica A, Mantovani A. Macrophage plasticity and polarization: in vivo veritas. *J Clin Invest* (2012) 122(3):787-95. Epub 2012/03/02. doi: 10.1172/JCI59643.
 73. Krzyszczyk P, Schloss R, Palmer A, Berthiaume F. The Role of Macrophages in Acute and Chronic Wound Healing and Interventions to Promote Pro-wound Healing Phenotypes. *Front Physiol* (2018) 9:419. Epub 2018/05/17. doi: 10.3389/fphys.2018.00419.
 74. Durafourt BA, Moore CS, Zammit DA, Johnson TA, Zaguia F, Guiot MC, et al. Comparison of polarization properties of human adult microglia and blood - derived macrophages. *Glia* (2012) 60(5):717-27.
 75. Leidi M, Gotti E, Bologna L, Miranda E, Rimoldi M, Sica A, et al. M2 Macrophages phagocytose Rituximab-Opsonized Leukemic Targets More Efficiently than M1 Cells In Vitro. *Journal of Immunology* (2009) 182(7):4415-22. doi: 10.4049/jimmunol.0713732.
 76. Wang YS, Chi KH, Chu RM. Cytokine profiles of canine monocyte-derived dendritic cells as a function of lipopolysaccharide- or tumor necrosis factor-α-induced maturation. *Veterinary Immunology and Immunopathology* (2007) 118(3-4):186-98. doi: 10.1016/j.vetimm.2007.05.010.
 77. Campos M, Kool MM, Daminet S, Ducatelle R, Rutteman G, Kooistra HS, et al. Upregulation of the PI3K/Akt pathway in the tumorigenesis of canine thyroid

- carcinoma. *J Vet Intern Med* (2014) 28(6):1814-23. Epub 2014/09/19. doi: 10.1111/jvim.12435.
78. Król M, Pawłowski KM, Majchrzak K, Gajewska M, Majewska A, Motyl T. Global gene expression profiles of canine macrophages and canine mammary cancer cells grown as a co-culture in vitro. *BMC Vet Res* (2012) 8:16. Epub 2012/02/23. doi: 10.1186/1746-6148-8-16.

7



General discussion

General discussion

Hsp70 has been considered as an immune target in many inflammatory diseases, such as in rheumatoid arthritis (1, 2). Hsp70 can promote the induction of Treg cells, and further boost the secretion of immunosuppressive cytokines like IL-10 and TGF- β (3). Therefore, Hsp70 mediated immunoregulation has been proposed as a way of therapy to regulate adaptive immunity through induction of Tregs. The role of Hsp70 in T cell-mediated diseases was reviewed in **chapter 2**.

Inducible Hsp70 has profound significance for both cell survival and the development of chronic inflammation, such as in the eye (4). Many eye diseases are associated with retinal pigment epithelium (RPE) degeneration (5). Previous studies have shown that upregulation of Hsp70 may ameliorate certain eye diseases and restore the function of RPE cells (6). In recent years, compounds from herb or approved drugs with low toxicity were shown to improve Hsp70 expression in RPE cells, and thereby to ameliorate eye diseases. Consequently, these results warrant a further exploration of these compounds as novel Hsp70 inducers or co-inducers.

Macrophages, a key member of innate immunity, are identified as one of the key drivers in immune disorders. Changes in macrophage function may disturb the balance between inflammation and resolution, which can be the main cause of chronic immune diseases, including uveitis (7). An increasing number of studies have shown that the induction of Hsp70 has impact on macrophage function by modulating inflammation related signaling pathways and cytokine production (8). Compared to other animals, dogs have a relatively high incidence of certain immunological diseases, such as rheumatoid arthritis and uveitis, that resemble the same condition in humans with respect to pathogenic etiology, clinical symptoms, and clinical responses. Thus, dogs provide a suitable model for studying immunological diseases affecting both species. Thus, understanding the role of Hsp70 in canine macrophages possesses the instructive significance for the corresponding human immune diseases.

Macrophages can be roughly classified into two groups, known as the classically activated macrophage (M1) and the alternatively activated macrophage (M2), which are present in different phases of inflammation or infection (1). Previous studies have shown that dysregulation of macrophage polarization is closely related to many immune diseases, such as autoimmune diseases, cancers, and chronic inflammatory diseases (2, 9, 10). However, despite representing an attractive animal model for immunological diseases, little is known about canine macrophages. Consequently, exploring the function of macrophages plays an important role in

studying the onset and progression of many diseases.

In this thesis, we identified a novel HSP co-inducer, leucinostatin, and investigated its enhancing effects on Hsp70 expression in arsenite-stressed dog retinal pigment epithelial cells. We also investigated the anti-inflammatory effect of Hsp70 in canine macrophages. Furthermore, we polarized both canine monocytes and O30D cells into M1 and M2 macrophages, and characterized the morphology, phenotypic properties, gene profiles, and functional properties of canine monocyte- and O30D-derived macrophages.

Hsp upregulation as therapeutic target in chronic inflammation

As mentioned above, Hsp70 plays a regulatory role in both the adaptive and innate immune system. In a previous study we showed that in mice after Hsp70 peptide B29 immunization Hsp70-specific Treg cells were induced, which had regulatory characteristics and ameliorated arthritis (11). As Treg cells have a wide range of immunosuppressive effects, theoretically, Hsp70-specific Treg cells may have a role in many T cell-mediated chronic inflammatory diseases. In **chapter 2**, we reviewed several T-cell driven autoimmune diseases such as rheumatoid arthritis and type I diabetes, and discussed the immunomodulatory effects of Hsp70 in current clinical trials and laboratory research, as well as the prospects of Hsp70 administration in other autoimmune diseases. We also pointed out that several eye diseases like uveitis and idiopathic retinal vasculitis, are Th1 or Th17 mediated diseases, which raises the possibility of regaining tolerance through the therapeutic induction of Hsp70 specific Treg cells. In **chapter 2**, we also discussed that not only exogenous Hsp70, but also the induction of endogenous Hsp70 is able to boost the frequency of Hsp70 specific Tregs (12). Since Hsp70 is upregulated in inflamed tissue, the application of a co-inducer may further increase Hsp70 abundance and lead to an enhanced Hsp70 specific Treg response, which may mitigate the progress of chronic diseases. This has been proven in a mouse arthritis model, in which the Hsp70 co-inducer carvacrol raised Hsp70 expression in the Peyer's patches and induced Hsp70 specific Tregs with CD4+CD25+Foxp3+ phenotype (13). These findings provided clues for our follow-up research on eye diseases.

Leucinostatin, a promising Hsp70 co-inducer in dog RPE cells

The retinal pigment epithelium (RPE) plays a central role in vision function; improper functioning of the RPE has been identified as the etiology of various eye diseases, such as age-related macular degeneration (AMD), retinal detachment, and uveitis. Although it would be ideal to perform studies in human RPE cells, it is difficult to obtain RPE cells from patients in the clinic. As an alternative, dog eyes share a lot

of similarities to human eyes in size, morphology and in density of photoreceptor distribution (14). In **chapter 3**, we successfully isolated and cultured dog RPE cells. In our culture, dog RPE cells exhibited typical RPE characterization, such as hexagonal morphology and pigmentation. Those characteristics are in line with the findings in human, mouse, rabbit, and pig (15-18). By testing the RPE specific marker, RPE65, we showed that the purity of our primary dog RPE cells reached approximately 95%. However, dog RPE cells changed their hexagonal morphology as well as decreased RPE65 expression and pigment production with an increasing number of passages, which was also observed in human and rat RPE cultures (19, 20). Those changes may be caused by epithelial-to-mesenchymal transition (EMT) of RPE in in vitro culture, by which epithelial cells change their phenotype into a mesenchymal phenotype (21). Unfortunately, little is known about EMT process.

The induction of Hsp70 has been proven to protect RPE cells, retinal ganglion cells and photoreceptors against degeneration (22, 23). It has been widely used in the clinic to treat eye diseases, such as by increasing the expression of Hsp70 in RPE cells via heating or laser irradiation (24, 25). Hsp70 co-inducers have a notable capacity to co-induce cellular Hsp70 expression in inflamed tissues or cells, but do not work on healthy tissues or cells (26). The utility of inducing Hsp70 expression by pharmacological agents (HSP co-inducers) is relatively safe and non-toxic. Therefore, identification of novel Hsp70 co-inducing compounds with enhanced potencies can be a novel strategy for the prevention and treatment of eye diseases. In our laboratory, we screened for Hsp70 co-inducers from a fungus library (CBS, Utrecht) and found that leucinostatin is probably a potential Hsp70 co-inducer. In **chapter 3**, we first showed that the stressor arsenite could time- and dose-dependently induce Hsp70 expression in dog RPE cells. Then, we showed that carvacrol, described as Hsp70 co-inducer (12), was able to co-induce Hsp70 in RPE cells, as detectable in flow cytometry analyses, which allowed us to analyze Hsp70 level at both single cell level and within defined cell subsets. Subsequently, leucinostatin was found to increase Hsp70 expression during arsenite stress, but not in the absence of arsenite. These results suggested that leucinostatin is a novel potent co-inducer of Hsp70. In addition, in the literature compounds such as glycyrrhizin, bimeclozole, and curcumin have been regarded as co-inducer of HSPs (26). Those compounds might also co-induce Hsp70 in RPE cells.

Hsp70 upregulation is mediated via different signaling strategies by different compounds. HSF1 mainly mediated the transcription of inducible HSPs. In resting cells, HSF1 forms complexes together with Hsp70, Hsp90 and other proteins. Dissociation or direct activation of HSF1 results in the release of HSF1 from these complexes, which facilitates HSF1 translocation and initiation of HSP-transcription. In our study, by using the DNAJB1-luc-O23 reporter cell line, we showed that

leucinostatin can boost Hsp70 expression in canine RPE cells, most likely by activating HSF1. The mechanism of Hsp70 co-induction by leucinostatin is in line with our previous findings using carvacrol. This finding suggested that leucinostatin as a Hsp70 co-inducer may have a possible therapeutic application in inflammatory diseases of the eye.

The role of Hsp70 in innate immunity

Cytokines and chemokines secreted by macrophages, as potent signaling molecules, are the major mediators in inflammatory and immune responses. Activation of macrophages is initiated by inflammatory stimuli, including T lymphocyte-derived cytokines (IFN- γ , TNF- α), immune complexes and microbial products (LPS), and leads to an enhanced capacity to produce cytokines and chemokines. As shown in **chapter 4 and 5**, LPS administration induced high levels of IL-6, TNF- α and IL-1 β expression in both the canine macrophage cell line O30D and monocyte-derived M1 cells. While macrophages produce both pro- and anti-inflammatory cytokines; the balance between these cytokines is determined by the macrophage activation status. As NF- κ B is a critical mediator of pro-inflammatory cytokine production, excessive activation of NF- κ B in macrophages contributes to the development of acute or chronic inflammatory diseases. Recent studies showed that overexpression of Hsp70 may affect the activation of NF- κ B. However, the precise nature of the regulatory role of Hsp70 in NF- κ B activity in canine immune cells remains unknown. Thus, in **chapter 4**, we investigated the potential anti-inflammatory role of Hsp70 in canine macrophages.

Endogenous Hsp70 in macrophages can be induced in many different ways, such as by heat stress, inflammatory environment and chemical stressors (sodium arsenite) (27, 28). In our study, we showed that sodium arsenite dose-dependently induced Hsp70 expression at both the protein and gene level in O30D cells. By treatment of O30D cells with both arsenite and LPS, we found that LPS-induced expression of the pro-inflammatory cytokine IL-6 and TNF- α was significantly inhibited in O30D cells pre-treated with arsenite. To further confirm that the reduction in pro-inflammatory cytokine expression was caused by upregulation of Hsp70, a gene-edited version of the O30D cell line lacking inducible Hsp70 was generated using CRISPR-Cas9 technology. Compared to wild-type canine macrophage cells, the inhibitory effect of arsenite was neutralized in these Hsp70-deficient cells. Similar to our finding in canine, it has been observed that in both murine and human macrophages upregulation of Hsp70 induced by hyperthermia decreased the expression of IL-6, IL-1 β and TNF- α (29, 30). Besides, Ding et al. showed that overexpression of Hsp70 in human macrophages resulted in inhibited expression of IL-1 β , TNF- α , IL-10 and IL-12, but not IL-6 (31). Moreover, Hsp70 induced by

arsenite decreased LPS-induced cytokine TNF- α and IL-6 production in murine Kupffer cells (27). It is worth mentioning that in our study IL-1 β expression was not inhibited by upregulated Hsp70 in both wild-type canine macrophage cells and in Hsp70-deficient cells. This may be due to the specific mechanism of IL-1 β production. As known, IL-1 β exists in two forms, inactive precursor IL-1 β (pro-IL-1 β) and mature IL-1 β . The inactive IL-1 β precursor accumulates in the cytosol until processed into an active cytokine by caspase-1(32). Moreover, apart from NF- κ B, other signaling pathway also regulate IL-1 β , such as the inflammasome, the p38 α -MAPK-MK2 pathway, and cAMP-PKA pathway (33, 34).

The expression of a large number of proinflammatory cytokine genes, such as IL-1, IL-6 and TNF- α , is regulated by NF- κ B. NF- κ B normally exists in an inactive complex, bound to the inhibitory protein I κ B. Activation of NF- κ B signaling is triggered by the release of NF- κ B dimers and its further phosphorylation. The p50/p65 dimer is the most studied and common form of NF- κ B (35), whereby activation of p65 is involved in transcription of pro-inflammatory cytokines (36). Phosphorylation of p65 at Ser536 contributes to its nuclear translocation and DNA binding (37). In **chapter 4**, we showed that treatment of canine macrophages with LPS led to enhanced phosphorylation of p65 at Ser536, while pre-treatment of the cells with arsenite inhibited LPS-induced p65 phosphorylation. Therefore, we hypothesized that arsenite-induced Hsp70 upregulation may result in the inactivation of p65. To test our hypothesis, we further analyzed the phosphorylation levels of p65 in Hsp70-deficient cells. Our results showed that the inhibitory effect of arsenite treatment is attenuated in Hsp70-deficient cells. Taken together, our study in **chapter 4** reveals that Hsp70 may regulate inflammatory responses through NF- κ B activation and cytokine expression in canine macrophages.

In line with our study, Hsp70 overexpression attenuated I κ B degradation and the translocation of p65 in a murine macrophage cell line (38). Similarly, sodium arsenite also inhibited NF- κ B activation by inducing Hsp70 in mouse kupffer cells (27). In addition, Hsp70 has been shown to interact with other molecules such as TRAF6, IKK or p50 and so affect the NF- κ B pathway (39-41). However, the exact molecular basis of Hsp70 and NF- κ B interaction is still unclear. In our study, we compared the amino acid sequences of murine and canine p65; and predicted the potential Hsp70 binding sites on the canine p65 protein. We found that the phosphorylation sites are located in proximity to the accessible chaperone binding peptides, suggesting that Hsp70 may stabilize p65 by occupying its phosphorylation sites.

On the contrary, some studies showed that induction of endogenous Hsp70 by hyperthermia promoted pro-inflammatory cytokine production by macrophages. Elevating the body temperature of LPS-treated mice increased the serum

concentrations of TNF- α , IL-6 and IL-1 β (42), and heat treatment induced Hsp70 expression and TNF- α production in macrophages, suggesting a pro-inflammatory role of Hsp70 (43). Further studies showed that elevating the body temperature of mice also resulted in an increase in LPS-induced NF- κ B activation (43). Since macrophages are highly plastic, the contradictory role of Hsp70 on macrophages might depend on their activation status.

Future perspectives

At present, the treatment of eye diseases by inducing Hsp70 is mostly based on the cell protective roles of HSP70. A great number of studies have demonstrated that Hsp70 enhances RPE or ganglion cell survival in various eye diseases (23, 44). However, the immunomodulatory effect of Hsp70 in the treatment of eye diseases has not been explored. Recently, Jiang, Shuhong, et al. reported that nasal immunization with a low dose of Hsp60 induced immune tolerance and increased the levels of Tregs in a mouse glaucoma model, and reduced RGC and functional loss (24). Our preliminary data also showed that nasal immunization with the Hsp70 peptide B29 had a promising neuroprotective effect in a mouse glaucoma model (personal communication). Furthermore, studies have shown that RPE cells in the presence of inflammatory mediators express MHC I and MHC II molecules (45-47). RPE cells could present extracellular peptides to CD4 T cells via MHC II, inducing anergic T cells (48). Previous studies have shown that both Hsp70 inducers and co-inducers promoted Hsp70 expression at the site of inflammation, led to the increased number of Treg cells and, finally, inhibited inflammation caused by autoimmune diseases, such as experimental autoimmune uveoretinitis and arthritis (13, 49). These studies suggest that in autoimmune eye diseases it is possible that induced endogenous Hsp70 is presented by RPE cells or professional APCs to induce Tregs, meeting the purpose of treating eye diseases. Therefore, based on the characteristics of HSPs co-inducers, leucinoastatin (**in chapter 3**) may have a promising therapeutic role in chronic eye diseases.

Moreover, the results described in **chapter 4** showed anti-inflammatory properties of Hsp70. Besides, stress responses in macrophages may also trigger phenotypic changes of macrophages, by regulating the M1/M2 balance (50). This effect may be mainly caused by HSP70 (51, 52). Except for macrophages, Hsp70 has been found capable of activating dendritic cells, monocytes, and natural killer cells (53). On the other hand, during cellular stress, increased Hsp70-chaperoned peptides in APCs can be presented on MHC class I, and further activate CD8 T cells. Macrophages are able to internalize HSP-chaperoned peptides via CD91, and then present antigenic peptides by MHC class I and II, leading to CD4 and CD8 T cell responses (54). A study from our group showed that a conserved Hsp70 epitope, B29,

presented by MHC II could lead to Treg induction (11). Based on what was discussed above, Hsp70 seems to be a link between innate and adaptive immunity. Combining its role in the induction of immune tolerance, the induction of Hsp70 shows a promising therapeutic effect in macrophages, with possible relevance for chronic diseases.

Comparison of polarization properties of canine monocyte-derived macrophages (MDMs) and canine 030D cell derived macrophages

Plasticity and heterogeneity of macrophages give rise to a continuum of polarization and activation states, represented by two extreme states: M1 and M2 macrophages (55). The shift between M1 and M2 polarization state is often associated with the onset and development of immunological and inflammatory diseases (56). Therefore, the definition and modulation of M1 and M2 polarization states in diseases may be useful for diagnosis and therapy. In *in vitro* studies, tissue-resident macrophages are either directly isolated from tissues such as lung for alveolar macrophages, liver for Kupffer macrophages, spleen, and peritoneal macrophages, or derived from bone marrow and monocytes (PBMC). Among them, PBMCs are widely used because of their many advantages. For example, circulating monocytes *in vivo* are the main source of replenished tissue-resident macrophages and infiltrating macrophages, thus monocyte-derived macrophages *in vitro* resemble natural macrophages quite well; compared to other macrophages, isolation and polarization of monocytes is relatively easy and leading to less animal sacrifice. In addition to monocytes, monocyte-like cell lines are an alternative source of macrophages. Both monocyte-derived and monocyte-like cell line-derived macrophages are widely adopted in human and mouse macrophage studies (57-59). However, there is no standard protocol for polarization and characterization of canine monocyte-derived and monocyte-like cell line-derived macrophages. Hence, in **chapter 5 and 6**, we first polarized canine monocyte and monocyte-like cells (030D cells) into macrophages. Subsequently, polarized macrophages were comprehensively characterized by morphology, phenotypes, gene expression and functional properties.

In our study, canine MDMs were polarized for 7 days in the presence of GM-CSF for M1 or M-CSF for M2 cells. At day 5, M1 and M2 MDMs were activated with IFN- γ and LPS, or IL-4 separately. 030D-derived macrophages were polarized for 3 days in the presence of IFN- γ and LPS for M1, or IL-4 for M2. These experiments showed significant morphological differences between the M0, M1 and M2 subsets. During a 7-day polarization, canine monocyte-derived M0 cells at day 1 had almost the same small and round morphology as monocytes. Compared to M0 cells, canine M1 MDMs

showed a bigger, round shape with pseudopods and amoeboid morphology. A similar change in morphology was observed in canine 030D-derived M1 cells. In contrast, canine M2 MDMs presented with an elongated, spindle-like morphology at day 5; the proportion of elongated cells was increased at day 7. Conversely, only a small portion of 030D-derived M2 macrophages appeared to have a spindle-like shape at day 3. These data are in line with previous findings in humans and mice, where the morphology of M1 cells is described as fired-egg shape, while M2-polarized macrophages present themselves in stretched and spindleoid shapes (60, 61). Besides, Gao, Jiye, et al. observed similar morphological differences between M1 and M2 polarized macrophage populations in pigs (62). Thus, these morphological changes are like our observations in canine M1 and M2 cells. In contrast with our study, one canine macrophage study described M2 cells as a heterogenous population (63). Both spindle-like cells and multinucleated giant cells were found within the M2 population (63). Another study did not find spindle-like cells in either canine blood-derived or cell line-derived (DH82) M2 macrophages (64). We found that in these two studies, macrophages were polarized from PBMCs, which may have led to contamination with granulocytes and dendritic cells. In addition, the continuous subculturing of cell lines such as DH82 may cause gene loss, resulting in an unexpected morphology. In addition, our results showed that canine M1 MDMs were larger and more granular than M0 and M2 MDMs. A similar description was found on pig M1 macrophages as well (62).

Morphological changes in macrophages have been associated with phenotypes and functional states, including surface makers, gene expression and phagocytosis (60, 65, 66). In our study, canine MDMs and 030D-derived macrophages were identified by the expression of the pan-macrophage markers CD14 and CD11b. Other macrophage-specific markers such as Mer tyrosine kinase receptor (MerTK) and CD115 were also measured on 030D-derived macrophages (67, 68). MerTK was widely expressed by all 030D-derived M0, M1 and M2 cells. CD115 expression was decreased in 030D-derived M1 cells, but not M0 and M2 cells, suggesting that CD115 might be a marker for M1/M2 in canine. M1 and M2 cells from both MDM and 030D can be distinguished by the expression of surface markers. As M1 markers, MHC II and co-stimulatory molecules, CD40, CD80 and CD86, were selected. Those markers were highly expressed under M1 polarizing states on both MDMs and 030D macrophages. In addition, all Fc γ receptors (CD16, CD32 and CD64) were expressed at a higher level in M1 cells derived from the 030D cell line. Unlike 030D-derived macrophages, the expression of CD32 was found higher in M2 than M1 in dog MDMs. Similarly, CD83 expression was slightly upregulated in 030D-derived M2 cells, but downregulated in dog M1 MDMs. The difference of M1 marker profiles between canine monocyte- and 030D-derived macrophages has not been elucidated. Likewise, a difference of surface marker expression between human

THP-1 and monocyte-derived macrophages was also reported (69). Therefore, a further study is needed to compare gene expression profiles between canine 030D- and monocyte-derived macrophages. M2 macrophages were generally characterized by the expression of CD206, CD209 and CD163 (70-72). Both canine monocyte- and 030D-derived M2 cells have a higher expression of CD206, CD209 and CD163, compared to corresponding M1 macrophages.

Next, cytokine profiles of 030D-derived M1 and M2 macrophages were compared in **chapter 6**. In most of the studies, pro-inflammatory cytokines, such as IL-6, IL-1 β , TNF- α , IL-12, COX2, are used to characterize M1 macrophages, whereas M2 macrophages express the anti-inflammatory cytokines IL-10 and TGF- β (73, 74). Besides, M1 and M2 activation states are also defined by nitric oxide production and arginase-1 expression respectively. Our results showed that 030D-derived M1 macrophages exhibited both M1 and M2 cytokine signatures by expressing IL-6, IL-1 β , TNF- α , IL-12p35/40, IL-23p19, COX2, CCL2, CCR7, TGF- β and IL-10. Both relatively higher levels of iNOS and arginase-1 were observed in 030D-derived M1 macrophages. However, neither M1 nor M2 macrophages produced detectable nitric oxide. Moreover, newly established M1 marker genes, LOX-1 and LXN, and M2 marker genes, MS4A2, are found to be expressed by canine 030D-derived M1 and M2 macrophages respectively (63, 75). The overlap of cytokine signature between M1 and M2 cells indicated that 030D-derived macrophages may be in a middle state of two extreme polarization states (M1 and M2).

To systematically investigate the difference between dog monocyte-derived M1 and M2 macrophages, global gene profiles of dog macrophages were characterized through mRNA sequencing in chapter 5. As expected, M0, M1 and M2 macrophages share a common set of genes, which may maintain the basic functions of macrophages, while each subset has a set of subset-specific expressed genes. Compared to M0 cells, 1649 differentially expressed genes (DEGs) ($p < 0.05$ and $|\log_2(\text{FC})| > 1$) were upregulated in M1 cells including pro-inflammatory cytokines and chemokines, such as IL-1 β , TNF- α , CCL and CXCL. Besides, MHC I and II were also increased in M1 cells. These genes were found to be upregulated in 030D-derived M1 cells as well. GO and KEGG analysis revealed that upregulated genes in M1 cells were mainly enriched for genes involved in inflammation- and immune-related processes and pathways, such as cytokine and chemokine activity, and Th1, Th2 and Th17 differentiation (supplementary Table S15 and S17). A total of 901 upregulated DEGs were identified in M2 cells compared to M0 cells. Similar to M1 cells, immune-related GO terms and pathways the most enriched DEGs of M2 cells. In the comparison of M1 and M2, 1688 DEGs were upregulated in M1 cells, which are significantly associated with immune-related GO terms and pathways, such as immune response, antigen processing and presentation, TNF signaling pathway and

IL-17 signaling pathway, etc. In contrast, 1436 DEGs were found to be upregulated in M2 cells, which are enriched in GO terms related to DNA and RNA metabolic processes, cell cycle, and helicase activity, etc., and pathways relative to cell cycle, DNA replication, ribosome and β -alanine metabolism, etc. In addition, phagocytosis-related genes were also highly enriched in M1 and M2 cells, suggesting an enhancement of phagocytotic capacity. Furthermore, principal component analysis of all genes showed that M1 cells were clearly separated from M2 cells, which confirms that they are distinct populations. Nevertheless, M0 and M2 cells were clustered together. In line with our observation, a study on mouse macrophages demonstrated also that M2 cells clustered with M0 rather than with M1 (76). Taken together, our results indicate that dog monocyte-derived M1 and M2 cells in vitro display distinct gene profiles, which are strongly associated with the immune response, inflammation and cellular proliferation.

As professional phagocytes, phagocytosis is the main function of macrophages in tissue repair, host defense and homeostasis maintenance. However, there is still controversy in comparison of phagocytosis between M1 and M2 macrophages. M1 macrophages with stronger phagocytosis were shown in some studies, while others demonstrated that M2 macrophages displayed a higher phagocytosis (77-80). In **chapter 5 and 6**, we showed that both monocyte- and O30D-derived macrophages possess the ability to strongly phagocytose latex beads, which may result from widely expressed phagocytic related receptors, such as CD14, MerTK, lectins and integrins (81-83). O30D-derived M1 macrophages developed the strongest phagocytosis among O30D-derived M0, M1 and M2 cells, while M2 cells from monocyte-derived macrophages have a higher phagocytosis capacity than M0 and M1 cells. Likewise, the difference in phagocytosis between cell line and primary monocytes was also found in a human macrophage study (84). Different activation states caused by pathogen infection may regulate phagocytosis of M1 and M2. It is reported that microbial pathogens could control phagocytosis during infection (85). In the early phase of infection, M1 cells dominate the inflammatory response. Non-opsonic receptors on M1 cells are activated by pathogen associated molecular patterns (PAMPs), which further assists in inducing phagocytosis (85). Activated M1 phagocytose and ingest invaded pathogens, secrete cytokines, and present antigens of pathogens. M2 cells obtain very high phagocytosis capacity in the late phase of infection (78). Highly expressed scavenger receptors and mannose receptors on M2 cells may contribute to phagocytosis for the removal of dead cells, and debris. Moreover, Fc γ receptors (CD64, CD32 and CD16) and complement receptors (CR3 and CR4) are major mediators of phagocytosis (85, 86). The treatment of cytokines, like M-CSF, TGF- β or IL-10 treatment was also shown to increase the phagocytic capacity of macrophages (87, 88). Thus, phagocytosis is a complex process, which is influenced by many factors, including activation state, cytokines, surface markers

and pathogens. A comprehensive investigation is needed when phagocytosis of M1 and M2 is compared.

Taken together, we successfully polarized canine monocytes and 030D cells into M0, M1 and M2 macrophages. Characterized canine macrophages shared many similarities to human and mouse macrophages in morphology, phenotypes, gene expression and phagocytosis. Well-characterized canine macrophages are instrumental in canine immunological studies of the future.

Future perspectives

Dogs can spontaneously and frequently develop plenty of immune diseases, such as cancers and autoimmune diseases, which are highly similar to human diseases. Therefore, the dog has been regarded as an attractive animal model for human diseases. For example, type 1 diabetes in dogs highly resembles the human disease (87). Thus, dog can be used as a translational animal model for certain human diseases. The investigation of canine macrophages would be useful for studies on human macrophage-related diseases in which canine is used as a translational animal model.

Reference

1. van Eden W, van der Zee R, Prakken B. Heat-shock proteins induce T-cell regulation of chronic inflammation. *Nat Rev Immunol* (2005) 5(4):318-30. Epub 2005/04/02. doi: 10.1038/nri1593.
2. Wendling U, Paul L, van der Zee R, Prakken B, Singh M, van Eden W. A conserved mycobacterial heat shock protein (hsp) 70 sequence prevents adjuvant arthritis upon nasal administration and induces IL-10-producing T cells that cross-react with the mammalian self-hsp70 homologue. *J Immunol* (2000) 164(5):2711-7. Epub 2000/02/29. doi: 10.4049/jimmunol.164.5.2711.
3. Borges TJ, Wieten L, van Herwijnen MJ, Broere F, van der Zee R, Bonorino C, et al. The anti-inflammatory mechanisms of Hsp70. *Front Immunol* (2012) 3:95. Epub 2012/05/09. doi: 10.3389/fimmu.2012.00095.
4. Sayed KM, Mahmoud AA. Heat shock protein-70 and hypoxia inducible factor-1 α in type 2 diabetes mellitus patients complicated with retinopathy. *Acta Ophthalmol* (2016) 94(5):e361-6. Epub 2016/01/05. doi: 10.1111/aos.12919.
5. Sparrow JR, Hicks D, Hamel CP. The retinal pigment epithelium in health and disease. *Curr Mol Med* (2010) 10(9):802-23. Epub 2010/11/26. doi: 10.2174/156652410793937813.
6. Kumar R, Soni R, Heindl SE, Wiltshire DA, Khan S. Unravelling the Role of HSP70 as the Unexplored Molecular Target in Age-Related Macular Degeneration. *Cureus* (2020) 12(7):e8960. Epub 2020/08/09. doi: 10.7759/cureus.8960.
7. Mérida S, Palacios E, Navea A, Bosch-Morell F. Macrophages and Uveitis in Experimental Animal Models. *Mediators Inflamm* (2015) 2015:671417. Epub 2015/06/17. doi: 10.1155/2015/671417.
8. Lee CT, Repasky EA. Opposing roles for heat and heat shock proteins in macrophage functions during inflammation: a function of cell activation state? *Front Immunol* (2012) 3:140. Epub 2012/06/08. doi: 10.3389/fimmu.2012.00140.
9. Takeda A, Sonoda K-H, Ishibashi T. Regulation of Th1 and Th17 cell differentiation in uveitis. *Inflammation and Regeneration* (2013) 33(5):261-8. doi: 10.2492/inflammregen.33.261.
10. Bazzazi H, Aghaei M, Memarian A, Asgarian-Omran H, Behnampour N, Yazdani Y. Th1-Th17 Ratio as a New Insight in Rheumatoid Arthritis Disease. *Iran J Allergy Asthma Immunol* (2018) 17(1):68-77. Epub 2018/03/08.
11. van Herwijnen MJ, Wieten L, van der Zee R, van Kooten PJ, Wagenaar-Hilbers JP, Hoek A, et al. Regulatory T cells that recognize a ubiquitous stress-inducible self-antigen are long-lived suppressors of autoimmune arthritis. *Proc Natl Acad Sci U S A* (2012) 109(35):14134-9. Epub 2012/08/15. doi: 10.1073/pnas.1206803109.
12. Wieten L, van der Zee R, Goedemans R, Sijtsma J, Serafini M, Lubsen NH, et al. Hsp70 expression and induction as a readout for detection of immune modulatory components in food. *Cell Stress Chaperones* (2010) 15(1):25-37. Epub 2009/05/28. doi: 10.1007/s12192-009-0119-8.
13. Wieten L, van der Zee R, Spiering R, Wagenaar-Hilbers J, van Kooten P, Broere F, et al. A novel heat-shock protein coinducer boosts stress protein Hsp70 to activate T cell regulation of inflammation in autoimmune arthritis.

- Arthritis Rheum* (2010) 62(4):1026-35. Epub 2010/02/05. doi: 10.1002/art.27344.
14. Petersen-Jones SM, Komáromy AM. Dog models for blinding inherited retinal dystrophies. *Hum Gene Ther Clin Dev* (2015) 26(1):15-26. Epub 2015/02/12. doi: 10.1089/humc.2014.155.
 15. Sonoda S, Spee C, Barron E, Ryan SJ, Kannan R, Hinton DR. A protocol for the culture and differentiation of highly polarized human retinal pigment epithelial cells. *Nat Protoc* (2009) 4(5):662-73. Epub 2009/04/18. doi: 10.1038/nprot.2009.33.
 16. Shang P, Stepicheva NA, Hose S, Zigler JS, Jr., Sinha D. Primary Cell Cultures from the Mouse Retinal Pigment Epithelium. *J Vis Exp* (2018) (133). Epub 2018/04/03. doi: 10.3791/56997.
 17. Amirpour N, Karamali F, Razavi S, Esfandiari E, Nasr-Esfahani MH. A proper protocol for isolation of retinal pigment epithelium from rabbit eyes. *Adv Biomed Res* (2014) 3:4. Epub 2014/03/05. doi: 10.4103/2277-9175.124630.
 18. Toops KA, Tan LX, Lakkaraju A. A detailed three-step protocol for live imaging of intracellular traffic in polarized primary porcine RPE monolayers. *Exp Eye Res* (2014) 124:74-85. Epub 2014/05/28. doi: 10.1016/j.exer.2014.05.003.
 19. Blenkinsop TA, Salero E, Stern JH, Temple S. The culture and maintenance of functional retinal pigment epithelial monolayers from adult human eye. *Methods Mol Biol* (2013) 945:45-65. Epub 2012/10/26. doi: 10.1007/978-1-62703-125-7_4.
 20. Heller JP, Kwok JC, Vecino E, Martin KR, Fawcett JW. A Method for the Isolation and Culture of Adult Rat Retinal Pigment Epithelial (RPE) Cells to Study Retinal Diseases. *Front Cell Neurosci* (2015) 9:449. Epub 2015/12/05. doi: 10.3389/fncel.2015.00449.
 21. Lee H, O'Meara S, O'Brien C, Kane R. The Role of Gremlin, a BMP Antagonist, and Epithelial to Mesenchymal Transition in Proliferative Vitreoretinopathy. *Investigative Ophthalmology & Visual Science* (2007) 48(13):5723-.
 22. Amirkavei M, Pitkänen M, Kaikkonen O, Kaarniranta K, André H, Koskelainen A. Induction of Heat Shock Protein 70 in Mouse RPE as an In Vivo Model of Transpupillary Thermal Stimulation. *Int J Mol Sci* (2020) 21(6). Epub 2020/03/21. doi: 10.3390/ijms21062063.
 23. Piri N, Kwong JM, Gu L, Caprioli J. Heat shock proteins in the retina: Focus on HSP70 and alpha crystallins in ganglion cell survival. *Prog Retin Eye Res* (2016) 52:22-46. Epub 2016/03/29. doi: 10.1016/j.preteyeres.2016.03.001.
 24. Pallasaho S, Pallasaho S, Wang J, Huie P, Dalal R, Lee S, et al., editors. Retinal Pigment Epithelium Heating Treatment for Age-Related Macular Degeneration
Heat shock protein expression as guidance for the therapeutic window of retinal laser therapy
Targeting HSP: Immune Tolerance to HSP60 Attenuates Neurodegeneration in Glaucoma. *SPIE BiOS*; 2019: SPIE.
 25. Wang J, Huie P, Dalal R, Lee S, Tan G, Lee D, et al. *Heat shock protein expression as guidance for the therapeutic window of retinal laser therapy*: SPIE (2016).
 26. Ohtsuka K, Kawashima D, Gu Y, Saito K. Inducers and co-inducers of molecular chaperones. *Int J Hyperthermia* (2005) 21(8):703-11. Epub 2005/12/13. doi: 10.1080/02656730500384248.

27. Sun D, Chen D, Du B, Pan J. Heat shock response inhibits NF-kappaB activation and cytokine production in murine Kupffer cells. *J Surg Res* (2005) 129(1):114-21. Epub 2005/10/26. doi: 10.1016/j.jss.2005.05.028.
28. Bachelet M, Adrie C, Polla BS. Macrophages and heat shock proteins. *Research in Immunology* (1998) 149(7):727-32. doi: 10.1016/S0923-2494(99)80047-9.
29. Hagiwara S, Iwasaka H, Matsumoto S, Noguchi T. Changes in cell culture temperature alter release of inflammatory mediators in murine macrophagic RAW264.7 cells. *Inflamm Res* (2007) 56(7):297-303. Epub 2007/07/31. doi: 10.1007/s00011-007-6161-z.
30. Fairchild KD, Viscardi RM, Hester L, Singh IS, Hasday JD. Effects of hypothermia and hyperthermia on cytokine production by cultured human mononuclear phagocytes from adults and newborns. *J Interferon Cytokine Res* (2000) 20(12):1049-55. Epub 2001/01/11. doi: 10.1089/107999000750053708.
31. Ding XZ, Fernandez-Prada CM, Bhattacharjee AK, Hoover DL. Overexpression of hsp-70 inhibits bacterial lipopolysaccharide-induced production of cytokines in human monocyte-derived macrophages. *Cytokine* (2001) 16(6):210-9. Epub 2002/03/09. doi: 10.1006/cyto.2001.0959.
32. Dinarello CA. Overview of the IL-1 family in innate inflammation and acquired immunity. *Immunol Rev* (2018) 281(1):8-27. Epub 2017/12/17. doi: 10.1111/imr.12621.
33. Wang C, Hockerman S, Jacobsen EJ, Alippe Y, Selness SR, Hope HR, et al. Selective inhibition of the p38 α MAPK-MK2 axis inhibits inflammatory cues including inflammasome priming signals. *J Exp Med* (2018) 215(5):1315-25. Epub 2018/03/20. doi: 10.1084/jem.20172063.
34. Zastona Z, Pålsson-McDermott EM, Menon D, Haneklaus M, Flis E, Prendeville H, et al. The induction of pro-IL-1 β by lipopolysaccharide requires endogenous prostaglandin E2 production. *The Journal of Immunology* (2017) 198(9):3558-64.
35. Oeckinghaus A, Ghosh S. The NF-kappaB family of transcription factors and its regulation. *Cold Spring Harb Perspect Biol* (2009) 1(4):a000034. Epub 2010/01/13. doi: 10.1101/cshperspect.a000034.
36. Giridharan S, Srinivasan M. Mechanisms of NF- κ B p65 and strategies for therapeutic manipulation. *J Inflamm Res* (2018) 11:407-19. Epub 2018/11/23. doi: 10.2147/jir.S140188.
37. Sakurai H, Chiba H, Miyoshi H, Sugita T, Toriumi W. IkappaB kinases phosphorylate NF-kappaB p65 subunit on serine 536 in the transactivation domain. *J Biol Chem* (1999) 274(43):30353-6. Epub 1999/10/16. doi: 10.1074/jbc.274.43.30353.
38. Shi Y, Tu Z, Tang D, Zhang H, Liu M, Wang K, et al. The inhibition of LPS-induced production of inflammatory cytokines by HSP70 involves inactivation of the NF-kappaB pathway but not the MAPK pathways. *Shock* (2006) 26(3):277-84. Epub 2006/08/17. doi: 10.1097/01.shk.0000223134.17877.ad.
39. Chen H, Wu Y, Zhang Y, Jin L, Luo L, Xue B, et al. Hsp70 inhibits lipopolysaccharide-induced NF-kappaB activation by interacting with TRAF6 and inhibiting its ubiquitination. *FEBS Lett* (2006) 580(13):3145-52. Epub 2006/05/16. doi: 10.1016/j.febslet.2006.04.066.
40. Bao X-Q, Liu G-T. Induction of overexpression of the 27-and 70-kDa heat

- shock proteins by bicyclol attenuates concanavalin A-induced liver injury through suppression of nuclear factor- κ B in mice. *Molecular pharmacology* (2009) 75(5):1180-8.
41. Guzhova IV, Darieva ZA, Melo AR, Margulis BA. Major stress protein Hsp70 interacts with NF- κ B regulatory complex in human T-lymphoma cells. *Cell Stress Chaperones* (1997) 2(2):132-9. Epub 1997/06/01. doi: 10.1379/1466-1268(1997)002<0132:msphiw>2.3.co;2.
 42. Ostberg JR, Taylor SL, Baumann H, Repasky EA. Regulatory effects of fever-range whole-body hyperthermia on the LPS-induced acute inflammatory response. *J Leukoc Biol* (2000) 68(6):815-20. Epub 2000/12/29.
 43. Lee CT, Zhong L, Mace TA, Repasky EA. Elevation in body temperature to fever range enhances and prolongs subsequent responsiveness of macrophages to endotoxin challenge. *PLoS One* (2012) 7(1):e30077. Epub 2012/01/19. doi: 10.1371/journal.pone.0030077.
 44. Valdés-Sánchez L, Calado SM, de la Cerda B, Aramburu A, García-Delgado AB, Massalini S, et al. Retinal pigment epithelium degeneration caused by aggregation of PRPF31 and the role of HSP70 family of proteins. *Mol Med* (2019) 26(1):1. Epub 2020/01/02. doi: 10.1186/s10020-019-0124-z.
 45. Chan CC, Detrick B, Nussenblatt RB, Palestine AG, Fujikawa LS, Hooks JJ. HLA-DR antigens on retinal pigment epithelial cells from patients with uveitis. *Arch Ophthalmol* (1986) 104(5):725-9. Epub 1986/05/01. doi: 10.1001/archophth.1986.01050170115034.
 46. Detrick B, Rodrigues M, Chan CC, Tso MO, Hooks JJ. Expression of HLA-DR antigen on retinal pigment epithelial cells in retinitis pigmentosa. *Am J Ophthalmol* (1986) 101(5):584-90. Epub 1986/05/15. doi: 10.1016/0002-9394(86)90949-9.
 47. Lipski DA, Dewispelaere R, Foucart V, Caspers LE, Defrance M, Bruyns C, et al. MHC class II expression and potential antigen-presenting cells in the retina during experimental autoimmune uveitis. *J Neuroinflammation* (2017) 14(1):136. Epub 2017/07/20. doi: 10.1186/s12974-017-0915-5.
 48. Gregerson DS, Heuss ND, Lew KL, McPherson SW, Ferrington DA. Interaction of retinal pigmented epithelial cells and CD4 T cells leads to T-cell anergy. *Invest Ophthalmol Vis Sci* (2007) 48(10):4654-63. Epub 2007/09/28. doi: 10.1167/iovs.07-0286.
 49. Kitamei H, Kitaichi N, Yoshida K, Nakai A, Fujimoto M, Kitamura M, et al. Association of heat shock protein 70 induction and the amelioration of experimental autoimmune uveoretinitis in mice. *Immunobiology* (2007) 212(1):11-8. Epub 2007/02/03. doi: 10.1016/j.imbio.2006.08.004.
 50. Vega VL, Crotty Alexander LE, Charles W, Hwang JH, Nizet V, De Maio A. Activation of the stress response in macrophages alters the M1/M2 balance by enhancing bacterial killing and IL-10 expression. *J Mol Med (Berl)* (2014) 92(12):1305-17. Epub 2014/08/29. doi: 10.1007/s00109-014-1201-y.
 51. Eastman AJ, He X, Qiu Y, Davis MJ, Vedula P, Lyons DM, et al. Cryptococcal heat shock protein 70 homolog Ssa1 contributes to pulmonary expansion of *Cryptococcus neoformans* during the afferent phase of the immune response by promoting macrophage M2 polarization. *J Immunol* (2015) 194(12):5999-6010. Epub 2015/05/15. doi: 10.4049/jimmunol.1402719.
 52. Kaczmarek M, Lagiedo M, Masztalerz A, Kozłowska M, Nowicka A, Brajer B, et al. Concentrations of SP-A and HSP70 are associated with polarization of

- macrophages in pleural effusions of non-small cell lung cancer. *Immunobiology* (2018) 223(2):200-9. Epub 2017/11/08. doi: 10.1016/j.imbio.2017.10.025.
53. Koliński T, Marek-Trzonkowska N, Trzonkowski P, Siebert J. Heat shock proteins (HSPs) in the homeostasis of regulatory T cells (Tregs). *Cent Eur J Immunol* (2016) 41(3):317-23. Epub 2016/11/12. doi: 10.5114/ceji.2016.63133.
 54. Srivastava P. Roles of heat-shock proteins in innate and adaptive immunity. *Nat Rev Immunol* (2002) 2(3):185-94. Epub 2002/03/27. doi: 10.1038/nri749.
 55. Parisi L, Gini E, Baci D, Tremolati M, Fanuli M, Bassani B, et al. Macrophage Polarization in Chronic Inflammatory Diseases: Killers or Builders? *J Immunol Res* (2018) 2018:8917804. Epub 2018/03/07. doi: 10.1155/2018/8917804.
 56. Bashir S, Sharma Y, Elahi A, Khan F. Macrophage polarization: the link between inflammation and related diseases. *Inflamm Res* (2016) 65(1):1-11. Epub 2015/10/16. doi: 10.1007/s00011-015-0874-1.
 57. Riddy DM, Goy E, Delerive P, Summers RJ, Sexton PM, Langmead CJ. Comparative genotypic and phenotypic analysis of human peripheral blood monocytes and surrogate monocyte-like cell lines commonly used in metabolic disease research. *PLoS One* (2018) 13(5):e0197177. Epub 2018/05/11. doi: 10.1371/journal.pone.0197177.
 58. Elisia I, Pae HB, Lam V, Cederberg R, Hofs E, Krystal G. Comparison of RAW264.7, human whole blood and PBMC assays to screen for immunomodulators. *J Immunol Methods* (2018) 452:26-31. Epub 2017/10/19. doi: 10.1016/j.jim.2017.10.004.
 59. Lewis ND, Hill JD, Juchem KW, Stefanopoulos DE, Modis LK. RNA sequencing of microglia and monocyte-derived macrophages from mice with experimental autoimmune encephalomyelitis illustrates a changing phenotype with disease course. *J Neuroimmunol* (2014) 277(1-2):26-38. Epub 2014/10/02. doi: 10.1016/j.jneuroim.2014.09.014.
 60. McWhorter FY, Wang T, Nguyen P, Chung T, Liu WF. Modulation of macrophage phenotype by cell shape. *Proc Natl Acad Sci U S A* (2013) 110(43):17253-8. Epub 2013/10/09. doi: 10.1073/pnas.1308887110.
 61. Vereyken EJ, Heijnen PD, Baron W, de Vries EH, Dijkstra CD, Teunissen CE. Classically and alternatively activated bone marrow derived macrophages differ in cytoskeletal functions and migration towards specific CNS cell types. *J Neuroinflammation* (2011) 8:58. Epub 2011/05/28. doi: 10.1186/1742-2094-8-58.
 62. Gao J, Scheenstra MR, van Dijk A, Veldhuizen EJA, Haagsman HP. A new and efficient culture method for porcine bone marrow-derived M1- and M2-polarized macrophages. *Vet Immunol Immunopathol* (2018) 200:7-15. Epub 2018/05/20. doi: 10.1016/j.vetimm.2018.04.002.
 63. Heinrich F, Lehmbecker A, Raddatz BB, Kegler K, Tipold A, Stein VM, et al. Morphologic, phenotypic, and transcriptomic characterization of classically and alternatively activated canine blood-derived macrophages in vitro. *PLoS One* (2017) 12(8):e0183572. Epub 2017/08/18. doi: 10.1371/journal.pone.0183572.
 64. Herrmann I, Gotovina J, Fazekas-Singer J, Fischer MB, Hufnagl K, Bianchini R, et al. Canine macrophages can like human macrophages be in vitro activated toward the M2a subtype relevant in allergy. *Developmental and Comparative Immunology* (2018) 82:118-27. doi: 10.1016/j.dci.2018.01.005.

65. Folkman J, Moscona A. Role of cell shape in growth control. *Nature* (1978) 273(5661):345-9. Epub 1978/06/01. doi: 10.1038/273345a0.
66. Aderem A, Underhill DM. Mechanisms of phagocytosis in macrophages. *Annu Rev Immunol* (1999) 17:593-623. Epub 1999/06/08. doi: 10.1146/annurev.immunol.17.1.593.
67. Briseño CG, Haldar M, Kretzer NM, Wu X, Theisen DJ, Kc W, et al. Distinct Transcriptional Programs Control Cross-Priming in Classical and Monocyte-Derived Dendritic Cells. *Cell Rep* (2016) 15(11):2462-74. Epub 2016/06/07. doi: 10.1016/j.celrep.2016.05.025.
68. Helft J, Böttcher J, Chakravarty P, Zelenay S, Huotari J, Schraml BU, et al. GM-CSF Mouse Bone Marrow Cultures Comprise a Heterogeneous Population of CD11c(+)MHCII(+) Macrophages and Dendritic Cells. *Immunity* (2015) 42(6):1197-211. Epub 2015/06/18. doi: 10.1016/j.immuni.2015.05.018.
69. Daigneault M, Preston JA, Marriott HM, Whyte MK, Dockrell DH. The identification of markers of macrophage differentiation in PMA-stimulated THP-1 cells and monocyte-derived macrophages. *PLoS One* (2010) 5(1):e8668. Epub 2010/01/20. doi: 10.1371/journal.pone.0008668.
70. Martinez FO, Helming L, Gordon S. Alternative activation of macrophages: an immunologic functional perspective. *Annu Rev Immunol* (2009) 27:451-83. Epub 2008/12/25. doi: 10.1146/annurev.immunol.021908.132532.
71. Frafjord A, Skarshaug R, Hammarstrom C, Stankovic B, Dorg LT, Aamodt H, et al. Antibody combinations for optimized staining of macrophages in human lung tumours. *Scand J Immunol* (2020) 92(1):e12889. Epub 2020/04/17. doi: 10.1111/sji.12889.
72. Genin M, Clement F, Fattaccioli A, Raes M, Michiels C. M1 and M2 macrophages derived from THP-1 cells differentially modulate the response of cancer cells to etoposide. *BMC Cancer* (2015) 15(1):577. doi: 10.1186/s12885-015-1546-9.
73. Orecchioni M, Ghosheh Y, Pramod AB, Ley K. Macrophage Polarization: Different Gene Signatures in M1(LPS+) vs. Classically and M2(LPS-) vs. Alternatively Activated Macrophages. *Front Immunol* (2019) 10:1084. Epub 2019/06/11. doi: 10.3389/fimmu.2019.01084.
74. Röszer T. Understanding the Mysterious M2 Macrophage through Activation Markers and Effector Mechanisms. *Mediators Inflamm* (2015) 2015:816460. Epub 2015/06/20. doi: 10.1155/2015/816460.
75. Chanput W, Mes JJ, Savelkoul HF, Wichers HJ. Characterization of polarized THP-1 macrophages and polarizing ability of LPS and food compounds. *Food Funct* (2013) 4(2):266-76. Epub 2012/11/09. doi: 10.1039/c2fo30156c.
76. Lu L, McCurdy S, Huang S, Zhu X, Peplowska K, Tiirikainen M, et al. Time Series miRNA-mRNA integrated analysis reveals critical miRNAs and targets in macrophage polarization. *Sci Rep* (2016) 6:37446. Epub 2016/12/17. doi: 10.1038/srep37446.
77. Zhang M, Hutter G, Kahn SA, Azad TD, Gholamin S, Xu CY, et al. Anti-CD47 Treatment Stimulates Phagocytosis of Glioblastoma by M1 and M2 Polarized Macrophages and Promotes M1 Polarized Macrophages In Vivo. *PLoS One* (2016) 11(4):e0153550. Epub 2016/04/20. doi: 10.1371/journal.pone.0153550.
78. Jaggi U, Yang M, Matundan HH, Hirose S, Shah PK, Sharifi BG, et al. Increased phagocytosis in the presence of enhanced M2-like macrophage responses correlates with increased primary and latent HSV-1 infection. *PLoS*

- Pathog* (2020) 16(10):e1008971. Epub 2020/10/09. doi: 10.1371/journal.ppat.1008971.
79. Lam RS, O'Brien-Simpson NM, Holden JA, Lenzo JC, Fong SB, Reynolds EC. Unprimed, M1 and M2 Macrophages Differentially Interact with *Porphyromonas gingivalis*. *PLoS One* (2016) 11(7):e0158629. Epub 2016/07/08. doi: 10.1371/journal.pone.0158629.
 80. Krzyszczyk P, Schloss R, Palmer A, Berthiaume F. The Role of Macrophages in Acute and Chronic Wound Healing and Interventions to Promote Pro-wound Healing Phenotypes. *Front Physiol* (2018) 9:419. Epub 2018/05/17. doi: 10.3389/fphys.2018.00419.
 81. Zizzo G, Hilliard BA, Monestier M, Cohen PL. Efficient clearance of early apoptotic cells by human macrophages requires M2c polarization and MerTK induction. *J Immunol* (2012) 189(7):3508-20. Epub 2012/09/04. doi: 10.4049/jimmunol.1200662.
 82. Moodley Y, Rigby P, Bundell C, Bunt S, Hayashi H, Misso N, et al. Macrophage recognition and phagocytosis of apoptotic fibroblasts is critically dependent on fibroblast-derived thrombospondin 1 and CD36. *Am J Pathol* (2003) 162(3):771-9. Epub 2003/02/25. doi: 10.1016/s0002-9440(10)63874-6.
 83. Erwig LP, Gordon S, Walsh GM, Rees AJ. Previous uptake of apoptotic neutrophils or ligation of integrin receptors downmodulates the ability of macrophages to ingest apoptotic neutrophils. *Blood* (1999) 93(4):1406-12. Epub 1999/02/09.
 84. Vaddi K, Newton RC. Comparison of biological responses of human monocytes and THP-1 cells to chemokines of the intercrine-beta family. *J Leukoc Biol* (1994) 55(6):756-62. Epub 1994/06/01. doi: 10.1002/jlb.55.6.756.
 85. Uribe-Querol E, Rosales C. Control of Phagocytosis by Microbial Pathogens. *Frontiers in Immunology* (2017) 8(1368). doi: 10.3389/fimmu.2017.01368.
 86. Acharya D, Li XR, Heineman RE-S, Harrison RE. Complement Receptor-Mediated Phagocytosis Induces Proinflammatory Cytokine Production in Murine Macrophages. *Frontiers in Immunology* (2020) 10(3049). doi: 10.3389/fimmu.2019.03049.
 87. Leidi M, Gotti E, Bologna L, Miranda E, Rimoldi M, Sica A, et al. M2 macrophages phagocytose rituximab-opsonized leukemic targets more efficiently than m1 cells in vitro. *J Immunol* (2009) 182(7):4415-22. Epub 2009/03/21. doi: 10.4049/jimmunol.0713732.
 88. Lingnau M, Höflich C, Volk HD, Sabat R, Döcke WD. Interleukin-10 enhances the CD14-dependent phagocytosis of bacteria and apoptotic cells by human monocytes. *Hum Immunol* (2007) 68(9):730-8. Epub 2007/09/18. doi: 10.1016/j.humimm.2007.06.004.

8



Summary in English

Summary

This thesis can be roughly divided into two parts. In the first three chapters, we discussed and studied the role of Hsp70 in retinal pigment epithelial (RPE) cells, and the innate and adaptive immune response. We reviewed the relationship of T cell-mediated diseases and HSPs, and pointed out that the induction of Hsp70 may contribute to therapeutic tolerance (**chapter 2**). Then, we explored a new Hsp70 co-inducer, leucinoastatin, and its role in canine RPE cells (**chapter 3**). Further, we studied the anti-inflammatory effects of Hsp70 in canine macrophages (**chapter 4**). In the last two chapters, we focus on various differently activated canine macrophage subsets originating from both primary monocytes and a monocyte-like cell line (O30D cell) (**chapter 5 and 6**). We successfully polarized canine monocyte-derived macrophages (MDMs) into M1 and M2 cells and thoroughly characterized their features (**chapter 5**). Meanwhile, we demonstrated that O30D cells can be differentiated into M1 and M2 macrophages and that each subset shares the characteristics of the corresponding canine monocyte-derived macrophage subset. Results and conclusions from each chapter are summarized hereafter.

In **chapter 1**, we give a general introduction of this thesis, including basic knowledge of HSPs and Hsp70, the role of Hsp70 in eye diseases and macrophages, and up-to-date research progress on macrophage polarization and characterization.

Inducible HSPs, especially Hsp70, play a crucial role in multiple inflammatory and immune diseases, such as cancer, rheumatoid arthritis, and eye diseases. Diagnosis and therapies targeting the retinal pigment epithelium (RPE) layer have been documented for numerous eye diseases in humans and canine. In recent years, the induction of Hsp70 in RPE has shown therapeutic effects in RPE-related eye diseases. Therefore, exploring non-toxic inducers or co-inducers of Hsp70 for RPE cells is a promising way to cure eye diseases.

An increasing number of studies, not restricted to eye diseases, has shown that the induction of Hsp70 has impact on macrophage function, by modulating inflammation-related signaling pathways and cytokine production. Dysfunction of macrophages affects the balance between inflammation and its resolution, which is the main cause of chronic diseases, including eye diseases and autoimmune diseases. Therefore, the role of Hsp70 in macrophages and macrophage-related diseases was reviewed in **chapter 1**. Furthermore, the effect of upregulated Hsp70 in canine macrophages was investigated in **chapter 4**.

In addition, macrophages represent a group of heterogeneous cells containing a

continuum of polarization and activation states, such as M1 and M2 macrophages. Imbalance of macrophage polarization is closely related to many immune diseases, such as autoimmune diseases, cancers, and chronic inflammatory diseases. However, the information about canine macrophage culturing and polarization is largely lacking. In this thesis, both canine monocyte- and O30D-derived macrophages were studied.

In **chapter 2**, a series of T cell-mediated chronic inflammatory diseases was reviewed. We discussed the immunomodulatory effects of Hsp70 in current clinical trials and laboratory research, as well as the application prospects of Hsp70 in other autoimmune diseases. We also pointed out that several eye diseases like uveitis and idiopathic retinal vasculitis, are Th1 or Th17 mediated diseases, which may establish therapeutic tolerance through the induction of Hsp70 specific Treg cells. We also discussed that both exogenous and endogenous Hsp70 are able to boost the frequency of Hsp70 specific Tregs. Hence boosting Hsp70 by its co-inducers may lead to enhanced Hsp70 specific Treg responses, and further mitigate the progress of chronic diseases. This provided clues for our follow-up research on eye diseases.

In **chapter 3**, we identified an Hsp70 co-inducer (leucinostatin) and developed a method for isolation and culture of canine RPE cells. Furthermore, we investigated whether the compound leucinostatin could enhance Hsp70 expression in arsenite-stressed RPE cells. Our data showed that canine RPE cells were isolated and cultured successfully. The purity of cells that strongly expressed RPE65 was over 90%. In addition, leucinostatin, which enhanced heat shock factor-1-induced transcription from the heat shock promoter in DNAJB1-luc-O23 reporter cell line, also enhanced Hsp70 expression in arsenite-stressed RPE cells, in a dose-dependent fashion. These findings demonstrate that leucinostatin can boost Hsp70 expression in canine RPE cells, most likely by activating heat shock factor-1, suggesting that leucinostatin might be applied as a new co-inducer of Hsp70 expression.

In **chapter 4**, we investigated the potential anti-inflammatory effects of Hsp70 in canine macrophages as well as the mechanisms underlying these effects. We first showed that non-toxic concentrations of arsenite induced Hsp70 expression in canine macrophages. Then we found that Hsp70 upregulation significantly inhibited the LPS-induced expression of the pro-inflammatory mediators, TNF- α and IL-6, as well as the activation of NF- κ B in canine macrophages. Furthermore, CRISPR-Cas9-mediated gene editing of inducible Hsp70 neutralized this inhibitory effect of cell stress on NF- κ B activation and pro-inflammatory cytokine expression. Collectively, our study revealed that Hsp70 may regulate inflammatory responses through NF- κ B activation and cytokine expression in canine macrophages.

In **chapter 5**, we isolated and polarized dog monocytes with GM-CSF, IFN- γ and LPS for M1, or M-CSF and IL-4 for M2. Further, polarized macrophage subsets were thoroughly characterized based on morphology, surface markers feature, gene profiles and functional properties. Our results showed M1-polarized macrophages appeared as round cells with a dominant amoeboid and “fried-egg” phenotype, while M2-polarized macrophages obtained an elongated spindle-like morphology. Phenotypically, M1-polarized MDMs expressed high levels of CD40, CD80, CD86 and MHC II, while a significant increase in the expression levels of CD206, CD209, CD163, and CD32 was observed in M2-polarized macrophages. RNA sequencing showed that M1 and M2-polarized macrophages have distinct gene expression profiles, related to the immune response, cell differentiation and phagocytosis. Functionally, all three polarization states of dog MDMs can phagocytose latex beads, but M2-polarized macrophages exhibited the strongest phagocytic capacity compared to M0- and M1-polarized macrophages. With our work, we contribute to a better understanding of canine macrophage biology in relation to the immune system.

In **chapter 6**, monocyte-like 030D cells were polarized into M1 and M2 macrophages for three days with either IFN- γ + LPS for M1 or IL-4 for M2. Subsequently, 030D-derived M0, M1 and M2 macrophages were comprehensively characterized on each day for morphology, phenotypic characteristics, marker gene expression and phagocytosis. Our results showed that 030D-derived M1 macrophages obtained a bigger, roundish, and amoeboid shape, i.e. a “fried-egg” morphology, whereas some of the M2 macrophages adopted an elongated morphology. Macrophages at all three polarization states expressed the pan-macrophage markers CD14 and CD11b. Flow cytometry analysis showed that 030D-derived M1 macrophages upregulated the expression of CD32, CD40, CD80, CD83, CD86 and MHC II, while M2 macrophages expressed a relatively high level of CD206 compared to M1 macrophages. 030D-derived M1 macrophages highly upregulated the expression of pro-inflammatory cytokines and chemokines, including IL-6, IL-1 β , TNF- α , IL-12p35/40, IL-23p19, COX2, CCL2, CCR7, TGF- β , and IL-10, while the novel identified M2 marker MS4A2 was significantly upregulated in M2 macrophages in comparison to M1 macrophages. Besides, qPCR analysis showed that mRNA levels of CD16, CD32, CD40, CD64, LOX-1, LXN, DLA I, MHC II, CIITA and arginase-1 were upregulated in M1 macrophages compared to M2 macrophages. Functionally, we found that M1 macrophages had a stronger phagocytic capacity than M0 and M2 macrophages. Taken together, in our study it became evident that canine 030D-derived M1 and M2 macrophages showed many similarities to M1 and M2 macrophages derived from other species, such as human, mouse, pig and ovine. Thus, the 030D-derived macrophage can be a powerful cell model for canine immunological studies.

Finally, in **chapter 7**, the results and insights from each chapter are discussed based on the latest research results from different species. We believe that the content of this thesis may contribute to a better understanding of canine Hsp70, eye diseases, macrophages, and the relationships between them.

Nederlandse samenvatting

Samenvatting

Dit proefschrift kan grofweg in twee delen worden verdeeld. In de eerste drie hoofdstukken hebben we de rol van Hsp70 in retinale pigmentepitheelcellen (RPE) en de aangeboren en adaptieve immuunrespons besproken en bestudeerd. We onderzochten de relatie tussen T-cel-gemedieerde ziekten en HSPs, en wezen erop dat de inductie van Hsp70 kan bijdragen aan therapeutische tolerantie (**hoofdstuk 2**). Vervolgens onderzochten we een nieuwe Hsp70 co-inductor, leucinostatine, en diens rol in RPE-cellen van honden (**hoofdstuk 3**). Verder hebben we de ontstekingsremmende effecten van Hsp70 in macrofagen bij honden bestudeerd (**hoofdstuk 4**). In de laatste twee hoofdstukken richtten we ons op verscheidene verschillend geactiveerde macrofaag subsets van honden, afkomstig uit zowel primaire monocytten als een monocyt-achtige cellijn (O30D cellijn) (**hoofdstuk 5 en 6**). We hebben met succes honden monocyt-afgeleide macrofagen gepolariseerd (MDMs) tot M1 en M2 cellen en hun kenmerken grondig gekarakteriseerd (**hoofdstuk 5**). Verder laten we zien dat ook O30D-cellen tot M1- en M2-macrofagen kunnen worden gedifferentieerd en dat beide subsets de kenmerken van de overeenkomstige hondenmonocytten afgeleide macrofaagsubsets delen. De resultaten en conclusies van elk hoofdstuk worden hieronder samengevat.

In **hoofdstuk 1**, geven we een algemene introductie van dit proefschrift, inclusief basis informatie over HSPs en Hsp70, de rol van Hsp70 in oogziekten en macrofagen, en actueel onderzoeksvoortgang op het gebied van macrofaagpolarisatie en karakterisering.

Induceerbare HSPs, vooral Hsp70, spelen een cruciale rol bij meerdere ontstekings- en immuunziekten, zoals kanker, reumatoïde artritis en oogziekten. Diagnose en therapieën die gericht zijn op de RPE-laag zijn gedocumenteerd voor tal van oogziekten bij mensen en honden. De afgelopen jaren is er aangetoond dat Hsp70 inductie in RPE therapeutische effecten heeft op RPE-gerelateerde oogziekten. Daarom kan onderzoek naar niet-toxische (co-) inductoren van Hsp70 in RPE-cellen bijdragen aan de ontwikkeling van nieuwe therapieën voor oogziekten.

Een toenemend aantal studies, niet allen op het gebied van oogziekten, laat zien dat de inductie van Hsp70 invloed heeft op de functie van macrofagen middels het moduleren van ontstekingsgerelateerde signaalroutes en cytokinen productie. Disfunctie van macrofagen beïnvloedt het evenwicht tussen ontsteking en de resolutie hiervan, wat de belangrijkste oorzaak is van chronische ziekten, waaronder oogziekten en auto-immuunziekten. Daarom werd de rol van Hsp70 in macrofagen en macrofaag-gerelateerde ziekten besproken in **hoofdstuk 1**. Verder werd het

effect van verhoogde Hsp70-expressie in macrofagen bij honden onderzocht in **hoofdstuk 4**.

Daarnaast vertegenwoordigen macrofagen een groep heterogene van cellen die een continuüm van verschillende polarisatie- en activeringstoestanden vertegenwoordigen, zoals M1- en M2-macrofagen. Een disbalans in macrofaagpolarisatie is nauw gecorreleerd aan veel immuunziekten, zoals auto-immuunziekten, kanker en chronische ontstekingsziekten. Informatie over het kweken en polariseren van macrofagen bij honden ontbreekt echter grotendeels. In dit proefschrift worden zowel monocyt- als van de cellijn O30D-afgeleide macrofagen van honden bestudeerd.

In **hoofdstuk 2**, wordt een serie T-cel-gemedieerde chronische ontstekingsziekten besproken. We bediscussieerden het immunomodulerende effect van Hsp70 dat wordt waargenomen in huidig klinisch- en laboratoriumonderzoek, evenals de toepassingsmogelijkheden van Hsp70 bij andere auto-immuunziekten. We wezen er ook op dat verschillende oogziekten, zoals uveïtis en idiopathische retinale vasculitis, Th1- of Th17-gemedieerde ziekten zijn. Deze T cellen kunnen therapeutisch getolereerd worden, door de inductie van Hsp70-specifieke Treg-cellen. We hebben ook besproken dat zowel exogeen als endogeen Hsp70 de frequentie van Hsp70-specifieke Tregs kan verhogen. Daarom kan het stimuleren van Hsp70 expressie door een co-inductor leiden tot een verbeterde Hsp70-specifieke Treg-respons, waardoor de verdere progressie van chronische ziekten wordt verminderd. Dit leverde aanknopingspunten op voor ons vervolgonderzoek naar oogziekten.

In **hoofdstuk 3**, identificeerden we een Hsp70 co-inducer (leucinostatine) en ontwikkelden we een methode voor isolatie en kweek van honden RPE cellen. Verder hebben we onderzocht of leucinostatine de Hsp70-expressie in arseniet-gestresste RPE-cellen kan verbeteren. We waren succesvol in het isoleren en kweken van honden RPE-cellen. De zuiverheid van cellen die de RPE marker RPE65 sterk tot expressie brachten, was meer dan 90%. Bovendien verhoogde leucinostatine, dat de door heatshock factor-1 geïnduceerde transcriptie van de heatshock promotor in een DNAJB1-luc-O23-reportercellijn verbeterde, ook de Hsp70-expressie in arseniet-gestresste RPE-cellen, op een dosisafhankelijke manier. Deze bevindingen tonen aan dat leucinostatine de Hsp70-expressie in RPE-cellen van honden kan verhogen, hoogstwaarschijnlijk door heatshock factor-1 te activeren, hetgeen suggereert dat leucinostatine zou kunnen worden toegepast als een nieuwe co-inductor voor Hsp70-expressie.

In **hoofdstuk 4**, hebben we de mogelijke ontstekingsremmende effecten van Hsp70

in honden macrofagen onderzocht, evenals de mechanismen die aan deze effecten ten grondslag liggen. We toonden eerst aan dat niet-toxische arseniet concentraties tot Hsp70-expressie in hondenmacrofagen leidden. Vervolgens ontdekten we dat Hsp70-inductie zowel de LPS-geïnduceerde expressie van de pro-inflammatoire mediators TNF- α en IL-6, als de activering van NF-KB in hondenmacrofagen significant remde. Andersom neutraliseerde CRISPR-Cas9-gemedieerde modificatie van het Hsp70 gen het remmende effect van celstress op NF-KB-activering en pro-inflammatoire cytokine expressie. Samenvattend laat onze studie zien dat Hsp70 in de honden in staat is om ontstekingsreacties te reguleren via activatie van NF-KB- en cytokine expressie in macrofagen.

In **hoofdstuk 5** hebben we hondenmonocyten geïsoleerd en gepolariseerd met GM-CSF, IFN- γ en LPS voor M1, of M-CSF en IL-4 voor M2. Verder werden gepolariseerde macrofaagsubsets uitvoerig gekarakteriseerd op basis van morfologie, eigenschappen van oppervlaktemarkers, genexpressieprofielen en functionele eigenschappen. Onze resultaten toonden aan dat M1-gepolariseerde macrofagen eruitzagen als ronde cellen met een dominant amoëboïde en "gebakken ei" fenotype, terwijl M2-gepolariseerde macrofagen een langwerpige spindelachtige morfologie verkregen. Fenotypisch vertoonden M1-gepolariseerde MDM's een hoog expressieniveau van CD40, CD80, CD86 en MHC II, terwijl in M2-gepolariseerde macrofagen een significante toename van CD206, CD209, CD163 en CD32 werd waargenomen. RNA-sequencing toonde in M1- en M2-gepolariseerde macrofagen verschillende genexpressieprofielen aan, die nauw verband houden met de immuunrespons, celdifferentiatie en fagocytose. Functioneel konden alle drie MDM-afgeleide macrofaag polarisatie vormen latexparels fagocyteren, maar M2-gepolariseerde macrofagen vertoonden de sterkste fagocytische capaciteit. Samenvattend verbeteren deze studies het begrip van macrofaagbiologie en het immuunsysteem in honden.

In **hoofdstuk 6** werd de monocyet-achtige cellijn 030D gepolariseerd tot M1 en M2 macrofagen, door de cellen gedurende drie dagen met ofwel IFN- γ + LPS voor M1 of IL-4 voor M2 te kweken. Vervolgens werden de 030D-afgeleide M0-, M1- en M2-macrofagen dagelijks bestudeerd m.b.t. morfologie, fenotypische kenmerken, expressie van markergenen en fagocytose. Onze resultaten lieten zien dat de van 030D afgeleide M1-macrofagen een grotere, rondere en amoëboïde vorm hadden aangenomen, oftewel een "gebakken ei" -morfologie, terwijl sommige M2-macrofagen een langwerpige vorm aannamen. Macrofagen in elk van de drie polarisatietoestanden brachten de pan-macrofaagmarkers CD14 en CD11b tot expressie. Flowcytometrie-analyse toonde aan dat 030D M1-macrofagen gekenmerkt werden door een hoge expressie van CD32, CD40, CD80, CD83, CD86 en MHC II, terwijl M2-in vergelijking tot M1 macrofagen meer CD206 tot expressie

brachten. Van 030D-afgeleide M1-macrofagen verhoogden de expressie van pro-inflammatoire cytokinen en chemokinen zoals IL-6, IL-1 β , TNF- α , IL-12p35/40, IL-23p19, COX2, CCL2, CCR7, TGF- β , en IL-10, terwijl de recent geïdentificeerde M2-marker MS4A2 significant verhoogd was in M2-macrofagen. Bovendien toonde qPCR-analyse aan dat de mRNA-niveaus van CD16, CD32, CD40, CD64, LOX-1, LXN, DLA I, MHC II, CIITA en arginase-1 verhoogd waren in M1-macrofagen, in vergelijking met M2-macrofagen. Functioneel vonden we dat M1-macrofagen een sterkere fagocytische capaciteit hadden dan M0- en M2-macrofagen. Alles bij elkaar genomen werd uit onze studie duidelijk dat van honden 030D-afgeleide M1- en M2-macrofagen veel overeenkomsten vertoonden met M1- en M2-macrofagen uit andere soorten, zoals mensen, muizen, varkens en schapen. De van 030D afgeleide macrofaag kan dus een krachtig celmodel zijn voor immunologische studies bij honden.

Ten slotte worden in **hoofdstuk 7**, de resultaten en inzichten uit elk hoofdstuk besproken op basis van de laatste onderzoeksresultaten in verschillende organismen. Wij zijn van mening dat de inhoud van dit proefschrift bijdraagt aan een beter begrip van Hsp70 bij honden, oogziekten, macrofagen en de relatie hiertussen.



Appendix

Acknowledgements

Curriculum vitae

List of publications

Acknowledgements

The four years research journey as a PhD candidate in the immunology section of Utrecht University is an amazing and unforgettable experience. Without the help and support from these wonderful people and organizations, I could not have made this thesis possible.

First of all, my heartfelt gratitude goes to **Prof. Dr. Willem van Eden** for your kindness to give me the chance to be one of your PhD students. I still remember how excited I was when I received the acceptance letter from you. You arranged a lot of things when I started my life in the Netherlands. You always respond to my emails as soon as possible, which makes our communication so effective. Thank you for giving me the chance to improve my poor English at the beginning. Thank you for all your helpful and constructive comments on our papers and my thesis, which certainly brought my work to a much higher level. I benefit a lot from your comments, corrections, and constructive suggestions. Thank you for your supervision and support. I am very lucky that I joined your retirement party. I was inspired by your scientific research experience. All my best wishes for your retirement. Enjoy every moment of it.

Meanwhile, I would like to express my sincere gratitude to the **China Scholarship Council (CSC)** for providing me the 4 years scholarship to pursue my PhD abroad. This opportunity helped me obtain more knowledge and research skills. Without the support from **CSC and Prof. Willem van Eden**, I would not have been here. I will never forget this.

My next sincere gratitude goes to my supervisors, **Prof. Dr. Femke Broere and Dr. Alice Sijts**. I am very lucky that I am under your supervision. You are the most responsible supervisors in my life. You are always patient and kind to me. You not only give a lot of suggestions on my project, but also care about my life in the Netherlands. I feel relaxed and happy working with you. You helped me a lot in science and taught me how to write scientifically. I really appreciate all of your useful suggestions and kind help to our papers and my thesis. Your optimistic attitude towards scientific research will accompany my future research career. **Alice**, thank you for inviting me for dinner at your place. You have a precious daughter. She is very talented in piano. I like her playing and her hobby in insect collecting. Thank you for your support and encouragement during my PhD.

I would also like to express my gratitude to **Prof. Dr. Victor P.M.G. Rutten** for guiding me along the way. You always respond very fast. Your critical reading and

constructive comments helped me a lot during my PhD. I really appreciate your kindness and support. Thanks for your time and feedback. I wish you nothing but the very best in your retirement.

For support of laboratory work, I would like to thank **Peter van Kooten**. I would not know how to start my PhD without your help. You taught me everything in the lab. You are always the first one I want to ask for help when I had problem in the lab. You are so warmhearted and willing to help. I really like working with you. You are a nice friend. Thank you for offering me a nice bike. Thank you for all the help that you offered during my PhD. I wish your life in retirement fill with joy and happiness. Enjoy spending time with your loved ones.

I would like to thank **Aad Hoek**. You are nice and talkative. I like to talk to you. your jokes and stories always make me laugh. You bring me a lot of happiness. Thank you for organizing activities for our department. I really enjoy it.

I would like to thank **Ger Arkesteijn**. Thanks for helping me sort cells and introducing me to FACS. I am very glad that you like Chinese tea. You are a good friend. I like to talk to you. All my best wishes to you.

During the last four and half years, I received enormous support and help from my other colleagues. **Robin van den Biggelaar**, thank you for lending me experimental material. Thank you for answering all my questions about our lab and practical skills in the lab. Also, thank you for teaching me swimming, which is a good skill, especially in the Netherlands. I can feel your enthusiasm on science. All my best wishes for your future research career and I believe you will be a great scientist in the future. I thank **Andreja Novak** for sharing antibodies and reagents to me. When I have questions about dog experiment, I always come to you. Thank you for your nice answers and patience. **Nathalie Meijerink**, you are also one of people I ask questions frequently. Thank you for your patience. I still remember **you, Robin and Danielle** taught me how to ice skate. Thank you for organizing activities for PhDs including me. Thank you for all the unforgettable moments we have shared together. You are also going to get your PhD this year. I wish everything goes well on your defense.

Magdalena Wawrzyniuk, thanks for bringing the crisper cas9 technique to our lab, which plays an important role in my publications. Thank you for your effort on our paper.

Danielle Ter Braake, it was a nice experience to have you as my officemate. You are a good organizer of all social activities. Thank you for all the activities that you

organized and all the stories that you shared. I really enjoy them. You bring a lot of happiness to me and the whole department. Thank you for sharing very nice tea with me. I really like the bachelor party **you** and **Lena** organized for me. Thank you both. Good luck with your PhD.

I thank **Irene Ludwig** for all your efforts on our paper. Thanks for your comments on our paper. You helped me a lot in the lab. I wish you a pleasant life.

I would like to thank my another good friend, **Michael Kahsay Ghebremariam**. You are so easy-going and understanding. You always understand me and give me good advice promptly. I wish you a bright future in science.

Shuyu Huang, it is so lucky we met in the Netherlands. Talking with you makes me feel relaxed. Thank you very much. You are so efficient in your work. I wish you the best for the rest of you PhD. **Wu tong**, it is very nice to see you in the Netherlands. Thank you for introducing me to a job, even though it went not well. You are so versatile. You will have a bright future. Hope to see you sometime in China.

Thank you all other PhD fellows **Adil Ljza**, **Lobna Medfai**, **Emanuele Nolfi** and **Miriam East** for your friendship, help and the good time we have had together. I thank all the researchers in our department **Christine Jansen**, **Daphne van Haarlem**, **Naomi Benne**, **Bart van den Eshof** and **Arjan Stoppelenburg** for any moment I may have had to run to you for questions, guidance, and advice. I also want to thank people who used to work in our department during my PhD. **Charlotte de Wolf**, **Anouk Platteel**, **Manon Jansen**, **Susan van Aalst**, **Karin Stumpf**, and **Peter Reinink**, you more or less helped me get through all good and tough situations during my stay in the Netherlands. I thank **Suttiwee Chermprapai** for teaching me qPCR and sharing material and experience to me. I wish all of you are doing good in your own field.

Finally, I want to thank the whole department and all the people that I met. Without any of you, my life would never have been so colorful and exciting. These four years filled with so many unforgettable moments and wonderful experience.

在荷兰的这四年我也认识了好多中国的朋友，他们或多或少都为我提供过帮助，使我枯燥的博士生活变得轻松、愉快，也增加了许多难忘的回忆。**杜文娟**，我们从申请 CSC 的时候就认识，后来一起飞到荷兰，感谢当时及时的信息交流，一切才能如此顺利。来到荷兰之后，我们实验室离的如此之近，感谢为我使用你们的

仪器提供方便。也感谢你邀请我和我媳妇王燕去你家聚餐。很高兴你在同一个实验室找到博后职位，祝你的科研生涯越来越好。

张小刚，在国内的时候就听说你发过很多文章，很庆幸在荷兰认识你。跟你的每次交谈都让我感到轻松，压力倍减。你总是对科研充满激情，相信你一定会有所成就，在此也祝你早日取得博士学位。

余博，很幸运我们能在荷兰成为室友，很怀念我们一起做饭的时刻，希望你能顺利拿到学位，多发好文章。

王晨宇，作为我的另外一个室友我们相处的时间有点短，但是还是要感谢你请我和余博吃饭，感谢你对我在生活上的帮助和支持，祝你早日毕业。

陈娜师姐，谢谢你在我申请学校时不厌其烦地回答我的问题，感谢你去车站接我，感谢你邀请我去你家吃饭。很荣幸能够认识你，祝你的生活越来越好。

李欣悦，感谢你组织的聚餐，让我认识了许多我们领域之外的朋友，你是一个很 social 的人，每次跟你交流都很开心，祝你在科研的道路上越走越远。

彭练慈，我仍然记得我们第一次认识是在学校组织的兽医学大会上。之后虽然交流不多但感觉你是一个外表柔弱内心坚强的女孩，感谢你在实验上对我的帮助和建议。祝你工作、生活一切顺利。

梁建，**丁云**，很幸运在荷兰认识你们，感谢你们的帮助和支持，祝你们能在各自的领域有所成就。

李文涛师兄，谢谢你在科研上给我的建议，你一定会成为一位非常好的科学家。

郎一飞师兄，**王春燕**，**赵珊**，感谢你们提供的帮助，祝你们一切顺利，心想事成。

李永涛老师，谢谢你对我的实验提出的宝贵意见。

陈宏伟老师，很荣幸在荷兰认识你，跟你一起吃饭交谈的日子，让我倍感轻松。祝你家庭美满，事业有成。

崔健男，**曹雪峰**，感谢你们为我提供方便，祝你们博士期间多发文章，早日毕业。感谢师弟**邱泊宁**，谢谢你帮我从国内带东西。

张敏，曾亚龙，土志伟，秦万海，我们都是从吉林大学来到荷兰的，每次见到你们如同见到亲人。感谢张敏邀请我和王燕去你家聚餐。祝你早日获得博士学位。曾亚龙，我们硕士时同出一门，又是室友，在荷兰又在同一所学校，真是太有缘了。虽然在荷兰的相处时间短暂，还是要感谢你的支持与帮助，感谢你新冠疫情期间虽然在国内还不忘给同胞邮寄口罩。祝你成就一番辉煌的事业。感谢土志伟在我女朋友王燕来荷兰时以及之后为我们提供的各种帮助。祝你早日毕业，多发好文章。

感谢UU学联的伙伴，李嘉欣，常晓，宇洁等等，你们组织的各种活动使我在荷兰的生活更加丰富多彩。

同时我也要感谢住在阿姆斯特丹的朋友们，感谢刘施琪，张亚辉，亓文熙，省慧，黄奕轩，谢谢你们分享的食物，跟你们做邻居很开心，就像回到国内一样。感谢江少杰，我们来自同一个县并且是邻村能在荷兰认识真是太难得了，谢谢邀请我和王燕去你家吃火锅。谢谢我的朋友李光尧，你是我唯一一个在荷兰校园外的朋友，感谢你为我免费理发，希望你的生意兴隆。感谢姚嘉俊，谢谢你带我参加基督徒的聚会，让我认识了好多真诚的朋友。祝你学业有成。谢谢我的韩国朋友朴恩卿和她的男朋友Wouter，仍然记得那次偶然的帮助使我们认识。喜欢跟你们一起聊天，享用晚餐，感谢你们提供的美味食物。

此外，我还要感谢我的硕士导师柳巨雄教授，谢谢您对我出国留学的帮助和支持。感谢我的同门和好友，黄炳旭，谢谢你帮我推荐博后职位。感谢我的其他吉大校友蔡桓，刘刚，祝你们在各自领域越走越远。

最后，我想感谢一直在背后支持我的家人。谢谢我的**父亲母亲**对我无条件的支持，无论我走多远你们永远是我坚实的后盾。感谢我的**姐姐（吕丹丹）**，**弟弟（吕庆博）**，**弟妹（陈肖）**，谢谢你们对父母的照顾，使我消除后顾之忧，在荷兰安心学习。谢谢**侄子（吕善浩）**，**侄女（吕紫萱）**，你们给家庭带来了无尽的欢乐。感谢我的爱人，**王燕**，为了能在一起不远万里来到荷兰，感谢你对我无偿的包容和支持。希望我能成为你们的骄傲。

Curriculum vitae

Qingkang Lyu (吕庆康) was born on October 18th, 1988 in Handan, Hebei Province, China. He grew up and finished primary, middle, and high school in his hometown. From September 2009 to June 2013, he studied Veterinary Medicine for 4 years in the undergraduate program at Hebei North University. He wrote his bachelor thesis under supervision of Prof. Fumei Zhang and obtained his bachelor's degree in 2013. In September of 2013, he started his master study in basic Veterinary Medicine in Jilin University, Changchun, China. During his master, he was supervised by Prof. Dr. Juxiong Liu. He mainly focused on the "Mycophenolate Mofetil modulates the differentiation of Th1/Th2 and the secretion of cytokines in active Chron's disease mice model". In June of 2016, he was awarded the master's degree of Agriculture. In September of 2016, he had an opportunity to get a scholarship from the China Scholarship Council to pursue a PhD study at Utrecht University, The Netherlands. He started working in the department of Infectious diseases and Immunology under the supervision of Prof. Dr. Willem van Eden, Prof. Dr. Femke Broere and Dr. Alice Sijts. Here, he studied the role of Hsp70 in canine eye and macrophages. Further, he investigated polarization and characterization of canine macrophages in vitro.

List of publications

Lyu, Qingkang, et al. "Comprehensive characterization of dog monocyte-derived macrophages at different polarization statuses: M1 and M2." (submitted).

Lyu, Qingkang, et al. "A canine macrophage cell line that can be polarized into classically activated M1 and alternatively activated M2 macrophages provides a model for the study of canine macrophage differentiation." (submitted).

Lyu, Qingkang, et al. "Hsp70 and NF- κ B Mediated Control of Innate Inflammatory Responses in a Canine Macrophage Cell Line." *International Journal of Molecular Sciences* 21.18 (2020): 6464.

Lyu, Qingkang, et al. "Leucinoctatin acts as a co-inducer for heat shock protein 70 in cultured canine retinal pigment epithelial cells." *Cell Stress and Chaperones* 25.2 (2020): 235-243.

Barbera Betancourt, Ariana, **Q Lyu**, F Broere et al. "T Cell-Mediated Chronic Inflammatory Diseases Are Candidates for Therapeutic Tolerance Induction with Heat Shock Proteins." *Frontiers in immunology* 8 (2017): 1408.

Qing-kang Lyu, Ju-xiong Liu, Su-nan Li et al. Mycophenolate Mofetil modulates the differentiation of Th1/Th2 and the secretion of cytokines in active Chron's disease mice model [J]. *Int J Mol Sci*. 2015 Nov 6;16(11):26654-66

Li, Sunan, Liu, Juxiong, **Lv, Qingkang**, et al. "AG and UAG induce β -casein expression via activation of ERK1/2 and AKT pathways." *Journal of molecular endocrinology* 56.3 (2016): 213.

LIU Hong-mei, HUANG Bing-xu, **LV Qing-kang** et al. Effects of NPY on TNF- α -induced Caco-2 cell apoptosis [J]. *Chin J Vet Sci*, 2015, 05: 005.

LIU Hong-mei, LI Su-nan, WU Ting-ting, FU Shou-peng, LI Zhi-qiang, **LV Qing-kang** et al. Effect of IL-21 on IL-1 β , IL-10 and IL-12 mRNA expression in LPS-induced macrophages[J]. *Chin J Vet Sci*, 2014, 10: 017.

XUE Wen-jing, ZHANG Hao-long, ZENG Ya-long, LIU Hong-mei, XIE Shan-shan, **LV Qing-kang** et al. The inhibits of the BHBA on the expression of CRH gene in hypothalamic cell[J]. *Chin J Vet Sci*, 2014, 12: 022.

List of publications

Fu SP, Wang JF, Xue WJ, Liu HM, Liu BR, Zeng YL, Li SN, Huang BX, **Lv QK** et al. Anti-inflammatory effects of BHBA in both in vivo and in vitro Parkinson's disease models are mediated by GPR109A-dependent mechanisms[J]. *Journal of neuroinflammation*, 2015, 12(1): 1-14.

Fu SP, Li SN, Wang JF, Li Y, Xie SS, Xue WJ, Liu HM, Huang BX, **Lv QK** et al. BHBA suppresses LPS-induced inflammation in BV-2 cells by inhibiting NF- κ B activation[J]. *Mediators of inflammation*, 2014, 2014.